Mechanistic insight into the MAP kinase signaling pathway during zygote polarization in *Arabidopsis thaliana*

Dissertation

der Mathematisch-Naturwissenschaftlichen Fakultät

der Eberhard Karls Universität Tübingen

zur Erlangung des Grades eines

Doktors der Naturwissenschaften

(Dr. rer. nat.)

vorgelegt von

Kai Wang

aus Anhui/China

Tübingen

2021

Gedruckt mit Genehmigung der Mathematisch-Naturwissenschaftlichen Fakultät der Eberhard Karls Universität Tübingen.

Tag der mündlichen Qualifikation:	20.12.2021
Dekan:	Prof. Dr. Thilo Stehle
1. Berichterstatter/-in:	Prof. Dr. Gerd Jürgens
2. Berichterstatter/-in:	Prof. Dr. Michael Nodine
3. Berichterstatter/-in	Dr. Martin Bayer

Acknowledgements

During my master's study, I was always wondering how to determine positions (upstream and downstream) of components in a regulatory pathway. I was especially confused when I read publications with similar results but different explanations of the regulatory relationships. At that time, I thought regulation should be logistic and pathways should be linear. I innocently thought there should be one experiment that can be universally utilized to determine positions of components in all pathways.

With this youthful naivety, I joined Dr. Martin Bayer's group focusing on the molecular regulation of early embryogenesis. After four years of doctoral research, I have learned a lot about regulation and realized my error. The regulation is complex and "pathways" are not linear. There is no agreed-upon experiment that allows us to identity regulatory relationships. Even when interpreting results of rescue experiments, we always need to explain carefully according to the known context and take into consideration functional redundancy, signal feedback and cell-cell communication in our model. I have learned that we know so little about molecular biology. The true situation is always more complex than what we think. This is why we always need to use proper controls and multiple approaches to address one question. This does not mean that we should not conceive models, but must carefully interpret our results no matter how correct our models appear. I am in favor of Occam's razor: entities should not be multiplied beyond necessity. I have learned to appreciate the difference between the use of "suggest" and "indicate". My understanding may still be naive, but I have learned to persevere in misunderstanding. Like Samuel Beckett's expression, used by my supervisor to encourage me: Ever tried. Ever failed. No matter. Try again. Fail again. Fail better.

First, I want to thank my supervisor Dr. Martin Bayer for his tremendous support in my PhD research. He helped me design experiments, develop methodologies, tackle problems and strengthened my understanding on molecular regulation. I really enjoy discussing scientific questions and exchanging ideas with him. He is always patient and enthusiastic to explain knowledge I am unfamiliar with or do not understand. In addition, he offered me many opportunities to participate in conferences and communicate with

other groups. Furthermore, I cannot forget that he bought me the drink I love but never found in the supermarket: Hochdorfer Wild Elder.

Second, I want to thank my co-supervisor Prof. Dr. Gerd Jürgens, as well as Prof. Dr. Marja Timmermans and Dr. Birgit Kemmerling for their assistance on my project. As my TAC advisors, they gave me many suggestions to improve my experiments. In particular, I want to thank Prof. Dr. Gerd Jürgens for the discussion during the department's monthly progress reports.

A great thank to Dr. Honour McCann for her suggestions and comments on this thesis. Her help strongly improved clarity and coherence of my description.

I want to thank my colleagues Martina Kolb, Marina Ortega-Perez, Yingjing Miao, Houming Chen and former colleagues Agnes Henschen, Daniel Slane and Ancilla Neu for their help in my experiments and for their assistance and entertainment in daily life. Especially, I want to thank Houming Chen and Marina Ortega-Perez for suggestions in my writing.

A special thank to our former secretary Birgit Moldovan for the support in administration affairs. Your spirit lives with us.

I also want to thank my Chinese friends Chuanfu Dong and others for playing sports together.

A thank to brezel and butter. They should be eaten together.

Finally, my appreciation of my parents and grandparents cannot be expressed in words.

Kai Wang

Table of Contents

Abbreviations

ACD: asymmetric cell division
ARF: Auxin Response Factor
APM: apical plasma membrane
BBM: BABY BOOM
BDL: BODENLOS
bHLH: basic helix-loop-helix
BIR3: BAK1-INTERACTING RECEPTOR-LIKE KINASE 3
BPM: basal plasma membrane
BRI1: BRASSINOSTEROID INSENSITIVE 1
BSK: BR-signaling kinase
CEPR: C-TERMINALLY ENCODED PEPTIDE RECEPTOR
CLV3: CLAVATA3
CLE: CLAVATA3/Embryo Surrounding Region-Related
DME: DEMETER
EC1: EGG CELL 1
EPF: Epidermal Pattern Factor
EPFL: EPF-like
ER: ERECTA
ERL: ERECTA-like
ERf: ERECTA family
ESF1: Embryo Surrounding Factor 1
FER: FERONIA
FIS2: FERTILISATION INDEPENDENT SEED 2
FLS2: FLAGELLIN-SENSITIVE 2
GMC: guard mother cell
GLV: GOLVEN
GRD: GROUNDED
GSK3: Glycogen Synthase Kinase 3
HAE: HAESA
HDG: HOMEODOMAIN GLABROUS
HSL: HAESA-like
IKU2: HAIKU2
LatB: latrunculin B
LRR-RK: Leucine-Rich Repeat Receptor Kinase
LRR-RLK: Leucine-Rich Repeat Receptor-like Kinases

MAPK: Mitogen-activated protein kinase
MEA: MEDEA
MEG: maternally expressed gene
MET1: METHYLTRANSFERASE 1
MMC: meristemoid mother cell
MP: MONOPTEROS
MKK: MAPK kinase
MKKK: MAPK kinase kinase
MZT: maternal-to-zygotic transition
PCD: programed cell death
PEG: Parentally expressed gene
PI: propidium iodide
PIP: PAMP-Induced Peptide
RPK2: Receptor-like Protein Kinase 2
RLK7: Receptor-like kinase 7
PIN: PIN-FORMED
RGI: RGF1 INSENSITIVE
ROP: Rho of Plants
RS2200: Renaissance 2200
SAM: shoot apical meristem
SCRM: SCREAM
SERK: Somatic Embryogenesis Receptor Kinase
SGN3: SCHENGEN 3
SGR2: Shoot Gravitropism 2
SLGC: stomata lineage ground cell
SMC: subsidiary mother cell
SPCH: SPEECHLESS
SSP: SHORT SUSPENSOR
STK: SEEDSTICK
TAA1: TRYPTOPHAN AMINOTRANSFERASE OF ARABIDOPSIS 1
TMM: TOO MANY MOUTHS
TPR: Tetratricopeptide repeat
WOX: WUSCHEL-RELATED HOMEOBOX
WUS: WUSCHEL
YDA: YODA
yda-CA: YDA constitutive active
YUC10: YUCCA 10

Summary

In Arabidopsis, the YDA pathway regulates stomata formation, inflorescence architecture and zygote polarity. Although many upstream components of the YDA pathway during stomata patterning have been revealed, upstream components of the embryonic YDA pathway are still largely unknown. In addition, how the YDA signaling confers zygote polarity is still elusive.

In the first project I was involved in, we found that BSK1/2 function upstream of the YDA cascade in addition to SSP. The *bsk1 bsk2 ssp* triple mutant shows severe zygote polarity defects, recapitulating the *yda* phenotype. It has been suggested that the intramolecular interaction between the BSK kinase domain and TPR domain represses BSK activity. We confirmed this repressive interaction within BSK1. Intriguingly, SSP lost this interaction, which confers a constitutive activity. Further swapping experiments between BSK1 and SSP indicate that the first and second TPR motifs of SSP are responsible for its hyperactivity.

Since BSKs and MAPK signals function downstream of receptors, we then wondered which receptor regulates the embryonic YDA pathway. I showed ER functions upstream of YDA with a sporophytic maternal effect. The functional ER mRNAs/proteins in the zygote are likely inherited pre-meiotically from the megaspore mother cell. The sporophytic maternal effect was also observed for BSK1. Furthermore, I confirmed the paternal regulator SSP can function in an ERf-independent manner. My results demonstrate that independent parental signal inputs converge on YDA activation to modulate zygote polarity, reminiscent of the parental conflict theory.

To detect whether other receptors can also activate YDA, we collaborated with Prof. Dr. Michael Hothorn to design an approach for constitutive activation of SERK-dependent LRR-RK pathways. We fused the BIR3 ectodomain with the kinase domain of several LRR-RKs and confirmed their constitutive activity in the corresponding tissues. In particular, when expressed in the epidermal meristemoid, oBIR3-iER blocked stomata formation while oBIR3-iFLS2 had no apparent influence, suggesting the signal specificity of BIR3 chimeras. Then I used this approach to screen the HAESA family receptors and found that most receptors of this family can potentially activate YDA.

Summary

In *yda-CA* transgenic lines, long filamentous embryos are formed. However, what identity these cells possess has not been studied. I designed a filamentous-embryo system to study the suspensor-embryo transition. Twin embryos are frequently developed from the early filamentous embryo. Then we proved that the early filamentous embryo has the identity of early basal cells. In addition, the maximum auxin response is shifted from the hypophysis to basal cells, which may directly contribute to the suspensor-embryo transition.

We then investigate how the YDA signal confers zygote polarity. I showed that SSP is polarly localized in the basal plasma membrane of the elongating zygote. Depolarized localization of SSP leaded to a severe zygote polarity defect, indicating that its asymmetric localization is potent for zygote polarity. As SSP interacts directly with YDA and functions in an ERf-independent way, these results shed light on a polarized YDA activity in the zygote.

These works collectively improved our understanding of the mechanism of zygote polarization.

Zusammenfassung

In der Blütenpflanze *Arabidopsis thaliana* werden viele Entwicklungsentscheidungen durch einen MAP Kinase Signalweg kontrolliert, der die MAPKK Kinase YODA beinhaltet. Unter Anderem werden Stomata-Bildung, die Architektur des Blütenstandes und die Polarität der Zygote reguliert. Während im Kontext der Stomata-Entwicklung einige der Komponenten der Signalkaskade oberhalb von YODA bekannt sind, gibt es im Kontext der Embryogenese bisher kaum molekulare Daten über die Zusammensetzung dieses Signalwegs. Darüber hinaus ist es momentan nicht klar, wie dieser Signalweg die Polarität der Zygote auf molekularer Ebene kontrolliert.

In einem ersten Projekt mit meiner Beteiligung konnten wir BSK1 und BSK2 als integrale Bestandteile von YODA-abhängigen Signalwegen identifizieren – membranständige Mitglieder der Proteinfamilie der BRASSINOSTEROID SIGNALING KINASES. Im Kontext der Embryogenese arbeiten BSK1 und BSK2 parallel zu BSK12 (SHORT SUSPENSOR, SSP) bei der Polarisierung der Zygote. Es wurde beschrieben, dass BSK Proteine durch eine Interaktion ihrer C-terminalen TPR Domäne mit der zentralen Kinase-Domäne in ihrer Signalfunktion gehemmt und dadurch negativ reguliert werden. Das BSK1 Paralog SSP scheint im Laufe der Evolution diese Protein-Interkation verloren zu haben und weißt daher die Eigenschaft auf, den YODA Signalweg konstitutiv zu aktivieren. SSP wird ausschließlich in den Spermienzellen des Pollens exprimiert und übt daher einen paternalen Effekt auf die frühe Embryogenese aus. Funktionale Analysen mit Proteinchimären aus SSP und BSK1 konnten zeigen, dass die ersten beiden TPR Einheiten für die SSP-spezifische Funktion verantwortlich sind.

Da MAP Kinase Signalwege in der Regel durch membranständige Rezeptorkomplexe aktiviert werden, suchten wir nach den Rezeptorkinase(n), die YODA im Embryo aktivieren. Wir konnten dabei zeigen, dass die Rezeptorkinase ERECTA (ER) und in deren Abwesenheit die paralogen ER-LIKE1 und ER-LIKE2 die Polarisierung der Zygote kontrollieren. Die Funktion von ER ist dabei unter sporophytisch-maternaler Kontrolle. Dies ist darauf zurückzuführen, dass ER prä-meiotisch von der Megasporen-Mutterzelle vererbt wird. Weitere Komponenten des embryonalen YODA Signalwegs, darunter BSK1 und BSK2, werden in ihrer Funktion ebenfalls sporophytisch maternal kontrolliert. Dies steht im Gegensatz zu SSP, das den embryonalen YODA Signalweg paternal kontrolliert. Wir konnten zeigen, dass SSP dabei unabhängig von funktionalem ER funktioniert. Zusammenfassend zeigen unsere Daten, dass unabhängige Signalmoleküle beider Eltern bei der Aktivierung von YODA zusammenkommen. Dieses Zusammenspiel von

maternalen und paternalen Einflüssen auf die Embryonalentwicklung diskutieren wir im Kontext der Parentalkonflikt-Theorie.

In einer Kollaboration mit dem Labor von Prof. Dr. Michael Hothorn untersuchten wir, ob weitere Rezeptorkinasen YODA-abhängige Signalwege aktivieren können. Dazu entwickelten wir eine Methode, konstitutiv-aktive Varianten der Rezeptorkinasen zu erstellen. Dabei nutzten wir die Interaktion der extrazellulären Domäne von BIR3 mit SERK Co-Rezeptoren in Abwesenheit von Liganden aus. Dabei zeigte sich, dass Chimären, die die extrazelluläre Domäne von BIR3 und den intrazellulären Teil der zu untersuchenden Rezeptorkinase tragen, nachgeschaltene Signalkaskaden in SERK-abhängigen Signalwegen mit unveränderter Spezifität konstitutiv aktivieren.

Wir nutzten diesen Effekt, um Rezeptorkinasen der HAESA Familie zu untersuchen und konnten dabei zeigen, dass die Mehrzahl dieser Rezeptorkinasen in der Lage ist, YODA zu aktivieren.

Wenn YODA konstitutiv aktiviert wird, wir anstatt eines Embryos eine lange fadenförmige Struktur gebildet. Welche Identität die Zellen in diesem Gebilde annehmen, war bisher unklar. Wir nutzten dieses System und aktivierten YODA vorübergehend. Dabei entwickeln sich aus der ursprünglich fadenförmigen Struktur mehrere Embryonen, die sich teilweise zu funktionalen Keimlingen in einem Samen entwickeln können. Analysen mit Reportergenen legen nahe, dass die Zellen der fadenförmigen Struktur die gleiche Identität aufweisen wie die basale Tochterzelle der asymmetrischen Zygotenteilung. Da nach wie vor unklar war, welche Rolle die Aktivierung von YODA in der Zygote bei der Polarisierung dieser Zelle spielt, untersuchten wir verschiedene transgene Linien, die YODA durch Eizell-spezifische Expression von *SSP* aktivieren. Dabei stellten wir fest, dass bei mittlerer bis starker Expression von *SSP*, das SSP Protein sich weiterhin am basalen Ende der Zygote befindet und zu einem Phänotyp führt, der an konstitutiv-aktives YODA erinnert. Bei sehr starker Expression von *SSP* jedoch befindet sich das SSP Protein an der gesamten Zygoten Plasmamembran wieder. Diese nicht-polare Lokalisierung des SSP Proteins führt zu einem Phänotyp, der an die *loss-of-function yda* Mutante erinnert, obwohl bei starker Expression von *SSP* eine starke Aktivierung von YODA zu erwarten wäre. Diese Ergebnisse deuten darauf hin, dass die einseitige Aktivierung von YODA bei der Polarisierung der Zygote wichtig ist.

Zusammengenommen haben uns die Ergebnisse dieser Projekte deutlichen Einblick in den Mechanismus der Zygotenpolarisierung gegeben und unser Verständnis der frühen Musterbildung in der Pflanzenentwicklung erweitert.

List of publications

Accepted publications

1. Independent parental contributions initiate zygote polarization in Arabidopsis thaliana.
***Kai Wang**, Houming Chen, Marina Ortega-Perez, Yingjing Miao, Yanfei Ma, Agnes Henschen, Jan U Lohmann, Sascha Laubinger, Martin Bayer. Current Biology*, *2021.*
https://doi.org/10.1016/j.cub.2021.08.033

2. Zygotic Embryogenesis in Flowering Plants.
*Houming Chen, Yingjing Miao, **Kai Wang**, Martin Bayer. Methods in Molecular Biology. 2288:73-88; 2021.* doi:10.1007/978-1-0716-1335-1_4.

3. Constitutive Activation of Leucine-Rich Repeat Receptor Kinase Signaling Pathways by BAK1-INTERACTING RECEPTOR-LIKE KINASE3 Chimera.
*Ulrich Hohmann, Priya Ramakrishna, **Kai Wang**, Laura Lorenzo-Orts, Joel Nicolet, Agnes Henschen, Marie Barberon, Martin Bayer, Michael Hothorn. The Plant Cell, October 2020.*
https://doi.org/10.1105/tpc.20.00138

4. Square one: zygote polarity and early embryogenesis in flowering plants.
***Kai Wang**, Houming Chen, Yingjing Miao, Martin Bayer. Current Opinion in Plant Biology, February 2020.* https://doi.org/10.1016/j.pbi.2019.10.002

5. Constitutive signaling activity of a receptor-associated protein links fertilization with embryonic patterning in Arabidopsis thaliana.
*Ancilla Neu, Emily Eilbert, Lisa Y Asseck, Daniel Slane, Agnes Henschen, **Kai Wang**, Patrick Bürgel, Melanie Hildebrandt, Thomas J Musielak, Martina Kolb, Wolfgang Lukowitz, Christopher Grefen, Martin Bayer. Proceedings of the National Academy of Sciences of the United States of America, May 2019.* https://doi.org/10.1073/pnas.1815866116

Manuscript ready for submission

6. A filament-like embryo system to study the suspensor-embryo transition.
***Kai Wang**, Yingjing Miao, Marina Ortega-Perez, Houming Chen, Martin Bayer*.

Contribution to the publications

1. Independent parental contributions initiate zygote polarization in Arabidopsis thaliana.

In this work, I designed experiments and wrote the manuscript together with *Martin Bayer*. I performed main experiments and prepared all figures. *Houming Chen*, *Yingjing Miao, Marina Ortega-Perez* and *Agnes Henschen* helped in some experiments. *Yanfei Ma* and *Jan U Lohmann* provided the Anti-GFP nanobody sequence. *Sascha Laubinger* provided the data of mRNA stability. *Jan U Lohmann* and *Sascha Laubinger* also helped in discussion on the manuscript.

2. Zygotic Embryogenesis in Flowering Plants.

For this review, I collected publications for shoot apical meristem initiation during embryogenesis. *Houming Chen* collected publications for hypophysis initiation and protoderm development, *Yingjing Miao* collected publications for early embryogenesis. *Martin Bayer* designed the manuscript structure. The manuscript was prepared by all authors.

3. Constitutive Activation of Leucine-Rich Repeat Receptor Kinase Signaling Pathways by BAK1-INTERACTING RECEPTOR-LIKE KINASE3 Chimera.

For this publication, I performed the experiment to check BIR3 chimera specificity. I made the *MUTE$_{pro}$:oBIR3-iER* and *MUTE$_{pro}$:oBIR3-iFLS2* transgenic lines, and checked the stomata phenotype and the expression of stomata-related genes. *Agnes Henschen* helped me in the experiment. Together with *Martin Bayer*, we made the Figure 4 and Figure S4. *Ulrich Hohmann*, *Martin Bayer* and *Michael Hothorn* designed the project and experiments. *Ulrich Hohmann, Priya Ramakrishna, Laura Lorenzo-Orts, Joel Nicolet* and *Michael Hothorn* performed the other experiments and made figures. The BIR3 chimera approach was then used in my project to identify the function of other LRR-RKs.

4. Square one: zygote polarity and early embryogenesis in flowering plants.

In this review, I collected publications for zygote elongation and polarity. *Houming Chen* collected publications for auxin response during embryogenesis. *Yingjing Miao* collected publications for zygotic transition. *Martin Bayer* designed the manuscript structure. The manuscript was prepared by all authors.

5. Constitutive signaling activity of a receptor-associated protein links fertilization with embryonic patterning in Arabidopsis thaliana.

In this publication, I checked the expression of target genes in protoplasts. I also made posters and gave oral presentations in the SFB1101 meetings. *Wolfgang Lukowitz, Christopher Grefen* and *Martin Bayer* designed this research and wrote the paper. *Ancilla Neu, Emily Eilbert, Lisa Y Asseck, Daniel Slane, Agnes Henschen, Patrick Bürgel, Melanie Hildebrandt, Thomas J Musielak, Martina Kolb, Wolfgang Lukowitz, Christopher Grefen* and *Martin Bayer* performed the other experiments and data analysis.

6. A filament-like embryo system to study the suspensor-embryo transition.

In this work, I designed the research together with *Martin Bayer*. I performed the main experiments, prepared figures and wrote the manuscript. *Yingjing Miao* dissected ovules and helped to check the *gWOX8Δ-nls-3xVenus* signals and the *DR5:GFP* signals. *Marina Ortega-Perez* detected the activity of the *S4* promoter, checked MP_{pro}*:MP-GFP* expression and other promoter lines. *Houming Chen* helped to detect *DR5:GFP* signals. Martin Bayer detected the $ARF13_{pro}$*:nls-tom* line. *Marina Ortega-Perez* and *Houming Chen* revised the manuscript as well.

EBERHARD KARLS
UNIVERSITÄT
TÜBINGEN

Mathematisch-Naturwissenschaftliche Fakultät

Erklärung nach § 5 Abs. 2 Nr. 8 der Promotionsordnung der Math.-Nat. Fakultät

-Anteil an gemeinschaftlichen Veröffentlichungen-

Nur bei kumulativer Dissertation erforderlich!

Declaration according to § 5 Abs. 2 No. 8 of the PhD regulations of the Faculty of Science

-Collaborative Publications-

For Cumulative Theses Only!

Last Name, First Name: Wang, Kai

List of Publications

1. Independent parental contributions initiate zygote polarization in *Arabidopsis thaliana*.

2. Zygotic Embryogenesis in Flowering Plants.

3. Constitutive Activation of Leucine-Rich Repeat Receptor Kinase Signaling Pathways by BAK1-INTERACTING RECEPTOR-LIKE KINASE3 Chimera.

4. Square one: zygote polarity and early embryogenesis in flowering plants.

5. Constitutive signaling activity of a receptor-associated protein links fertilization with embryonic patterning in *Arabidopsis thaliana*.

6. A filament-like embryo system to study the suspensor-embryo transition.

Nr.	**Accepted publication yes/no**	**List of authors**	Position of candidate in list of authors	Scientific ideas by the candidate (%)	Data generation by the candidate (%)	Analysis and Interpretation by the candidate (%)	Paper writing done by the candidate (%)
			The contribution to each publication and manuscript is stated in the section “Contribution to the publications”.				
1							
2							
3							

I confirm that the above-stated is correct.

Date, Signature of the candidate

I/We certify that the above-stated is correct.

Date, Signature of the doctoral committee or at least of one of the supervisors

Introduction

1 Embryogenesis

1.1 Plant embryogenesis

Embryogenesis is the fundamental step to establish body structures in multicellular organisms. Angiosperm embryogenesis initiates from a horizontal division of the zygote. In many angiosperm species, the zygote divides asymmetrically to generate an apical-basal axis [1]. The apical and basal daughter cells then differentiate and form an embryo containing an embryo proper and a suspensor. The suspensor is a plant-specific structure to connect the embryo with the mother tissue (Figure 1A) [2-4]. It is considered to

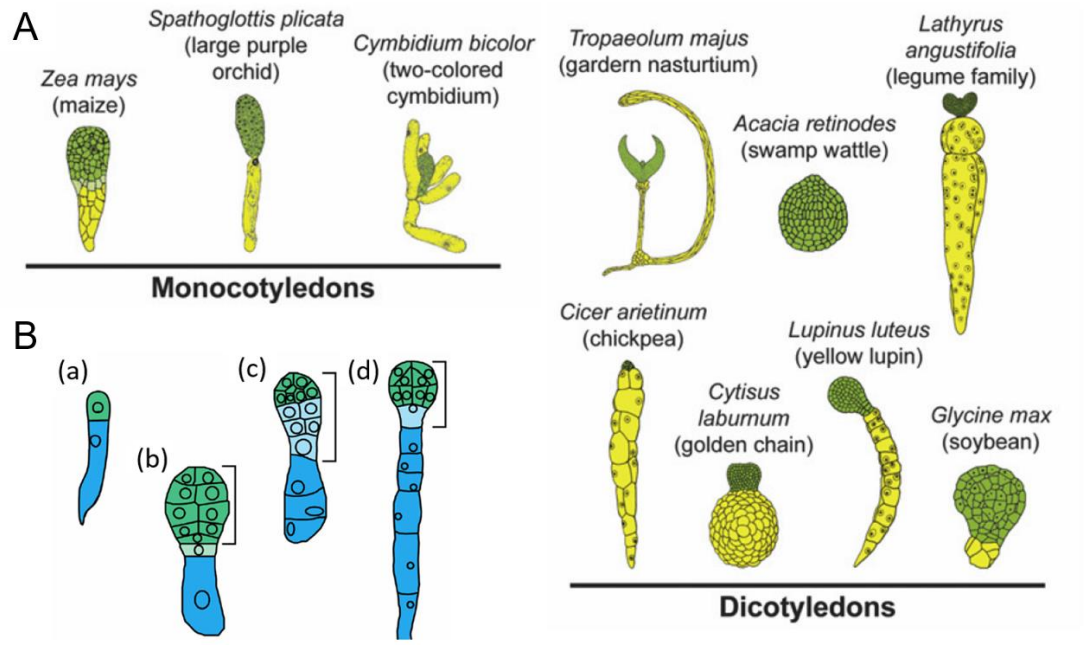

Figure 1. Diversity of the suspensor in angiosperm species [2, 3].

(A) The suspensor (yellow) and the embryo proper (green) of monocots and dicots ([2], modified). (B) Origin of embryonic structures [3]. (a) The first cell division generates an apical (green) and basal (blue) daughter cells. (b) Descendants (light green) of the apical cell in *Sagina procumbens* contribute to the suspensor. (c) Cells (light blue) derived from the basal cell incorporate into the embryo proper in *Geum urbanum*. (d) The uppermost basal cell (light blue) contributes to the embryo proper in *Brassicaceae*. Brackets indicate the embryo proper.

hold the embryo proper and promote its development through the delivery of nutrition and phytohormones [2]. In many species, the basal daughter cell does not solely contribute to the suspensor: several of its descendant cells also contribute to the embryo proper

(Figure 1B). In contrast, in some species several apical descendant cells can incorporate with basal cells to form the suspensor. During seed maturation, most cells of the suspensor is eventually degraded [2, 4]. Despite their conserved function and destiny, suspensor structures are quite diverse among angiosperms (Figure 1A) [2]. In many species, because of irregular embryonic configuration, embryogenesis is hard to follow and the boundary between the suspensor and the embryo proper is difficult to discern [2-4]. In comparison, *Brassicaceae* follows a stereotypical developmental process during embryogenesis, providing a remarkable model to study the molecular regulations of plant embryogenesis [3].

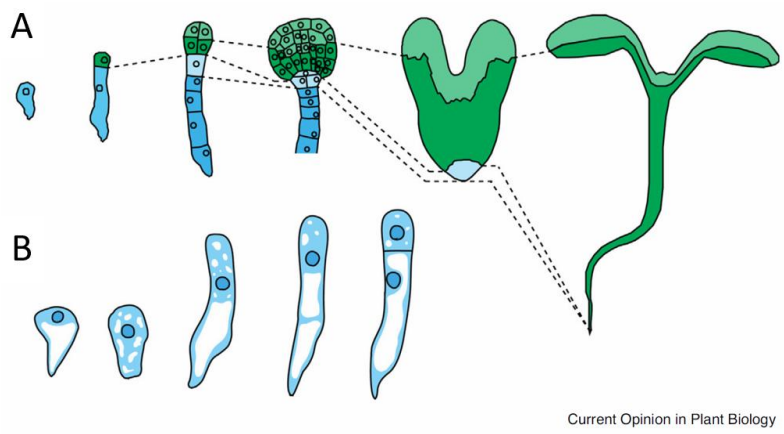

Figure 2. Embryogenesis in Arabidopsis [3].

(A) Development of the Arabidopsis embryo. After fertilization, the zygote elongates and then divides into two daughter cells with different sizes. The apical daughter cell (green) then forms a spherical embryo proper (the upper tier (light green) and lower tier (dark green)) which develops into the aboveground part of a seedling. The basal daughter cell (blue) divides into the mostly extra-embryonic filamentous suspensor (dark blue) except the uppermost cell that will contribute to the formation of the hypophysis (light blue). Hypophysis eventually forms the underground root meristem. (B) The asymmetric zygote division. The egg cell contains a large vacuole (white) at the basal pole and a small nucleus at the apex (dark blue). After fertilization, cell polarity is temporarily lost in the very early zygote, reflected by the movement of the nucleus from the top to the middle and the fragmentation of the large vacuole. During cell elongation, the zygote repolarizes and divides asymmetrically. A large vacuole is reformed at the basal pole of the elongating zygote.

1.2 Arabidopsis embryogenesis

Arabidopsis embryogenesis is well described compared with other *Brassicaceae* species (Figure 2A) [3, 5-7]. During Arabidopsis embryogenesis, the zygote first shrinks and then

elongates approximately three times in a tip-grown manner. It then divides asymmetrically, giving birth to a small apical cell and a large basal cell. The apical daughter cell undergoes two longitudinal divisions followed by a transverse division, forming an 8-cell proembryo. These cells then undergo an oblique division to generate a 16-cell dermatogen embryo, of which the outer layer finally differentiates into the epidermis while the inner cells develop into the endodermis, the shoot apical meristem (SAM), the hypocotyl and the vasculature. In comparison to the diverse cell divisions and differentiations of the apical-cell lineage, the basal daughter cell only divides horizontally to form the suspensor containing ultimately a file of 6 to 8 cells. The uppermost suspensor cell will contribute to the formation of hypophysis, the precursor of the root meristem. The other suspensor cells will eventually undergo programed cell death (PCD).

1.3 Zygote polarization

In angiosperms, after fertilization the dicot zygote elongates whereas the monocot zygote does not show apparent elongation. However, both monocot and dicot zygotes undergo an asymmetric cell division (ACD) to generate two daughter cells with distinct destinies, indicating that angiosperm zygotes are polarized [3, 8]. The mechanism of zygote polarity establishment, however, is still elusive.

Some understanding of zygote polarization has been achieved in the model plant Arabidopsis. The Arabidopsis egg cell harbors a large vacuole at the bottom and a small nucleus at the apex (Figure 2B), and microtubules and actin filaments (F-actins) are oriented mainly in the vertical direction [9, 10]. After fertilization, the zygote is temporarily depolarized. The nucleus moves to the middle and the large vacuole is shattered into evenly distributed small vacuoles. Microtubules and F-actins seem to be oriented randomly at this stage [9, 10]. Zygote polarity is acquired during cell elongation. The zygote nucleus moves to the apical region and a large vacuole is reformed at the basal pole (Figure 2B). The microtubules and F-actins are rearranged. In the zygote apex, microtubules form a transverse ring and F-actins form an apical cap [9].

The influence of the cytoskeleton and the vacuole on zygote development was only recently revealed. The microtubule polymerization inhibitor oryzalin can suppress zygote elongation, whereas the actin polymerization inhibitor latrunculin B (LatB) has no obvious

effect on zygote elongation. However, the polar migration of the zygote nucleus is inhibited by LatB, resulting in a symmetric division of the zygote [9]. These results indicate that microtubules affect zygote elongation while F-actins affect zygote division. Moreover, vacuole distribution also influences zygote polarity. Shoot Gravitropism 2 (SGR2) is a phospholipase A1-like protein localized on the vacuolar membrane. In the *sgr2-1* loss-of-function mutant, polarized vacuole distribution in the elongating zygote is blocked. Large vacuoles are localized both in the apical and basal parts of the zygote. While the zygote seems to elongate normally, it divides more symmetrically. Furthermore, F-actin cables are associated with tubular vacuoles in wild type but not in *sgr2-1*. LatB does not affect vacuolar distribution in the *sgr2-1* zygote, implying that F-actins regulate the zygote polarity by modulating the polarized vacuolar distribution [10].

2 The YDA signaling pathway

2.1 The MAPK cascade

The Mitogen-activated protein kinase (MAPK) phosphorylation cascade is composed of a MAPK kinase kinase (MKKK), a MAPK kinase (MKK) and a MAPK. In plants, the MAPK cascades play versatile roles in plant growth, development, immune response and abiotic resistance [11-14]. Arabidopsis has 20 MAPKs, 10 MAPKKs and approximately 60 MAPKKKs [12, 15]. The MKKK3/5-MKK4/5-MPK3/6 and MEKK1-MKK1/2-MPK4 cascades positively and negatively regulate the flg22-induced immune response, respectively [11, 13, 14]. Zygote polarity, inflorescence architecture and stomata pattering are controlled by the YODA (YDA, MKKK4)-MKK4/5/-MPK3/6 cascade [5, 16-19]. Moreover, MKK4/5 and MPK3/6 modulate the floral abscission and the lateral root emergency with an unknown MKKK in Arabidopsis [20]. The MAPK cascades also play pivotal functions in other species [14, 21-23]. In particular, a MAPK cascade is reported to regulate the expansion of phragmoplast microtubules during cytokinesis in tobacco and Arabidopsis [23].

2.2 The YDA signaling pathway during stomata development

Stomata are microscopic structures in plant epidermis for gas exchange between plants and the environment. They consist of a pair of guard cells that flank a central pore [24, 25]. In many plant species, the stomata development initiates from an ACD of the meristemoid

mother cell (MMC) [25]. In Arabidopsis, the small daughter cell serves as a meristemoid that can either develop into a guard mother cell (GMC) or undergo several rounds of ACDs before entering differentiation (Figure 3A). The large daughter cell, named the

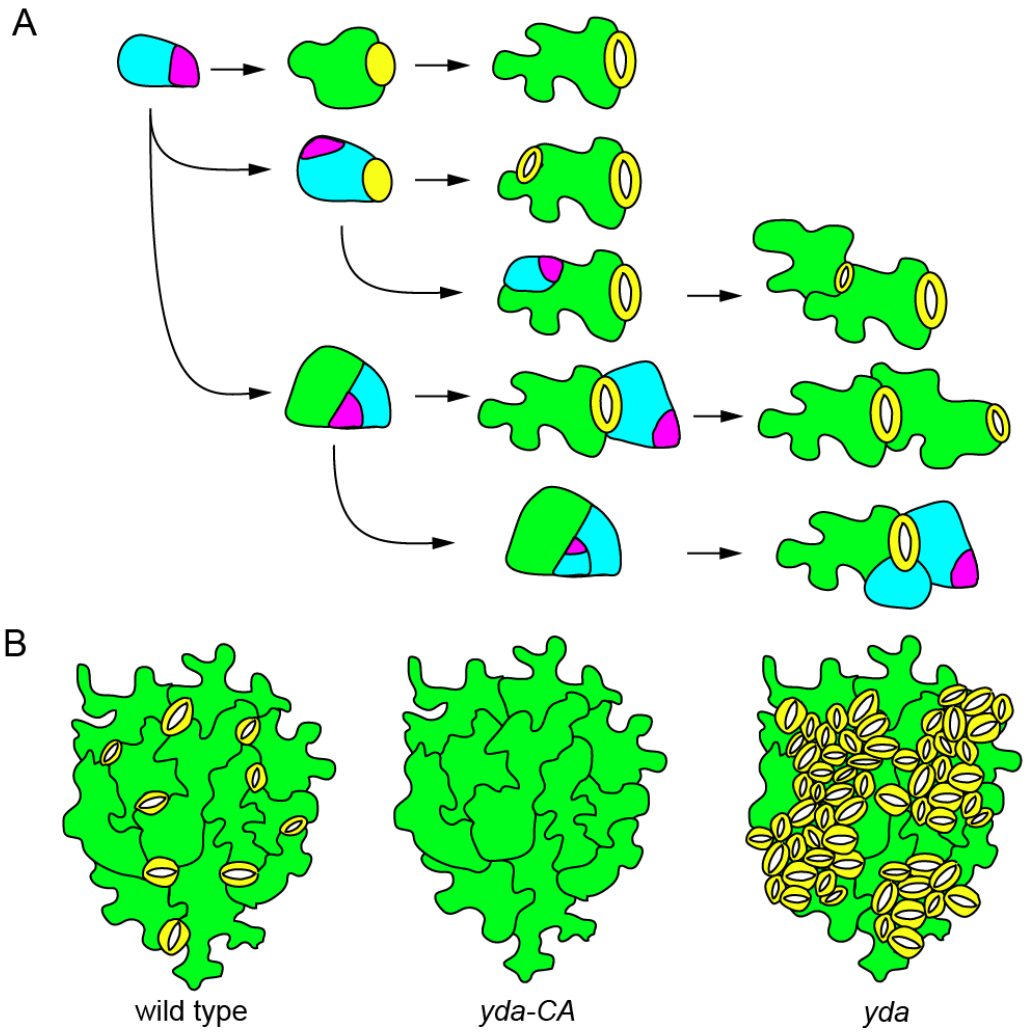

Figure 3. Stomata development in Arabidopsis.

(A) Development of guard cells. The MMC divides asymmetrically to generate a small meristemoid (magenta) and a SLGC (light blue). The meristemoid can either differentiate into two guard cells (yellow) or undergo another ACD to generate a new meristemoid and another SLGC. The SLGC can either form a pavement cell or divide asymmetrically to form another SLGC and a new meristemoid. (B) The epidermal phenotypes of the *yda-CA* lines and the *yda* mutants.

stomata lineage ground cell (SLGC), will either differentiate into a pavement cell or divide asymmetrically again to generate another meristemoid. In contrast, the stomatal lineage is less flexible in grasses. Their MMC only experiences a single ACD to form a GMC and

a large sister cell that becomes a pavement cell. The flanking neighboring cells at both sides of the GMC, called the subsidiary mother cells (SMCs), undergo an ACD to yield two subsidiary cells that facilitate the function of guard cells [25].

The distribution of stomata in leaf epidermis is always discrete. Stomata are usually separated by pavement cells so that they are not adjacent to each other, according to the so called the one-cell spacing rule (Figure 3) [26]. The *yda*, *mkp3*$^{+/-}$ *mpk6* loss-of-function mutants and the *mkk4/mkk5 amiRNA* lines show clustered stomata while expressing a constitutively active version of *YDA (yda-CA)* can severely block stomata formation (Figure 3B). These results demonstrate that the YDA signaling inhibits stomata generation in Arabidopsis [16, 27]. In addition, YDA also inhibits stomata formation in *Brachypodium*, indicating conserved function of YDA in both monocots and dicots [28].

Leucine-Rich Repeat Receptor Kinases (LRR-RKs) / Leucine-Rich Repeat Receptor-like Kinases (LRR-RLKs) contain an extracellular leucine-rich repeat domain, a transmembrane part and an intracellular kinase domain. There are more than 200 LRR-RKs or LRR-RLKs in Arabidopsis [29]. The ERECTA family (ERf) LRR-RKs is composed of ERECTA (ER), ERECTA-like 1 (ERL1) and ERL2. This family plays versatile functions during plant vegetative and reproductive development, including stomata patterning, leaf initiation and development of the vasculature, SAM, reproductive organs and cotyledons [30-37]. Similar to *yda*, the *er erl1 erl2* mutant shows severe clustered stomata [38]. Its stomatal defect can be rescued by introducing yda-CA, indicating that ERf functions upstream of YDA during stomata patterning (Figure 4) [31].

TOO MANY MOUTHS (TMM) is a receptor-like protein lacking the intracellular domain. It interacts with ERf to create a binding pocket for perceiving Epidermal Pattern Factor 1/2 (EPF1/2) in leaf epidermis [38-40]. EPF-like 9 (EPFL9)/STOMAGEN negatively regulates the ERf signal by competing with EPF1/2 for binding to ERf [32]. Intriguingly, while the *tmm* loss-of-function mutant has clustered stomata in leaf epidermis, no stomata is formed in its stem epidermis [38, 41]. Recent protein structure evidence indicates that TMM suppresses the binding of EPFL4/6 to ERf [40]. EPFL4/6 are expressed in endodermal cells. It is proposed that once TMM is abolished, EPFL4/6 secreted from stem endodermis activate ERf in stem epidermis to inhibit stomata formation [32, 42]. The activation of EPF signals also requires the interaction between ERf and the Somatic Embryogenesis

Receptor Kinases (SERKs) upon EPF binding. The ERf-SERK interaction will trans-activate each other for signal transduction [43]. SERKs also belong to LRR-RKs. In addition to serving as co-receptors for ERf, they are also co-receptors of many other LRR-RKs, such as HAE/HSL2, HSL1, FLS2 and BRI1 [44-47].

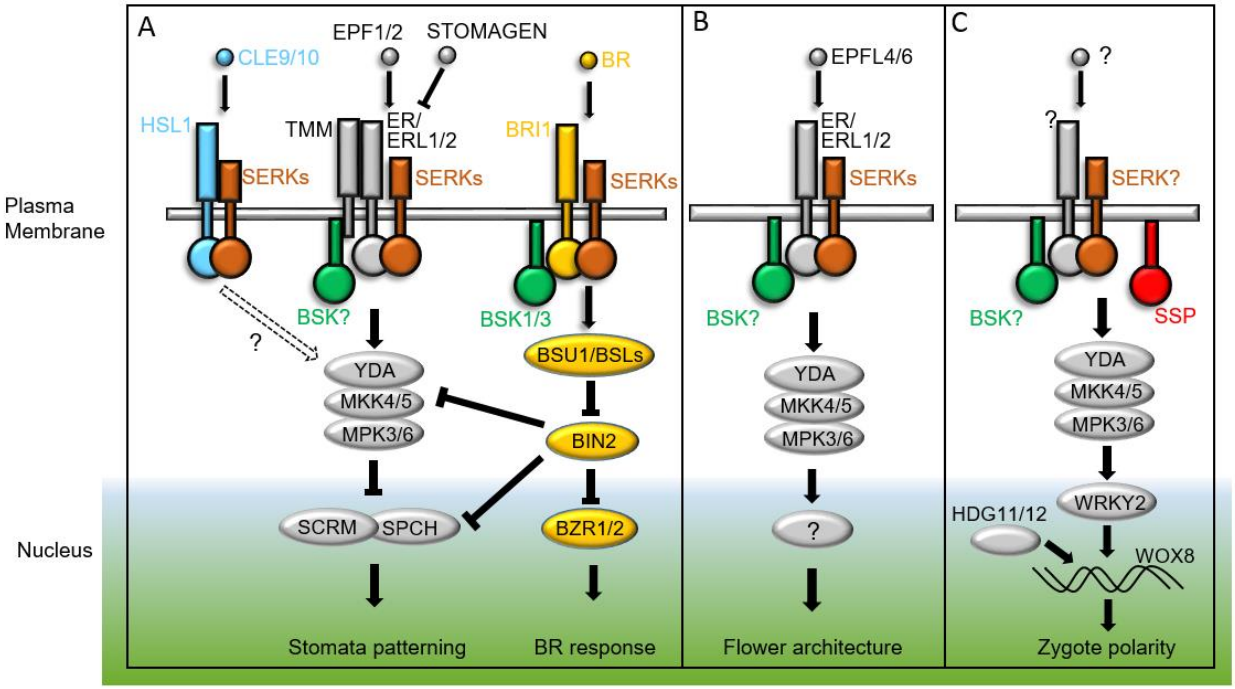

Figure 4. The YDA pathway in Arabidopsis.

(A) During stomata patterning, the ERECTA family receptors ER/ERL1/ERL2 interact with TMM and SERKs to perceive EPF1/2. STOMAGEN/EPFL9 competes with EFP1/2 for binding with ERf and inhibits the ERf signaling. The YDA cascade regulates stomata patterning by phosphorylating and inhibiting the transcription factors SPCH and SCRM. Moreover, the BR signaling pathway affects stomata pattern through BIN2 phosphorylation and inhibition of YDA and SPCH. In addition, CLE9/10 bind with HSL1 and SERKs to modulate stomata patterning, probably through activating the YDA cascade. (B) During inflorescence development, ERECTA family receptors interact with SERKs upon binding of EPFL4/6, activating the YDA cascade to control the SAM size. The downstream transcription factors are unknown. (C) SSP (BSK12) functions upstream of the YDA cascade to regulate zygote polarity. MPK3/6 phosphorylates the transcription factor WRKY2, which then activates the expression of *WOX8*. The transcription factors HDG 11/12 also promote WOX8 expression. The upstream receptor was unknown. Whether other BSKs also function upstream of YDA was also unrevealed.

The BR-signaling kinases (BSKs) are membrane-anchored proteins functioning downstream of LRR-RKs. According to their structure and kinase activity, BSKs are considered pseudokinases [48]. In Arabidopsis, this protein family contains 12 members:

BSK1-BSK12. BSK1/3/5/6/7/8/11 can be phosphorylated by BRASSINOSTEROID INSENSITIVE 1 (BRI1) in BR signaling [49, 50]. BRI1 activates BSK1 by phosphorylating its Ser-230 site [49]. Additionally, FLAGELLIN-SENSITIVE 2 (FLS2) interacts with BSK1 to regulate the innate immune response [51]. It was unknown Whether BSKs function downstream of ERf and other LRR-RKs.

SPEECHLESS (SPCH), MUTE and FAMA are the basic helix-loop-helix (bHLH) transcription factors that modulate three consecutive steps during stomata formation: initiation, meristemoid differentiation and guard cell morphogenesis [52]. SCREAM (SCRM) and SCRM2 are paralogous proteins in the bHLH family. They directly interact with SPCH, MUTE and FAMA, and specify their sequential actions [53]. The activity of SPCH is suppressed by MPK3/6 through direct phosphorylation [17]. Recent evidences indicate that SCRM functions as a scaffold to recruit MPK3/6 to SPCH. MPK6 directly binds to the SCRM bipartite motif, phosphorylating SCRM and activating its degradation [54]. In addition, SPCH directly binds the promoter of *EPF2* and *TMM* to activate their expression, thereby forming a negative feedback loop to fine-tune the stomata patterning [55]. The functions of SPCH, MUTE and FAMA during stomata formation seem to be conserved in tomato and grasses [25, 56]. Moreover, the BR signaling pathway affects stomata pattern through the phosphorylation and inhibition of YDA and SPCH by the Glycogen Synthase Kinase 3 (GSK3) kinase BIN2 [57].

2.3 The YDA signaling pathway during inflorescence development

The YDA pathway also regulates inflorescence architecture in Arabidopsis (Figure 4). Compact flowers are observed in *yda*, *mkp3*$^{+/-}$ *mpk6* and the *mkk4/mkk5 amiRNA* lines while expressing *yda-CA* or constitutively active *MKK4/MKK5* increases the pedicel length [18, 31]. Suppressing the function of ERf and SERKs also cause compact flowers [31, 43]. In *er erl1 erl2,* the SAM size expands strikingly. ERFL1/2/4/6 expressed in the boundary of the SAM are suggested to activate ERf in the SAM region [35, 58]. ERf also regulates inflorescence architecture in tomato, suggesting that the function of ERf receptors might be conserved [59]. It is worth mentioning that expressing yda-CA only weakly rescues the inflorescence architecture of *er erl1 erl2* and partially rescues the

pedicel length of the *er* single mutant, suggesting that other MKKKs might also function downstream of ERf during inflorescence development [18, 31].

The WUSCHEL-CLAVATA3 (WUS-CLV3) negative feedback loop is well known to regulate SAM homeostasis. WUS is expressed in the organizing center. It activates CLV3 expression in the SAM which in turn suppresses *WUS* expression [60]. In *er erl1 erl2*, the expression domain of *WUS* and *CLV3* is exaggerated [31, 61, 62]. Interestingly, while SAM development and *CLV3* expression are entirely blocked in the *wus* loss-of-function mutant, *CLV3* expression of the L1 layer and the SAM size are restored in the *wus er erl1 erl2* mutant. This result suggests that the *CLV3* expression of the L1 layer is regulated by ERf in a WUS-independent way [62]. How the YDA pathway regulates inflorescence architecture and the SAM size is still ambiguous. As *WUS* and *CLV3* expressions are affected in *er erl1 erl2*, whether the YDA pathway directly regulates *WUS* and *CLV3* expressions needs to be investigated.

2.4 The YDA signaling pathway during embryogenesis

The YDA cascade plays an indispensable role during embryogenesis in Arabidopsis (Figure 4). The zygote loses polarity and divides symmetrically when the function of the YDA-MKK4/5-MPK3/6 cascade is blocked. Then the basal daughter cell adopts an embryo-like development, leading to an embryo without a suspensor [19, 27, 63]. In contrast, in *yda-CA* the first division becomes more asymmetric and a filamentous embryo without an embryo proper is formed, resulting in embryonic lethality [63]. Thus, the YDA cascade promotes zygote polarity and suspensor differentiation while inhibiting proembryo identity. YDA regulates embryogenesis with a zygotic effect [63]. MKK4/5 and MPK3/6, however, modulate this process with a combination of zygotic effect and maternal effect [19].

SHORT SUSPENSOR (SSP) functions upstream of the YDA cascade to modulate embryogenesis with a paternal effect [64, 65]. It is presumed that functional *SSP* transcripts in the zygote are delivered from the sperm cell [64]. The embryonic phenotype of the *ssp* loss-of-function mutant is weaker than *yda*, suggesting there are other signal inputs for YDA activation. SSP (BSK12) belongs to the BSK family. Whether other BSKs function upstream of the embryonic YDA pathway was unreported. Embryo Surrounding Factor 1 (ESF1) is expressed in the endosperm and secreted to the embryo to affect suspensor

development. This small protein is suggested to function upstream of SSP [66]. The WRKY transcription factors are a large family in plants that recognize the W box motif of DNA. There are up to 100 WRKY proteins in Arabidopsis. The name WRKY is defined by the conserved N-terminal WRKYGQK sequence within a conserved 60 amino acid region called the WRKY domain [67]. During embryogenesis, *WRKY2* is expressed in the zygote, the basal daughter cell and the suspensor (Figure 5). The *wrky2* loss-of-function mutant exhibits reduced zygote elongation and more symmetric zygote division, recapitulating the *yda* phonotypes. WRKY2 can be phosphorylated by MPK3/6, which then enforces the expression of the *WUSCHEL-RELATED HOMEOBOX (WOX)* transcription factor *WOX8* (Figure 4) [68, 69].

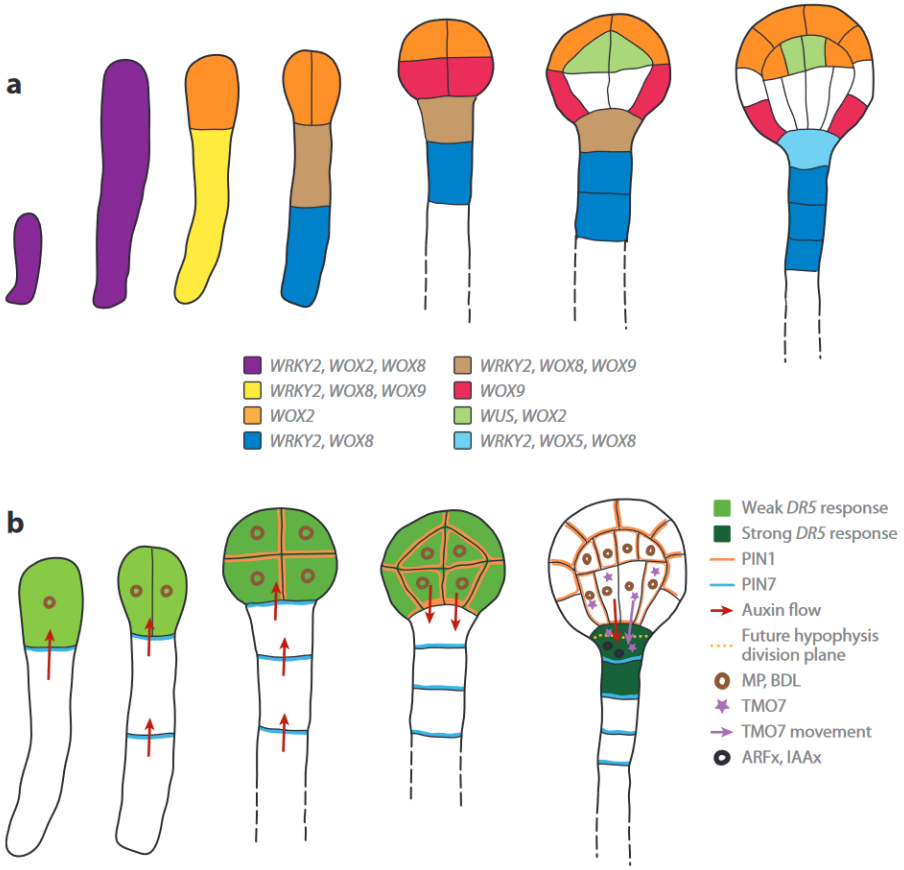

Figure 5. The apical-basal patterning and auxin response during early embryogenesis in Arabidopsis [70]. (a) Expression patterns of *WRKY2* and *WOX* genes. (b) Auxin signaling and hypophysis specification.

WOX8 has a similar expression pattern to *WRKY2* during embryogenesis (Figure 5). It regulates development of the whole embryo together with *WOX9* [71]. *WOX9* initially has

an overlapping expression pattern with *WOX8*. Then it is expressed in the lower tier of the proembryo and the upper tier of the suspensor (Figure 5). Interestingly, while the embryonic development is significantly deregulated in the *wox8 wox9* mutant, the initial zygote division seems unaffected. *WOX2* is expressed in the zygote, the apical daughter cell and the proembryo (Figure 5). Its expression is blocked in *wox8 wox9*. When *WOX2* driven by the *WOX9* promoter was introduced into *wox8 wox9*, a prominent zygote polarity defect was observed while the apical cell fate was restored, suggesting a coordination between WOX8/9 and WOX2 in controlling zygote polarity and cell fates [71]. Despite the obvious phenotype, the zygote polarity defect of *wrky2* is still weaker than that of *yda* and *mpk3 mpk6*, suggesting the direct involvement of other transcription factors downstream of the YDA cascade. In addition, *WOX8* expression is regulated by the HOMEODOMAIN GLABROUS (HDG) transcription factors HDG11/12 which show a maternal effect on zygote polarization (Figure 4)[69]. Whether HDG11/12 function downstream of MPK3/6, however, has not been deciphered by far. GROUNDED (GRD) is a RWP-RK transcription factor broadly expressed during early embryogenesis. Although Genetic evidence suggests that GRD functions downstream of YDA, GRD is not a direct target of MPK3/6 [72]. How GRD affects zygote polarity and whether it regulates the expression of *WOX* genes are remain ambiguous.

3 Auxin signal during early embryogenesis

Auxin signal plays a fundamental role in embryogenesis [70]. PIN-FORMED (PIN) proteins are auxin efflux carriers anchored in the plasma membrane. After zygote division, PIN7 is localized in the basal-cell plasma membrane adjacent to the apical cell for auxin transport (Figure 5). The apical cell shows an auxin response while the auxin response is compromised in the basal cell [73]. PIN1 is expressed in the proembryo and is responsible for the auxin transport to the putative hypophysis. From the 16/32-cell stage onward, PIN7 is reversely localized in suspensor cells, presumably mediating the auxin transport to the suspensor. Strong auxin response then takes place in the hypophysis, the precursor of root meristem. Later, it also occurs in cotyledon primordium tips and the developing vasculature [70, 73-75].

The auxin response is mediated by Aux/IAAs and Auxin Response Factors (ARFs). MONOPTEROS (MP)/ARF5 and its inhibitor BODENLOS (BDL)/IAA12 are expressed in the apical cell lineage. When the apical auxin response is suppressed either by directly stabilizing BDL to inhibit ARF activities or by knocking out PINs to retard auxin influx, the apical daughter cell divides horizontally. Then an abnormal embryo proper is formed, indicating importance of the auxin response in determining the apical cell identity and the proembryo formation [73, 74]. Recent data suggest that auxin transported from surrounding maternal tissue facilitates the auxin response in the apical cell [76]. Auxin signal also controls the ACD from the 8-cell embryo to the 16-cell embryo where the outer-layer protoderm is generated. In addition, auxin signal is also essential for hypophysis initiation and its ACD. The *mp* loss-of-function mutant and the stabilized *bdl* mutant fail to specify the hypophysis [74, 77], probably because of reduced PIN1 expression in the proembryo that impedes auxin transport to the hypophysis [78]. According to 3D imaging, auxin affects embryonic cell divisions and differentiations by overriding the “shortest wall” rule which is usually complied in symmetric cell divisions [79]. Furthermore, embryo-like proliferations are observed when the auxin response is suppressed in the suspensor, suggesting that the auxin response inhibits embryonic transition of suspensor cells [80].

In *yda-CA*, the apical daughter cell divides horizontally, reminiscent of the suppressed auxin response [63, 73]. However, it is still elusive whether auxin signal modulates zygote polarity and whether the embryonic auxin response is blocked in *yda-CA*.

4 Gene expression states during reproduction

In animals and plants, the egg cell is much larger than the sperm cell, thus providing more proteins and RNAs for initiation of embryogenesis. Transcriptional activation of zygote genome then conducts development. In animals, the maternal-to-zygotic transition (MZT) undergoes two steps: (i) the elimination of maternal transcripts and (ii) the activation of *de novo* zygotic transcription [81]. In flowering plants, conflicting descriptions about timing of the MZT and degree of parental contribution to early embryogenesis have been reported [82-88]. Recent evidences from manually isolated single cells illuminate that the progressive MZT in flowering plants is similar to the animal MZT [89, 90].

During the MZT and embryogenesis of flowering plants, many genes show parent-of-origin expression (binary imprinting) [89-91]. Paternally expressed genes (PEGs) and maternally expressed genes (MEGs) have been shown to play pivotal roles in nutrition transfer, endosperm proliferation, embryogenesis and the control of seed size [92]. For instance, the PEGs *BABY BOOM (BBM)* control the initiation of embryogenesis in rice [93]; the auxin biosynthesis enzymes YUCCA 10 (YUC10) and TRYPTOPHAN AMINOTRANSFERASE OF ARABIDOPSIS 1 (TAA1) are paternally imprinted for endosperm proliferation in Arabidopsis [94]. During Arabidopsis embryogenesis, parental genomes contribute equally to the transcriptomes of both the apical-cell lineage and the basal-cell lineage. Intriguingly, more PEGs and MEGs are detected in the suspensor than in the embryo proper [95].

Genomic imprinting is conferred mainly by DNA methylation and histone methylation. While some epigenetic regulators have been extensively studied such as the FIS-PRC2 complex, the DEMETER (DME) glycosylase and the DNA METHYLTRANSFERASE 1 (MET1), it is still largely unknown how genomic imprinting is established in plants [92]. Notably, some imprinting regulators are themselves imprinted, such as MEDEA (MEA) and FERTILISATION INDEPENDENT SEED 2 (FIS2) [96-98]. Besides binary imprinting, abundant genes have differential expression levels of parental alleles, which is called parental biased expression or differential imprinting.

5 Polarized protein localization during cell polarization

In many animal species, the sperm entry site can function as positional cue [99, 100]. Similarly, the sperm entry site in the brown alga *Fucus* can also function as positional cue in the absence of other polarizing cues [101]. In contrast to animals and algae, the egg cell of flowering plants is embedded in ovule tissues, and their zygote polarity is always set up along a putative apical-basal axis. The sperm entry side, therefore, seems not to affect zygote polarity. Consistently, in vitro experiments with rice gametes argue against the correlation between sperm entry side and zygote polarity [102].

Although the YDA pathway has been described for more than 10 years, it remains unclear how elongating zygote is polarized by this pathway. Similar to the Arabidopsis zygote, some cell types adopt a tip-grown manner, such as the root hair and the germinated pollen

[9, 10]. Many cell types also divide asymmetrically to generate daughter cells with different sizes, shapes or identities, such as the MMC mentioned above, the lateral root founder cell, root meristem cells, the hypophysis, the procambium and the monocot SMC [103]. Collective evidence suggests that polarized protein localization contributes prominently to cell polarity.

PAN1 is a LRR-RLK in maize lacking kinase activity. It is localized in the SMC at the conjunction sites to the GMC. Loss of PAN1 causes formation of abnormal subsidiary cells as a result of loss of SMC polarity [104]. Polarized localization of PAN1 requires PAN2 which is also a LRR-RLK and has a similar localization to PAN1 [105]. In addition, the polarized accumulation of PAN receptors is regulated by the SCAR/WAVE complex [106]. It is suggested that ligands secreted from the GMC may activate PAN receptors in the SMC. GOLVEN 6 (GLV6) and GLV10 are CLAVATA3/Embryo Surrounding Region-Related (CLE)-like peptides regulating lateral root initiation in Arabidopsis. After the first ACD of lateral root founder cells, GLV6/10 peptides inhibit a second ACD of flanking cells through RGF1 INSENSITIVE (RGI) receptors and MPK6. In addition, the overexpression of *GLV6* results in a symmetric division of pericycle cells, suggesting that the GLV gradient is important for the first ACD [107]. SOSEKI proteins are ancient polar proteins across the plant kingdom, and their polar accumulation sheds light on global polarity cues in Arabidopsis [108, 109].

Rho of Plants (ROP) are plant-specific small G proteins that switch between an inactive GDP-binding version and an active GTP-binding version [110, 111]. In maize, ROP2/9 are required for normal subsidiary cell formation. ROP2/9 show similar localization to PAN1 and their polarized accumulation necessitates PAN1 [112]. In Arabidopsis, ROPs show polarized accumulation in the formation side of future root hairs, and in the tips of both growing root hairs and elongating pollen tubes. They control cell elongation through interacting with Receptor-like Protein Kinase 2 (RPK2) in pollen tubes or with FERONIA (FER) in root hairs [110, 111]. In addition, ROP2 and ROP6 are polarly localized at pavement cell plasma membrane to modulate pavement cell interdigitation [111]. During root development, ROP3 regulates the polarized localization of PIN1 and PIN3 but not PIN2 [113]. Furthermore, ROP3 also modulates zygote polarity and hypophysis development [113]. Arabidopsis zygote also adopts a tip-grown manner, resembling the root hair and the

pollen tube. Whether ROP3 is polarly localized in the tip of the elongating zygote has not been unfolded yet. Since ROP3 affects PIN localization, it is tempting to investigate whether the auxin response also affects zygote polarity.

During stomata development, BASL is localized in the nucleus and on the edge distal to the putative division plane in the MMC. BASL interacts with YDA and polarizes its localization to the same edge. After the activation of the YDA cascade, MPK6 phosphorylates BASL, which is important for the polarized localization of BASL. Thus, a positive feedback loop is formed to affect SPCH abundance in the two daughter cells of the MMC, generating a SLGC and a meristemoid [153]. Furthermore, BASL is required for the polarized localization of POLAR in stomatal cell lineages which serves as a scaffold for the polarization of BIN2 and ATSK12 [154, 155].

6 The HAESA family receptors

Plant LRR-RKs are divided into 15 subfamilies based on the kinase domain phylogeny. LRR-RK XI subfamily contains 27 members, including the HAESA subgroup that consists of 8 proteins: HAESA (HAE), HAESA-like 1 (HSL1), HSL2, HSL3, Receptor-like kinase 7 (RLK7), HAIKU2 (IKU2), C-TERMINALLY ENCODED PEPTIDE RECEPTOR 1 (CEPR1) and CEPR2 (Figure 6) [29, 114]. According to the phylogeny of LRR-RK XI in vascular plants and bryophytes, HAE and IKU2 are likely novel genes resulted from gene duplication events in the eudicot lineage [115].

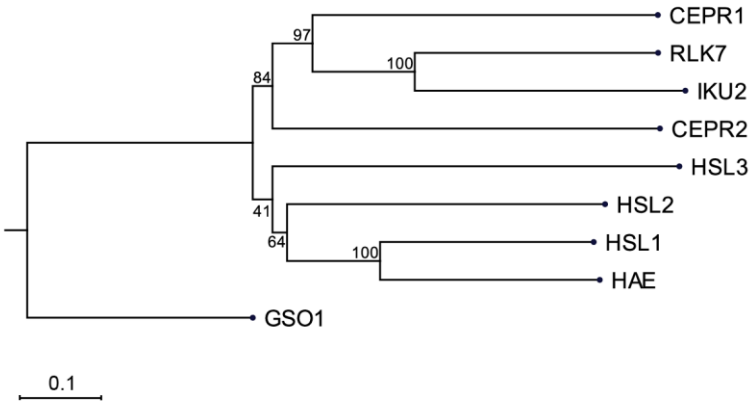

Figure 6. The phylogeny of the HAESA subgroup of the LRR-RK XI subfamily in Arabidopsis.

Based on the protein sequence, the tree is constructed using the Neighboring Joining method with 1000 bootstrap replicates. The protein distance measure method is Jukes-Cantor. GASSHO1 (GSO1), another

LRR-RK XI receptor, is used as the outgroup. Bootstrap values are shown as percentage at branch points. Scale bar represents 0.1 nucleotide substitutions per site.

HAE/HSL2 are expressed in the abscission zone and the lateral root. By perceiving IDA, HAE/HSL2 function redundantly to regulate floral organ abscission and lateral root emergence which also involve MKK4/5 and MPK3/6 [45, 116, 117]. HSL1 recognizes CLE9/10 to mediate stomata development [46]. HSL3 represses stomatal closure through mediating the H_2O_2 level in guard cells [118]. IKU2 is expressed in early endosperms and regulates endosperm cellularization and seed size. Interestingly, *iku2* loss-of-function mutants also show slightly delayed embryogenesis [119]. RLK7 is expressed in vegetative tissues, in the micropylar region of the ovule, and in embryos from the globular stage onward. It regulates seed germination speed and the tolerance to oxidative stress [120]. In addition, it enhances immune response by perceiving PAMP-Induced Peptide 1 (PIP1) [120, 121]. Furthermore, a recent research indicates RLK7 binds PIP-Like 3 (PIPL3) to regulate the spacing of lateral root funder cells by suppressing the new funder cell initiation near a specified one [122]. CEPR1/2 control lateral root development upon interacting with the C-terminally encoded peptides (CEPs) [123].

Aim of the thesis

While the YDA signaling pathway in stomata patterning has been explicitly investigated, the embryonic YDA signaling pathway is still poorly understood. Dissecting how the YDA signaling pathway establishes zygote polarity is an interesting topic. Many important components of this pathway are still missing and whether the YDA signaling itself is polarized temporally or spatially in the zygote has not been reported. This thesis aims to enhance our understanding on the embryonic YDA pathway by focusing on the following aims:

1. Although the *ssp* loss-of-function mutant shows obvious defects in zygote polarity and embryonic development, the embryo phenotype is not as severe as that of the *yda* loss-of-function mutant, suggesting that other signal inputs may also stimulate the embryonic YDA pathway. SSP belongs to the BSK family which consists of 12 members in Arabidopsis. Thus, our first aim was to investigate whether other BSKs also modulate the embryonic YDA pathway.

2. While EPF1/2 and ERf function upstream of YDA during stomata patterning, the upstream receptor signal of the embryonic YDA pathway remains unrevealed. my aim was to determine which receptors function upstream of YDA to regulate zygote polarity. In addition, I aimed to identify LRR-RKs that may activate the YDA cascade in other tissues.

3. In *yda-CA* transgenic lines, long filamentous embryos are formed, indicating that the YDA pathway inhibits embryonic identity. However, what identity these cells possess in these filaments has not been studied. The filamentous embryos are also observed when auxin response is compromised, possibly linking the YDA signal with auxin response. My third aim was to illuminate the altered cell identities upon YDA activation and the auxin response state in these cells.

4. The YDA signal is polarized in the MMC. However, whether it is also polarized in the zygote has not been unfolded. By checking the localization of key components in the ovule, my fourth aim was to investigate whether some components of the embryonic YDA pathway are polarly localized and to disentangle how their localization affects zygote polarity.

Chapter I

SSP is a robust signaling input of the embryonic YDA pathway

Results

1. BSK1/2 function upstream of the YDA cascade

BSK1 and BSK2 are close homologs of SSP (BSK12). Broadly expressed in plant tissues, BSK1/2 have been uncovered to regulate both developmental and immune processes [49-51]. We found that BSK1 and BSK2 function redundantly to mediate stomata patterning, inflorescence architecture and embryonic development [124]. The phenotype of clustered stomata in the *bsk1 bsk2* loss-of-function mutant can be rescued by expressing *yda-CA*, indicating that BSK1/2 function upstream of YDA. Notably, a significant zygote polarity defect was observed in the *bsk1 bsk2 ssp* triple mutant, almost mimicking the *yda* defect. These results reveal that BSK1/2 and SSP are pivotal regulators functioning upstream of YDA [124].

2. SSP is a constitutively active version of BSK1

Although SSP and BSK1/2 are homologous genes, the *ssp* single mutant already exhibits strong embryonic defects, implying that SSP and BSK1/2 may possess different protein properties. When expressed by the sperm cell-specific *MGH3* promoter, BSK1 did not rescue the zygote polarity defect of *bsk1 bsk2 ssp* while SSP partially rescued the defect. Thus, the difference between BSK1 and SSP cannot be simply explained by different expression patterns. When expressed in protoplasts, SSP apparently affected the expression of target genes and increased the phosphorylation of MPK3/6. Similar results were observed for yda-CA but not for BSK1. These results suggest that SSP is a constitutively active version of BSK1.

3. The TPR domain of SSP confers the hyperactivity

The intramolecular interaction between the kinase domain and the Tetratricopeptide repeat (TPR) domain of OsBSK3 has been suggested to suppress OsBSK3 activity [125]. Different from BSK1, SSP has lost this interaction, making itself a constitutively active

form of BSK1. By swapping domains between SSP and BSK1, we further found that the TPR domain is responsible for the hyperactivity of SSP. SSP has four TPR motifs in its TPR domain. A close inspection revealed that the first and the second TPR motifs are necessary for SSP hyperactivity [124]. SSP has been shown to directly interact with YDA [65]. We further found that the TPR domains of SSP and BSK1 can bind with the kinase domain of YDA in a yeast-two hybrid experiment. Thus, it seems plausible that the loss of intramolecular binding in SSP facilitates the YDA activation.

Discussion

1. BSK1/2 and SSP have extremely different expression patterns

Although SSP is a constitutively active version of BSK1, their expression patterns are extremely different. *SSP* transcripts are only detected in the sperm cell and the zygote [64, 90]. *BSK1/2* are ubiquitously expressed during development. Notwithstanding, the *BSK1/2* transcriptional level in the sperm cell is very low according to experimental and transcriptomic data [64, 126-128]. When SSP is expressed by the CaMV 35S promoter (*$35S_{pro}$:SSP*), stomata development is entirely blocked, reminiscent of the *yda-CA* lines. Those transgenic seedlings are dwarfed and show lethality [64], demonstrating that increasing SSP dosage in other tissues is deleterious. In contrast, *$35S_{pro}$:BSK1* only rescues the *bsk1 bsk2* stomata defect to the wild-type level [124]. Thus, the specific temporal and spatial expression of *SSP* seems both advantageous and inalterable for Arabidopsis development. It would be intriguing to investigate the mechanism of the specific expression pattern of SSP in comparison with BSK1/2.

The functional SSP transcripts in the zygote is suggested to be inherited from the sperm cell [64]. However, recent evidence challenges this presumption. In the sperm cell, the repressive histone methylation marker H3K27me3 is generally erased. Instead, the positive histone methylation marker H3K4me3 is enriched in PEGs but not in MEGs. The transcriptionally primed state of the sperm chromatin probably accelerates the expression of PEGs after fertilization [129]. As the histone methylation state of SSP is similar to that of many PEGs, newly transcribed *SSP* mRNA from the paternal allele may also contribute to zygote polarity after plasmogamy [129]. If *SSP* is indeed a PEG, it is still extremely different from other PEGs since *SSP* transcripts cannot be detected any more after zygote

division [90]. A new question arises: how its transcription is shut down before the first asymmetric division.

2. The TPR domains of SSP and BSK1 interact with YDA

Previously, the 3D structure of the Arabidopsis BSK8 catalytic domain (kinase domain) was revealed. BSK8 harbors an unusual CFG motif within the ATP-binding region. It is considered a pseudokinase because its catalytic domain is unable to bind ATP analogues and shows no catalytic activity [48]. In rice, the interaction between the kinase domain and the TPR domain of OsBSK3 is able to suppress the binding of AtBSU1 to OsBSK3 kinase domain *in vitro*. OsBRI1 can phosphorylate OsBSK3 kinase domain, which blocks the intramolecular interaction of OsBSK3 [125]. The current model is that BRI1 directly phosphorylates BSK3 kinase domain, prohibiting the suppressive binding between BSK3 kinase domain and its TPR domain. Then the open conformation of BSK3 functions as a scaffold to recruit BSU1 through BSK3 kinase domain to provoke the BR signaling. Consistent with this model, we found that BSK1 activity is also suppressed by this intramolecular interaction. In contrast, this interaction has been lost in SSP and its hyperactivity necessitates its first two TPR motifs. However, rather than the kinase domains of SSP and BSK1, their TPR domains interact with YDA in our yeast-two hybrid experiment [124]. TPR domains are considered to serve as platforms for protein-protein interactions [130]. It is tempting to speculate that the kinase and TPR domains of BSKs may be involved in recruitment of different substrates in different contexts such as recruiting BSU1 and YDA. Intriguingly, BIN2, the substrate of BSU1, can directly phosphorylate and inhibit YDA [57]. How BSKs activate downstream targets might be more elusive than our current understanding.

Since the swapping of kinase domains between SSP and BSK1 did not alter their activity [124], it is pivotal to dissect the mechanism by which specific TPR motifs determine BSK activity. The 3D structures of both the TPR domains and the full-length proteins of SSP and BSK1 will enable a better understanding of the activity difference. Nevertheless, it remains to be elucidated whether the suppression of the intramolecular interaction of BSK is a prerequisite for binding and activation of substrates

Chapter II

Independent parental contributions initiate zygote polarization in *Arabidopsis thaliana*

Results

1. ERf regulates zygote polarity

As shown in Chapter I, BSK1/2 and SSP function upstream of the embryonic YDA pathway [124]. In other contexts, BSKs directly interact with LRR-RKs, such as FLS2 and BRI1 [49-51]. However, the receptor of the embryonic YDA pathway was still unknown. The YDA cascade functions downstream of ERf during stomata patterning, thus it is important to dissect whether ERf also regulates zygote polarity. First, I found ERf modulates zygote polarity and suspensor development with ER taking the main function [131]. The *er erl1* and *er erl2* phenotypes were weaker than *yda*. I was not able to directly check the embryos of the *er erl1 erl2* triple mutant because of its infertility [30, 31, 63]. In *YDA/yda* heterozygous mutants, a quarter of zygotes are extremly short and symmetrically divide, indicating that YDA regulates embryogenesis with a zygotic effect [63, 131]. Although the genotype segregation ratio of the offspring in the *ER/er erl1 erl2* plant followed the Mendelian law, the distribution of offspring zygote length was similar to that of wild type, suggesting a non-zygotic effect of ER on zygote polarity. By reciprocal crosses of *er erl1* or *er erl2* with wild type, I observed a maternal effect of ERf on zygote polarity and suspensor length.

2. ER and BSK1 show a sporophytic maternal effect on zygote polarization

Maternal effects can be divided into two cases: The phenotype of the zygote is determined (i) by the genotype of the female gamete (so called gametophytic maternal effect) or (ii) by the genotype of the female sporophyte (so called sporophytic maternal effect). In the case of ER, as the offspring genotypes of *ER/er erl1 erl2* follow the Mendelian law, the genotype of 50% female gametes should be *er erl1 erl2*. However, the distribution of zygote length did not show a 1:1 ratio in the *ER/er erl1 erl2* plant, excluding the possibility

of a gametophytic maternal effect for ER. Using similar experiments, I found that BSK1 is also under a sporophytic maternal control.

3. ERf directly functions in the zygote

We then investigate how sporophytic tissue-derived ER regulates embryogenesis. Using the *ER$_{pro}$:3xVenus-N7* promoter lines and *ER$_{pro}$:ER-YPet* rescued lines, I observed strong YFP signal in the integument. In contrast, I was not able to detect clear YFP signals in the egg cell and early zygotes. A similar result was observed in the RNA in-situ hybridization experiment. Nonetheless, according to published data, the ER mRNA is detected in the egg cell and early zygotes, albeit at weak levels [90]. Because the YDA signal does happen in the zygote and the *er erl2* zygote defect was rescued by introducing *yda-CA*, we believe that the ERf signal still directly functions in the zygote [131]. Considering that very low amounts of ER-YFP proteins were able to rescue the phenotype of clustered stomata in *er erl1 erl2*, we believe the ER protein level in the zygote is just too low to be detected with microscopy [131]. To further determine this possibility, I took advantage of the anti-GFP nanobody which has been used to specifically degrade GFP/YFP-containing proteins in mammalian cells, *Drosophila* and Arabidopsis [132-134]. In our case, the anti-GFP nanobody was introduced to an *ER$_{pro}$:ER-YPet er erl1 erl2* rescued line. When the *ER* promoter was used to drive NSlm-vhhGFP4, an extreme dwarf phenotype was observed, indicating that the nanobody can be used to degrade ER-YPet. Then I use the egg cell-specific *EGG CELL 1 (EC1)* promoter to strongly express this nanobody in the egg cell. An obvious zygote polarity defect was observed, which indicates that the ER undoubtedly functions in the zygote. Although YFP signal in the zygote was not observed in *ER$_{pro}$:3xVenus-N7* and *ER$_{pro}$:ER-Ypet er erl1 erl2*, distinguishable YFP signal was detected in the megaspore mother cell and the megaspore of these lines. This implies the functional ER mRNA or protein is inherited premeiotically from the megaspore mother cell. This hypothesis explains why ER directly regulates zygote polarity but with a sporophytic maternal effect.

4. SSP activates YDA independently of ERf

It has been shown that some factors of the embryonic YDA pathway, such as MKK4/5, MPK3/6 and HDG11/12, are partially or fully under the maternal control [19, 69]. Here we show ERf and BSK1/2 are also under the maternal control [131]. As these genes are conserved in flowering plants, a conserved maternal pathway and a *Brassicaceae*-specific paternal SSP input seems to function together to regulate early embryogenesis in Arabidopsis. As SSP is a constitutively active version of BSK1 [124], we wonder whether SSP can activate YDA in an ERf-independent way. The *er erl1 erl2* triple mutant is infertile, so we cannot directly test this hypothesis in the zygote. Since the YDA pathway also suppresses stomata formation, I checked whether ectopic expression of *SSP* could inhibit stomata formation in the absence of ERf. When introduced into *er erl1 erl2*, $35S_{pro}$*:SSP* fully blocked stomata formation while $35S_{pro}$*:BSK1* did not rescue the phenotype of clustered stomata at all. This result indicates that SSP can function in an ERf-independent manner. *ssp* can further enhance the zygote polarity defect when crossed as pollen donor with *er erl1*, *er erl2* and *bsk1 bsk2*, indicating that *ssp* is additive to these mutants. Furthermore, adding a single copy of *SSP* is able to partially rescue the zygote defect of *er erl2*. Taken together, these results suggest independent parental contributions converge on the YDA activation to establish zygote polarity.

Discussion

1. The origin of functional zygotic ER

In this chapter, we demonstrate that ERf function upstream of YDA to modulate zygote polarity and early embryogenesis. ER and BSK1 show a sporophytic maternal effect. Sporophytic maternal effects on embryogenesis and endosperm development have been reported for more than two decades [135-137]. Recently, *Robert et al.* showed that auxin synthesized in the micropolar region of the integument can be transported into the zygote to affect early embryogenesis, indicating that the sporophytic maternal auxin supplement is indispensable for normal embryogenesis [76]. Given that the integument development of *er erl* mutants is abnormal, the easiest explanation for the *er erl* maternal influence might be that the defective integument of *er erl* indirectly affects zygote development. For example, the delivery of maternal molecules from the integument might be retarded in *er*

erl mutants. This correlation seems plausible as the ovule size and the zygote polarity in *ER/er erl1 erl2* plant are both normal. This correlation is further reinforced by a strong ovule defect observed in *bsk1 bsk2* (unpublished data, not shown) as BSK1 also shows a sporophytic maternal effect. However, when *ER-YPet* is specifically expressed in the *er erl1* integument using the *SEEDSTICK (STK)* promoter [138], the integument defect was rescued while the zygote polarity was not restored (Figure 6, additional experiment not included in this publication), indicating that the zygote defect of *er erl1* is not caused indirectly by its ovule defect.

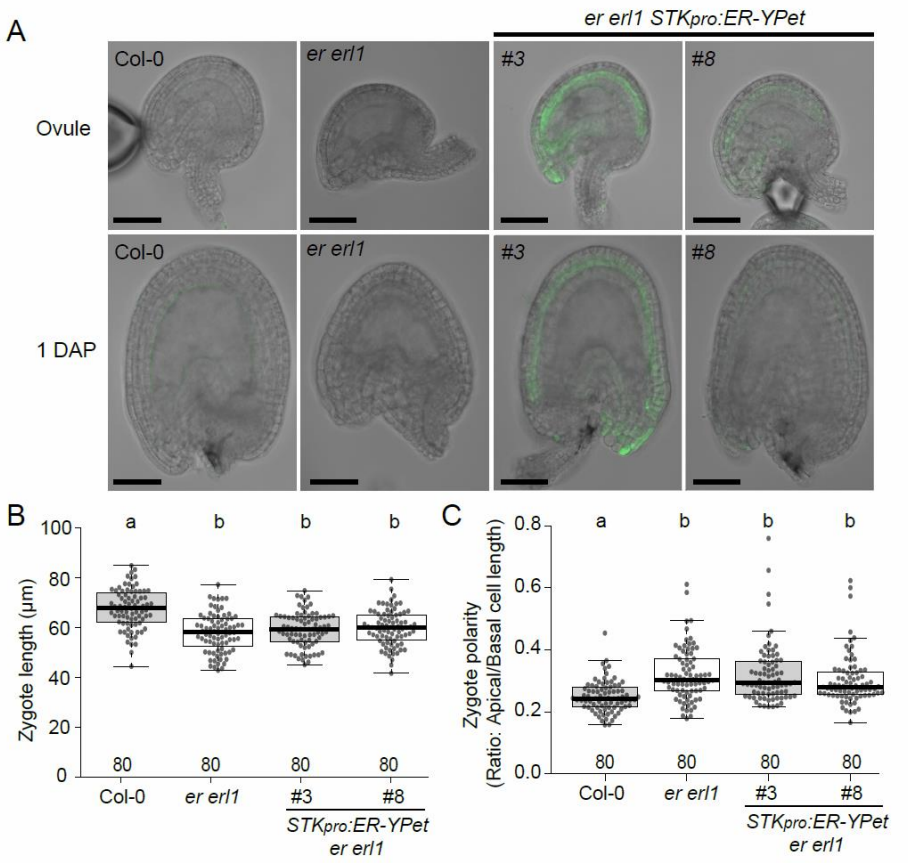

Figure 6. Expressing *ER-YPet* with the *STK* promoter does not rescue the zygote defect of *er erl1.*

(A) The ovule shapes of *er erl1* and *er erl1 STK$_{pro}$:ER-YPet* lines before and after fertilization. 1DAP: 1 day after pollination. These images are merged images of the bright field image and the confocal image detecting YFP signals. The scale bars represent 50 µm in all panels. (B-C) The zygote length (B) and the ratio of apical/basal cell length (C) of Col-0, *er erl1*, and *er erl1 STK$_{pro}$:ER-YPet* lines. Letters above boxes refer to individual groups in a one-way ANOVA with a post hoc Tukey test ($p < 0.05$).

Combining the *yda-CA* rescue experiment, the anti-GFP nanobody experiment, the *ER* expression pattern and the available transcriptomic data together, we presume that the

functional ER mRNA or protein in the zygote is inherited from the megaspore mother cell. Although a zygotic effect is not observed for ER and BSK1, it does not mean that the zygotic *ER* gene and *BSK1* gene are not active during this stage. In fact, biallelic transcripts of *ER* and *BSK1* are detected in the zygotes of reciprocal crosses between Col-0 and Ler [90]. These paternal transcripts are unlikely inherited from the sperm cell because both the transcriptional levels of *ER* and *BSK1* are very low in the sperm cell [127]. ER and BSK1 need to be first delivered to plasma membrane for their function. As zygote polarization happens in a short period of time, the newly translated ER and BSK1 proteins of the zygote genome might be too late to function in the zygote.

Through the reciprocal crosses between Col-0 and Ler, the recent research shows that zygote length and suspensor length are determined by the maternal ecotype [95]. The authors presumed that these developments are mainly modulated by MEGs [95]. Since Ler (Landsberg *erecta*) is an *er* mutant, their observation is in agreement with our results that ER regulates these developments with a maternal effect [131]. However, biallelic *ER* transcripts are detected both in the zygote and the early suspensor, demonstrating that *ER* is not a maternal imprinting gene [95]. Our results suggest that the functional ER component in the zygote is probably inherited from the megaspore mother cell. In addition, we show that ER affects suspensor development also with a sporophytic maternal effect. Because the basal daughter cell generates the suspensor, the zygote polarity defect should successively lead to the suspensor defect.

2.The possible ligand for the embryonic YDA pathway

During stomata patterning and SAM development, EPFs/EPFLs directly bind and regulate the ERf activity [35, 39, 40, 139]. However, *EPFs/EPFLs* transcripts are barely detected in the egg cell and early zygotes [90]. It is tempting to check whether *EPFs/EPFLs* are expressed in the endosperm or the surrounding mother tissue. It is worth mentioning that some secreted small proteins and peptides have been shown to affect embryogenesis. CLE8 regulates both embryo development and endosperm proliferation [140]. It was shown to be expressed in the endosperm and early embryos using RNA in-situ hybridization and promoter activity detection [140]. Contradictorily, *CLE8* transcripts are not detected in the egg cell, the zygote, the 1-cell embryo and the 32-cell embryo in more elaborate

transcriptomic data [90]. This expression pattern implies CLE8 non-cell-autonomously affects the whole embryogenesis, rather than just affect suspensor development as suggested by *Fiume et al.* [140]. CLE8 might be secreted from the endosperm to influence embryogenesis. In contrast, *CLE9/10* transcripts are detected in the egg cell and early zygotes [90]. CLE9/10 bind with HSL1 and SERKs to regulate stomata patterning, probably functioning upstream of YDA [46]. Thus, they might also regulate the YDA activity during embryogenesis. *CLE19* is expressed in both the embryo and the endosperm, and regulates cotyledon development in a non-cell-autonomous manner [141]. However, as the size of IDA and CLE peptides for the HAESA family is much smaller than EPFs/EPFLs, it seems unlikely that these small peptides serve as ligands for zygotic ERf proteins. Instead, they may activate the HAESA family receptors during early embryogenesis with either cell-autonomous or non-cell-autonomous manners. The endosperm ESF1 is shown to affect suspensor development [66]. It would be interesting to investigate whether it also influences zygote polarity.

If the sporophytic maternal control of ER and BSK1 is conserved in the zygotes of flowering plants, this manner may also apply to the ligand for ERf. The ligand, therefore, is more likely to be secreted from sporophytic mother tissues than from the endosperm or the zygote. It is intriguing to inspect whether *EPFs/EPFLs* are expressed in the integument surrounding the zygote.

3. Whether SERKs and TMM are involved in early embryogenesis

During stomata patterning, SERKs and TMM are co-receptors of ERf [32, 39, 43]. SERKs also serve as co-receptors of many other LRR-RKs [44-47]. Recently, SERKs are shown to regulate the division pattern of embryonic vascular precursors [142]. Resembling the reported role of ERf [33], SERKs also affect late embryogenesis [142]. As the transcripts of *SERKs* and *TMM* are detected in early zygotes [90], it is extremely tempting to check their roles in establishing zygote polarity. Because the *serk1 serk2* double mutant is male sterile due to defects in tapetum specification [143], we are unable to directly check the embryo of the *serk1/2/3/4* quadruple mutant. Instead, we checked the suspensor length of the F1 embryos generated from the crossing between *serk1/2/3/4* (female) and *serk1/2$^{+/-}$/3/4* (male). Using this crossing direction, we can also detect parental effects if

existing. However, the suspensor development in these F1 embryos is normal (data not shown). The easiest explanation is that SERKs are not involved in early embryogenesis. Alternatively, SERK5 may still compensate the loss of other SERKs during early embryogenesis although it is previously considered as a pseudo-receptor [44, 47, 144]. Whether zygote polarity is retarded when TMM or all 5 SERKs are knocked out needs further inspection.

4. SSP functions independently of ERf

We showed that SSP can in principle function independently of ERf. We are not able to directly check this scenario in the zygote because the *er erl1 erl2* plant produces no ovules. Thus, we turn into the epidermal system. Similar to *yda-CA*, ectopically expressed SSP influences stomata patterning in an ERf-independent manner. We propose in Chapter I that SSP constitutively adopts an active conformation. These results together suggest that SSP acts as an ERf-independent strong input for the YDA activation. In the beginning, we wonder whether zygote polarization is fully blocked if all ERf proteins are erased. As development of the ovule is entirely hindered in the *er erl1 erl2* triple mutant [30, 31], we are unable to directly address this question. We presume that zygote polarity will not be entirely lost if all ERf proteins are removed because SSP functions independently of ERf.

Does the ERf-independent manner indicate that the YDA activation can be receptor-independent? As BSKs are considered as pseudokinase, it is unlikely that BSKs directly phosphorylate YDA. It is also unknown how yda-CA becomes constitutively active. Detecting the interaction among ERf, SSP/BSK1 and YDA/yda-CA will facilitate our understanding on SSP hyperactivity and YDA activation.

5. The conflict of different parental interests

When we carefully look at the embryonic YDA pathway, many components show maternal effect, containing ERf, BSK1/2, MKK4/5, MPK6 and HDG11/12 [19, 69, 131]. As these elements are evolutionally conserved in flowering plants, there seems to be a conserved pathway under the maternal control to regulate early embryogenesis. Despite the probably conserved maternal control, SSP, a strong paternal input to the YDA activation,

functions independently of the maternal ERf signal input [64, 124, 131]. This is reminiscent of the "parental conflict model" proposed by Haig and Westoby to explain the evolution of imprinting genes [145]. According to this model, parental imprinting genes are evolved because of conflicting interests of parents: The interest of the mother is the equal growth of all its progeny whereas the competing fathers want their own progeny to be preferentially nourished at the expense of other progeny [91, 146]. Recently, *Picard er al.* showed that the imprinting of Arabidopsis PEGs is strongest in the chalazal endosperm compared to other endosperm regions. The chalazal endosperm is the region for nutrition uptake to the endosperm, supporting the parental conflict theory [147].

This theory fits our results for three reasons: (i) the most obvious influence of the independent parental inputs is on development of the suspensor which connects the embryo with the mother tissue for nutrient delivery; (ii) SSP functions in an ERf-independent manner which overcomes the maternal control of YDA activation. However, as MKK4/5 and MPK6 are partially under the maternal control, SSP in fact cannot entirely override the maternal influence, resembling the tug-of-war. Nonetheless, a strong transient SSP boost just in the beginning may have been beneficial enough for these progeny to defeat other progeny of the same mother; (iii) the function of ER and BSK1 in early embryos is under a sporophytic maternal control. The effect of imprinting genes belongs to the gametophytic control. However, from the maternal point of view, the sporophytic control seems to make more sense because it also avoids the competition between progeny even when the mother plant is heterogeneous for the controlling gene. The "parental conflict" is used in outcrossing species where the sperm and the egg cell are from different individuals. A pivotal issue we should not overlook is that *Arabidopsis thaliana* is a self-crossing species. The evolution of the paternal SSP input in *Arabidopsis thaliana* might be just a coincidence since having the SSP input is advantageous. However, *SSP* is a *Brassicaceae*-specific gene [124]. Many species in the family are outcrossing species, including the close-relative species of *Arabidopsis thaliana*: *Arabidopsis lyrata* and *Arabidopsis halleri*. Therefore, this parental SSP contribution of *Arabidopsis thaliana* may have evolved in its ancestral species. Deciphering whether the paternal effect of SSP is conserved in *Brassicaceae* or at least in *Arabidopsis* genus will facilitate the understanding of SSP evolution.

Chapter III

Screening for receptors functioning upstream of the YDA cascade

Background

LRR-RKs function together with SERKs to activate BSKs and a downstream MAPK signaling pathway in different contexts. Arabidopsis contains more than 200 LRR-RKs [29]. In comparison, it has 5 SERKs [148], 12 BSKs [124], 20 MAPKs, 10 MAPKKs and approximately 60 MAPKKKs [12, 15, 29, 124, 148, 149]. Some LRR-RKs have been revealed to share SERK co-receptors and some downstream BSKs, MAPKKs and MAPKs. Thus, the specificity of LRR-RK signals largely depends on the receptors themselves.

The extracellular LRR domains of LRR-RKs are quite diverse, and they bind to specific ligands or peptides. Recently, *Hohmann et al* showed that brassinolide (BL) could induce the HAE signaling when the BRI1 LRR was fused with HAESA kinase domain, suggesting that the kinase domain of LRR-RK determines the cytoplasmic signaling specificity [150]. BAK1-INTERACTING RECEPTOR-LIKE KINASE 3 (BIR3) is a LRR-receptor pseudokinase that can constitutively bind with both LRR-RKs and their SERK co-receptors through its extracellular domain in a ligand-independent manner. The BIR3 binding is suppressive as it does not activate receptor signals and blocks the interaction between LRR-RKs and SERKs. Once the corresponding ligands are present, LRR-RKs and SERKs are released from BIR3 for interaction [150-155].

Results

1. The BIR3 chimera enables a constitutive activation of SERK-dependent LRR-RK pathways

Combining (i) the constitutive binding between BIR3 and SERKs, and (ii) the cytoplasmic signaling specificity conferred by LRR-RK kinase domain, we designed an approach to constitutively activate SERK-dependent LRR-RK signals in collaboration with Prof. Dr. *Michael Hothorn* at the University of Geneva (Figure 6) [156].

We demonstrated that when the ectodomain and transmembrane domain of BIR3 were fused with the intercellular domain of BRI1, HAE, ER or SCHENGEN 3 (SGN3), related

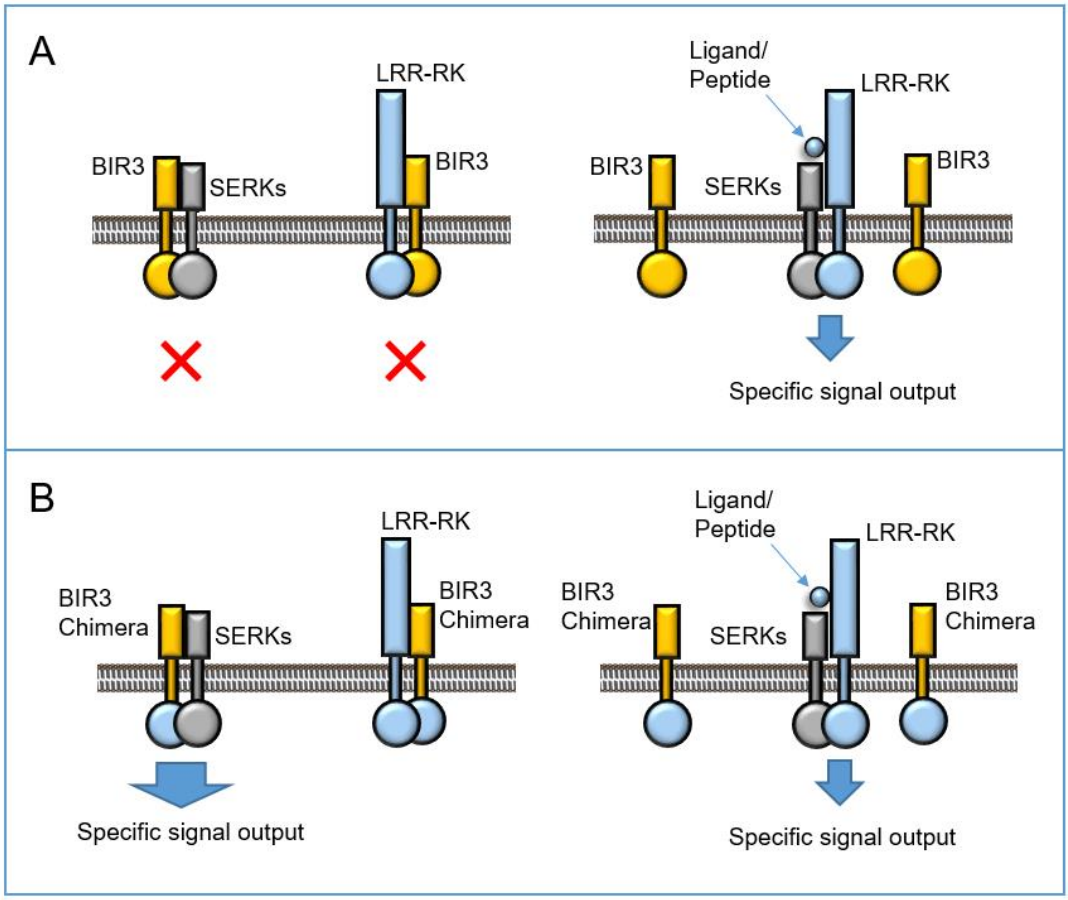

Figure 6. The mechanism of the constitutive activation of LRR-RK signals by the BIR3 chimera

(A) In wild type, BIR3 interacts constitutively with LRR-RKs or their SERK co-receptors through their extracellular domains to inhibit the interaction between LRR-RKs and SERKs when ligands do not exist. The intercellular domain of BIR3 does not have a kinase activity, thus it cannot activate receptors. When ligands exist, LRR-RKs and SERKs are released from BIR3 for binding with ligands. The interaction of their extracellular domains brings their kinase domains together to activate downstream targets. (B) In the BIR3 chimera, the BIR3 intercellular domain is replaced by the kinase domain of a LRR-RK. The extracellular interaction between the BIR3 chimera and SERKs brings the kinase domains together. Thus, the receptor signal is activated independently of the ligand binding. When the corresponding ligand exists, LRR-RK and SERKs might be released from the BIR3 chimera to transduce the ligand signal. Therefore, the receptor signaling will be always active with and without the ligand.

receptor signals were constitutively activated in a SERK-dependent manner [156]. Driven by the *MUTE* promoter that is active in the epidermal meristemoid, the *oBIR3-iER* chimera significantly inhibited stomata initiation. In contrast, when ERECTA kinase domain in this chimera was replaced by FLS2 kinase domain, stomata formation was not influenced, suggesting BIR3 chimeras exhibit signal specificity [156].

2. Chimeras of BIR3 and the HAESA family inhibited stomata formation when expressed with the *MUTE* promoter

Both *er erl1 erl2* and *yda* are extremely dwarfed with highly clustered stomata and aberrant inflorescence architectures [31]. However, vegetative defects of *yda* are still generally stronger than that of *er erl1 erl2*, arguing that other receptors may also regulate the YDA cascade. Recent research demonstrates that HSL1, another LRR-RK, functions together with SERKs to modulate stomata patterning by perceiving CLE9/10 peptides. It is speculated that the CLE9/10-HSL1 signaling and the EPF-ERf signaling converge on the YDA cascade to fine tune stomata spacing [46]. Given that some receptors in the HAESA family are related to seed development or the MAPK signaling pathway, it is possible that they are components in the YDA signaling pathway.

Since SERKs also serve as co-receptors of the HAESA family [46, 156], we then applied this "BIR3 chimera" strategy to the HAESA family receptors to investigate whether these receptors are competent to activate YDA or not. Because *MUTE$_{pro}$:oBIR3-iER* lines showed the activation of the stomatal YDA pathway, we used the *MUTE* promoter to drive our different chimeras and measured their stomatal phenotype to evaluate the ability to activate YDA. Considering that the *HAE$_{pro}$:oBIR3-iHAE* construct rescued the floral abscission defect of *hae hsl2* [156], we strongly believe that BIR chimeras of the HAESA family should suppress stomata initiation if they can activate YDA.

As described in our approach, extracellular, transmembrane and cytoplasmic domains of the HAESA family were predicted by Phobius (https://phobius.sbc.su.se/, Table 1) [156].

Protein	Signal peptide	Non cytoplasmic	Transmembrane	Cytoplasmic
BIR3	1 ~ 24 aa	25 ~ 218 aa	219 ~ 245 aa	246 ~ 601 aa
ER	1 ~ 24 aa	25 ~ 580 aa	581 ~ 601 aa	602 ~ 976 aa
FLS2	1 ~ 23 aa	25 ~ 806 aa	807 ~ 828 aa	602 ~ 1173 aa
HAE	1 ~ 22 aa	23 ~ 622 aa	623 ~ 648 aa	649 ~ 999 aa
HSL1	1 ~ 15 aa	16 ~ 618 aa	619 ~ 641 aa	642 ~ 996 aa
HSL2	1 ~ 28 aa	29 ~ 631 aa	632 ~ 653 aa	654 ~ 993 aa
HSL3	1 ~ 22 aa	23 ~ 627 aa	628 ~ 651 aa	652 ~ 1005 aa
RLK7	1 ~ 28 aa	29 ~ 608 aa	609 ~ 631 aa	632 ~ 977 aa
IKU2	1 ~ 19 aa	20 ~ 617 aa	618 ~ 635 aa	636 ~ 991 aa
CEPR1	1 ~ 24 aa	25 ~ 593 aa	594 ~ 613 aa	614 ~ 966 aa
CEPR2	1 ~ 31 aa	32 ~ 621 aa	622 ~ 641 aa	642 ~ 977 aa

Table 1. Domains of the HAESA family receptors predicted by Phobius.

Then the CDS of BIR3 ectodomain and transmembrane domain was combined with the CDS of the cytoplasmic region of the HAESA family together with a YPet YFP at the C terminal (Figure 7). The *MUTE* promoter was used to drive these chimeras. *MUTE$_{pro}$:oBIR3-iER* and *MUTE$_{pro}$:oBIR3-iFLS2* were used as a positive and negative control, respectively [156].

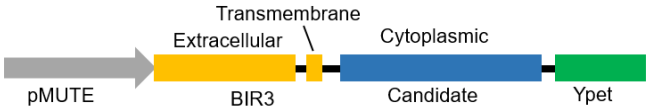

Figure 7. The construct of BIR3 chimeras.

These constructs were transformed into Col-0. The epidermal cell layer of the cotyledon abaxial side were imaged with propidium iodide (PI) staining in 5-day old T_2 transgenic seedlings. As described previously, stomata formation was prohibited in all 4 *oBIR3-iER* lines while all 12 *oBIR3-iFLS2* lines generated normal stomata patterning (Figure 8 and Table 2).

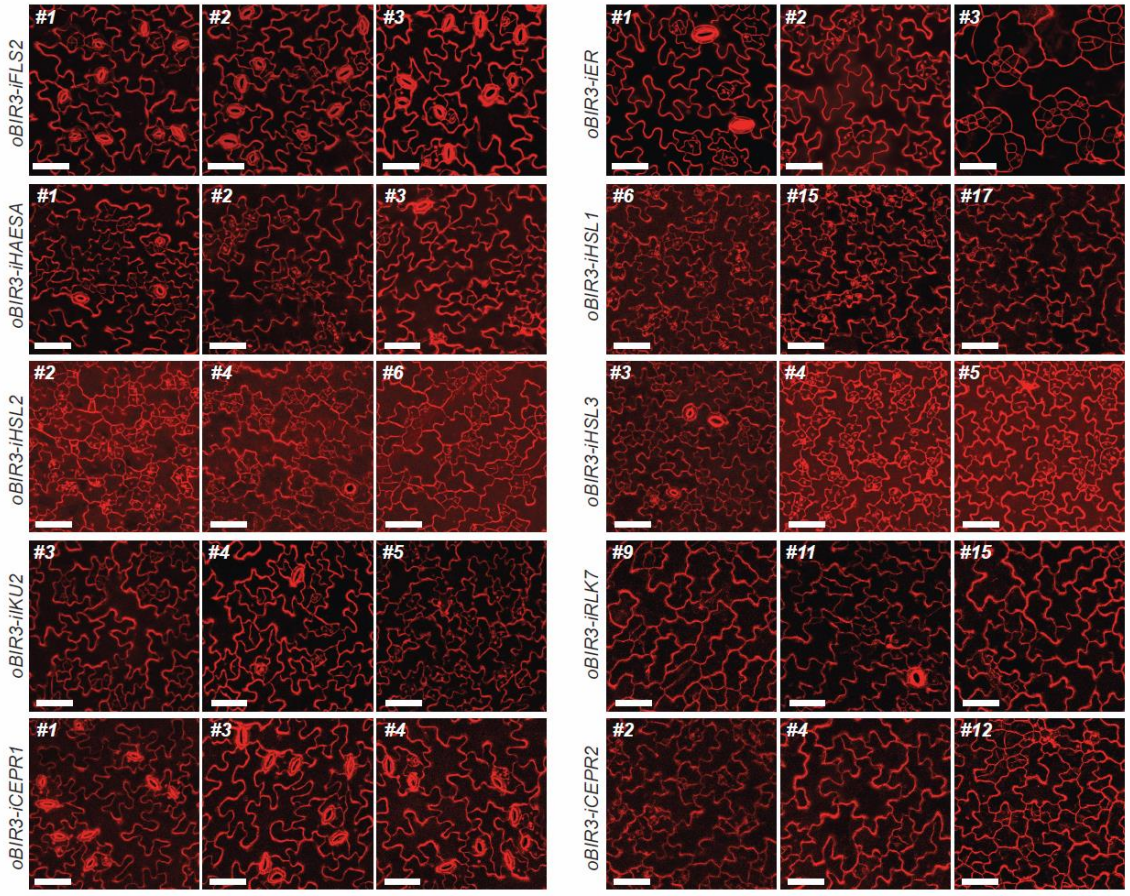

Figure 8. PI staining of the cotyledon epidermis of BIR3 chimera lines.

The epidermal cell layer of the cotyledon abaxial side were imaged with PI staining in 5-day old T_2 transgenic seedlings. Three individual lines were shown for each construct. Scale bars represent 50 μm in all panels.

For the HAESA family, seven of the eight chimera constructs suppressed stomata development to different extents (Figure 8 and Table 2). Interestingly, oBIR3-iCEPR1 appeared not to affect stomata patterning as only one transgenic line exhibits a weak stomata defect. These result suggests that most of the HAESA family receptors can potentially activate the YDA pathway.

Transgenic lines	Total lines	Lines with reduced stomata density
MUTE$_{pro}$:oBIR3-iFLS2	12	0
MUTE$_{pro}$:oBIR3-iER	4	4
MUTE$_{pro}$:oBIR3-iHAE	16	16
MUTE$_{pro}$:oBIR3-iHSL1	19	8
MUTE$_{pro}$:oBIR3-iHSL2	16	10
MUTE$_{pro}$:oBIR3-iHSL3	13	13
MUTE$_{pro}$:oBIR3-iIKU2	16	16
MUTE$_{pro}$:oBIR3-iRLK7	19	10
MUTE$_{pro}$:oBIR3-iCEPR1	15	1
MUTE$_{pro}$:oBIR3-iCEPR2	13	6

Table 2. Number of transgenic lines of each BIR3 chimera.

3. The constitutive activity of oBIR3-iHSL1 is YDA-dependent

HSL1 has been speculated to function upstream of the stomatal YDA pathway [46]. To determine whether these BIR3 chimeras really repressed stomata initiation through YDA, we crossed *oBIR3-iER #1* and *oBIR3-iHSL1 #15* with *yda-11* which is a new loss-of-function allele in Col-0 background [131]. The constitutive activations of *oBIR3-iER* and *oBIR3-iHSL1* were blocked in *yda-11*, indicating that the function of these oBIR3 chimeras is YDA-dependent (Figure 9).

Taken together, according to the stomatal phenotype of these BIR3 chimera lines, we deduce that the HAESA family receptors are potential upstream receptors of YDA. Similar to ERf, HSL1 also functions upstream of YDA to regulate stomata formation. Further research is required to investigate whether YDA really functions downstream of the other HAESA family receptors.

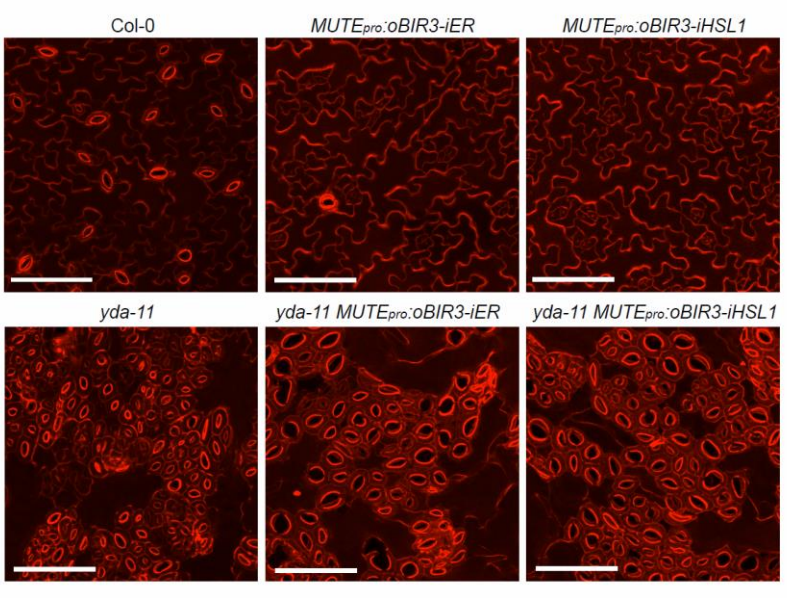

Figure 9. The constitutive activity of BIR3 chimeras is blocked in *yda-11*

MUTE$_{pro}$:oBIR3-iER and *MUTE$_{pro}$:oBIR3-iHSL1* were crossed with *yda-11* respectively. 10-day-old cotyledon epidermis were stained with PI and then imaged with confocal microscopy. Scare bars represent 100 μm in all panels.

Discussion

1. Whether yda-CA functions in a receptor-independent way

Based on the results from the specific expression of BIR3 chimeras in epidermal meristemoid, we conclude that most receptors of the HAESA family can potentially activate the YDA cascade. However, as these receptors are involved in different processes in different tissues, whether YDA really functions downstream of these receptors need explicit inspection. In principle, elaborate description of the phenotype of *yda* mutants should have revealed whether YDA is indeed an indispensable regulator in these tissues. However, the severe dwarfism and lethality features of *yda* impede further study [16, 63]. Another strategy to inspect the involvement of YDA is to introduce yda-CA in receptor mutants [16, 63], as exemplified by the rescue of defects of ERf loss-of-function mutants during stomata development, inflorescence development and embryogenesis [18, 31, 131]. HSL1 regulates stomata patterning [46], and our results indicate that the oBIR3-iHSL1 inhibition of stomata formation is YDA-dependent.

Although yda-CA can function in an ERf-independent way, its functionality might be still receptor-dependent. If HSL1 is another signal input for YDA, there is one question that

should be addressed immediately: whether HSL1 can activate yda-CA in the *er erl1 erl2* background. This question is not trivial because if HSL1 also activates YDA independently, the rescue of *er erl1 erl2* stomata defect by yda-CA cannot be simply explained by YDA functioning downstream of ERf. It is necessary to check whether yda-CA can still block stomata formation in an *er erl1 erl2 hsl1* quadruple mutant background. Furthermore, expressing *MUTE$_{pro}$:oBIR3-iHSL1* in the *er erl1 erl2* background may manifest whether HSL1 functions in an ERf-independent way. It is possible that ERf forms complexes with HSL1, considering that ERf can form homomers [43].

If yda-CA still functions in the receptor-dependent way, and if ERf are the only receptors functioning upstream of YDA during inflorescence development, this might explain why yda-CA cannot fully rescue the inflorescence architecture defect of *er erl1 erl2*. This hypothesis is important because yda-CA may have been introduced in other receptor mutants in unpublished trials. For example, HAESA/HSL2 have been shown to function upstream of MKK4/5 and MPK3/5 while the corresponding MKKK is still unknown so far [116, 117, 157]. If YDA is indeed involved but yda-CA functionality still relies on functional HAE/HSL2, the rescue of *hae hsl2* defect by yda-CA may never be achieved. In essence, a basic question is how yda-CA becomes a dominant-active version of YDA. The protein-protein interaction test among receptors, BSKs and YDA or yda-CA will strengthen our understanding on the functional mechanism of YDA. Then another question arises: whether SSP functions in a receptor-independent manner or just in the ERf-independent manner.

2. Possible receptors for the embryonic YDA pathway

If HSL1 and ERf receptors converge on the YDA cascade to modulate stomata patterning, whether the HAESA family receptors also regulate the zygotic YDA cascade needs to be further addressed. In our BIR3 chimera constructs, only *oBIR3-iCEPR1* lines showed normal stomata formation, implying that CEPR1 may not activate the YDA. Intriguingly, *CEPR1* is also the only HAESA family gene of which the transcripts is not detected at all in the egg cell and the zygote. Similar to *oBIR3-iER*, all *oBIR3-iHAE*, *oBIR3-iHSL3* and *oBIR3-iIKU2* lines showed obvious stomata defects, implying that HAE, HSL3 and IKU2 kinase domains possess higher competence to stimulate YDA compared to other HAESA

family receptors. Coincidentally, *HAE*, *HSL3* and *IKU2* also shows higher transcriptional levels in early zygotes in comparison with other HAESA family genes (Table 3) [90]. Combining our BIR3 chimera results with the published transcriptomic data, we consider HAESA, HSL3 and IKU2 potential upstream receptors of the zygotic YDA pathway. *HAE* and *IKU2* have been suggested to be novel genes in the eudicot lineage [115]. Whether HAESA, HSL3 and IKU2 regulate zygote polarity requires further inspection.

Gene	Egg cell	Zygote 14h	Zygote 24 h	1-cell
ER	70.87	25.50	8.08	5.19
HAE	1.31	6.75	0.00	1.56
HSL1	0.00	1.33	1.71	1.02
HSL2	0.70	2.22	0.20	1.36
HSL3	0.00	3.88	1.59	0.00
IKU2	22.79	12.72	0.06	1.15
RLK7	0.00	0.56	0.01	1.45
CEPR1	0.00	0.00	0.00	0.00
CEPR2	1.35	0.64	2.79	0.00

Table 3. Transcription of the *HAESA* family genes in the egg cell, zygotes and the 1-cell embryo. This table is generated from the published data [90]. Zygote 14h, zygote of 14h after pollination. Zygote 24h, zygote of 24h after pollination. 1-cell, 1-cell embryo. Numbers indicate reads per million matched reads (RPM). >3 RPMs are marked in red. The *ER* transcriptional level is also listed here.

Materials and Methods

The materials and methods are as described in *Hohmann et al*.[156]

Primer sequence

Primer	sequence	Function
HAE-KD-IF-F1	TTCTGGTGGTTCTTCAAGTGTAGAAAACTCAGAGC	Clone HAE kinase domain
HAE-KD-IF-R1	TTTAGACACCATCCCAACGCTGTTCAAGTCTTCCGTG	
HSL1-KD-IF-F1	TTCTGGTGGTTCTTCAAGTACAGGACTTTCAAGAAAGC	Clone HSL1 kinase domain
HSL1-KD-IF-R1	TTTAGACACCATCCCAGCTATACTTCCTTGGTCTGAG	
HSL2-KD-IF-F1	TTCTGGTGGTTCTTCAAAACCAAACCGTTATTCAAGAG	Clone HSL2 kinase domain
HSL2-KD-IF-R1	TTTAGACACCATCCCCTCTAGTGATTTCTTCTCTTTAAGC	
HSL3-KD-IF-F1	TTCTGGTGGTTCTTCAGGGACTACACAAGGAAACAAAG	Clone HSL3 kinase domain
HSL3-KD-IF-R1	TTTAGACACCATCCCTACAAAACCTAAATCTTCATCTTC	
IKU2-KD-IF-F1	TTCTGGTGGTTCTTCAAGATAAGACGAGATAAGTTG	Clone IKU2 kinase domain
IKU2-KD-IF-R1	TTTAGACACCATCCCTACAACTTTAGTAATCTCATC	

RLK7-KD-IF-F1	TTCTGGTGGTTCTTCAAGAAAACAGAGAAGAAGGAG	Clone RLK7 kinase domain
RLK7-KD-IF-R1	TTTAGACACCATCCCACTTATTTCTTTGACCTTGAC	
CEPR1-KD-IF-F1	TTCTGGTGGTTCTTCAGACAACGGATGAGTAAAAACAG	Clone CEPR1 kinase domain
CEPR1-KD-IF-R1	TTTAGACACCATCCCGAGTCTTGTTTGCGTGAGATG	
CEPR2-KD-IF-F1	TTCTGGTGGTTCTTCCGTTACAGAGTTGTGAAGATAC	Clone CEPR2 kinase domain
CEPR2-KD-IF-R1	TTTAGACACCATCCCTACTGTAATCTTTCCAGTTGTG	

Chapter IV

A filament-like embryo system to study the suspensor-embryo transition (*manuscript attached*)

Declaration of contributions

Author	Author position	Scientific ideas %	Data generation %	Analysis & interpretation %	Paper writing %
Kai Wang	1	50%	65%	80%	90%
Yingjing Miao	2	10%	10%	5%	0
Marina Ortega-Perez	3	5%	15%	5%	5%
Houming Chen	4	5%	5%	5%	5%
Martin Bayer	5	30%	5%	5%	0
Title of paper:		A filament-like embryo system to study the suspensor-embryo transition			
Status in publication process:		Ready for submission			

Results

By enhancing the YDA signal at early embryonic stages using *S4$_{pro}$:SSP-YFP*, we designed a filamentous-embryo system to study the suspensor-embryo transition. The filamentous embryos showed the identity of early basal cells, implying that they were in an undifferentiated state. Secondary embryos were initiated from the basal cells, and healthy twin embryos/seedlings were generated eventually. Auxin response was suppressed primarily in the apical cell cluster and shifted to the basal cells. We also observed the maximum auxin response in vertically divided basal cells. We presume that the vertical division of the basal cells results from an increased auxin response, which may directly contribute to the suspensor-embryo transition.

Discussion

In wild type, auxin transported through PIN proteins enables a strong auxin response in the hypophysis [70]. The strong auxin response in the basal cells of *S4$_{pro}$:SSP-YFP* probably reflects an altered auxin sink generated through auxin transport from neighboring cells. Future study is required to check the auxin concentration in different basal cells and whether the localization of PIN proteins has been changed. Controversial

evidences are reported to explain the role of auxin in the suspensor-embryo transition [80, 158-161]. Whether an increased auxin response is responsible for the vertical division and the embryonic transition of the basal cells remains to be addressed.

Which basal lineage ground cells will get a higher auxin response? Will that follow a certain role regarding the distance between each cell? Or is the position of a high auxin response a stochastic event? The *S4$_{pro}$:SSP-YFP* transgene seems to set up a positive feedback on its own expression, which makes the analysis complicated. Thus, activating the YDA signaling by a strong egg cell-specific promoter, if also creating filamentous embryos at the beginning, will make the analysis easier.

Chapter V

Polarized SSP localization affects zygote polarity

Results

1. ER and BSK1 are not polarly localized in epidermal cells

As YDA is polarly localized in the epidermal MMC by BASL, I first checked whether BASL is expressed in the zygote. According to recent transcriptomic data, BASL seems not to be expressed in the zygote [90, 162]. Then I investigate whether ER and BSK1, two upstream components of the stomatal YDA pathway, have polarized accumulation on the MMC plasma membrane or not. The *ER$_{pro}$:ER-YPet* [131] and *BSK1$_{pro}$:BSK1-YPet* constructs rescued the developmental defects of *er erl1 erl2* and *bsk1 bsk2*, respectively (Figure 10). Thus, these lines were used to detect the localizations of ER and BSK1 in the abaxial epidermal layer. The YFP signals were equally distributed in the putative MMC/SLGC and the small meristemoid (Figure 10), suggesting that ER and BSK1 are not polarly localized in these cells.

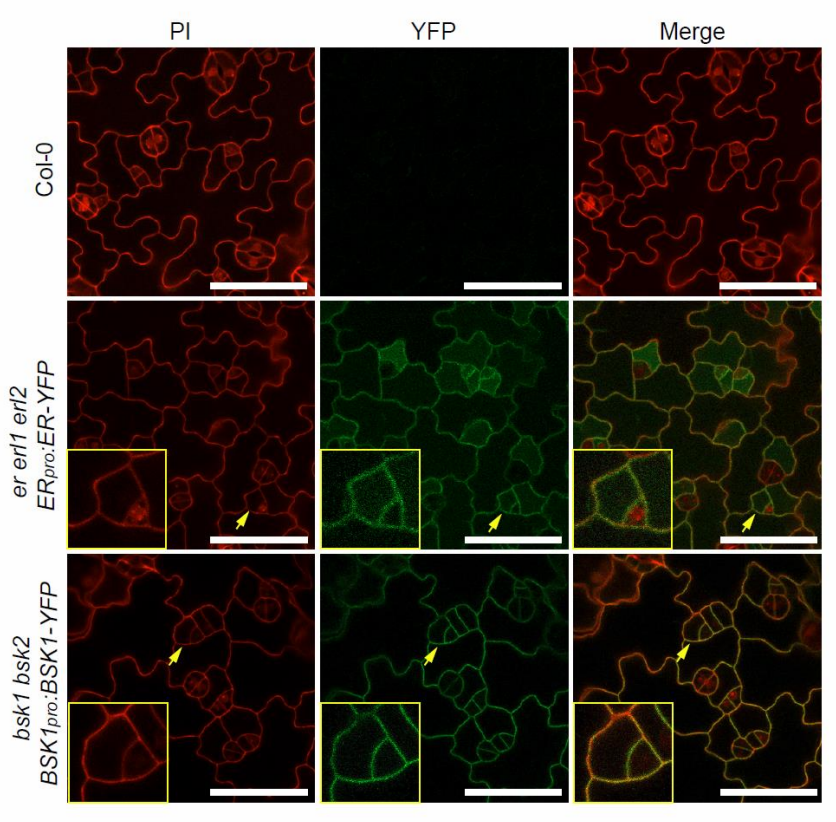

Figure 10. The localizations of ER and BSK1 in epidermal cells.

5-day-old cotyledons of *ER$_{pro}$:ER-YPet* and *BSK1$_{pro}$:BSK1-YFP* rescued lines were stained with PI. PI staining (red) and YFP signals (green) were imaged on cotyledon epidermis. The arrow indicates one putative MMC/SLGC and one meristemoid which are also enlarged in the yellow box. Scale bars represent 50 μm in all panels. In the enlarged image of BSK1-YPet, the strength of PI signal is not equal because of this staining is artificial. The PI staining strength is not corelated with the YFP signal strength, indicating that the equal destribution of YFP signals is intrinsic.

2. SSP is polarly localized in elongating zygotes

Then I investigated whether ER, BSK1 and SSP are polarly localized in the zygote or not. Unfortunately, the ER-YPet signal in the egg cell and the zygote of the *er erl1 erl2 ER$_{pro}$:ER-YPet* rescue line is below the detection limit of our confocal microscopy [131]. Therefore, ER was excluded from further detection. The *SSP$_{pro}$:SSP-YFP* line that rescued *ssp-2* defects was used to visualize SSP localization [64]. Consistent with previous observation and transcriptomic data, SSP-YFP signal was not detected in the egg cell and was only shortly detected after fertilization (Figure 11A-E). After zygote division, the YFP signal was difficult to detect, indicating that SSP-YFP proteins were only generated in the zygote [64, 90]. Notably, SSP-YFP proteins were mainly localized on the basal plasma membrane (BPM here afterwards) of the elongating zygotes (Figure 11D).

3. BSK1 is broadly expressed in the ovule

BSK1 is broadly expressed in plant tissues compared with *SSP* [124]. In agreement with this, we observed board expression of BSK1-YPet in the ovule (Figure 11L). Different from SSP-YFP, BSK-YPet signals were equally distributed surrounding elongating zygotes (Figure 11I). Moreover, BSK1-YPet aggregates were frequently observed after fertilization (Figure 11G-J). Before fertilization, strong YPet signal seemed to be localized at the central cell while only very weak YPet signal was detected at the egg cell (Figure 11F). As the egg cell/zygote plasma membrane and the central cell/endosperm plasma membrane are closely located, it is in general hard to discriminate both membranes. However, we did observe strong YPet signal on the endosperm plasma membrane after fertilization (Figure 11H). Extremely weak YPet signal was observed on embryo plasma membranes in the distal side to the endosperm. In contrast, the signal surrounding the whole embryos was much brighter (Figure 11J-K). These observations suggest the BSK1-YPet proteins surrounding the egg cell/zygote/embryo were mainly localized at the central

cell/endosperm. To further determine the localization of BSK1-YPet, gentle vacuum was performed on the fertilized ovule to separate the zygote and the endosperm, followed by the Renaissance 2200 (RS2200) staining to visualize cell wall [163]. Most membrane-localized BSK1-YPet proteins were not localized at the zygote, indicating that these BSK1-YPet proteins were mainly localized at the endosperm (Figure 11M-O). Thus, the even distribution of BSK1-YPet surrounding the zygote does not reflect how BSK1-YPet is localized on the zygote plasma membrane.

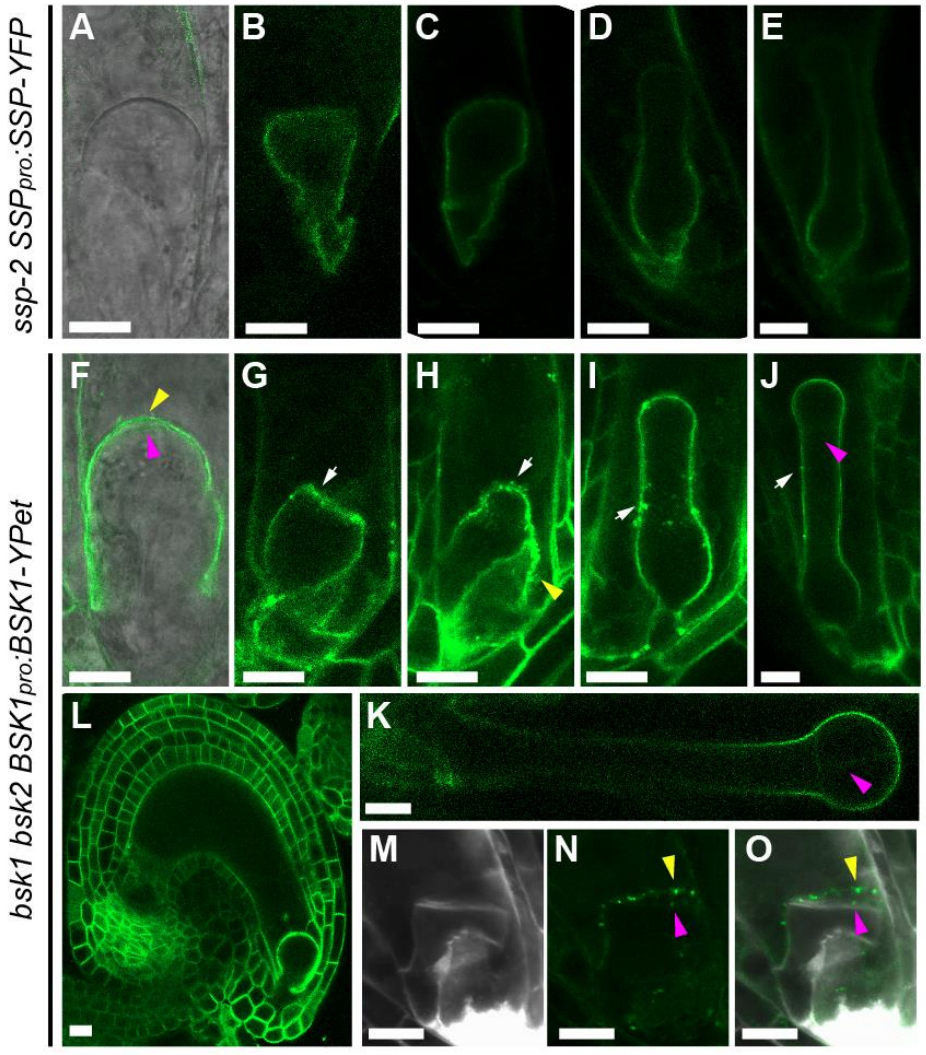

Figure 11. The localization of BSK1 and SSP in the egg cell, zygotes and embryos.

(A-E) SSP-YFP expression and localization in the egg cell (A), the shrunken zygote (B), the elongating zygotes (C and D) and the 1-cell embryo (E) of the *ssp-2 SSP$_{pro}$:SSP-YFP* rescued line. (F-O) BSK1-YPet expression and localization in the *bsk1 bsk2 BSK1$_{pro}$:BSK1-Ypet* rescued line. (F-K) BSK1-YPet expression and localization around the female gametophyte (F), the shrunken zygote (G), the elongating zygotes (H and I), the 1-cell embryo (J) and the 2-cell embryo (K). (L) BSK1-YPet expression pattern in the unfertilized

ovule. (M-O) BSK1-YPet localization on the zygote plasma membrane and the endosperm plasma membrane after RS2200 staining and gentle vacuum. (M) RS2200 staining of the zygote cell wall. (N) BSK1-YPet signal. (O) the merged image of M and N. Yellow arrowheads indicate YFP signals on the control cell plasma membrane (F) or the endosperm plasma membrane (H,N-O). White arrowheads in G-J indicate the BSK1-YFP aggregrates. Magenta arrowheads indicate YFP signals on the egg cell membrane (F) or the zygote plasma membrane (N-O) or the embryo plasma membrane (J-K). The scale bars represent 10 μm in all panels.

4. Polarized SSP localization is not promoter-dependent

Since SSP can function independently of ERf receptors and SSP directly interacts with YDA [65, 124, 131], the polarized localization of SSP-YFP suggests polarized YDA activity. Considering that SSP is only shortly transcribed in the early zygote [90], we wonder whether the polarized SSP-YFP localization is just a result of the specific

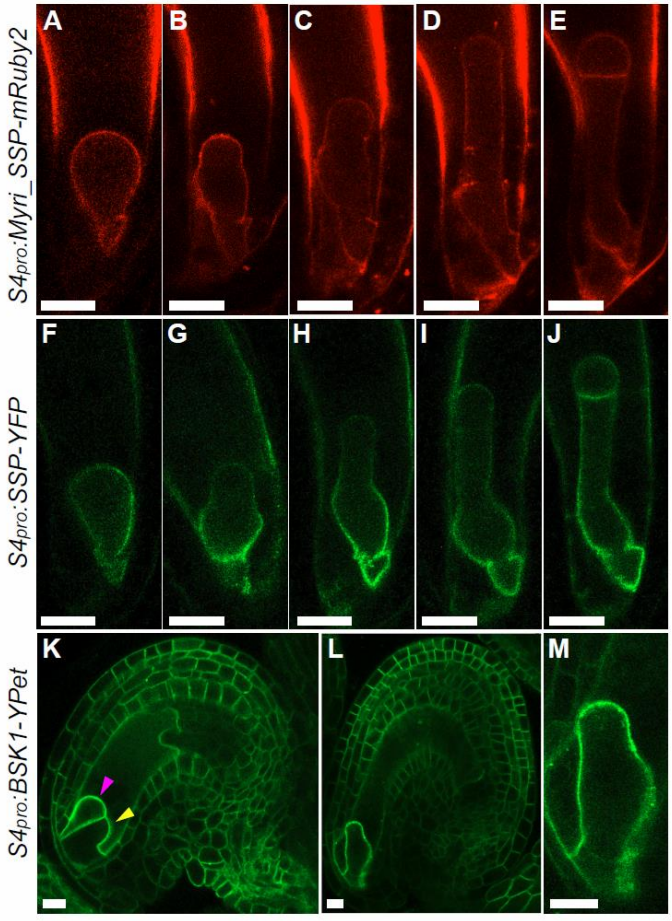

Figure 12. Localization of SSP-YFP and BSK1-YPet under the S4 promoter

(A-E) Localization of Myri_SSP-mRuby2 in the egg cell (A), zygotes (B-D) and the 1-cell embryo (E) of the *S4$_{pro}$:Myri_SSP-mRuby2* line. (F-J) Localization of SSP-YFP in the egg cell (F), zygotes (G-I) and the 1-cell embryo (J) of the *S4$_{pro}$:SSP-YFP* line. (K-M) Localization of BSK1-YPet in the unfertilized ovule (K) and the

fertilized ovule (L) of the *S4$_{pro}$:BSK1-YPet* line. (M) The enlarged image of L. The pink and the yellow arrowleads in K indicate the YPet signal in the egg cell plasma membrane and the centrol cell plasma membrane, respcetively. The scale bars represent 20 μm in all panels.

temporal expression. The *S4* promoter is specifically active during early embryonic phase [164]. We then used the *S4* promoter to prolong SSP-YFP expression in the zygote to check whether the zygotic localization of SSP-YFP is altered or not. As control, the *S4* promoter was used to drive the expression of a membrane-localized mRuby2 RFP fluorescent protein. The membrane-localized mRuby2 was made by fusing mRuby2 with SSP myristoylation motif which is necessary for SSP membrane-localization [64]. The Myri_SSP-mRuby2 proteins were equally localized on the membranes of the egg cell, zygotes and 1-cell embryo (Figure 12A-E), indicating that the *S4* promoter itself does not generate any polarity cue. However, while SSP-YFP proteins were evenly distributed on the egg cell membrane, they were still polarly localized on the BPM of elongating zygotes and the 1-cell embryo (Figure 12F-J). Taken together, these results suggest that the SSP polarized localization is determined by SSP cytoplasmic domain rather than its promoter or membrane-localization motif.

Then we used the *S4* promoter to check BSK1-YPet localization in the zygote. Unfortunately, BSK1-YPet was strongly expressed on the membranes of the egg cell and the central cell besides broad expression in the integument, making it again difficult to dissect the zygote localization of BSK1 (Figure 12K-M).

5. Depolarized SSP localization suppresses zygote polarity

To check whether the polarized SSP localization is necessary for zygote polarity, we tried to depolarize SSP localization. In maize, depolarizing ROP2 localization can be achieved by overexpression [112]. Hence, we over-expressed SSP-YFP in *ssp-2* mutant with the *EC1* promoter. Three representative lines were chosen according to their expression levels in the egg cell: moderate, strong and extremely strong. In the *#1* line with moderate expression, SSP-YFP proteins were still polarly localized on the BPM of the zygote, and the zygote elongation and polarity defects were rescued (Figure 13A-C). In the #7 line that showed strong SSP-YFP expression, although SSP-YFP proteins were still mainly localized on the zygote BPM, obvious YFP signal was also observed on the apical plasma

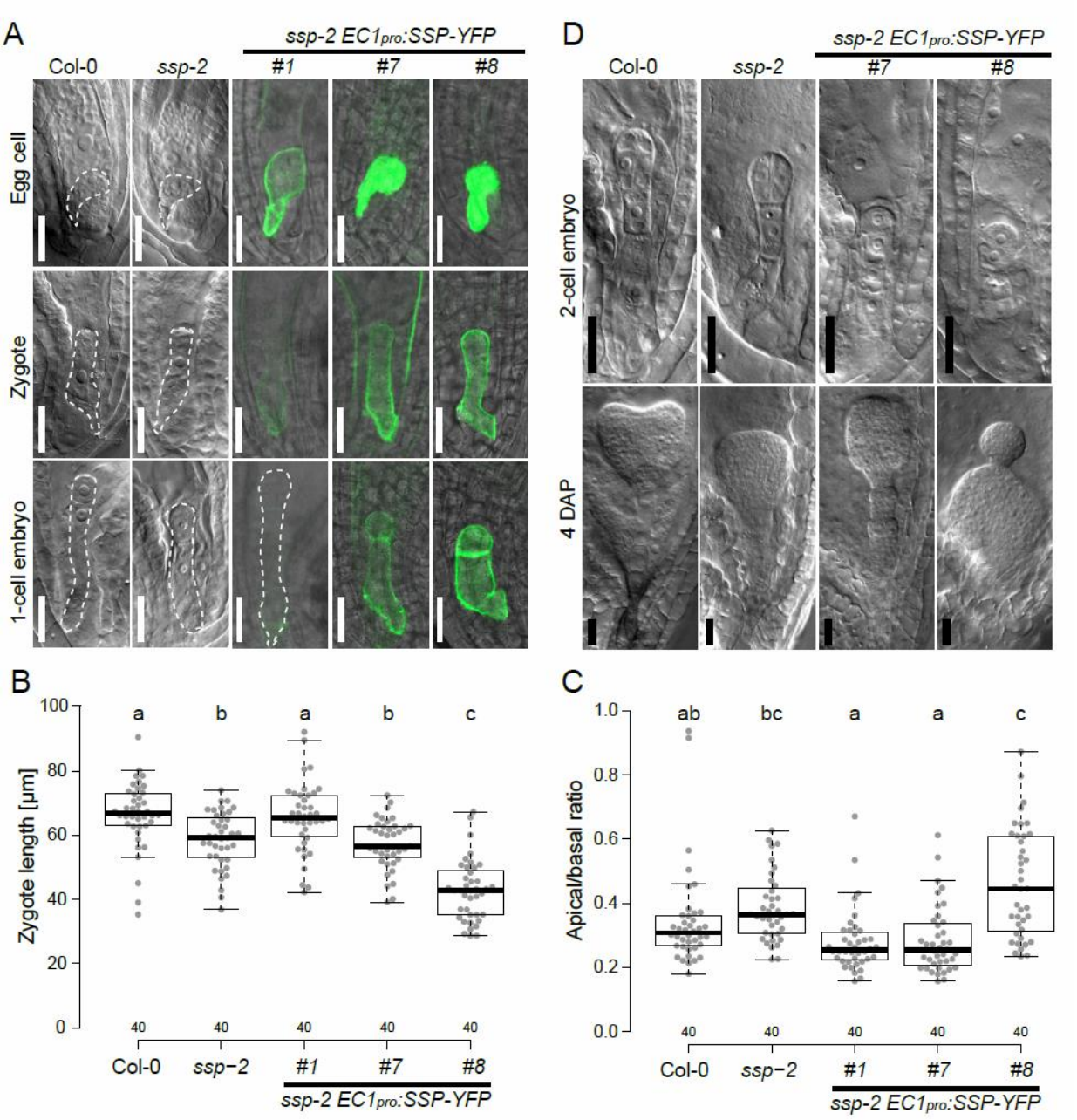

Figure 13. SSP-YFP localization and embryonic phenotypes of *ssp-2 EC1$_{pro}$:SSP-YFP* lines.
(A) SSP-YFP expression levels and localizations, and zygotic phenotypes of *ssp-2 EC1$_{pro}$:SSP-YFP* lines. Left two columns: Egg cells, zygotes and 1-cell embryos of Col-0 and *ssp-2* shown with DIC images and dashed lines. Right three columns: The merged images of confocal and bright field images in three *ssp-2 EC1$_{pro}$:SSP-YFP* lines showing different expression levels of SSP-YFP. The 1-cell embryo of the *#1* line is marked with dashed lines. (B-C) Zygote length (B) and apical/basal ratio (C) of Col-0, *ssp-2* and *ssp-2 EC1$_{pro}$:SSP-YFP* lines. Letters above boxes refer to individual groups in a one-way ANOVA with a post hoc Tukey test ($p < 0.05$). (D) Phenotypes of *ssp-2 EC1$_{pro}$:SSP-YFP #7* and *#8* lines at the 2-cell stage and at 4 days after pollination. DAP, days after pollination. The scale bars represent 20 µm in all panels.

membrane (APM here afterwards). In contrast to the *#1* line, the zygote defect was not rescued in *#7*. The *#8* line showed extremely strong expression of SSP-YFP. In contrast to *#1* and *#7*, the localization of SSP-YFP proteins was not polarized in #8 zygotes. Accordingly, the zygote defect was even stronger than that of *ssp-2*. Strong expression may block SSP-YFP protein function, causing loss-of-function phenotypes. However, frequent horizontal division of the apical daughter cell, and twin embryos were observed in *#7* and *#8* lines (Figure 14 and Table 4).

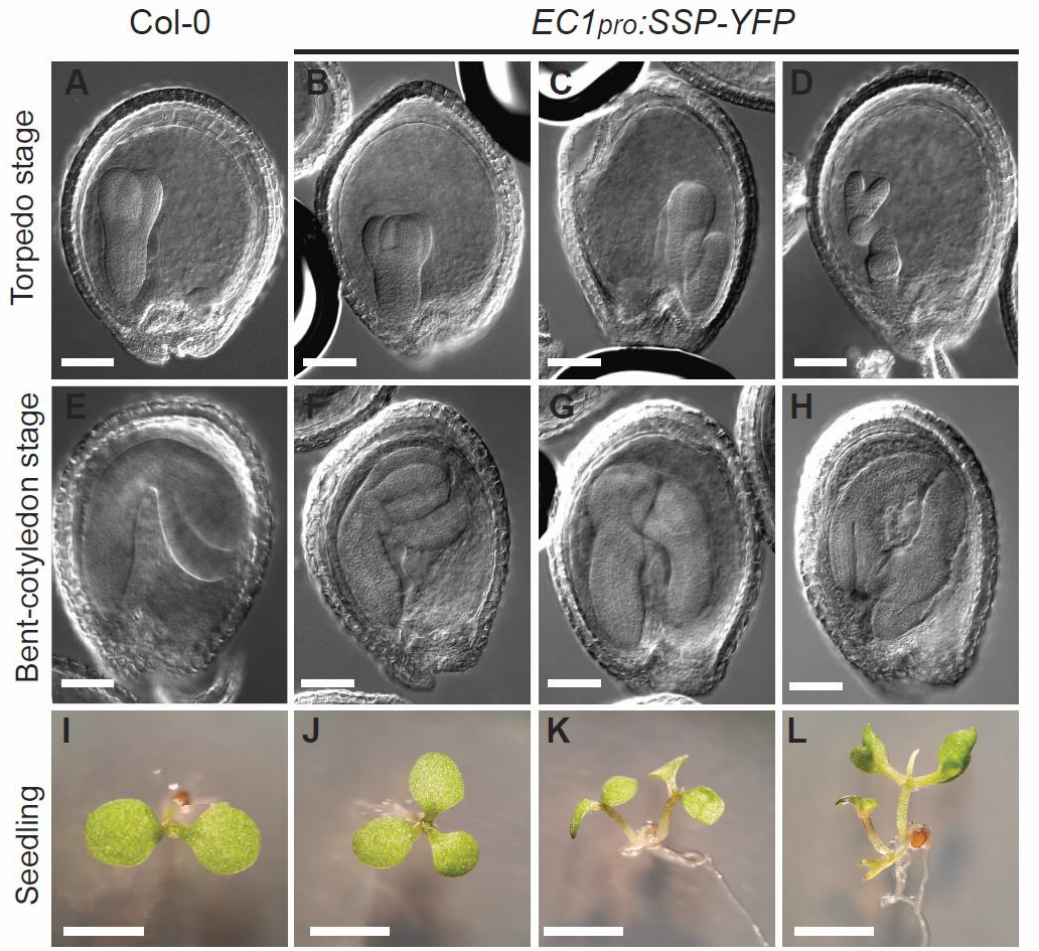

Figure 14. Late embryonic phenotypes and seedling phenotypes of the *ssp-2 EC1$_{pro}$:SSP-YFP* line

(A-H) Embryonic phenotypes of Col-0 (A, E) and *ssp-2 EC1$_{pro}$:SSP-YFP* (B-D, F-H) at the torpedo stage (A-D) and the bent-cotyledon stage (E-H). Phenotypes of triple cotyledons (B, F), twin embryos (C, G) and multiple embryos (D, H) are observed in *ssp-2 EC1$_{pro}$:SSP-YFP* lines. (I-L) 5-day-old Col-0 seedlings (I) and *ssp-2 EC1$_{pro}$:SSP-YFP* lines (J-L) with triple cotyledons (J), twin seedlings (K) or triple seedlings (L).

In addition, triple-cotyledon seedlings, twin seedlings and even triple seedlings were generated after germination. These seedlings phenotypes resemble the *S4$_{pro}$:SSP-YFP*

phenotypes (Chapter IV), suggesting that SSP-YFP proteins are functional in #7 and #8 lines. Thus, zygote phenotypes of line *#7* and *#8* are likely caused by partial and full loss of SSP polarity in line *#7* and *#8*, respectively. These results suggest that the polarized SSP localization is essential for zygote polarity. How SSP is polarized and whether YDA localization or activation is also polarized are still to be elucidated.

	Line	Vertical	Horizontal
Division of the apical daughter cell	Col-0	207/214 (96.73%)	7/214 (3.27%)
	#7	7/32 (21.86%)	25/32 (78.13%)
	#8	52/197 (26.40%)	145/197 (73.60%)

	Line	One embryos	Multiple embryos
Embryos	#7	435/457 (95.19%)	22/257 (4.81%)
	#8	406/460 (88.26%)	54/460 (11.74%)

	Line	Normal seedlings	Triple cotyledons	Multiple seedlings
Seedlings	Col-0	264/264 (100%)	0/264 (0%)	0/264 (0%)
	#7	178/185 (96.22%)	0/185 (0%)	7/185(3.78%)
	#8	141/171 (76.61%)	25/171 (14.62%)	15/171(8.77%)

Table 5. Ratio of abnormal embryos and seedlings in *ssp-2 EC1$_{pro}$:SSP-YFP #7* and *#8* lines

Discussion

1. Whether ERf and BSK1/2 signals are polarized in epidermal cells

Although YDA is polarly localized in ACD precursor cells during stomata generation [162], the localization of ER and BSK1 seems even in epidermal cells. During stomata patterning, the function of BSK1 is ERf-dependent and ERf is activated upon binding of EPFs [39, 131]. It is suggested that EPFs are secreted from meristemoids to activate the ERf signal in neighboring cells [165, 166]. As a result, the ER and BSK1 activity might be stimulated preferentially on the plasma membranes adjacent to meristermoids, irrespective of their protein localization. Using the same transgenic lines, we could not determine whether ER and BSK1 are polarly localized on the zygote plasma membrane due to the invisible ER-YPet signal in the zygote and the strong endosperm expression of BSK1-YPet. To overcome the drawback of using BSK1 native promoter, the *S4* promoter was used to express *BSK1* in the embryo. However, BSK1-YPet was expressed

almost ubiquitously in the ovule, mimicking the *BSK1$_{pro}$:BSK1-YFP* pattern. This result implies existence of strong cis elements in *BSK1* genomic sequence. Similarly, when *BSK1-YPet* and *ER-YPet* were driven by the *EC1* promoter, defects of vegetative development were also partially rescued (data not shown), supporting our speculation that cis elements promoting their broad expression exist in the genomic sequences of *BSK1* and *ER*. When *ER* CDS was driven by the *EC1* promoter, expression was barely observed in the egg cell (data not shown), consistent with a previous report that *ER* introns are indispensable for its stable expression [167]. Thus, confocal microscopy can only provide limited knowledge on BSK1 and ER localization. Interesting, extreme supplement of ER, BSK1 and SSP does not cause any visible damage to the egg cell, since fertilization undergoes normally (data not shown).

As discussed in Chapter II, related ligands may be secreted form surrounding mother tissues, which might lead to a polarized ERf signal. Therefore, polarized localizations of ER and BSK1 on the zygote plasma membrane seems unnecessary. As BSK1 is also localized on the endosperm plasma membrane adjacent to the zygote, it may be involved in a signal transduction from the zygote to the former.

2. SSP is polarly localized

Different from ER and BSK1, SSP is only expressed in early zygotes [64, 90]. In the *ssp-2 SSP$_{pro}$:SSP-YFP* rescued line, SSP-YFP is polarly localized on the zygote BPM. As SSP can function in an ERf-independent manner and directly interacts with YDA [65, 124, 131], the polarized SSP localization suggests a polarized YDA activity in the basal part of the zygote. Strikingly, depolarized SSP localizations strongly affected zygote polarity, suggesting that the polarized SSP/YDA activity is indispensable for zygote polarity. Expressing YDA under an embryo-specific promoter, similar to the use of *SPCH$_{pro}$:YDA-YFP* and *SPCH$_{pro}$::DNyda-YFP* in leaf epidermis [162], may shed light on YDA polarity in the zygote. In addition, we also tried to ectopically express SSP-YFP with the *BSK1* promoter to check whether SSP-YFP localization were also polarized in epidermis. However, YFP signal in epidermal cells of our transgenic lines was too weak to be identified. As the *BSK1* promoter is ubiquitously active during embryogenesis, we may select against transgenic lines with strong SSP-YFP expression.

SSP is a *Brassicaceae*-specific gene which evolved much later than *ERf*, *BSK1/2* and *YDA*. If the zygotic YDA signal is polarized, the ligand-ERf-BSK1/2 signal transduction should also contribute to this polarity. As ERf and BSK1/2 are evolutionarily conserved in flowering plants, we presume that the corresponding ligand may also show a sporophytic maternal effect. The unknown ligand, therefore, is likely secreted from surrounding mother tissues to trigger zygote polarization. Thus, it seems plausible that zygote polarization is a further reflection of the highly polarized ovule in flowering plant. Hence, it is necessary to identify where the ligand is secreted from.

3. The mechanism of SSP polarized localization

When plasma membrane-localized mRuby2 was expressed with the *S4* promoter, the proteins were distributed evenly on the zygote plasma membrane. In contrast, SSP-YFP proteins expressed under the same promoter were still polarly localized on the BPM of both the elongating zygote and the basal daughter cell, suggesting that SSP protein localization is somehow regulated. Even when SSP-YFP was strongly expressed by the *EC1* promoter, polarized localization was still observed. It was only when SSP-YFP was produced to an extreme level that the mechanism polarizing SSP-YFP seemed nonfunctional. As the localization of BSK1 in the zygote could not be easily monitored in our hands, whether the potential mechanism also applies to BSK1/2 is unknown. Although SSP can function in an ERf-independent way, we are not sure whether ERf facilitates SSP polarity in wild type. Checking SSP localization in the zygotes of *er erl1*, *er erl2* or *er erl1/+ erl2* mutants might help to answer this question. When SSP was depolarized, zygote polarity was strongly suppressed, suggesting that polarized YDA signal is necessary for zygote polarity.

Notwithstanding, it is still possible that the zygote polarity defect is just a result of an oversupply of nonfunctional SSP-YFP proteins that blocked normal molecular regulation, although more functional SSP-YFP proteins were also produced simultaneously (For example, because of its extreme expression, non-functional SSP-YFP proteins were generated and gradually transited into functional SSP-YFP. The nonfunctional SSP-YFP prevailed in the zygote and YDA is barely activated. In the apical daughter cell, the strong expression of SSP-YFP is eliminated. The ratio of functional to nonfunctional SSP-YFP

increased with the nonfunctional-to-function transition. The functional SSP-YFP prevailed in the apical daughter cell. Thus, YDA is activated and the apical cell divided horizontally). Therefore, using the *EC1* promoter to express a nonfunctional SSP as control, such as the G2A version [64], will be helpful to exclude this possibility.

ROPs are polarly localized on the tip plasma membranes of the tip-grown pollen tube and root hair. Zygote elongation also adopts a tip-grown manner. As ROP3 regulates zygote polarity [113], it may be also polarly localized on the APM of the elongating zygote. As SSP and ROP3 may be distributed in opposite sites, it seems unlikely that ROP3 directly regulates SSP localization. However, it is still tempting to dissect whether ROP3 functions in the YDA pathway and whether SSP localization is influenced in the *rop3* loss-of-function mutant. Since ROP3 affects the polar localization of PIN proteins in the root [113], it may affect zygote polarity through auxin response. Whether auxin response regulates zygote polarity and whether it intertwines with the YDA signal remain to be deciphered.

Materials and Methods

Main materials and methods are as described in the attached manuscript for Chapter IV.

Plasmid construction

The *ER$_{pro}$:ER-YPet* [131] and *S4$_{pro}$:SSP-YFP* are described in Chapter II and Chapter IV, respectively. To make *BSK1$_{pro}$:BSK1-YPet* lines, the *ER* promoter and *ER* genomic sequence in *ER$_{pro}$:ER-YPet* was replaced by a 2780 bp *BSK1* promoter fused with the *BSK1* genomic sequence. The construct was transformed into the *bsk1 bsk2* mutant [124]. To make *EC1$_{pro}$:SSP-YFP*, the *S4* promoter in *S4$_{pro}$:SSP-YFP* was replaced by the 464 bp *EC1* promoter. The construct was transformed into the *ssp-2* mutant. To construct *S4$_{pro}$:Myri_SSP-mRuby2*, the *S4* promoter was fused with the 60 bp *SSP* myristoylation motif and the *mRuby2 RFP* sequence in pBay-bar vector [131].

Primer sequence

Primer	sequence	Function
pBSK1-IF-F1	ATAAAATAATGTCGACTCGATTACTTTAGTAAATCC	Clone BSK1 promoter
pBSK1-IF-R1	ATGGCGCGCCCTCGAGCAAACTCTTTTTCCTTAC	
BSK1-IF-F1	TTGCTCGAGGGCGCGCCATGGGTTGTTGTCAATCCTTG	Clone BSK1

BSK1-IF-R1	TTTAGACACCATCCCGGGAGATCCTCTGCCGCCTCG	genomic sequence
pEC1-IF-F1	ATAAAATAATGTCGACCGCCTTATGATTTCTTCGG	Clone EC1 promoter
pEC1-IF-R1	ACAGAGCCATGGATCCCCTTCTCAACAGATTGATAAGGT	
Myri_SSP-IF-F1	TAGTAAAAAAGGATCCATGGGTTGTTGTTACTC	Clone SSP myristoylation motif
Myri_SSP-IF-R1	GCCCTTAGACACCATAGATCGCGTGTGGTC	
mRuby2-IF-F1	GACCACACGCGATCTATGGTGTCTAAGGGC	Clone mRuby2 sequence
mRuby2-IF-R1	TGGTTACCTTTTTAGGGCCCCTACTTGTACAGCTCG	

Prospect

In this dissertation, we investigated several aspects of the embryonic YDA pathway in Arabidopsis. The maternal ERf-BSK1/2 signal input and the paternal strong SSP signal input converge on YDA activation to control zygote polarity. The independent parental inputs reflect the hyperactivity of SSP and are reminiscent of the parental conflict theory. In addition, the polarized localization of SSP in the zygote is essential for zygote polarity. We further demonstrated that the HAESA family receptors can potentially activate the YDA signaling pathway through the BIR3 chimera assay. In addition, we designed a system to study the suspensor-embryo transition by using the hyperactivity of SSP.

In the future, identifying the interaction among YDA/yda-CA, BSK1/SSP or ERf/HSL1 will shed light on the molecular mechanism of YDA activation. Furthermore, comparing the structural difference between full-length BSK1 and SSP or between their TPR domains will enable better comprehension of function manners of BSKs. Since SSP is just *Brassicaceae*-specific, identifying the related ligand for ERf will further improve our understanding of both the parental conflict model and ancient polarity cues of flowering plants.

SSP can be used as a great tool to explore biological questions. As it is a constitutively active version of BSK1, it may facilitate the revealing of how BSKs are activated and how active BSKs recruit downstream substrates. BSK1/2 are broadly expressed in Arabidopsis tissues, and their expressions and functions might be conserved in flowering plants. BSKs seem to function redundantly and over-expression of BSK1 does not cause obvious phenotypes, SSP therefore may be utilized to replace BSK1 for activating BSK1-related pathways in Arabidopsis or in other flowering plants, enhancing our understanding of other BSK1-related regulations. Multiple embryos and seedlings are generated when SSP expression is prolonged in the embryo. This phenotype would be an appealing trait for agriculture as more seedlings are produced without post-embryonic growth inhibition. The multiple-seedling system should be improved, considering only approximately 10% seeds produce multiple seedlings. This may be refined by using other promoters to generate longer filamentous embryos in early stages. Prolonging SSP expression actually delays embryogenesis in Arabidopsis, an implication that SSP dosage needs to be precisely controlled. As an early SSP boost is beneficial, embryogenesis of non-*Brassicaceae* species might be accelerated by transiently expressing SSP in the zygote, thus producing larger embryos and seeds.

References

1. Friedman, W.E., *Comparative embryology of basal angiosperms.* Curr Opin Plant Biol, 2001. **4**(1): p. 14-20.
2. Kawashima, T. and R.B. Goldberg, *The suspensor: not just suspending the embryo.* Trends Plant Sci, 2010. **15**(1): p. 23-30.
3. Wang, K., et al., *Square one: zygote polarity and early embryogenesis in flowering plants.* Curr Opin Plant Biol, 2020. **53**: p. 128-133.
4. Hawkins, R.R., *An Introduction to the Embryology of Angiosperms.* Library Journal, 1950. **75**(18): p. 1830-1830.
5. Musielak, T.J. and M. Bayer, *YODA signalling in the early Arabidopsis embryo.* Biochem Soc Trans, 2014. **42**(2): p. 408-12.
6. ten Hove, C.A., K.J. Lu, and D. Weijers, *Building a plant: cell fate specification in the early Arabidopsis embryo.* Development, 2015. **142**(3): p. 420-30.
7. Bayer, M., D. Slane, and G. Jurgens, *Early plant embryogenesis-dark ages or dark matter?* Curr Opin Plant Biol, 2017. **35**: p. 30-36.
8. Khanday, I. and V. Sundaresan, *Plant zygote development: recent insights and applications to clonal seeds.* Current Opinion in Plant Biology, 2021. **59**.
9. Kimata, Y., et al., *Cytoskeleton dynamics control the first asymmetric cell division in Arabidopsis zygote.* Proc Natl Acad Sci U S A, 2016. **113**(49): p. 14157-14162.
10. Kimata, Y., et al., *Polar vacuolar distribution is essential for accurate asymmetric division of Arabidopsis zygotes.* Proceedings of the National Academy of Sciences of the United States of America, 2019. **116**(6): p. 2338-2343.
11. Meng, X. and S. Zhang, *MAPK cascades in plant disease resistance signaling.* Annu Rev Phytopathol, 2013. **51**: p. 245-66.
12. Xu, J. and S. Zhang, *Mitogen-activated protein kinase cascades in signaling plant growth and development.* Trends Plant Sci, 2015. **20**(1): p. 56-64.
13. Zhang, M., et al., *Conveying endogenous and exogenous signals: MAPK cascades in plant growth and defense.* Curr Opin Plant Biol, 2018. **45**(Pt A): p. 1-10.
14. Cui, F., W. Sun, and X. Kong, *RLCKs Bridge Plant Immune Receptors and MAPK Cascades.* Trends Plant Sci, 2018. **23**(12): p. 1039-1041.
15. Group, M., *Mitogen-activated protein kinase cascades in plants: a new nomenclature.* Trends Plant Sci, 2002. **7**(7): p. 301-8.
16. Bergmann, D.C., W. Lukowitz, and C.R. Somerville, *Stomatal development and pattern controlled by a MAPKK kinase.* Science, 2004. **304**(5676): p. 1494-7.
17. Lampard, G.R., C.A. MacAlister, and D.C. Bergmann, *Arabidopsis Stomatal Initiation Is Controlled by MAPK-Mediated Regulation of the bHLH SPEECHLESS.* Science, 2008. **322**(5904): p. 1113-1116.
18. Meng, X.Z., et al., *A MAPK Cascade Downstream of ERECTA Receptor-Like Protein Kinase Regulates Arabidopsis Inflorescence Architecture by Promoting Localized Cell Proliferation.* Plant Cell, 2012. **24**(12): p. 4948-4960.
19. Zhang, M.M., et al., *Maternal control of embryogenesis by MPK6 and its upstream MKK4/MKK5 in Arabidopsis.* Plant Journal, 2017. **92**(6): p. 1005-1019.
20. Zhu, Q., et al., *A MAPK cascade downstream of IDA-HAE/HSL2 ligand-receptor pair in lateral root emergence.* Nat Plants, 2019. **5**(4): p. 414-423.
21. Xu, R., et al., *Control of Grain Size and Weight by the OsMKKK10-OsMKK4-OsMAPK6 Signaling Pathway in Rice.* Mol Plant, 2018. **11**(6): p. 860-873.

22. Li, F.J., et al., *Regulation of cotton (Gossypium hirsutum) drought responses by mitogen-activated protein (MAP) kinase cascade-mediated phosphorylation of GhWRKY59.* New Phytologist, 2017. **215**(4): p. 1462-1475.
23. Sasabe, M. and Y. Machida, *Regulation of organization and function of microtubules by the mitogen-activated protein kinase cascade during plant cytokinesis.* Cytoskeleton (Hoboken), 2012. **69**(11): p. 913-8.
24. Bertolino, L.T., R.S. Caine, and J.E. Gray, *Impact of Stomatal Density and Morphology on Water-Use Efficiency in a Changing World.* Front Plant Sci, 2019. **10**: p. 225.
25. Nunes, T.D.G., D. Zhang, and M.T. Raissig, *Form, development and function of grass stomata.* Plant J, 2020. **101**(4): p. 780-799.
26. Kagan, M.L. and T. Sachs, *Development of immature stomata: evidence for epigenetic selection of a spacing pattern.* Dev Biol, 1991. **146**(1): p. 100-5.
27. Wang, H., et al., *Stomatal development and patterning are regulated by environmentally responsive mitogen-activated protein kinases in Arabidopsis.* Plant Cell, 2007. **19**(1): p. 63-73.
28. Abrash, E., et al., *Conservation and divergence of YODA MAPKKK function in regulation of grass epidermal patterning.* Development, 2018. **145**(14).
29. Shiu, S.H. and A.B. Bleecker, *Receptor-like kinases from Arabidopsis form a monophyletic gene family related to animal receptor kinases.* Proc Natl Acad Sci U S A, 2001. **98**(19): p. 10763-8.
30. Pillitteri, L.J., et al., *Haploinsufficiency after successive loss of signaling reveals a role for ERECTA-family genes in Arabidopsis ovule development.* Development, 2007. **134**(17): p. 3099-109.
31. Bemis, S.M., et al., *Regulation of floral patterning and organ identity by Arabidopsis ERECTA-family receptor kinase genes.* J Exp Bot, 2013. **64**(17): p. 5323-33.
32. Shpak, E.D., *Diverse roles of ERECTA family genes in plant development.* J Integr Plant Biol, 2013. **55**(12): p. 1238-50.
33. Chen, M.K. and E.D. Shpak, *ERECTA family genes regulate development of cotyledons during embryogenesis.* FEBS Lett, 2014. **588**(21): p. 3912-7.
34. Shpak, E.D., et al., *Synergistic interaction of three ERECTA-family receptor-like kinases controls Arabidopsis organ growth and flower development by promoting cell proliferation.* Development, 2004. **131**(7): p. 1491-501.
35. Kosentka, P.Z., et al., *EPFL Signals in the Boundary Region of the SAM Restrict Its Size and Promote Leaf Initiation.* Plant Physiol, 2019. **179**(1): p. 265-279.
36. Tameshige, T., et al., *Stem development through vascular tissues: EPFL-ERECTA family signaling that bounces in and out of phloem.* Journal of Experimental Botany, 2017. **68**(1): p. 45-53.
37. Jorda, L., et al., *ERECTA and BAK1 Receptor Like Kinases Interact to Regulate Immune Responses in Arabidopsis.* Front Plant Sci, 2016. **7**: p. 897.
38. Shpak, E.D., et al., *Stomatal patterning and differentiation by synergistic interactions of receptor kinases.* Science, 2005. **309**(5732): p. 290-3.
39. Lee, J.S., et al., *Direct interaction of ligand-receptor pairs specifying stomatal patterning.* Genes Dev, 2012. **26**(2): p. 126-36.
40. Lin, G.Z., et al., *A receptor-like protein acts as a specificity switch for the regulation of stomatal development.* Genes & Development, 2017. **31**(9): p. 927-938.
41. Geisler, M., M. Yang, and F.D. Sack, *Divergent regulation of stomatal initiation and patterning in organ and suborgan regions of the Arabidopsis mutants too many mouths and four lips.* Planta, 1998. **205**(4): p. 522-30.
42. Uchida, N., et al., *Regulation of inflorescence architecture by intertissue layer ligand-receptor communication between endodermis and phloem.* Proc Natl Acad Sci U S A, 2012. **109**(16): p. 6337-42.

43. Meng, X., et al., *Differential Function of Arabidopsis SERK Family Receptor-like Kinases in Stomatal Patterning.* Curr Biol, 2015. **25**(18): p. 2361-72.
44. He, K., et al., *BAK1 and BKK1 regulate brassinosteroid-dependent growth and brassinosteroid-independent cell-death pathways.* Curr Biol, 2007. **17**(13): p. 1109-15.
45. Meng, X., et al., *Ligand-Induced Receptor-like Kinase Complex Regulates Floral Organ Abscission in Arabidopsis.* Cell Rep, 2016. **14**(6): p. 1330-1338.
46. Qian, P., et al., *Author Correction: The CLE9/10 secretory peptide regulates stomatal and vascular development through distinct receptors.* Nat Plants, 2019. **5**(2): p. 238.
47. Roux, M., et al., *The Arabidopsis leucine-rich repeat receptor-like kinases BAK1/SERK3 and BKK1/SERK4 are required for innate immunity to hemibiotrophic and biotrophic pathogens.* Plant Cell, 2011. **23**(6): p. 2440-55.
48. Grutter, C., et al., *Structural characterization of the RLCK family member BSK8: a pseudokinase with an unprecedented architecture.* J Mol Biol, 2013. **425**(22): p. 4455-67.
49. Tang, W.Q., et al., *BSKs mediate signal transduction from the receptor kinase BRI1 in Arabidopsis.* Science, 2008. **321**(5888): p. 557-560.
50. Sreeramulu, S., et al., *BSKs are partially redundant positive regulators of brassinosteroid signaling in Arabidopsis.* Plant J, 2013. **74**(6): p. 905-19.
51. Shi, H., et al., *BR-SIGNALING KINASE1 physically associates with FLAGELLIN SENSING2 and regulates plant innate immunity in Arabidopsis.* Plant Cell, 2013. **25**(3): p. 1143-57.
52. Pillitteri, L.J., et al., *Termination of asymmetric cell division and differentiation of stomata.* Nature, 2007. **445**(7127): p. 501-5.
53. Kanaoka, M.M., et al., *SCREAM/ICE1 and SCREAM2 specify three cell-state transitional steps leading to arabidopsis stomatal differentiation.* Plant Cell, 2008. **20**(7): p. 1775-85.
54. Putarjunan, A., et al., *Bipartite anchoring of SCREAM enforces stomatal initiation by coupling MAP kinases to SPEECHLESS.* Nat Plants, 2019. **5**(7): p. 742-754.
55. Horst, R.J., et al., *Molecular Framework of a Regulatory Circuit Initiating Two-Dimensional Spatial Patterning of Stomatal Lineage.* PLoS Genet, 2015. **11**(7): p. e1005374.
56. Ortega, A., et al., *The Tomato Genome Encodes SPCH, MUTE, and FAMA Candidates That Can Replace the Endogenous Functions of Their Arabidopsis Orthologs.* Front Plant Sci, 2019. **10**: p. 1300.
57. Kim, T.W., et al., *Brassinosteroid regulates stomatal development by GSK3-mediated inhibition of a MAPK pathway.* Nature, 2012. **482**(7385): p. 419-22.
58. Abrash, E.B., K.A. Davies, and D.C. Bergmann, *Generation of signaling specificity in Arabidopsis by spatially restricted buffering of ligand-receptor interactions.* Plant Cell, 2011. **23**(8): p. 2864-79.
59. Kwon, C.T., et al., *Rapid customization of Solanaceae fruit crops for urban agriculture.* Nature Biotechnology, 2020. **38**(2): p. 182-+.
60. Barton, M.K., *Twenty years on: the inner workings of the shoot apical meristem, a developmental dynamo.* Dev Biol, 2010. **341**(1): p. 95-113.
61. Uchida, N., M. Shimada, and M. Tasaka, *ERECTA-family receptor kinases regulate stem cell homeostasis via buffering its cytokinin responsiveness in the shoot apical meristem.* Plant Cell Physiol, 2013. **54**(3): p. 343-51.
62. Kimura, Y., et al., *ERECTA-family genes coordinate stem cell functions between the epidermal and internal layers of the shoot apical meristem.* Development, 2018. **145**(1).
63. Lukowitz, W., et al., *A MAPKK kinase gene regulates extra-embryonic cell fate in Arabidopsis.* Cell, 2004. **116**(1): p. 109-19.
64. Bayer, M., et al., *Paternal control of embryonic patterning in Arabidopsis thaliana.* Science, 2009. **323**(5920): p. 1485-8.

65. Yuan, G.L., H.J. Li, and W.C. Yang, *The integration of G beta and MAPK signaling cascade in zygote development.* Scientific Reports, 2017. **7**.
66. Costa, L.M., et al., *Central cell-derived peptides regulate early embryo patterning in flowering plants.* Science, 2014. **344**(6180): p. 168-72.
67. Eulgem, T., et al., *The WRKY superfamily of plant transcription factors.* Trends Plant Sci, 2000. **5**(5): p. 199-206.
68. Ueda, M., Z. Zhang, and T. Laux, *Transcriptional activation of Arabidopsis axis patterning genes WOX8/9 links zygote polarity to embryo development.* Dev Cell, 2011. **20**(2): p. 264-70.
69. Ueda, M., et al., *Transcriptional integration of paternal and maternal factors in the Arabidopsis zygote.* Genes Dev, 2017. **31**(6): p. 617-627.
70. Lau, S., et al., *Early embryogenesis in flowering plants: setting up the basic body pattern.* Annu Rev Plant Biol, 2012. **63**: p. 483-506.
71. Breuninger, H., et al., *Differential expression of WOX genes mediates apical-basal axis formation in the Arabidopsis embryo.* Dev Cell, 2008. **14**(6): p. 867-76.
72. Jeong, S., T.M. Palmer, and W. Lukowitz, *The RWP-RK factor GROUNDED promotes embryonic polarity by facilitating YODA MAP kinase signaling.* Curr Biol, 2011. **21**(15): p. 1268-76.
73. Friml, J., et al., *Efflux-dependent auxin gradients establish the apical-basal axis of Arabidopsis.* Nature, 2003. **426**(6963): p. 147-53.
74. Hamann, T., U. Mayer, and G. Jurgens, *The auxin-insensitive bodenlos mutation affects primary root formation and apical-basal patterning in the Arabidopsis embryo.* Development, 1999. **126**(7): p. 1387-1395.
75. Chen, H., et al., *Zygotic Embryogenesis in Flowering Plants.* Methods Mol Biol, 2021. **2288**: p. 73-88.
76. Robert, H.S., et al., *Maternal auxin supply contributes to early embryo patterning in Arabidopsis.* Nat Plants, 2018. **4**(8): p. 548-553.
77. Berleth, T. and G. Jurgens, *The Role of the Monopteros Gene in Organizing the Basal Body Region of the Arabidopsis Embryo.* Development, 1993. **118**(2): p. 575-587.
78. Weijers, D., et al., *Auxin triggers transient local signaling for cell specification in Arabidopsis embryogenesis.* Dev Cell, 2006. **10**(2): p. 265-70.
79. Yoshida, S., et al., *Genetic control of plant development by overriding a geometric division rule.* Dev Cell, 2014. **29**(1): p. 75-87.
80. Rademacher, E.H., et al., *Different auxin response machineries control distinct cell fates in the early plant embryo.* Dev Cell, 2012. **22**(1): p. 211-22.
81. Tadros, W. and H.D. Lipshitz, *The maternal-to-zygotic transition: a play in two acts.* Development, 2009. **136**(18): p. 3033-42.
82. Meyer, S. and S. Scholten, *Equivalent parental contribution to early plant zygotic development.* Curr Biol, 2007. **17**(19): p. 1686-91.
83. Pillot, M., et al., *Embryo and endosperm inherit distinct chromatin and transcriptional states from the female gametes in Arabidopsis.* Plant Cell, 2010. **22**(2): p. 307-20.
84. Autran, D., et al., *Maternal epigenetic pathways control parental contributions to Arabidopsis early embryogenesis.* Cell, 2011. **145**(5): p. 707-19.
85. Zhao, J., et al., *Dynamic changes of transcript profiles after fertilization are associated with de novo transcription and maternal elimination in tobacco zygote, and mark the onset of the maternal-to-zygotic transition.* Plant J, 2011. **65**(1): p. 131-145.
86. Nodine, M.D. and D.P. Bartel, *Maternal and paternal genomes contribute equally to the transcriptome of early plant embryos.* Nature, 2012. **482**(7383): p. 94-7.
87. Del Toro-De Leon, G., D. Lepe-Soltero, and C.S. Gillmor, *Zygotic genome activation in isogenic and hybrid plant embryos.* Curr Opin Plant Biol, 2016. **29**: p. 148-53.

88. Schon, M.A. and M.D. Nodine, *Widespread Contamination of Arabidopsis Embryo and Endosperm Transcriptome Data Sets.* Plant Cell, 2017. **29**(4): p. 608-617.
89. Chen, J., et al., *Zygotic Genome Activation Occurs Shortly after Fertilization in Maize.* Plant Cell, 2017. **29**(9): p. 2106-2125.
90. Zhao, P., et al., *Two-Step Maternal-to-Zygotic Transition with Two-Phase Parental Genome Contributions.* Dev Cell, 2019.
91. Dilkes, B.P. and L. Comai, *A differential dosage hypothesis for parental effects in seed development.* Plant Cell, 2004. **16**(12): p. 3174-80.
92. Batista, R.A. and C. Kohler, *Genomic imprinting in plants-revisiting existing models.* Genes Dev, 2020. **34**(1-2): p. 24-36.
93. Khanday, I., et al., *A male-expressed rice embryogenic trigger redirected for asexual propagation through seeds.* Nature, 2019. **565**(7737): p. 91-95.
94. Figueiredo, D.D. and C. Kohler, *Auxin: a molecular trigger of seed development.* Genes Dev, 2018. **32**(7-8): p. 479-490.
95. Zhao, P., et al., *Equal parental contribution to the transcriptome is not equal control of embryogenesis.* Nature Plants, 2020. **6**(11): p. 1354-+.
96. Kinoshita, T., et al., *Imprinting of the MEDEA polycomb gene in the Arabidopsis endosperm.* Plant Cell, 1999. **11**(10): p. 1945-52.
97. Grossniklaus, U., et al., *Maternal control of embryogenesis by MEDEA, a polycomb group gene in Arabidopsis.* Science, 1998. **280**(5362): p. 446-50.
98. Luo, M., et al., *Expression and parent-of-origin effects for FIS2, MEA, and FIE in the endosperm and embryo of developing Arabidopsis seeds.* Proc Natl Acad Sci U S A, 2000. **97**(19): p. 10637-42.
99. Piotrowska, K. and M. Zernicka-Goetz, *Role for sperm in spatial patterning of the early mouse embryo.* Nature, 2001. **409**(6819): p. 517-521.
100. Marston, D.J. and B. Goldstein, *Symmetry breaking in C-elegans: Another gift from the sperm.* Developmental Cell, 2006. **11**(3): p. 273-274.
101. Hable, W.E. and D.L. Kropf, *Sperm entry induces polarity in fucoid zygotes.* Development, 2000. **127**(3): p. 493-501.
102. Nakajima, K., T. Uchiumi, and T. Okamoto, *Positional relationship between the gamete fusion site and the first division plane in the rice zygote.* Journal of Experimental Botany, 2010. **61**(11): p. 3101-3105.
103. Rasmussen, C.G., J.A. Humphries, and L.G. Smith, *Determination of symmetric and asymmetric division planes in plant cells.* Annu Rev Plant Biol, 2011. **62**: p. 387-409.
104. Cartwright, H.N., J.A. Humphries, and L.G. Smith, *PAN1: A Receptor-Like Protein That Promotes Polarization of an Asymmetric Cell Division in Maize.* Science, 2009. **323**(5914): p. 649-651.
105. Zhang, X., et al., *Identification of PAN2 by quantitative proteomics as a leucine-rich repeat-receptor-like kinase acting upstream of PAN1 to polarize cell division in maize.* Plant Cell, 2012. **24**(11): p. 4577-89.
106. Facette, M.R., et al., *The SCAR/WAVE complex polarizes PAN receptors and promotes division asymmetry in maize.* Nat Plants, 2015. **1**: p. 14024.
107. Fernandez, A.I., et al., *GOLVEN peptide signalling through RGI receptors and MPK6 restricts asymmetric cell division during lateral root initiation.* Nat Plants, 2020. **6**(5): p. 533-543.
108. Yoshida, S., et al., *A SOSEKI-based coordinate system interprets global polarity cues in Arabidopsis.* Nat Plants, 2019. **5**(2): p. 160-166.
109. van Dop, M., et al., *DIX Domain Polymerization Drives Assembly of Plant Cell Polarity Complexes.* Cell, 2020. **180**(3): p. 427-439 e12.

110. Feiguelman, G., Y. Fu, and S. Yalovsky, *ROP GTPases Structure-Function and Signaling Pathways.* Plant Physiol, 2018. **176**(1): p. 57-79.
111. Craddock, C., I. Lavagi, and Z.B. Yang, *New insights into Rho signaling from plant ROP/Rac GTPases (vol 22, pg 492, 2012).* Trends in Cell Biology, 2013. **23**(2): p. 102-102.
112. Humphries, J.A., et al., *ROP GTPases act with the receptor-like protein PAN1 to polarize asymmetric cell division in maize.* Plant Cell, 2011. **23**(6): p. 2273-84.
113. Huang, J.B., et al., *ROP3 GTPase contributes to polar auxin transport and auxin responses and is important for embryogenesis and seedling growth in Arabidopsis.* Plant Cell, 2014. **26**(9): p. 3501-18.
114. Yamaguchi, Y., et al., *PEPR2 Is a Second Receptor for the Pep1 and Pep2 Peptides and Contributes to Defense Responses in Arabidopsis.* Plant Cell, 2010. **22**(2): p. 508-522.
115. Furumizu, C., et al., *The sequenced genomes of non-flowering land plants reveal the innovative evolutionary history of peptide signaling.* Plant Cell, 2021.
116. Jinn, T.L., J.M. Stone, and J.C. Walker, *HAESA, an Arabidopsis leucine-rich repeat receptor kinase, controls floral organ abscission.* Genes Dev, 2000. **14**(1): p. 108-17.
117. Cho, S.K., et al., *Regulation of floral organ abscission in Arabidopsis thaliana.* Proc Natl Acad Sci U S A, 2008. **105**(40): p. 15629-34.
118. Liu, X.S., et al., *The LRR-RLK Protein HSL3 Regulates Stomatal Closure and the Drought Stress Response by Modulating Hydrogen Peroxide Homeostasis.* Front Plant Sci, 2020. **11**: p. 548034.
119. Luo, M., et al., *MINISEED3 (MINI3), a WRKY family gene, and HAIKU2 (IKU2), a leucine-rich repeat (LRR) KINASE gene, are regulators of seed size in Arabidopsis.* Proc Natl Acad Sci U S A, 2005. **102**(48): p. 17531-6.
120. Pitorre, D., et al., *RLK7, a leucine-rich repeat receptor-like kinase, is required for proper germination speed and tolerance to oxidative stress in Arabidopsis thaliana.* Planta, 2010. **232**(6): p. 1339-53.
121. Hou, S., et al., *The secreted peptide PIP1 amplifies immunity through receptor-like kinase 7.* PLoS Pathog, 2014. **10**(9): p. e1004331.
122. Toyokura, K., et al., *Lateral Inhibition by a Peptide Hormone-Receptor Cascade during Arabidopsis Lateral Root Founder Cell Formation.* Dev Cell, 2019. **48**(1): p. 64-75 e5.
123. Tabata, R., et al., *Perception of root-derived peptides by shoot LRR-RKs mediates systemic N-demand signaling.* Science, 2014. **346**(6207): p. 343-6.
124. Neu, A., et al., *Constitutive signaling activity of a receptor-associated protein links fertilization with embryonic patterning in Arabidopsis thaliana.* Proc Natl Acad Sci U S A, 2019. **116**(12): p. 5795-5804.
125. Zhang, B.W., et al., *OsBRI1 Activates BR Signaling by Preventing Binding between the TPR and Kinase Domains of OsBSK3 via Phosphorylation.* Plant Physiology, 2016. **170**(2): p. 1149-1161.
126. Loraine, A.E., et al., *RNA-seq of Arabidopsis pollen uncovers novel transcription and alternative splicing.* Plant Physiol, 2013. **162**(2): p. 1092-109.
127. Borges, F., et al., *Comparative transcriptomics of Arabidopsis sperm cells.* Plant Physiol, 2008. **148**(2): p. 1168-81.
128. Zhao, P., et al., *Two-Step Maternal-to-Zygotic Transition with Two-Phases of Parental Genome Contributions.* Available at SSRN 3307384, 2018.
129. Borg, M., et al., *Targeted reprogramming of H3K27me3 resets epigenetic memory in plant paternal chromatin.* Nat Cell Biol, 2020. **22**(6): p. 621-629.
130. Zeytuni, N. and R. Zarivach, *Structural and functional discussion of the tetra-trico-peptide repeat, a protein interaction module.* Structure, 2012. **20**(3): p. 397-405.
131. Wang, K., et al., *Independent parental contributions initiate zygote polarization in Arabidopsis thaliana.* Curr Biol, 2021.

132. Harmansa, S., et al., *A nanobody-based toolset to investigate the role of protein localization and dispersal in Drosophila.* Elife, 2017. **6**.
133. Caussinus, E., O. Kanca, and M. Affolter, *Fluorescent fusion protein knockout mediated by anti-GFP nanobody.* Nature Structural & Molecular Biology, 2012. **19**(1): p. 117-U142.
134. Ma, Y.F., et al., *WUSCHEL acts as an auxin response rheostat to maintain apical stem cells in Arabidopsis.* Nature Communications, 2019. **10**.
135. Grossniklaus, U. and K. Schneitz, *The molecular and genetic basis of ovule and megagametophyte development.* Semin Cell Dev Biol, 1998. **9**(2): p. 227-38.
136. Ray, S., T. Golden, and A. Ray, *Maternal effects of the short integument mutation on embryo development in Arabidopsis.* Dev Biol, 1996. **180**(1): p. 365-9.
137. Golden, T.A., et al., *SHORT INTEGUMENTS1/SUSPENSOR1/CARPEL FACTORY, a Dicer homolog, is a maternal effect gene required for embryo development in Arabidopsis.* Plant Physiology, 2002. **130**(2): p. 808-822.
138. Mizzotti, C., et al., *SEEDSTICK is a Master Regulator of Development and Metabolism in the Arabidopsis Seed Coat.* Plos Genetics, 2014. **10**(12).
139. Lee, J.S., et al., *Competitive binding of antagonistic peptides fine-tunes stomatal patterning.* Nature, 2015. **522**(7557): p. 439-43.
140. Fiume, E. and J.C. Fletcher, *Regulation of Arabidopsis embryo and endosperm development by the polypeptide signaling molecule CLE8.* Plant Cell, 2012. **24**(3): p. 1000-12.
141. Xu, T.T., et al., *CLE19 expressed in the embryo regulates both cotyledon establishment and endosperm development in Arabidopsis.* Journal of Experimental Botany, 2015. **66**(17): p. 5217-5227.
142. Li, H., et al., *SERK Receptor-like Kinases Control Division Patterns of Vascular Precursors and Ground Tissue Stem Cells during Embryo Development in Arabidopsis.* Mol Plant, 2019. **12**(7): p. 984-1002.
143. Albrecht, C., et al., *The Arabidopsis thaliana SOMATIC EMBRYOGENESIS RECEPTOR-LIKE KINASES1 and 2 control male sporogenesis.* Plant Cell, 2005. **17**(12): p. 3337-49.
144. Gou, X., et al., *Genetic evidence for an indispensable role of somatic embryogenesis receptor kinases in brassinosteroid signaling.* PLoS Genet, 2012. **8**(1): p. e1002452.
145. Haig, D. and M. Westoby, *Parent-Specific Gene-Expression and the Triploid Endosperm.* American Naturalist, 1989. **134**(1): p. 147-155.
146. Wilkins, J.F. and D. Haig, *What good is genomic imprinting: The function of parent-specific gene expression.* Nature Reviews Genetics, 2003. **4**(5): p. 359-368.
147. Picard, C.L., et al., *Transcriptional and imprinting complexity in Arabidopsis seeds at single-nucleus resolution.* Nature Plants, 2021. **7**(6): p. 730-+.
148. Ma, X., et al., *SERKing Coreceptors for Receptors.* Trends Plant Sci, 2016. **21**(12): p. 1017-1033.
149. Lehti-Shiu, M.D., et al., *Evolutionary history and stress regulation of plant receptor-like kinase/pelle genes.* Plant Physiol, 2009. **150**(1): p. 12-26.
150. Hohmann, U., et al., *Mechanistic basis for the activation of plant membrane receptor kinases by SERK-family coreceptors.* Proc Natl Acad Sci U S A, 2018. **115**(13): p. 3488-3493.
151. Imkampe, J., et al., *The Arabidopsis Leucine-Rich Repeat Receptor Kinase BIR3 Negatively Regulates BAK1 Receptor Complex Formation and Stabilizes BAK1.* Plant Cell, 2017. **29**(9): p. 2285-2303.
152. Moussu, S. and J. Santiago, *Structural biology of cell surface receptor-ligand interactions.* Curr Opin Plant Biol, 2019. **52**: p. 38-45.
153. Hohmann, U., K. Lau, and M. Hothorn, *The Structural Basis of Ligand Perception and Signal Activation by Receptor Kinases.* Annu Rev Plant Biol, 2017. **68**: p. 109-137.

154. Hohmann, U., et al., *The SERK3 elongated allele defines a role for BIR ectodomains in brassinosteroid signalling.* Nat Plants, 2018.
155. Hohmann, U., et al., *Publisher Correction: The SERK3 elongated allele defines a role for BIR ectodomains in brassinosteroid signalling.* Nat Plants, 2018. **4**(9): p. 732.
156. Hohmann, U., et al., *Constitutive Activation of Leucine-Rich Repeat Receptor Kinase Signaling Pathways by BAK1-INTERACTING RECEPTOR-LIKE KINASE3 Chimera.* Plant Cell, 2020. **32**(10): p. 3311-3323.
157. Stenvik, G.E., et al., *The EPIP peptide of INFLORESCENCE DEFICIENT IN ABSCISSION is sufficient to induce abscission in arabidopsis through the receptor-like kinases HAESA and HAESA-LIKE2.* Plant Cell, 2008. **20**(7): p. 1805-17.
158. Liu, Y., et al., *Direct evidence that suspensor cells have embryogenic potential that is suppressed by the embryo proper during normal embryogenesis.* Proceedings of the National Academy of Sciences of the United States of America, 2015. **112**(40): p. 12432-12437.
159. Xiang, D., et al., *POPCORN functions in the auxin pathway to regulate embryonic body plan and meristem organization in Arabidopsis.* Plant Cell, 2011. **23**(12): p. 4348-67.
160. Zhang, M., et al., *Expression of a plastid-localized sugar transporter in the suspensor is critical to embryogenesis.* Plant Physiology, 2020.
161. Radoeva, T., et al., *A Robust Auxin Response Network Controls Embryo and Suspensor Development through a Basic Helix Loop Helix Transcriptional Module.* Plant Cell, 2019. **31**(1): p. 52-67.
162. Zhang, Y., et al., *The BASL polarity protein controls a MAPK signaling feedback loop in asymmetric cell division.* Dev Cell, 2015. **33**(2): p. 136-49.
163. Musielak, T.J., et al., *A simple and versatile cell wall staining protocol to study plant reproduction.* Plant Reprod, 2015. **28**(3-4): p. 161-9.
164. Slane, D., et al., *Cell type-specific transcriptome analysis in the early Arabidopsis thaliana embryo.* Development, 2014. **141**(24): p. 4831-40.
165. Hara, K., et al., *The secretory peptide gene EPF1 enforces the stomatal one-cell-spacing rule.* Genes Dev, 2007. **21**(14): p. 1720-5.
166. Hunt, L. and J.E. Gray, *The signaling peptide EPF2 controls asymmetric cell divisions during stomatal development.* Curr Biol, 2009. **19**(10): p. 864-9.
167. Karve, R., et al., *The presence of multiple introns is essential for ERECTA expression in Arabidopsis.* Rna, 2011. **17**(10): p. 1907-1921.

Appendix:

Accepted publications

1. Independent parental contributions initiate zygote polarization in *Arabidopsis thaliana*.

2. Zygotic Embryogenesis in Flowering Plants.

3. Constitutive Activation of Leucine-Rich Repeat Receptor Kinase Signaling Pathways by BAK1-INTERACTING RECEPTOR-LIKE KINASE3 Chimera.

4. Square one: zygote polarity and early embryogenesis in flowering plants.

5. Constitutive signaling activity of a receptor-associated protein links fertilization with embryonic patterning in *Arabidopsis thaliana*.

Manuscript ready for submission

6. A filament-like embryo system to study the suspensor-embryo transition.

Report

Current Biology

Independent parental contributions initiate zygote polarization in *Arabidopsis thaliana*

Graphical abstract

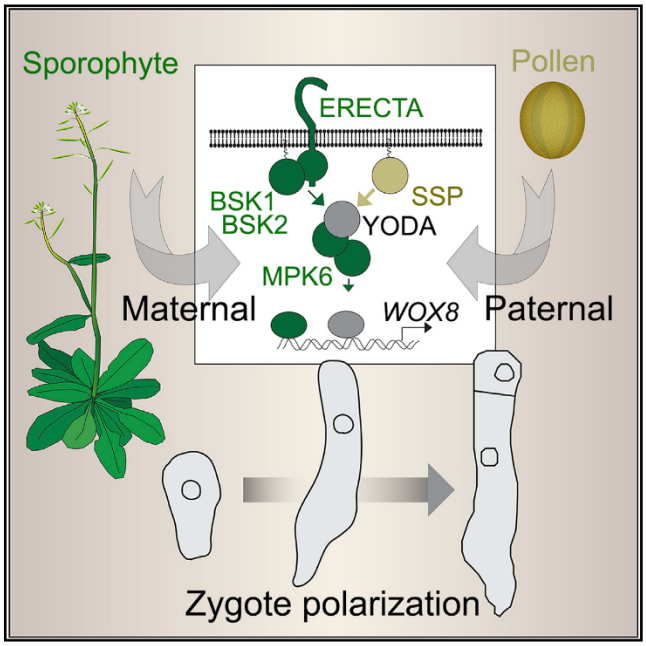

Authors

Kai Wang, Houming Chen, Marina Ortega-Perez, ..., Jan U. Lohmann, Sascha Laubinger, Martin Bayer

Correspondence

martin.bayer@tuebingen.mpg.de

In brief

Cell polarization and asymmetric division of the zygote initiate axis formation of the embryo in the model plant *Arabidopsis*. Wang et al. show in this context that a maternal receptor complex and a paternally provided constitutively active signaling protein independently contribute to MAP kinase signaling controlling zygote polarization.

Highlights

- Independent maternal and paternal factors influence *Arabidopsis* zygote polarity
- Maternal ERECTA family receptor kinases activate the MAP3K YODA in the zygote
- Paternal SHORT SUSPENSOR protein activates YODA independently of maternal ERECTA

Wang et al., 2021, Current Biology *31*, 1–7
November 8, 2021
https://doi.org/10.1016/j.cub.2021.08.033

CellPress

Please cite this article in press as: Wang et al., Independent parental contributions initiate zygote polarization in *Arabidopsis thaliana*, Current Biology (2021), https://doi.org/10.1016/j.cub.2021.08.033

Current Biology

CellPress

Report

Independent parental contributions initiate zygote polarization in *Arabidopsis thaliana*

Kai Wang,[1] Houming Chen,[1] Marina Ortega-Perez,[1] Yingjing Miao,[1] Yanfei Ma,[2] Agnes Henschen,[1] Jan U. Lohmann,[2] Sascha Laubinger,[3] and Martin Bayer[1,4,*]

[1]Max Planck Institute for Developmental Biology, Department of Cell Biology, Max-Planck-Ring 5, 72076 Tübingen, Germany
[2]Centre for Organismal Studies, Heidelberg University, Department of Stem Cell Biology, Im Neuenheimer Feld 230, 69120 Heidelberg, Germany
[3]University of Oldenburg, Institute for Biology and Environmental Sciences, Carl-von-Ossietzky-Str. 9-11, 26111 Oldenburg, Germany
[4]Lead contact
*Correspondence: martin.bayer@tuebingen.mpg.de
https://doi.org/10.1016/j.cub.2021.08.033

SUMMARY

Embryogenesis of flowering plants is initiated by polarization of the zygote, a prerequisite for correct axis formation in the embryo. The daughter cells of the asymmetric zygote division form the pro-embryo and the mostly extra-embryonic suspensor.[1] The suspensor plays a pivotal role in nutrient and hormone transport and rapid growth of the embryo.[2,3] Zygote polarization is controlled by a MITOGEN-ACTIVATING PROTEIN (MAP) kinase signaling pathway including the MAPKK kinase (MAP3K) YODA (YDA)[4] and the upstream membrane-associated proteins BRASINOSTEROID SIGNALING KINASE 1 (BSK1) and BSK2.[5,6] Furthermore, suspensor development is controlled by cysteine-rich peptides of the EMBRYO SURROUNDING FACTOR 1 (ESF1) family.[7] While they act genetically upstream of YDA, the corresponding receptor to perceive these potential ligands is unknown. In other developmental processes, such as stomata development, YDA activity is controlled by receptor kinases of the ERECTA family (ERf).[8–12] While the receptor kinases upstream of BSK1/2 in the embryo have so far not been identified,[1] YDA is in part activated by the sperm cell-derived BSK family member SHORT SUSPENSOR (SSP) that represents a naturally occurring, constitutively active variant of BSK1.[5,13] It has been speculated that SSP might be a paternal component of a parental tug-of-war controlling resource allocation toward the embryo.[2,13] Here, we show that in addition to SSP, the receptor kinase ERECTA plays a crucial role in zygote polarization as a maternally contributed part of the embryonic YDA pathway. We conclude that two independent parental contributions initiate zygote polarization and control embryo development.

RESULTS AND DISCUSSION

Despite its central role in zygote polarization and controlling embryonic versus non-embryonic development, it is still unclear if the embryonic YDA pathway is activated in response to extracellular signals. In many aspects of *Arabidopsis* development, YDA activity is controlled by receptor kinases of the ERECTA family, including ERECTA (ER), ER-LIKE 1 (ERL1), and ERL2.[9,10,12] As transcripts of *ER* can be detected in the zygote (Table S1),[14] a critical function of *ER* in controlling zygote polarity seems plausible. Homozygous *er erl1 erl2* triple mutants are sterile and produce no embryos.[11] We therefore addressed a possible function of *ER* in early embryogenesis by examining homozygous single, double, and segregating triple mutants of *ERf* genes. As mutants in Ler background used in previous studies contain a non-functional *ER* gene, we performed all genetic experiments with alleles in Col-0 background.[4,13,15] When comparing *er* mutants with wild type, weak defects in zygote elongation, zygote polarization, and suspensor length became apparent (Figure 1) as well as aberrant division plane orientations in the suspensor (Figure S1). These defects are hallmarks of reduced YDA activity[4] and mimic the phenotypes of *ssp* or *bsk1 bsk2* double mutants.[5,13] Loss of *ERL1* and *ERL2* function only showed detectable defects in the absence of functional *ER* by enhancing the *er* phenotype, indicating that ERL1 and ERL2 play a minor role in early embryogenesis but can partially take over *ER* function in its absence (Figure 1), as previously described for *ERf* function during stomata development.[10,16–18] To test if ER acts upstream of YDA in the context of zygote polarization as it does in other developmental contexts,[10,18,19] we performed genetic rescue experiments with a constitutively active version of YDA (*yda-CA*;[4] Figure S1). Constitutive YDA activity rescued the *er erl2* double mutant phenotype and caused increased zygote elongation, suggesting that YDA acts downstream of ER in a common signaling cascade. As *yda-CA* was hemizygous in the parental plant and therefore segregated in the analyzed embryos, a quarter of the embryos did not carry the *yda-CA* transgene, resulting in slightly lower median values in the *er erl2* background compared to wild-type background. These results suggest that the ER/YDA pathways involved in embryogenesis and stomata development share a common overall architecture.[20] Triple *ERf* mutants with segregating *er* (*ER/er erl1 erl2*), however, did not show defects in zygote

Please cite this article in press as: Wang et al., Independent parental contributions initiate zygote polarization in *Arabidopsis thaliana*, Current Biology (2021), https://doi.org/10.1016/j.cub.2021.08.033

CellPress

Current Biology
Report

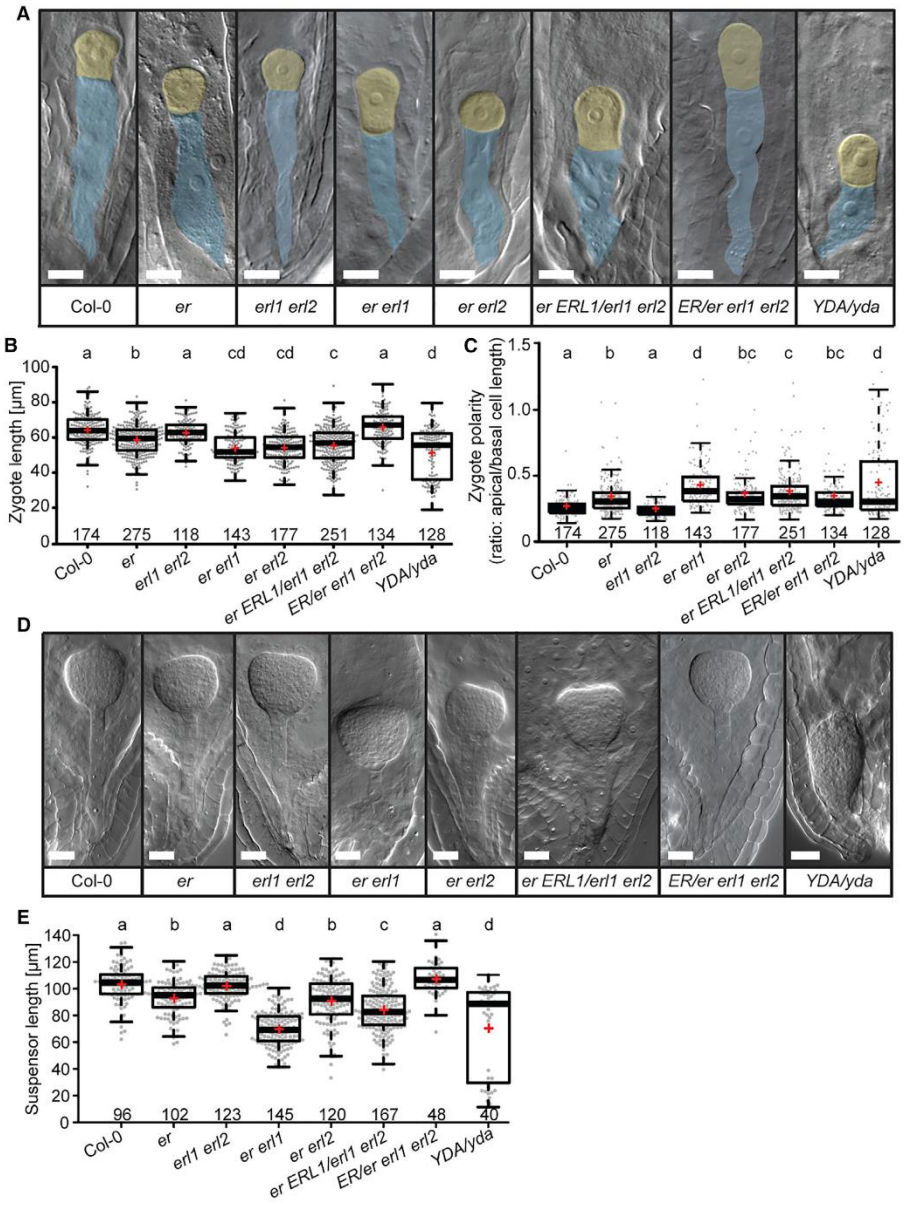

Figure 1. Zygote polarity and suspensor development

(A) DIC images of cleared ovules showing representative one-cell embryos (apical cell false-colored in yellow, basal cell in blue). Genotypes are given below images. Scale bar, 10 µm.

(B and C) Boxplot diagram of zygote length (B) and zygote polarity (C).

(D) DIC images of transition stage embryos. Genotypes are given below images. Scale bar, 20 µm.

(E) Boxplot diagram of suspensor length at transition stage.

(legend continued on next page)

Please cite this article in press as: Wang et al., Independent parental contributions initiate zygote polarization in *Arabidopsis thaliana*, Current Biology (2021), https://doi.org/10.1016/j.cub.2021.08.033

Current Biology
Report

CellPress

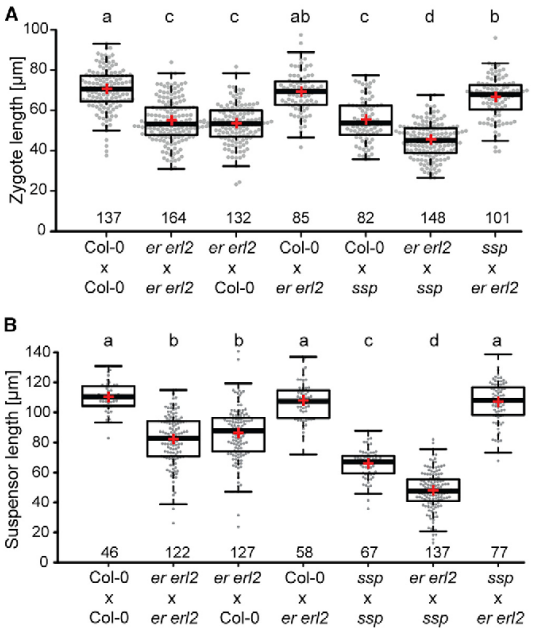

Figure 2. Parental effects in reciprocal crosses

Boxplot diagrams of zygote elongation (A) and suspensor length (B) in F1 embryos of reciprocal crosses. Genotypes are given as female × male. Boxplot data presentation as described in Figure 1. Different letters above boxes refer to individual groups in a one-way ANOVA with a post hoc Tukey test ($p < 0.05$). See also Figures S2 and S4 and Table S3.

elongation or suspensor formation despite normal transmission of the *er* mutant allele (Figure 1; Table S2). The fact that phenotypic defects in homozygous *er* embryos only became apparent if the parental plants were homozygous for *er*, but not in homozygous offspring of heterozygous *ER/er* parents, led us to test for possible parent-of-origin effects. In reciprocal crosses of *er erl* double mutants and wild type (Figures 2 and S2), we could only observe defects in F1 embryos if maternal plants carried the *er erl* mutations, but not if these alleles were transmitted by the pollen donors (Figures 2 and S2). Furthermore, zygote elongation defects could not be observed if maternal plants were heterozygous for the *er* mutation (Figure 1), although slightly altered zygote polarity can be observed in segregating triple *ER/er erl1 erl2* mutants (Figure 1). The phenotype of the embryo therefore seems to be predominantly determined by the genotype of the maternal sporophyte while loss of *ER* function in the haploid phase or the embryo in segregating plants did not have a major effect on the embryonic phenotype. This unusual parental effect may explain why a role of *ERECTA* in zygote polarization has so far been overlooked.

Two possible scenarios could explain the sporophytic maternal effect: zygote polarization could be affected by a non-cell-autonomous function of ER in sporophytic tissue. Such a scenario has, for example, been described for early auxin signaling in the embryo.[21] Alternatively, ER could function in the zygote but rely on *ER* transcripts and/or ER proteins inherited to the zygote via the pre-meiotic megaspore mother cell (MMC).

A transcriptional (ER_{pro}*:3xVenus-N7*) and a functional translational fusion (ER_{pro}*:ER-YPet*) reporter gene as well as RNA *in situ* hybridization revealed *ER* expression in the sporophytic seed coat as well as the female germline (Figure S3). As *ER* transcripts can be detected at low level in isolated zygotes[14] (Table S1) but are below detection limit in RNA *in situ* hybridization and very weak *ER-YPet* expression was sufficient to rescue the mutant phenotype in seedlings, we were not able to draw a definite conclusion about the location of ER function based on the observed expression pattern. However, *yda* has been reported as a zygotic recessive mutant,[4,15] and we confirmed this for the *yda-11* allele (Figures 1 and S1). On the other hand, *SSP* acts as sperm-derived activator.[5,13] Both genes would therefore argue for a function of the embryonic ERECTA/YDA pathway in the zygote. This is further supported by the function of WRKY2, a direct downstream target of MPK6 phosphorylation.[22] Consistently, loss-of-function *wrky2* null mutations are zygotic recessive without detectable parent-of-origin effects.[22] When looking at mRNA stability, *ER* transcripts showed a moderate half-life in seedlings at roughly the same level as typical housekeeping genes, such as *ACTIN 2*, for which rapid mRNA turnover does not appear necessary (Table S3).[23] *ER* transcripts can be detected in the egg cell, but transcript levels decline after fertilization, indicating that there is little or no *de novo* transcription of *ER* in the zygote (Table S1).[14] In order to address the question of where ER function is necessary for zygote polarization, we specifically reduced ER protein function in the zygote using the ER_{pro}*:ER-YPet* line in *er erl1 erl2* background. Genetically encoded anti-GFP nanobodies fused to ubiquitin ligases have been used as an elegant tool to specifically target GFP/YFP-tagged proteins for degradation.[24,25] To test its functionality, we expressed the NSlmb-vhhGFP4 nanobody under the *ER* promoter. The resulting seedlings mimicked the *er erl1 erl2* triple-mutant phenotype,[11] albeit with a slightly weaker phenotype (Figure 3), indicating that the nanobody is functional but does not completely abolish ER-YPet activity. In the next step, we expressed the nanobody under the strong egg cell-specific *EC1* promoter[26] to specifically reduce ER-YPet levels in the egg cell/zygote. This resulted in a significant reduction of zygote length in the ER_{pro}*:ER-YPet* rescue line (Figure 3), indicating that zygote polarization critically depends on functional *ER* protein in the zygote. Taken together, the available data suggest that the sporophytic maternal control of ER function can be explained by the inheritance of pre-meiotically produced *ER* transcripts/proteins to the zygote and that very low amounts of ER are sufficient to provide function in the zygote.

In (B)–(E), the sample size is given above the x axis. Center lines show the medians; box limits indicate the 25th and 75th percentiles; whiskers extend 1.5 times the interquartile range from the 25th and 75th percentiles; red crosses represent sample means; data points are plotted as gray dots. Letters above boxes refer to individual groups in a one-way ANOVA with a post hoc Tukey test ($p < 0.05$). In embryos of heterozygous *yda* plants, two distinct populations of data points can be observed, with approximately a quarter showing strong zygote elongation (B) and polarity defects (C), and reduced suspensor length (E) possibly representing the homozygous offspring. See also Figure S1 and Tables S1–S3.

Please cite this article in press as: Wang et al., Independent parental contributions initiate zygote polarization in *Arabidopsis thaliana*, Current Biology (2021), https://doi.org/10.1016/j.cub.2021.08.033

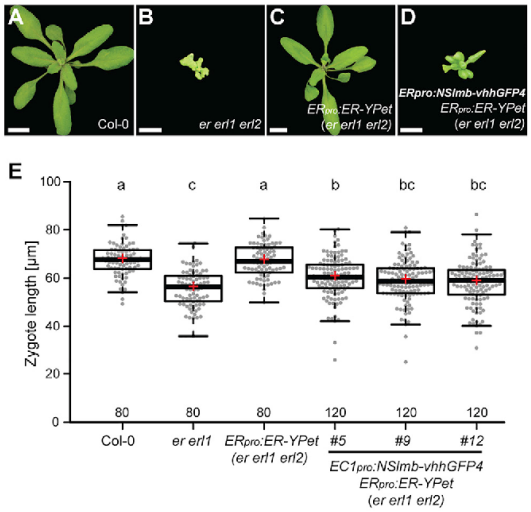

Figure 3. Cell-autonomous function of ER protein in the zygote

(A–D) Vegetative growth phenotype of wild-type Col-0 (A), *er erl1 erl2* triple homozygous (B), genetically rescued plants (ER_{pro}:*ER-YPet* in *er erl1 erl2*; C), and genetically recued plants expressing anti-GFP nanobody (ER_{pro}:*NSImb-vhhGFP4* in ER_{pro}:*ER-YPet er erl1 erl2*; D). Scale bar, 1 cm. See also Figure S3. (E) Egg cell-specific expression of the anti-GFP nanobody ($EC1_{pro}$:*NSImb-vhhGFP4*) in the ER_{pro}:*ER-YPet er erl1 erl2* plant leads to reduced zygote length. Boxplot diagram of zygote elongation. Boxplot data presentation as described in Figure 1. Different letters above boxes refer to individual groups in a one-way ANOVA with a post hoc Tukey test ($p < 0.05$).

Different mechanisms that cause maternal effects on plant embryogenesis including inheritance of cytoplasmic factors have been proposed more than two decades ago.[27] Furthermore, sporophytic maternal effects have previously been identified in the mutant *sin1-2* allele of the SHORT INTEGUMENTS 1 (SIN1)/DICER-LIKE 1 (DCL1) gene.[28,29] A comprehensive survey of essential genes in *Arabidopsis* showed that many mutations in essential genes can be transmitted through the female germline and only become deleterious in the early embryo.[30] This suggests that genetic compensation by premeiotic gene products prevents lethality in the female gametophyte for many essential genes and might therefore not be a rare event.[30]

BSK1 and BSK2 have been shown to act upstream of YDA, presumably linking ERECTA signaling with YDA activation.[5] Reciprocal crosses with *bsk1 bsk2* double mutants and wild type showed similar sporophytic maternal effects as observed for *er* (Figure S4). As maternal effects have been described for mutations in genes acting downstream of YDA,[31,32] not just *ER* but several components of this signaling pathway appear to be under maternal sporophytic control. This is quite intriguing, as the non-canonical BSK family member SSP activates YDA as paternal factor contributed by the sperm cell.[13] SSP has been shown to resemble a naturally occurring, constitutively active form of BSK that directly interacts with YDA via its TPR motif.[5] This raises the question of whether the two parental contributions to YDA activation can function independently. We tested this hypothesis in seedlings, where ectopic expression of *SSP* leads to constitutive activation of the YDA pathway[5,13] resulting in cotyledons lacking mature stomata. This was also observed for *SSP* expression in *er erl1 erl2* triple-mutant background, indicating that SSP can activate YDA in the absence of a functional receptor complex (Figure 4A). Overexpression of *BSK1* in *bsk1 bsk2* double-mutant background rescued the *bsk1 bsk2* phenotype, indicating that the construct is functional. In contrast to *SSP*, however, it failed to rescue the *er erl1 erl2* triple-mutant phenotype, despite having similar or higher transcript levels when compared to $35S_{pro}$:*SSP* (Figures 4B and 4C).

If SSP serves as an independent signal for YDA activation in the zygote, loss of *SSP* should have an additive effect to loss of *ER* function. The further loss of *SSP* in *er erl1* and *er erl2* mutants indeed led to further reduction in zygote length and an almost complete loss of zygote polarity (Figures 2 and S2), indicating that *SSP* provides additional YDA activation independently of *ER* function. If the embryonic YDA pathway indeed relies on two independent signaling inputs, additional SSP activity should compensate for the loss of ER function. To test this, we introduced an additional copy of *SSP* (SSP_{pro}:*SSP-YFP*) in the *er erl2* double mutant and found that additional *SSP* activity indeed partially rescued the loss-of-function phenotype of *er erl2* (Figure 4D).

Taken together, our data outline a signaling pathway (Figure 4E) with a maternally controlled receptor complex and a paternally provided activating protein that converge at the level of MAP3K activation. *SSP* is a *Brassicaceae*-specific gene while *ER*, *BSK1*, and *BSK2* are evolutionarily conserved in flowering plants.[33,34] *SSP* has been shown to be critical for correct suspensor development,[13] an organ that serves as a conduit for nutrients to the embryo,[3] and for rapid development of the embryo.[2] Therefore, suspensor development could be a possible target of a parental conflict over nutrient allocation to the embryo.[35] It has recently been observed that there are preferentially maternal expressed genes in the suspensor while there is mainly biparental expression in descendants of the apical cell.[36] This maternal bias in the suspensor could be interpreted in the context of the parental conflict theory enforcing equal nutrient distribution to all embryos by the maternal genome.[35] In this context, it might be significant that ER function is under sporophytic control as the sporophytic maternal effect would ensure uniform suspensor development of all embryos irrespective of segregating maternal alleles. In this scenario, *SSP* could be seen as a *Brassicaceae*-specific paternal contribution that circumvents the maternal control of suspensor development, bypassing ERECTA signaling as a strong independent activator of the YDA pathway.

This raises the question if suspensor development in other plant species is also under maternal control and whether the two independent inputs for YDA activation indeed are part of a parental tug-of-war over nutrient allocation to the embryo. Or are *Brassicaceae* shifting from ligand-/receptor-based zygote polarization to a sperm-based activation mechanism via SSP to fine-tune the timing of YDA activation as SSP naturally links fertilization with YDA activation?

The receptor kinase ER implies extra-cellular ligands in the control of zygote polarization, and the known ESF1 peptides are prime candidates. However, at present it is unclear if they have a function in zygote polarization or influence suspensor development after zygote polarization.[7] Future research will be needed to address the question of where the ligand for the ER

Please cite this article in press as: Wang et al., Independent parental contributions initiate zygote polarization in *Arabidopsis thaliana*, Current Biology (2021), https://doi.org/10.1016/j.cub.2021.08.033

Current Biology
Report

CellPress

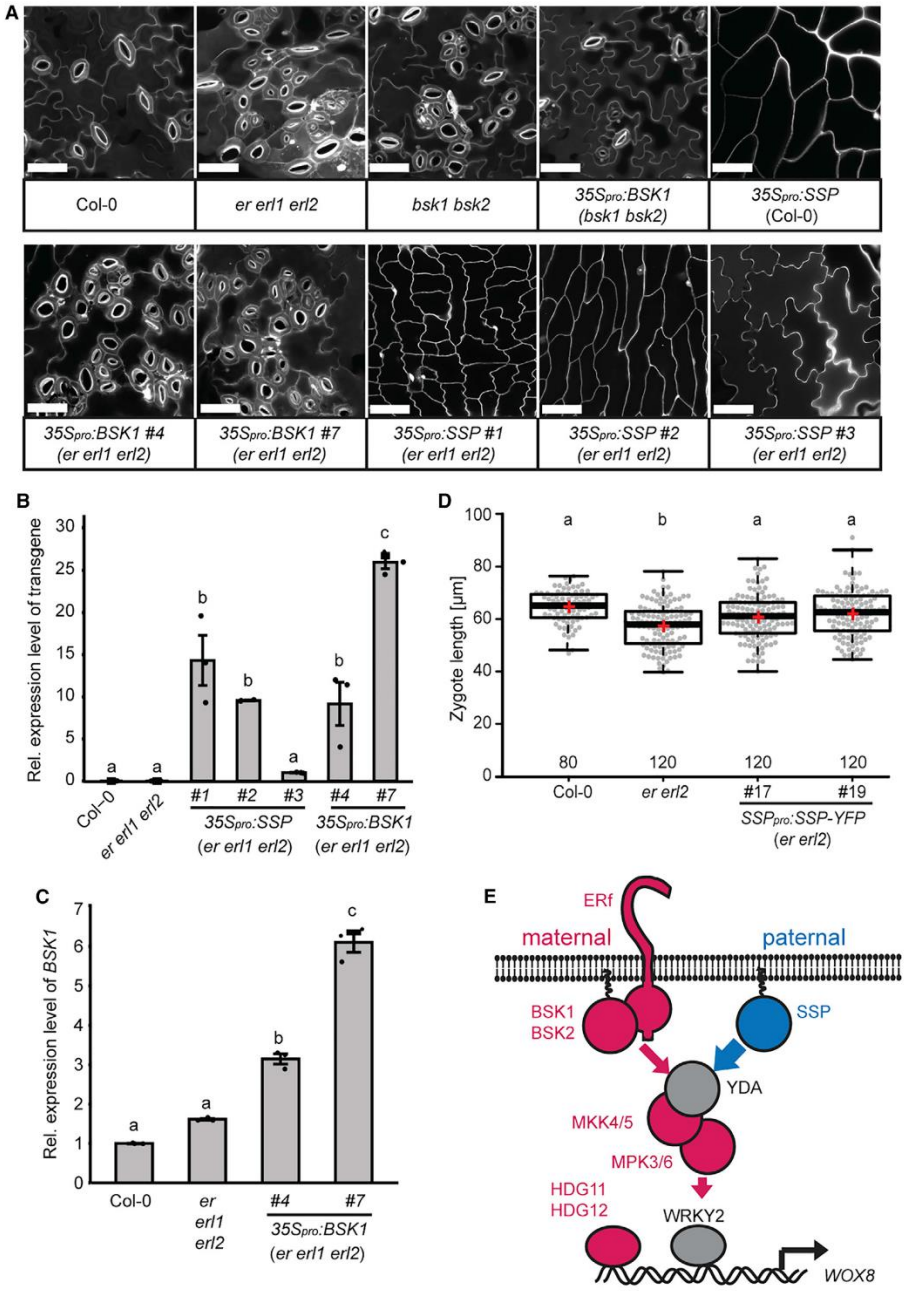

Figure 4. Independent parental contributions to YDA activation in the zygote

(A) Maximum projections of epidermal confocal images. Genotypes are given under each figure panel. Cell walls are stained with propidium iodide. Scale bar, 20 μm.

(B) Expression level of *35S$_{pro}$:SSP* and *35S$_{pro}$:BSK1* in *er erl1 erl2* seedlings shown in (A) as determined by qRT-PCR. Bar graph shows mean values of three technical replicates with standard error.

(legend continued on next page)

Please cite this article in press as: Wang et al., Independent parental contributions initiate zygote polarization in *Arabidopsis thaliana*, Current Biology (2021), https://doi.org/10.1016/j.cub.2021.08.033

receptor kinase is originating and how conserved this mode of zygote polarization is in land plants.

STAR★METHODS

Detailed methods are provided in the online version of this paper and include the following:

- KEY RESOURCES TABLE
- RESOURCE AVAILABILITY
  - Lead contact
  - Materials availability
  - Data and code availability
- EXPERIMENTAL MODEL AND SUBJECT DETAILS
- METHOD DETAILS
  - Mutant lines
  - Genotyping
  - Plasmid construction
  - Transgenic plants
  - DIC and Confocal microscopy
  - RNA *in situ* hybridization
  - Quantitative RT-PCR analysis
  - Phenotypic analysis of rosette leaves
  - RNA stability
- QUANTIFICATION AND STATISTICAL ANALYSIS
  - Measurement of zygote/suspensor length
  - Statistical analysis

SUPPLEMENTAL INFORMATION

Supplemental information can be found online at https://doi.org/10.1016/j.cub.2021.08.033.

ACKNOWLEDGMENTS

We would like to thank Gerd Jürgens for helpful discussions and comments on the manuscript. We also thank the Salk Institute Genomic Analysis Laboratory as well as the Nottingham *Arabidopsis* Stock Centre (NASC) for providing the sequence-indexed *Arabidopsis* tDNA insertion mutants and the Light Microscopy Facility at the Max Planck Institute for Developmental Biology for support. Research in our groups is supported by the German Research Foundation (Deutsche Forschungsgemeinschaft - DFG SFB1101/B01 to M.B. and SFB1101/B07 to J.U.L.), the Chinese Scholarship Council (fellowship no. 201806320131 to Y. Miao), and the Max Planck Society.

AUTHOR CONTRIBUTIONS

K.W. and M.B. designed the study with critical comments and modifications by H.C., M.O.-P., Y. Miao, Y. Ma, J.U.L., and S.L. K.W., H.C., M.O.-P., Y. Miao, and A.H. performed the experiments. K.W., H.C., M.O.-P., Y. Miao, Y. Ma, A.H., J.U.L., S.L., and M.B. evaluated the data and interpreted the experimental results. K.W. and M.B. wrote the initial manuscript draft, and all authors commented on and edited the manuscript.

DECLARATION OF INTERESTS

The authors declare no competing interests.

Received: March 26, 2021
Revised: July 9, 2021
Accepted: August 11, 2021
Published: September 7, 2021

REFERENCES

1. Wang, K., Chen, H., Miao, Y., and Bayer, M. (2020). Square one: zygote polarity and early embryogenesis in flowering plants. Curr. Opin. Plant Biol. *53*, 128–133.
2. Babu, Y., Musielak, T., Henschen, A., and Bayer, M. (2013). Suspensor length determines developmental progression of the embryo in Arabidopsis. Plant Physiol. *162*, 1448–1458.
3. Kawashima, T., and Goldberg, R.B. (2010). The suspensor: not just suspending the embryo. Trends Plant Sci. *15*, 23–30.
4. Lukowitz, W., Roeder, A., Parmenter, D., and Somerville, C. (2004). A MAPKK kinase gene regulates extra-embryonic cell fate in Arabidopsis. Cell *116*, 109–119.
5. Neu, A., Eilbert, E., Asseck, L.Y., Slane, D., Henschen, A., Wang, K., Bürgel, P., Hildebrandt, M., Musielak, T.J., Kolb, M., et al. (2019). Constitutive signaling activity of a receptor-associated protein links fertilization with embryonic patterning in *Arabidopsis thaliana*. Proc. Natl. Acad. Sci. USA *116*, 5795–5804.
6. Kim, T.W., and Wang, Z.Y. (2010). Brassinosteroid signal transduction from receptor kinases to transcription factors. Annu. Rev. Plant Biol. *61*, 681–704.
7. Costa, L.M., Marshall, E., Tesfaye, M., Silverstein, K.A., Mori, M., Umetsu, Y., Otterbach, S.L., Papareddy, R., Dickinson, H.G., Boutiller, K., et al. (2014). Central cell-derived peptides regulate early embryo patterning in flowering plants. Science *344*, 168–172.
8. Torii, K.U., Mitsukawa, N., Oosumi, T., Matsuura, Y., Yokoyama, R., Whittier, R.F., and Komeda, Y. (1996). The Arabidopsis ERECTA gene encodes a putative receptor protein kinase with extracellular leucine-rich repeats. Plant Cell *8*, 735–746.
9. Bergmann, D.C., Lukowitz, W., and Somerville, C.R. (2004). Stomatal development and pattern controlled by a MAPKK kinase. Science *304*, 1494–1497.
10. Shpak, E.D., McAbee, J.M., Pillitteri, L.J., and Torii, K.U. (2005). Stomatal patterning and differentiation by synergistic interactions of receptor kinases. Science *309*, 290–293.
11. Shpak, E.D., Berthiaume, C.T., Hill, E.J., and Torii, K.U. (2004). Synergistic interaction of three ERECTA-family receptor-like kinases controls Arabidopsis organ growth and flower development by promoting cell proliferation. Development *131*, 1491–1501.
12. Meng, X., Wang, H., He, Y., Liu, Y., Walker, J.C., Torii, K.U., and Zhang, S. (2012). A MAPK cascade downstream of ERECTA receptor-like protein kinase regulates Arabidopsis inflorescence architecture by promoting localized cell proliferation. Plant Cell *24*, 4948–4960.
13. Bayer, M., Nawy, T., Giglione, C., Galli, M., Meinnel, T., and Lukowitz, W. (2009). Paternal control of embryonic patterning in Arabidopsis thaliana. Science *323*, 1485–1488.

(C) Expression level of *BSK1* in Col-0, *er erl1 erl2*, and $35S_{pro}$:*BSK1 er erl1 erl2* seedlings. Bar graph shows mean values of three technical replicates with standard error.
(D) An additional copy of *SSP* (SSP_{pro}:*SSP-YFP*) partially rescues the *er erl2* loss-of-function phenotype in the zygote. The boxplot diagram shows zygote length. Boxplot data presentation as described in Figure 1.
Different letters above bars and boxes in (B)–(D) refer to individual groups in a one-way ANOVA with a post hoc Tukey test ($p < 0.05$).
(E) Simplified schematic depiction of the embryonic YDA pathway. YDA is activated by the maternally supplied receptor complex consisting of ER and the membrane-associated proteins BSK1 and BSK2. YDA is also activated by the paternally contributed BSK family member SSP. Signaling components are colored according to genetic contribution: maternal effect (magenta), paternal effect (blue), and zygotic recessive (gray).

Please cite this article in press as: Wang et al., Independent parental contributions initiate zygote polarization in *Arabidopsis thaliana*, Current Biology (2021), https://doi.org/10.1016/j.cub.2021.08.033

14. Zhao, P., Zhou, X., Shen, K., Liu, Z., Cheng, T., Liu, D., Cheng, Y., Peng, X., and Sun, M.X. (2019). Two-step maternal-to-zygotic transition with two-phase parental genome contributions. Dev. Cell *49*, 882–893.e5.
15. Del Toro-De León, G., García-Aguilar, M., and Gillmor, C.S. (2014). Non-equivalent contributions of maternal and paternal genomes to early plant embryogenesis. Nature *514*, 624–627.
16. Qi, X., Han, S.K., Dang, J.H., Garrick, J.M., Ito, M., Hofstetter, A.K., and Torii, K.U. (2017). Autocrine regulation of stomatal differentiation potential by EPF1 and ERECTA-LIKE1 ligand-receptor signaling. eLife *6*, e24102.
17. Ho, C.M., Paciorek, T., Abrash, E., and Bergmann, D.C. (2016). Modulators of stomatal lineage signal transduction alter membrane contact sites and reveal specialization among ERECTA kinases. Dev. Cell *38*, 345–357.
18. Shpak, E.D. (2013). Diverse roles of ERECTA family genes in plant development. J. Integr. Plant Biol. *55*, 1238–1250.
19. Hara, K., Kajita, R., Torii, K.U., Bergmann, D.C., and Kakimoto, T. (2007). The secretory peptide gene EPF1 enforces the stomatal one-cell-spacing rule. Genes Dev. *21*, 1720–1725.
20. Zoulias, N., Harrison, E.L., Casson, S.A., and Gray, J.E. (2018). Molecular control of stomatal development. Biochem. J. *475*, 441–454.
21. Robert, H.S., Park, C., Gutièrrez, C.L., Wójcikowska, B., Pěnčík, A., Novák, O., Chen, J., Grunewald, W., Dresselhaus, T., Friml, J., and Laux, T. (2018). Maternal auxin supply contributes to early embryo patterning in Arabidopsis. Nat. Plants *4*, 548–553.
22. Ueda, M., Zhang, Z., and Laux, T. (2011). Transcriptional activation of Arabidopsis axis patterning genes WOX8/9 links zygote polarity to embryo development. Dev. Cell *20*, 264–270.
23. Szabo, E.X., Reichert, P., Lehniger, M.K., Ohmer, M., de Francisco Amorim, M., Gowik, U., Schmitz-Linneweber, C., and Laubinger, S. (2020). Metabolic labeling of RNAs uncovers hidden features and dynamics of the Arabidopsis transcriptome. Plant Cell *32*, 871–887.
24. Caussinus, E., Kanca, O., and Affolter, M. (2011). Fluorescent fusion protein knockout mediated by anti-GFP nanobody. Nat. Struct. Mol. Biol. *19*, 117–121.
25. Ma, Y., Miotk, A., Šutiković, Z., Ermakova, O., Wenzl, C., Medzihradszky, A., Gaillochet, C., Forner, J., Utan, G., Brackmann, K., et al. (2019). WUSCHEL acts as an auxin response rheostat to maintain apical stem cells in Arabidopsis. Nat. Commun. *10*, 5093.
26. Sprunck, S., Rademacher, S., Vogler, F., Gheyselinck, J., Grossniklaus, U., and Dresselhaus, T. (2012). Egg cell-secreted EC1 triggers sperm cell activation during double fertilization. Science *338*, 1093–1097.
27. Grossniklaus, U., and Schneitz, K. (1998). The molecular and genetic basis of ovule and megagametophyte development. Semin. Cell Dev. Biol. *9*, 227–238.
28. Ray, S., Golden, T., and Ray, A. (1996). Maternal effects of the short integument mutation on embryo development in Arabidopsis. Dev. Biol. *180*, 365–369.
29. Golden, T.A., Schauer, S.E., Lang, J.D., Pien, S., Mushegian, A.R., Grossniklaus, U., Meinke, D.W., and Ray, A. (2002). SHORT INTEGUMENTS1/SUSPENSOR1/CARPEL FACTORY, a Dicer homolog, is a maternal effect gene required for embryo development in Arabidopsis. Plant Physiol. *130*, 808–822.
30. Muralla, R., Lloyd, J., and Meinke, D. (2011). Molecular foundations of reproductive lethality in Arabidopsis thaliana. PLoS ONE *6*, e28398.
31. Zhang, M., Wu, H., Su, J., Wang, H., Zhu, Q., Liu, Y., Xu, J., Lukowitz, W., and Zhang, S. (2017). Maternal control of embryogenesis by MPK6 and its upstream MKK4/MKK5 in Arabidopsis. Plant J. *92*, 1005–1019.
32. Ueda, M., Aichinger, E., Gong, W., Groot, E., Verstraeten, I., Vu, L.D., De Smet, I., Higashiyama, T., Umeda, M., and Laux, T. (2017). Transcriptional integration of paternal and maternal factors in the *Arabidopsis* zygote. Genes Dev. *31*, 617–627.
33. Liu, S.L., and Adams, K.L. (2010). Dramatic change in function and expression pattern of a gene duplicated by polyploidy created a paternal effect gene in the Brassicaceae. Mol. Biol. Evol. *27*, 2817–2828.
34. Caine, R.S., Chater, C.C., Kamisugi, Y., Cuming, A.C., Beerling, D.J., Gray, J.E., and Fleming, A.J. (2016). An ancestral stomatal patterning module revealed in the non-vascular land plant Physcomitrella patens. Development *143*, 3306–3314.
35. Haig, D. (1987). Kin conflict in seed plants. Trends Ecol. Evol. *2*, 337–340.
36. Zhao, P., Zhou, X., Zheng, Y., Ren, Y., and Sun, M.X. (2020). Equal parental contribution to the transcriptome is not equal control of embryogenesis. Nat. Plants *6*, 1354–1364.
37. Van Larebeke, N., Engler, G., Holsters, M., Van den Elsacker, S., Zaenen, I., Schilperoort, R.A., and Schell, J. (1974). Large plasmid in Agrobacterium tumefaciens essential for crown gall-inducing ability. Nature *252*, 169–170.
38. Scholl, R.L., May, S.T., and Ware, D.H. (2000). Seed and molecular resources for Arabidopsis. Plant Physiol. *124*, 1477–1480.
39. Mcelroy, D., Chamberlain, D.A., Moon, E., and Wilson, K.J. (1995). Development of gusa reporter gene constructs for cereal transformation - availability of plant transformation vectors from the Cambia Molecular-Genetic Resource Service. Mol. Breed. *1*, 27–37.
40. Hajdukiewicz, P., Svab, Z., and Maliga, P. (1994). The small, versatile pPZP family of Agrobacterium binary vectors for plant transformation. Plant Mol. Biol. *25*, 989–994.
41. Spitzer, M., Wildenhain, J., Rappsilber, J., and Tyers, M. (2014). BoxPlotR: a web tool for generation of box plots. Nat. Methods *11*, 121–122.
42. Schneider, C.A., Rasband, W.S., and Eliceiri, K.W. (2012). NIH Image to ImageJ: 25 years of image analysis. Nat. Methods *9*, 671–675.
43. Murashige, T., and Skoog, F. (1962). A revised medium for rapid growth and bio assays with tobacco tissue cultures. Physiol. Plant. *15*, 473–497.
44. Musielak, T.J., Schenkel, L., Kolb, M., Henschen, A., and Bayer, M. (2015). A simple and versatile cell wall staining protocol to study plant reproduction. Plant Reprod. *28*, 161–169.
45. Musielak, T.J., Bürgel, P., Kolb, M., and Bayer, M. (2016). Use of SCRI Renaissance 2200 (SR2200) as a versatile dye for imaging of developing embryos, whole ovules, pollen tubes and roots. Bio. Protoc. *6*, e1935.
46. Mayer, K.F., Schoof, H., Haecker, A., Lenhard, M., Jürgens, G., and Laux, T. (1998). Role of WUSCHEL in regulating stem cell fate in the Arabidopsis shoot meristem. Cell *95*, 805–815.
47. Pillitteri, L.J., Bemis, S.M., Shpak, E.D., and Torii, K.U. (2007). Haploinsufficiency after successive loss of signaling reveals a role for ERECTA-family genes in Arabidopsis ovule development. Development *134*, 3099–3109.
48. Slane, D., Kong, J., Berendzen, K.W., Kilian, J., Henschen, A., Kolb, M., Schmid, M., Harter, K., Mayer, U., De Smet, I., et al. (2014). Cell type-specific transcriptome analysis in the early Arabidopsis thaliana embryo. Development *141*, 4831–4840.
49. Czechowski, T., Stitt, M., Altmann, T., Udvardi, M.K., and Scheible, W.R. (2005). Genome-wide identification and testing of superior reference genes for transcript normalization in Arabidopsis. Plant Physiol. *139*, 5–17.
50. Livak, K.J., and Schmittgen, T.D. (2001). Analysis of relative gene expression data using real-time quantitative PCR and the 2(-Delta Delta C(T)) method. Methods *25*, 402–408.

Please cite this article in press as: Wang et al., Independent parental contributions initiate zygote polarization in *Arabidopsis thaliana*, Current Biology (2021), https://doi.org/10.1016/j.cub.2021.08.033

STAR★METHODS

KEY RESOURCES TABLE

REAGENT or RESOURCE	SOURCE	IDENTIFIER
Bacterial and virus strains		
Stellar competent cells	Takara	Cat#636763
Agrobacterium tumefaciens GV3101	[37]	N/A
Chemicals, peptides, and recombinant proteins		
Murashige and Skoog Plant Salts	SERVA	Cat#47516.03
Propidium iodide	SIGMA-ALDRICH	Cat#P4170
SCRI Renaissance 2200	Renaissance Chemicals Ltd	N/A
Triton X-100	Carl Roth GmbH	Cat#3051.1
Glycerol	SIGMA-ALDRICH	Cat#G5516
Para-formaldehyde	SIGMA-ALDRICH	Cat#P6148
GUM arabic	SIGMA-ALDRICH	Cat#G9752
Chloral hydrat	Carl Roth GmbH	Cat#K318.1
Digoxigenin-11-UTP	Roche	Cat#11209256910
Anti-Digoxigenin-AP	Roche	Cat#11093274910; RRID: AB_514497
DIG-labeled Control	Roche	Cat#11585746910
Protease (Pronase)	SIGMA-ALDRICH	Cat#73702
T7 Polymerase	Thermo Scientific	Cat#EP0111
Q5 High-Fidelity DNA polymerase Kit	NEW ENGLAND BioLabs	Cat#M0491
In-Fusion HD Cloning Kit	TAKARA	Cat#639650
Dream Taq Green PCR Master Mix	Thermo Scientific	Cat#K1081
RNeasy Plant Mini Kit	QIAGEN	Cat#74904
RevertAid First Strand cDNA Synthesis Kit	Thermo Scientific	Cat#K1622
Luna Universal qPCR Master Mix	NEW ENGLAND BioLabs	Cat#M3003
Phosphinothricin	SIGMA-ALDRICH	Cat#45520
Hygromycin B	Carl Roth GmbH	Cat#CP13.1
Experimental models: Organisms/strains		
Arabidopsis thaliana: Col-0	N/A	N/A
Arabidopsis thaliana: er	[5]	SALK_066455
Arabidopsis thaliana: erl1	[5]	GK_109G04
Arabidopsis thaliana: erl2	[5]	GK_486E03
Arabidopsis thaliana: YDA/yda-11	NASC[38]	SALK_078777
Arabidopsis thaliana: bsk1-2	[5]	SALK_122120
Arabidopsis thaliana: bsk2-2	[5]	SALK_001600
Arabidopsis thaliana: BSK1/bsk1 bsk2	[5]	N/A
Arabidopsis thaliana: ssp-2	[13]	SALK_051462
Arabidopsis thaliana: er erl1	This paper	N/A
Arabidopsis thaliana: er erl2	This paper	N/A
Arabidopsis thaliana: erl1 erl2	This paper	N/A
Arabidopsis thaliana: er erl1 erl2	[5]	N/A
Arabidopsis thaliana: ER/er erl1	This paper	N/A
Arabidopsis thaliana: ER/er erl1 erl2	This paper	N/A
Arabidopsis thaliana: er ERL1/erl1 erl2	[5]	N/A
Arabidopsis thaliana: er erl1 ssp	This paper	N/A
Arabidopsis thaliana: ER_{pro}*:3xVenus-N7*	This paper	N/A
Arabidopsis thaliana: ER_{pro}*:ER-YPet; er erl1 erl2*	This paper	N/A
Arabidopsis thaliana: YDA_{pro}*:yda-CA*	This paper	N/A

(*Continued on next page*)

Please cite this article in press as: Wang et al., Independent parental contributions initiate zygote polarization in *Arabidopsis thaliana*, Current Biology (2021), https://doi.org/10.1016/j.cub.2021.08.033

Continued

REAGENT or RESOURCE	SOURCE	IDENTIFIER
Arabidopsis thaliana: YDA_{pro}:yda-CA; er erl2	This paper	N/A
Arabidopsis thaliana: ER_{pro}:NSlmb-vhhGFP4; ER_{pro}:ER-YPet; er erl1 erl2	This paper	N/A
Arabidopsis thaliana: $EC1_{pro}$:NSlmb-vhhGFP4; ER_{pro}:ER-YPet; er erl1 erl2	This paper	N/A
Arabidopsis thaliana: $35S_{pro}$:BSK1; bsk1 bsk2	This paper	N/A
Arabidopsis thaliana: $35S_{pro}$:BSK1; er erl1 erl2	This paper	N/A
Arabidopsis thaliana: $35S_{pro}$:SSP	This paper	N/A
Arabidopsis thaliana: $35S_{pro}$:SSP; er erl1 erl2	This paper	N/A
Arabidopsis thaliana: SSP_{pro}:SSP-YFP; er erl2	This paper	N/A
Oligonucleotides		
Listed in Table S4	This paper	N/A
Recombinant DNA		
pCambia 3300	[39,40]	N/A
pCambia 1300	[39,40]	N/A
pBay-bar	[5]	N/A
pBay-hyg	[5]	N/A
ER_{pro}:3xVenus-N7	This paper	N/A
ER_{pro}:ER-YPet	This paper	N/A
YDA_{pro}:yda-CA	[4]	N/A
ER_{pro}:NSlmb-vhhGFP4	This paper	N/A
$EC1_{pro}$:NSlmb-vhhGFP4	This paper	N/A
$35S_{pro}$:BSK1	This paper	N/A
$35S_{pro}$:SSP	This paper	N/A
SSP_{pro}:SSP-YFP	[5,13]	N/A
Software and algorithms		
R version 3.6.1	N/A	https://www.r-project.org/
R: multcompView package	N/A	https://cran.r-project.org/web/packages/multcompView/index.html
Adobe Illustrator CS6	Adobe	https://www.adobe.com/products/illustrator.html
Adobe Photoshop CS6	Adobe	https://www.adobe.com/products/photoshop.html
BoxPlotR	[41]	http://shiny.chemgrid.org/boxplotr/
ImageJ 1.52p	[42]	https://imagej.nih.gov/ij/
ZEN 2.0 blue edition	ZEISS	https://www.zeiss.de/messtechnik/produkte/software.html
AxioVision 4	ZEISS	https://www.micro-shop.zeiss.com/en/de/softwarefinder/

RESOURCE AVAILABILITY

Lead contact

Further information and requests for resources and reagents should be directed to and will be fulfilled by the lead contact, Martin Bayer (martin.bayer@tuebingen.mpg.de).

Materials availability

All plasmids and *Arabidopsis* lines generated in this study are available from the Lead Contact without restrictions.

Data and code availability

All data reported in this paper will be shared by the lead contact upon request. This paper does not report original code. Any additional information required to reanalyze the data reported in this paper is available from the lead contact upon request.

Please cite this article in press as: Wang et al., Independent parental contributions initiate zygote polarization in *Arabidopsis thaliana*, Current Biology (2021), https://doi.org/10.1016/j.cub.2021.08.033

CellPress

Current Biology
Report

EXPERIMENTAL MODEL AND SUBJECT DETAILS

All *Arabidopsis thaliana* mutant and transgenic lines used in this study are in Col-0 background. Seeds were washed with 70% (v/v) ethanol for 5 min, followed by washing with 100% ethanol for 1 min. Then seeds were dried under clean bench. Surface-sterilized seeds were stratified at 4°C in dark for 2 days on half-strength Murashige and Skoog (½ MS) medium containing 1% (w/v) sucrose and 1% (w/v) agar (pH = 5.7)[43] then transferred to long-day conditions (16 h at 3000 photons per square meter per second, 8 h at dark) at 23°C for 1-2 weeks in custom-built walk-in growth chambers (Induplan, 8118140). Afterward, seedlings were transferred to soil and were grown under long-day conditions (16 h at 80 micromoles per square meter per second, 8 h at dark) at 23°C and 65% relative humidity as described before.[2] Mature seeds were harvested in seed bags and stored at room temperature.

METHOD DETAILS

Mutant lines

The *ssp-2* (SALK_051462), *bsk1-2* (SALK_122120), *bsk2-2* (SALK_001600), *er* (SALK_066455), *erl1* (GK_109G04), *erl2* (GK_486E03)[5,13] have been described previously. The *yda-11* (SALKseq_078777) allele in Col-0 background carries a T-DNA insertion in the second exon. As the truncated gene product lacks essential parts of the YDA coding region[4] and the mutant phenotype is similar to *yda-1*,[4] the *yda-11* presumably represents a null allele. Insertion lines were provided by the Nottingham *Arabidopsis* Stock Center (NASC).[38] *bsk1 bsk2* double mutant, *er ERL1/erl1 erl2* and *er erl1 erl2* triple mutants have been described before.[3] All other homozygous or heterozygous multiple mutant combinations were obtained by crossing. Crosses were performed by manual dissection of anthers before anthesis, followed by manual pollination approximately 24 h later.

Genotyping

For genotyping of mutant plants, PCR was performed with Dream Taq Green PCR Master Mix (Thermo Scientific). Gene-specific primers (LP and RP; Table S4) were used for the wild-type allele. Left border primers in combination with a gene-specific primer (RP) were used to detect the insertion allele. Segregation analysis of *ER/er erl1 erl2*, *er ERL1/erl1 erl2* and *BSK1/bsk1 bsk2* was based on counting the number of strong dwarfed mutant seedlings (phenotype of the *er erl1 erl2* triple homozygous and *bsk1 bsk2* double mutant seedlings) in the offspring.

Plasmid construction

Q5 High-Fidelity DNA polymerase Kit (NEW ENGLAND BioLabs) was used to clone DNA fragments from *Arabidopsis* Col-0. Plasmid construction was performed by in-fusion cloning using In-Fusion HD Cloning Kit (TAKARA) and transformed into Stellar competent cell (TAKARA). Oligonucleotide sequences for molecular cloning are summarized in Table S4. For plant transformation, transgenes were constructed in pCambia 3300[39] as well as pBay-bar and pBay-hyg binary vectors.[5] pBay-bar and pBay-hyg are modified versions of the pCambia binary vectors pCambia 3300 and pCambia 1300,[39] respectively. pCambia 3300 and pCambia 1300 (https://cambia.org) were modified from pPZP vectors.[40] In pBay-bar and pBay-hyg, the T-DNA has been replaced by a synthetic DNA fragment harboring unique restriction enzyme sites as well as plant codon-optimized selectable marker genes (conferring phosphinothricin and hygromycin resistance, respectively) under control of the *Arabidopsis RPL10A* promoter (−960 bp to +287 bp of At1g14320 including the first intron).[5] To generate ER_{pro}*:3xVenus-N7*, a 1934 bp genomic region immediately upstream of the start codon of *ER* was transcriptionally fused with the coding region of 3 copies of Venus *YFP* with a C-terminal N7 nuclear localization sequence and *UBQ10* terminator in pCambia 3300. ER_{pro}*:ER-YPet* contains a fragment of the *ER* locus including a 1934 bp region upstream of the start codon and the genomic sequence. The *ER* genomic sequence was fused in-frame at the 3′ end with the sequence of *YPet YFP* and *UBQ10* terminator. To generate ER_{pro}*:NSlmb-vhhGFP4*, the *ER-YPet* sequence in ER_{pro}*:ER-YPet* was replaced by the *NSlmb-vhhGFP4* coding sequence,[25] and the whole cassette was introduced into pBay-hyg. For $EC1_{pro}$*:NSlmb-vhhGFP4*, a 465 bp region of *EC1.1* was fused with *NSlmb-vhhGFP4* in pBay-hyg. To generate $35S_{pro}$*:BSK1* and $35S_{pro}$*:SSP*, *BSK1* CDS and *SSP* CDS, respectively, were fused with 2x 35S promoter and 35S terminator in pBay-bar backbone. SSP_{pro}*:SSP-YFP and* YDA_{pro}*:yda-CA* have been described previously.[4,13] In SSP_{pro}*:SSP-YFP*, 6630 bp *SSP* 5′ UTR, whole *SSP* genomic sequence and 153 bp *SSP* 3′ UTR of *SSP* were cloned to pCambia 3300. Citrine YFP sequence was fused in between the kinase domain sequence and TPR domain sequence of *SSP*. In YDA_{pro}*:yda-CA*, 3762 bp *YDA* 5′ UTR and 1217 *YDA* 3′ UTR were fused with truncated *YDA* genomic sequence in pCambia 3300. The truncated *YDA* genomic sequence contains a 447 bp deletion (+650 bp to +1096 bp) in the second exon.

Transgenic plants

All initial transgenic plants were transformed by floral dip using *Agrobacterium tumefaciens* GV3101.[37] ER_{pro}*:3xVenus-N7* was transformed into Col-0. ER_{pro}*:ER-YPet*, $35S_{pro}$*:BSK1* and $35S_{pro}$*:SSP* were transformed into *er erl1/ERL1 erl2* plants. $35S_{pro}$*:BSK1* and $35S_{pro}$*:SSP* were also transformed into *BSK1/bsk1 bsk2* and Col-0, respectively. YDA_{pro}*:yda-CA* and SSP_{pro}*:SSP-YFP* were transformed into *er erl2*. T_1 transgenic seedlings of these constructs were screened on $^3/_4$ $^3/_4$ $^3/_4$ MS plates containing 1% (w/v) sucrose and 50 mg/L phosphinothricin. ER_{pro}*:NSlmb-vhhGFP4* and $EC1_{pro}$*:NSlmb-vhhGFP4* in pBay-hyg were transformed into ER_{pro}*:ER-YPet #4* in *er erl1 erl2*, and T_1 seedlings were screened on $^3/_4$ $^3/_4$ $^3/_4$ MS plates containing 1% (w/v) sucrose, 50 mg/L phosphinothricin

Please cite this article in press as: Wang et al., Independent parental contributions initiate zygote polarization in *Arabidopsis thaliana*, Current Biology (2021), https://doi.org/10.1016/j.cub.2021.08.033

Current Biology
Report

CellPress

and 20 mg/L hygromycin. T_3 plants were used for phenotypic analyses, except for *35S$_{pro}$:SSP*, *35S$_{pro}$:SSP er erl1 erl2* and *35S$_{pro}$:BSK1 er erl1 erl2*, where T_1 seedlings were directly used because of sterility of the transgenic plants. Two independent transgenic lines of *YDA$_{pro}$:yda-CA* in *er erl2* (*#16* and *#19*) were crossed with Col-0 and offspring homozygous for the *ER ERL2* wild-type alleles were selected in the F2 generation. Transgene expression was determined by RT-PCR using M13rev and transgene-specific reverse primers (listed in Table S4).

DIC and Confocal microscopy

For differential interference contrast (DIC) imaging, ovules were dissected by hand and incubated overnight in Hoyer's solution (7.5g gum arabic, 5 mL glycerol, 100 g chloral hydrate and 30 mL water, diluted 2:1 with 10% (w/v) gum arabic solution). DIC images were taken with a Zeiss Axio Imager. Z1 microscope equipped with AxioCam HRc camera and AxioVision 4 software as described before.[5] Confocal microscopy was conducted with a Zeiss LSM 780 NLO microscope with ZEN 2.0 blue edition. SCRI Renaissance 2200 (SR2200) staining were performed according to published protocols[44,45] and confocal images were obtained with excitation at 405 nm and detection wavelength from 415 nm to 475 nm. For SR2200 staining of early ovules containing developing megaspore mother cell, early ovules were incubated in SR2200 solution (0.1% (v/v) SR2200, 1% (v/v) DMSO, 0.05% (w/v) Triton X-100, 5% (w/v) glycerol, 4% (w/v) para-formaldehyde in PBS buffer, pH 8.0) for 5 min. Then ovules were washed with water once and incubated in 5% (w/v) glycerol for imaging. For SR2200 staining of ovules containing megaspores or mature female gametes, both incubation and washing steps were performed with gentle vacuum to have a better staining. For YFP imaging, a 514 nm laser wavelength was used for excitation, a wavelength between 526 nm and 553 nm was recorded. For propidium iodide (PI) staining, cotyledons of seedlings (5 days after germination) were dissected and incubated in 10mg/L PI solution in water for 30 min, followed by brief washing with water. Afterward, cotyledons were transferred to microscopy slides and the abaxial side was imaged. PI fluorescence was detected from 571 nm to 656 nm with an excitation wavelength of 561 nm.

RNA *in situ* hybridization

RNA *in situ* hybridization were conducted according to Mayer et al.[46] with modifications (see below). The probes were amplified directly from cDNA from Col-0 seedlings using the primers ER-insitu-s: GTAAAGATCTCGGTGTGG and T7+ER-insitu-as: TAATACGACTCACTATAGGGCTGAAGACATATTCACA (T7 promoter sequence is the first 20bp) modified from Pillitteri et al.[47] They were transcribed and labeled with up to a 1:3 ratio of UTP: Digoxigenin-11-UTP (Roche) using the T7 Polymerase (Thermo Scientific). High specific labeling was by dot blot analysis using DIG-labeled Control RNA (Roche) as reference. For the plant material, unfertilized siliques were collected from Col-0, *ER/er*, and er plants. They were fixed and embedded as described previously,[48] shortening the ethanol series to 45 min and using 10 µm sections. Paraffin was removed by immersing twice in Histoclear (National Diagnostics) for 10 min. The samples were first rehydrated by ethanol series, then digested with 0.125 mg/mL Pronase (Sigma) for 10 min, treated shortly with Glycine 0.2% (w/v) in 1x PBS and 1x PBS before fixation in 4% (w/v) PFA for 10 min. Sections were dehydrated by ethanol series and 200 µl hybridization solution was applied per slide. After incubation in a humid box at 50°C overnight, the samples were shortly immersed in 2x SCC and washed three times in 0.2x SCC for 50 min at 50°C. The slides were incubated in 0.5% (w/v) blocking reagent (Boehringer) in TBS for 45 min. The Anti-Digoxigenin-alkaline-phosphatase-coupled antibody (Roche) was diluted 1:1250 in BXT (1% (w/v) BSA, 0.3% (w/v) Triton X-100 in TBS), 160 µl/slide applied and incubated for 1.5 h. Sections were washed 4 times in BXT for 20 min and incubated for 5 min in detection buffer (100 mM Tris (pH 9.5), 50 mM $MgCl_2$, 100 mM NaCl). Hundred twenty microliters of staining solution (450 µg/mL NBT, 175 µg/mL BCIP, 2% (w/v) Polyvinyl alcohol in detection buffer) were applied per slide and incubated overnight. They were immersed shortly in detection buffer, added 15% (w/v) glycerol to each slide and applied a coverslip for brightfield microscopy.

Quantitative RT-PCR analysis

RNA was extracted with the RNeasy Plant Mini Kit (QIAGEN) and quantified with a Nanodrop spectrophotometer. Col-0, *er erl1 erl2* and transgenic T_1 seedlings were grown on ½ MS media containing sucrose and agar for 14 days under long-day conditions. After 4 h in light, seedlings were collected and directly frozen in liquid nitrogen. 12 seedlings were collected for Col-0, *er erl1 erl2* and *35S$_{pro}$:BSK1 bsk1 bsk2* each. Single T_1 seedlings were collected for *35S$_{pro}$:SSP*, *35S$_{pro}$:SSP er erl1 erl2* and *35S$_{pro}$:BSK1 er erl1 erl2*. cDNA was synthesized with RevertAid First Strand cDNA Synthesis Kit (Thermo Scientific) from 1 µg total RNA of each sample, and was diluted 2-fold before quantitative PCR (qPCR) reaction. The qPCR was performed in a CFX Connect (Bio-Rad) with Luna Universal qPCR Master Mix (NEW ENGLAND Biolabs) in a total reaction volume of 20 µL (10 µL Luna Universal qPCR Master Mix, 0.5 µL 10 µM/L forward primers and reverse primers, 2 µL cDNA and 7 µL H_2O). The qPCR program was run as suggested by the qPCR Master Mix supplier (95°C for 60 s, 40 cycles: 95°C for 15 s and 60°C for 30 s). Melting curves were generated by increasing temperature from 65°C to 95°C with measurement every 0.5°C increment. Gene-specific primers were used for amplification (Table S4). *Actin2* (*At3g18780*) was used to normalize gene expression.[49] Relative gene expression level was shown as $2^{-\Delta\Delta Ct}$.[50] Three replicates per reaction were carried out. Biological replicates were not possible because T_1 lines of *35S$_{pro}$:SSP*, *35S$_{pro}$:SSP er erl1 erl2* and *35S$_{pro}$:BSK1 er erl1 erl2* were tiny and sterile.

Phenotypic analysis of rosette leaves

For Images of rosette leaves, three-week old plants were photographed with Canon EOS 1000D camera. To increase the visual contrast, images of rosette leaves were separated from background soil using Adobe Photoshop.

Please cite this article in press as: Wang et al., Independent parental contributions initiate zygote polarization in *Arabidopsis thaliana*, Current Biology (2021), https://doi.org/10.1016/j.cub.2021.08.033

RNA stability

Arabidopsis RNA half-live (stability) was derived from published data by Szabo et al.[23] using an exponential decay model. All data, a detailed description of the analysis and a hands-on protocol have been previously published.[23]

QUANTIFICATION AND STATISTICAL ANALYSIS

Measurement of zygote/suspensor length

After DIC imaging, size measurements were performed using measurement tools of ImageJ software (version 1.52p).[42] The length of the fully elongated zygote was inferred from the sum of apical and basal daughter cell length of the 1-cell embryo. Zygote polarity was determined as ratio of apical and basal cell length. Suspensor length during transition stage was measured from the micropylar end of the basal suspensor cell to the center of uppermost suspensor cell. In crossing experiments, anthers were removed before anthesis, followed by manual pollination approximately 24 h later. Ovules were collected 24-30 h after pollination to image the 1-cell embryos and 4 days after pollination to image transition stage embryos.

Statistical analysis

Boxplot diagrams were made online with BoxPlotR.[41] For statistical analysis of phenotypic data and expression data, the one-way ANOVA analysis with post hoc Tukey test was performed in R (version 3.6.1) with multcompView package (https://cran.r-project.org/web/packages/multcompView/index.html). The number of data points in each group was listed at the bottom of each diagram. The segregation analysis was statistically analyzed with Chi-Square test.

Chapter 4

Zygotic Embryogenesis in Flowering Plants

Houming Chen, Yingjing Miao, Kai Wang, and Martin Bayer

Abstract

In the context of plant regeneration, in vitro systems to produce embryos are frequently used. In many of these protocols, nonzygotic embryos are initiated that will produce shoot-like structures but may lack a primary root. By increasing the auxin-to-cytokinin ratio in the growth medium, roots are then regenerated in a second step. Therefore, in vitro systems might not or only partially execute a similar developmental program as employed during zygotic embryogenesis. There are, however, in vitro systems that can remarkably mimic zygotic embryogenesis such as *Brassica* microspore-derived embryos. In this case, the patterning process of these haploid embryos closely follows zygotic embryogenesis and all fundamental tissue types are generated in a rather similar manner. In this review, we discuss the most fundamental molecular events during early zygotic embryogenesis and hope that this brief summary can serve as a reference for studying and developing in vitro embryogenesis systems in the context of doubled haploid production.

Key words Axis formation, Pattern formation, Radial patterning, Root formation, Shoot apical meristem, Zygote polarization, Zygotic embryogenesis

1 Introduction

Land plants form most of their body shape postembryonically in response to environmental cues [1, 2]. During embryogenesis, therefore, only a simple yet stereotypic manifestation of a small plant is set up. This seedling invariably consists of a few readily recognizable structures along its apical–basal axis, namely, the embryonic leave(s), the hypocotyl, and the embryonic root. Less obviously, the stem cell niches (meristems) for postembryonic development of the shoot and the root are also already established at the opposite ends of the apical–basal axis. The plant embryo is further partitioned along the radial axis into vasculature, ground tissue, and epidermis.

These different tissue types are generated by consecutive steps of patterning along the apical–basal as well as the radial axis [3]. Many of the molecular players orchestrating this development

Jose M. Seguí-Simarro (ed.), *Doubled Haploid Technology: Volume 2: Hot Topics, Apiaceae, Brassicaceae, Solanaceae*, Methods in Molecular Biology, vol. 2288, https://doi.org/10.1007/978-1-0716-1335-1_4,

have been identified in *Arabidopsis thaliana*, but other model species such as maize and rice have also significantly contributed to our understanding of embryonic patterning in plants. In this review, we mainly focus on *Brassicaceae* embryogenesis as the stereotypic patterning process in this plant family facilitates the identification of different cell types by position. The invariant patterning also makes it possible to trace the origin of cells back to decisive cell divisions without live imaging [4]. In order to keep this review concise, we limit our overview to key factors that seem to have a conserved function in flowering plants and will refer to more comprehensive or specialized reviews where necessary.

2 Early Steps of Axis Formation

2.1 Zygote Polarization

In Arabidopsis, the fertilized egg cell (zygote) seems to undergo a brief phase in which cell polarity is lost, before it repolarizes, elongates about threefold, and finally divides asymmetrically to form an apical and a basal cell [5, 6] (Fig. 1).

The apical cell will invariably develop into the embryo. Descendants of the basal cell will foremost contribute to an extraembryonic support structure, called suspensor. In *Brassicaceae*, the suspensor is a filamentous structure formed by a series of stereotypic horizontal divisions of the basal cell and its descendants. The early embryo and suspensor are clonally derived from the apical and basal cell, respectively. However, in other angiosperms, this boundary is less clear and cells originating from the apical cell can also contribute to the suspensor (i.e. in members of the *Caryophyllaceae*) or cells derived from the basal cell can form part of the embryo, as in members of the Asteraceae family [7, 8].

In Arabidopsis, the elongation of the zygote is accomplished by tip growth [9]. This rather specialized mechanism of cell elongation can also be seen during pollen tube growth and root hair growth. While zygote elongation is a common feature of many angiosperm species [7], it does not seem to be a necessity for zygote polarization. In some members of the grasses, such as maize and rice, the egg cell undergoes an asymmetric division right after fertilization without any apparent cell elongation [10, 11].

The correct positioning of the zygote nucleus during this repolarization phase depends on actin filaments and vacuolar dynamics [9, 12]. The intrinsic polarity of the zygote does not necessarily result in size differences of the daughter cells and there are quite a number of plant species in which the apical cell is equal in size or larger than the basal cell [10, 13]. Independently of their size, however, the apical cell pointing toward the central cell and the chalaza will always form (at least part of) the embryo proper. The basal cell that is positioned toward the micropyle and is in physical

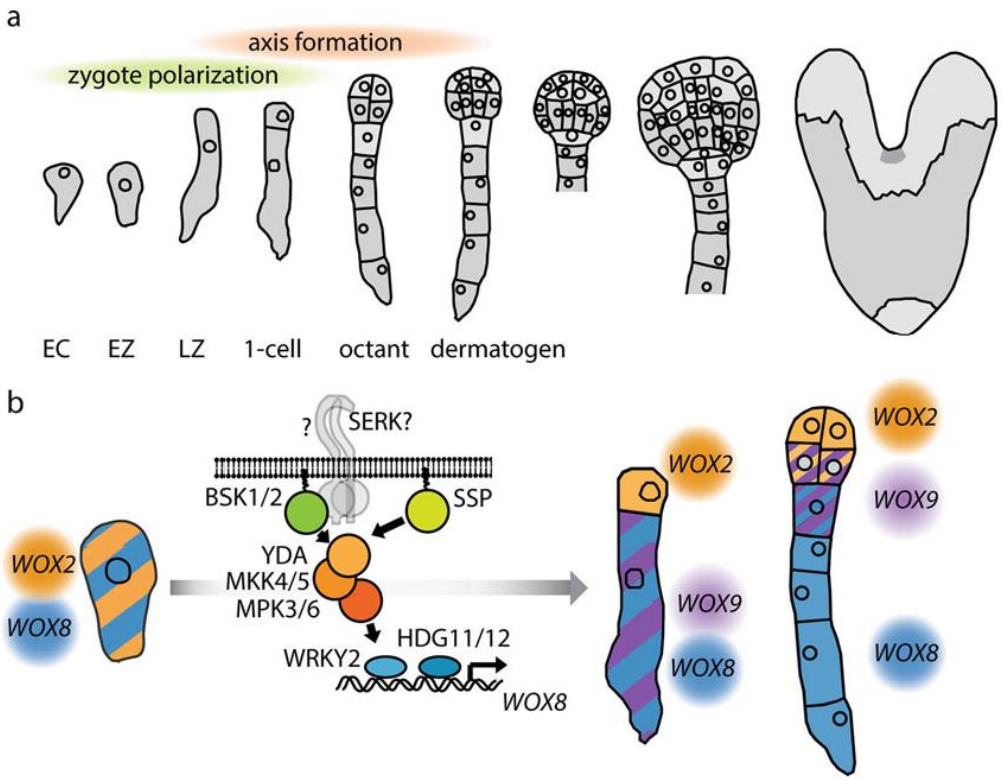

Fig. 1 Apical–basal axis formation. (**a**) Overview of early embryo morphology in Arabidopsis. Developmental stages are indicated below the graphic. *EC* egg cell, *EZ* early zygote, *LZ* late zygote. (**b**) Zygote polarization and patterning along the apical–basal axis. A simplified model of the embryonic YDA pathway is shown on the left. Differential expression of *WOX* gene family members along the apical–basal axis is depicted on the right

contact with sporophytic tissue of the seed coat will always contribute to the extraembryonic suspensor [14].

2.2 MAP Kinase Signaling

Zygote elongation and zygote polarization are at least in part regulated by a MITOGEN- ACTIVATED PROTEIN (MAP) kinase-dependent pathway (Fig. 1). This MAP kinase cascade includes the MAP2K kinase (MAP3K) YODA (YDA) [15], the MAPK kinases (MAP2K/MKK) MKK4 and MKK5, and the MAP kinases (MAPK/MPK) MPK3 and MPK6 [16, 17]. Upstream of YDA in this signaling cascade, two members of the BRASSINOSTEROID SIGNALING KINASE (BSK) family—BSK1 and BSK2—work in parallel [18]. These membrane-associated proteins typically function as signaling relay in SOMATIC EMBRYOGENESIS RECEPTOR-LIKE KINASE (SERK)-dependent receptor kinase pathways [19]. It is therefore a likely scenario that the YDA-dependent MAP kinase cascade is controlled by an extracellular signal received by a SERK-dependent receptor complex

[18]. Possible candidates for the extra-cellular signal include a family of small proteins termed EMBRYO SURROUNDING FACTOR [20] and the possible peptide ligand CLAVATA3/ESR-RELATED (CLE) 8 [21]. These extra-cellular molecules influence suspensor formation, but their direct involvement in activating the embryonic YDA pathway has not been shown and is therefore still hypothetical.

In *Brassicaceae*, an additional mechanism of YDA activation exists [22]. The atypical *BSK* family member *SHORT SUSPENSOR* (*SSP*) evolved as sister gene of *BSK1* [23]. In contrast to BSK1, which functions in a phosphorylation-dependent manner [24], the SSP protein seems to constitutively adopt an activated conformation [18]. *SSP* is tightly controlled at both transcriptional and translational levels. *SSP* transcripts accumulate at high level exclusively in sperm cells and seem to be paternally inherited to the zygote where the SSP protein transiently accumulates [25]. Since SSP directly interacts with YDA, the presence of SSP in the zygote links YDA activation with the fertilization event [18].

The rather mild defects in zygote polarization and suspensor development seen in *ssp* mutants are accompanied by strikingly slower embryo development possibly due to a malformed suspensor [26]. Therefore, the *Brassicaceae*-specific SSP protein might provide an additional, beneficial boost of early YDA activity in parallel to a BSK1/BSK2-dependent YDA activation [18].

One of the targets of this pathway is the transcription factor WRKY DNA-BINDING PROTEIN 2 (WRKY2) that is phosphorylated and activated by MPK6 [6, 27].

WRKY2 together with HOMEODOMAIN GLABROUS (HDG) HDG11 and HDG12 transcriptionally activates the homeodomain transcription factor gene *WUSCHEL RELATED HOMEOBOX 8* (*WOX8*) in the basal cell [6, 27, 28]. This possibly indicates that the embryonic YDA pathway is active at the basal pole of the zygote and/or in the basal daughter cell. Loss of *WOX8* and its close homolog *WOX9* leads to developmental defects in the suspensor. However, expression of the *WOX* gene family member *WOX2* as well as other genes that are normally confined to the apical daughter cell and its descendants is also lost in *wox8 wox9* double mutants, indicating a possible non–cell autonomous function [29].

Additional transcription factor complexes that include the RWP-RK domain–containing (RKD) protein GROUNDED (GRD)/RKD4 may be further targets of the embryonic YDA pathway as suggested by the genetic interaction of these mutants and the strikingly similar loss-of-function phenotype [30]. However, as members of this family seem to play a role in egg-to-zygote transition, a more general role in establishing a zygotic or embryonic transcriptional program and therefore setting the stage for

a functional embryonic YDA pathway might also be possible [30–32].

2.3 Auxin Taking the Stage

The two daughter cells shaped by the first zygotic cell division are characterized by differential gene expression [33]. Among the differentially expressed genes are members that control auxin transport and transcriptional auxin response [33, 34]. Consequently, with the formation of the embryogenic apical cell, auxin becomes one of the central players in the patterning process of the embryo. According to current data, sporophyte-derived auxin is transported by the auxin efflux facilitator PIN-FORMED 7 (PIN7) in the apical membrane of the basal cell to the terminal apical cell [34, 35]. Rising auxin levels in the apical cells lead to transcriptional auxin responses as well as a deviation of the stereotypic horizontal cell divisions by a 90° turn of the division plane [36]. If auxin responses are blocked in the early embryo, a stereotypic horizontal division plane following simple geometric rules of a local minimum in division plane size is formed [36, 37]. The initial apical transport of auxin and the corresponding differential auxin responses in the apical cell therefore seem to initiate the three-dimensional growth of the embryo.

It has been shown that auxin synthesis is coupled to auxin transport and response [38–40] and early in development of the embryo, the suspensor is a prominent source of auxin [39]. With rising auxin concentrations, the embryo proper itself will become the dominant source of auxin around globular stage, initiating a reversal of auxin transport in apical–basal direction [39, 41–43].

The differential auxin response in the apical cell vs. basal cell and their descendants is accomplished by directional auxin flow toward the apical cell and by different auxin response modules in the embryo vs. suspensor [44]. At this early stage, suspensor cells still possess embryogenic potential and cell proliferation seems to be repressed by a suspensor-specific auxin response module [44]. This is highlighted by laser ablation of the embryo or by suspensor-specific expression of certain embryo-specific factors initiating suspensor-derived secondary embryos [45, 46].

This raises the question how polar auxin transport and different auxin response modules are set up early in embryogenesis. As many factors in auxin synthesis, transport and response are expressed in an auxin-dependent manner, this could be in principle a self-organizing system [47]. However, since *wox8 wox9* double mutants show expanded auxin responses in the suspensor and lack the expression of some components of the embryo-specific auxin response module, a link between MAP kinase signaling in the zygote and differential auxin responses in the zygotic daughter cells seems to exist [6, 27, 29]. How direct this connection is, however, needs to be determined.

3 Patterning Along the Apical–Basal Axis

3.1 WOX Gene Expression

Three-dimensional growth of the embryo is initiated by two rounds of vertical divisions in the apical lineage of Arabidopsis. These four cells then divide each horizontally to form an upper and lower tier in the eight-cell preglobular embryo. The order of these cell divisions does not seem to be strictly necessary as other plant species (i.e., in the *Solanaceae* family) form a similar structure by an initial horizontal division of the apical cell followed by two rounds of vertical divisions in the upper and lower tier of the embryo, respectively [7].

At the eight-cell stage, the embryo can be functionally divided along its apical–basal axis. The four cells of the upper tier are the precursors of the embryonic leaves and the shoot apical meristem (SAM). Cells of the lower tier will form the hypocotyl, vasculature, and parts of the root meristem. The uppermost suspensor cell or hypophysis is the founder cell of the quiescent center (QC) of the root meristem as well as the columella. The rest of the suspensor remains extraembryonic. This organizational segmentation along the apical–basal axis is paralleled by overlapping expression domains of three *WOX* family genes [28] (Fig. 1).

The upper tier is characterized by *WOX2* expression, while in the lower tier, *WOX2* expression overlaps with the expression domain of *WOX9*. In the hypophysis, *WOX9* is coexpressed with *WOX8*. In the suspensor, *WOX8* is the only member of these three genes that is expressed [28] (Fig. 1). While the loss of *WOX2* or *WOX8* and *WOX9* lead to patterning defects in the embryo and the suspensor, respectively [29], their exact role during early embryogenesis is not fully understood. In the seedling, *WOX* family members control the proliferation of stem cells in various meristems (reviewed in [48]), a similar role in cell cycle regulation during early embryogenesis seems therefore possible [49].

3.2 Setting Boundaries

As the expression patterns of *WOX* genes illustrate, there seem to be clear boundaries between expression domains in the early Arabidopsis embryo that often are confined to single cell files. How this is achieved mechanistically is not clear. However, the GATA transcription factor HANABA TARANU (HAN) seems to play a critical role in setting up or maintaining the embryo–suspensor boundary [50]. In *han* mutants, genes typically expressed in the suspensor expand their expression domain to the lower tier. How *HAN* restricts the expression of these genes to the suspensor, however, and if/how this relates to the transcriptional network of *WOX* transcription factor genes, still needs to be investigated [50].

4 Radial Patterning

4.1 Protoderm Formation

Radial patterning is initiated with tangential divisions that form the 16-cell or dermatogen stage embryo [51]. This step depends on *WOX* gene function, as indicated by occasional anticlinal cell divisions in the upper tier in *wox2* mutants [29]. Similar incorrect orientation of cell divisions at this stage can be achieved by expression of a nondegradable version of the transcriptional repressor *BODENLOS* (*BDL*)/ *INDOLE-3-ACETIC ACID INDUCIBLE 12* (*IAA12*) [36], a critical component of the transcriptional auxin response module [37, 52]. This indirectly implies that asymmetric divisions forming the protoderm layer involve transcriptional auxin responses. Despite these early defects in division plane orientation, these embryos still form a functional epidermis [44], indicating that protoderm formation might be a rather robust process. Only a few molecular players involved in protoderm initiation are known (reviewed in [53]). However, the involvement of receptor kinases such as RECEPTOR-LIKE PROTEIN KINASE1 (RPK1) and RPK2 (TOADSTOOL2 (TOAD2) would suggest that protoderm formation relies on signaling at the outer cell surface [54, 55].

A key player in protoderm formation is the homeodomain leucine zipper class IV (HD-ZIP IV) transcription factor *A. thaliana* MERISTEM LAYER1 (AtML1) that is necessary and sufficient for epidermal cell identity [56–60]. Double mutants of *ATML1* and its closest homolog *PROTODERMAL FACTOR2 (PDF2)* show strong defects associated with misspecification of the protoderm while overexpression of *AtML1* can induce epidermal cell differentiation in nonepidermal cells [56, 58–60]. *AtML1* is initially expressed in all cells of the embryo but then confined to the outer cells (L1 layer) from the 16-cell stage onward [61].

How L1-specific expression of *AtML1* is controlled on a molecular level is not clear. However, this seems to involve posttranscriptional regulation [62, 63]. *AtML1* and *PDF2* activate the epidermis-specific expression of target genes by binding to a cis-regulatory element termed L1 box. As this element can be found in the *AtML1* and *PDF2* promoter region and is necessary for L1-specific expression of *PDF2*, a feedforward regulation seems to play a central role in controlling *AtML1* expression [56, 57, 61].

4.2 Patterning in the Lower Tier

Radial patterning in the lower tier establishes the initials for the vasculature, ground tissue and epidermis (Fig. 2; reviewed in [64]). By periclinal division, the ground tissue initials will then form endodermis and cortex. Many factors for differentiation and maintenance of different cell identities in the vasculature are known (reviewed in detail in [10, 65]). However, the initial setup in the embryo is less well understood. Radial patterning of the vasculature critically depends on auxin responses mediated by the auxin

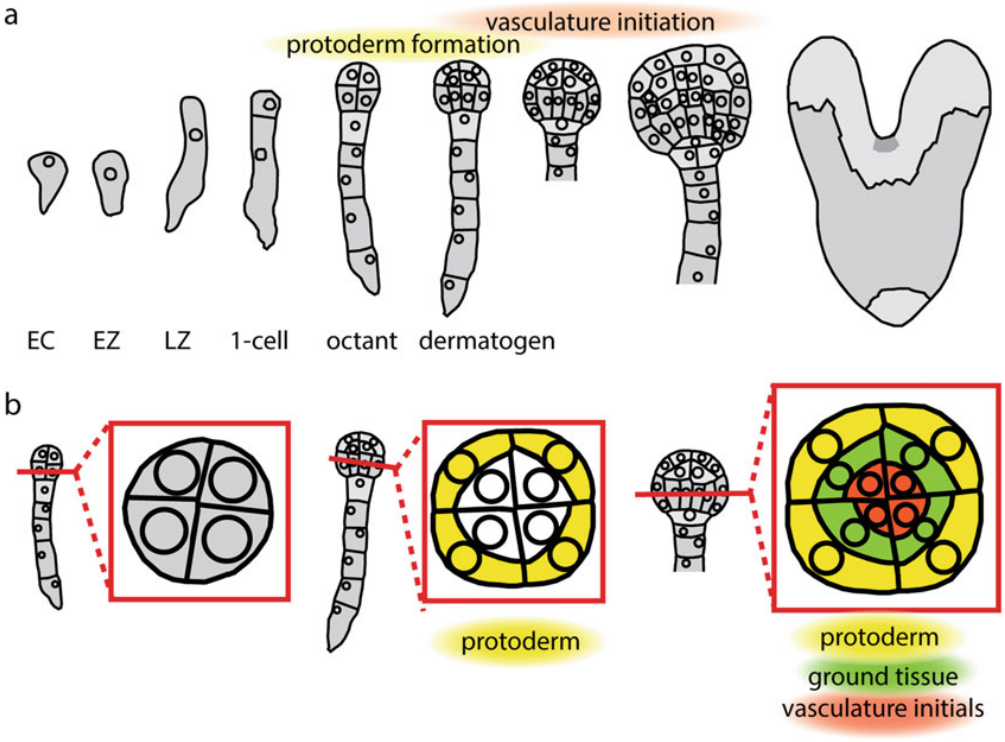

Fig. 2 Radial patterning in the Arabidopsis embryo. (**a**) Overview of early embryo morphology in Arabidopsis. Developmental stages are indicated below the graphic. *EC* egg cell, *EZ* early zygote, *LZ* late zygote. (**b**) Patterning along the radial axis in the lower tier of the embryo. Cross sections are illustrated in red squares. Yellow, protoderm; green, ground tissue; red, vasculature precursor cells

response factor (ARF) MONOPTEROS (MP) [66, 67] (Fig. 3). MP transcriptionally activates the bHLH transcription factor gene *TARGET OF MONOPTEROS 5* (*TMO5*) in the vasculature initials. TMO5 forms heterodimers with the bHLH transcription factor LONESOME HIGHWAY (LHW) and stimulates the expression of the cytokinin synthesis genes *LONELY GUY* (*LOG*) *3* and *LOG 4*. Together, this transcriptional complex controls periclinal divisions and therefore the number of cell files in the vasculature bundle (for comprehensive review, *see* ref. 68).

5 Establishing the Stem Cell Niches

5.1 Root Initiation

The first step of root meristem formation in Arabidopsis is the specification of the hypophysis [69]. This uppermost suspensor cell will form the QC that is responsible for stem cell maintenance [70]. The QC is characterized by expression of *WOX5* that maintains quiescence by controlling the cell cycle [28, 71, 72] (Fig. 3).

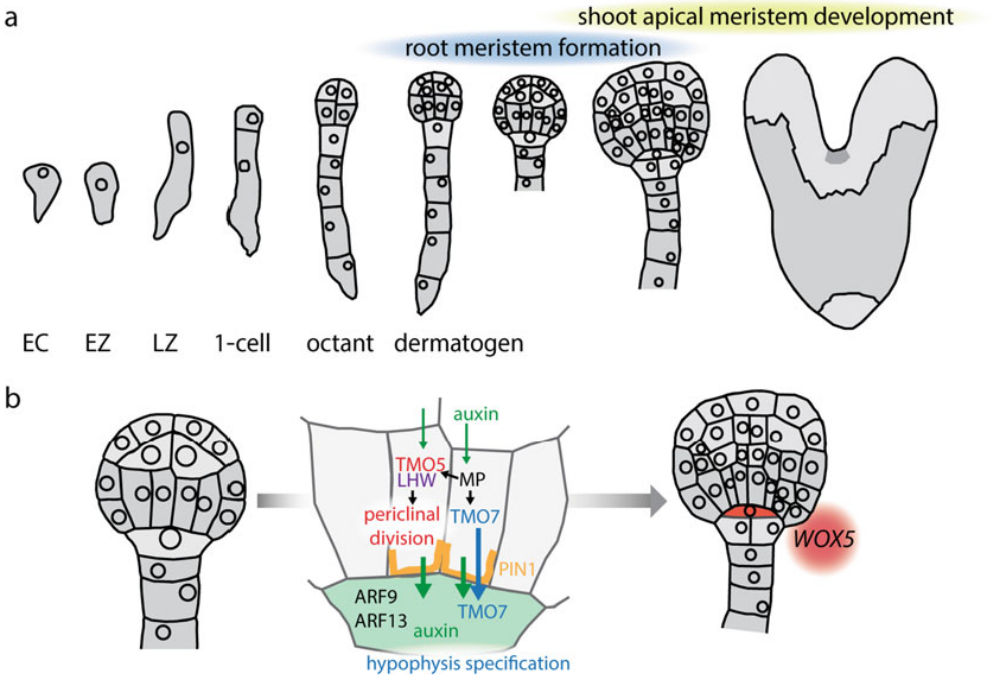

Fig. 3 Auxin signaling in vasculature formation and root meristem initiation. (**a**) Overview of early embryo morphology in Arabidopsis. Developmental stages are indicated below the graphic. *EC* egg cell, *EZ* early zygote, *LZ* late zygote. (**b**) A schematic overview of auxin responses leading to periclinal divisions in prevasculature cells and hypophysis specification. Auxin responses in the central cells of the lower tier and in the future hypophysis require cell-type specific auxin response machineries. After the asymmetric division of the hypophysis, expression of the *WOX* gene family member *WOX5* marks the quiescent center precursor cell

An intricate interaction of cells of the lower tier and the future hypophysis precedes the asymmetric division of the hypophysis that forms the QC. Auxin responses in the central cells of the lower tier lead to MP-dependent expression of *TMO7* [69]. This small bHLH transcription factor moves to the neighboring hypophysis where it plays a critical role in initiating QC formation [69]. This process also depends on the transcription factors NO TRANSMITTING TRACT (NTT)/WIP DOMAIN PROTEIN 2 (WIP2), WIP4, and WIP5 [73] that are expressed in the hypophysis, possibly in an auxin-dependent manner (reviewed in [64]).

Basal transport of auxin via PIN1 in the neighboring proembryo results in high auxin levels in the hypophysis as inferred from strong activity of synthetic auxin response reporters [34, 44, 69, 74]. Accumulation of auxin triggers transcriptional auxin responses mediated by a suspensor-specific auxin response machinery including ARF9, ARF13 and IAA10 [44] (Fig. 3).

Root initiation is also controlled by AP2 domain transcription factors of the PLETHORA (PLT) family [75]. *PLT1* and *PLT2* are expressed in the lower tier from the 8-cell embryo on and in the suspensor [50, 75]. PLT transcription factors can be considered to be master regulators of root identity. Loss of the four *PLT* gene family members *PLT1*, *PLT2*, *PLT3*, and *PLT4/BABY BOOM* (*BBM*) leads to misspecification of the hypophysis and rootless seedlings [76]. Ectopic expression of *PLT1* and *PLT2* in the shoot region or in the apical region of the embryo can induce ectopic root formation [75–77]. Expression of *PLT1* and *PLT2* depends on *MP*-dependent auxin signaling, emphasizing the importance of auxin in root formation [78].

5.2 The Shoot Apical Meristem

In tissue culture and in vitro plant regeneration, it has been known for a long time that the auxin-to-cytokinin ratio is crucial for the induction of shoots or roots, respectively. Under growth conditions where cytokinin is dominating, shoots can be regenerated, indicating an important role of cytokinin in formation of the SAM [79].

In the Arabidopsis embryo, this stem cell niche is first recognized at late heart stage as organized cell layers between the cotyledons [1, 80]. The organizing center of the SAM is characterized by the expression of the *WOX* gene family member *WUSCHEL* (*WUS*) [80, 81]. WUS moves to the neighboring stem cells where it suppresses differentiation [80–82]. The expression domain of *WUS* is negatively controlled by a receptor kinase pathway including the receptor kinase CLV1 [83–85]. WUS activates the expression of the corresponding peptide ligand CLV3 in the stem cells [86] and promotes its own expression in the organizing center by modulating cytokinin signaling [87, 88]. These (positive and negative) feedback loops restrict the size of the shoot meristem (reviewed in detail in [89]).

The position of stem cells underneath the shoot apex is controlled by L1-specific *miR394* [90]. This microRNA moves to the L2 and L3 layer and downregulates the expression of the F-box gene *LEAF CURLING RESPONSIVENESS* (*LCR*). LCR inhibits WUS activity. The *miR394/LCR* pathway therefore promotes WUS activity in the subepidermal region and ensures the correct position of the stem cell region in a growing shoot [90].

Although *WUS* expression starts at the 16-cell stage in the inner cells of the upper tier, it is dispensable for SAM formation. Instead, *WOX2* (together with *WOX1*, *WOX3*, and *WOX5*) is a key factor in meristem initiation [91]. In *wox1/2/3/5* quadruple mutant, a correct shoot meristem is not formed and the apical region of the embryo is characterized by increased auxin signaling [91]. Furthermore, the expression of the HD-ZIP III family members *PHABULOSA* (*PHB*), *PHAVOLUTA* (*PHV*), and *REVOLUTA* (*REV*) [92, 93] is strongly reduced or absent in the shoot meristem region of the embryo [91]. Therefore, *WOX2* seems to

promote HD-ZIP III expression in the shoot meristem initials. The HD-ZIPIII genes *PHB*, *PHV*, and *REV* are key players in shoot formation as ectopic accumulation in the basal part of the embryo leads to transformation of the root pole into shoot structures [77]. Since *PHB* and *PHV* control cytokinin production [94], *WOX2* regulates shoot meristem formation in part by promoting cytokinin levels in the upper tier of the embryo [91].

6 Outlook

While many molecular players in tissue differentiation and maintenance of cell types have emerged in recent years, our knowledge about the very first steps of initiating different identities in the early zygotic embryo is still fragmentary. What signals polarize the zygote and set up different auxin transport and response machineries in its daughter cells? How are different cell identities along the radial axis initiated? And how is the origin of the stem cell region for the shoot apical meristem controlled on a molecular level? Many fundamental questions about the early steps of zygotic embryogenesis are still waiting to be answered. Nevertheless, much less information is available about how microspore-derived embryos develop from dividing microspores, and about the genetic basis of some of the anatomical and functional abnormalities found in some cases. The knowledge summarized here may serve as a reference to compare with for the genetic dissection of microspore embryogenesis.

Acknowledgments

We would like to thank Gerd Jürgens for comments on the manuscript and apologize to our colleagues whose work we have not included in the chapter due to our focus on Brassicaceae embryogenesis. Research in our group is supported by the German Science Foundation (Deutsche Forschungsgemeinschaft—DFG: SFB1101/B01 to M.B.), the Chinese Scholarship Council (Fellowship No. 201806320131 to Y.M.), and the Max Planck Society.

References

1. Jurgens G (2003) Growing up green: cellular basis of plant development. Mech Dev 120 (11):1395–1406. https://doi.org/10.1016/j.mod.2003.03.001
2. Wang B, Smith SM, Li J (2018) Genetic regulation of shoot architecture. Annu Rev Plant Biol 69:437–468. https://doi.org/10.1146/annurev-arplant-042817-040422
3. Lau S, Slane D, Herud O, Kong JX, Jurgens G (2012) Early embryogenesis in flowering plants: setting up the basic body pattern. Annu Rev Plant Biol 63:483–506
4. ten Hove CA, Lu KJ, Weijers D (2015) Building a plant: cell fate specification in the early Arabidopsis embryo. Development 142

(3):420–430. https://doi.org/10.1242/dev.111500

5. Mansfield SG, Briarty LG (1991) Early embryogenesis in Arabidopsis-thaliana. 2. The developing embryo. Can J Bot 69(3):461–476
6. Ueda M, Zhang Z, Laux T (2011) Transcriptional activation of Arabidopsis axis patterning genes WOX8/9 links zygote polarity to embryo development. Dev Cell 20 (2):264–270. https://doi.org/10.1016/j.devcel.2011.01.009
7. Maheshwari P (1950) An introduction to the embryology of the angiosperms. McGraw-Hill, New York
8. Bayer M, Slane D, Jurgens G (2017) Early plant embryogenesis-dark ages or dark matter? Curr Opin Plant Biol 35:30–36. https://doi.org/10.1016/j.pbi.2016.10.004
9. Kimata Y, Higaki T, Kawashima T, Kurihara D, Sato Y, Yamada T, Hasezawa S, Berger F, Higashiyama T, Ueda M (2016) Cytoskeleton dynamics control the first asymmetric cell division in Arabidopsis zygote. Proc Natl Acad Sci U S A 113(49):14157–14162. https://doi.org/10.1073/pnas.1613979113
10. Johri BM, Ambegaokar KB, Srivastava PS (1992) Comparative embryology of angiosperms. Springer-Verlag, Berlin
11. Bommert P, Werr W (2001) Gene expression patterns in the maize caryopsis: clues to decisions in embryo and endosperm development. Gene 271(2):131–142. https://doi.org/10.1016/s0378-1119(01)00503-0
12. Kimata Y, Kato T, Higaki T, Kurihara D, Yamada T, Segami S, Morita MT, Maeshima M, Hasezawa S, Higashiyama T, Tasaka M, Ueda M (2019) Polar vacuolar distribution is essential for accurate asymmetric division of Arabidopsis zygotes. Proc Natl Acad Sci U S A 116(6):2338–2343. https://doi.org/10.1073/pnas.1814160116
13. Sivaramakrishna D (1978) Size relationships of apical cell and basal-cell in 2-celled embryos in angiosperms. Can J Bot 56(12):1434–1438. https://doi.org/10.1139/b78-166
14. Wang K, Chen H, Miao Y, Bayer M (2019) Square one: zygote polarity and early embryogenesis in flowering plants. Curr Opin Plant Biol. https://doi.org/10.1016/j.pbi.2019.10.002
15. Lukowitz W, Roeder A, Parmenter D, Somerville C (2004) A MAPKK kinase gene regulates extra-embryonic cell fate in Arabidopsis. Cell 116(1):109–119
16. Wang H, Ngwenyama N, Liu Y, Walker JC, Zhang S (2007) Stomatal development and patterning are regulated by environmentally responsive mitogen-activated protein kinases in Arabidopsis. Plant Cell 19(1):63–73. https://doi.org/10.1105/tpc.106.048298
17. Zhang M, Wu H, Su J, Wang H, Zhu Q, Liu Y, Xu J, Lukowitz W, Zhang S (2017) Maternal control of embryogenesis by MPK6 and its upstream MKK4/MKK5 in Arabidopsis. Plant J 92(6):1005–1019. https://doi.org/10.1111/tpj.13737
18. Neu A, Eilbert E, Asseck LY, Slane D, Henschen A, Wang K, Burgel P, Hildebrandt M, Musielak TJ, Kolb M, Lukowitz W, Grefen C, Bayer M (2019) Constitutive signaling activity of a receptor-associated protein links fertilization with embryonic patterning in Arabidopsis thaliana. Proc Natl Acad Sci U S A 116(12):5795–5804. https://doi.org/10.1073/pnas.1815866116
19. Shi H, Yan H, Li J, Tang D (2013) BSK1, a receptor-like cytoplasmic kinase, involved in both BR signaling and innate immunity in Arabidopsis. Plant Signal Behav 8(8). https://doi.org/10.4161/psb.24996
20. Costa LM, Marshall E, Tesfaye M, Silverstein KA, Mori M, Umetsu Y, Otterbach SL, Papareddy R, Dickinson HG, Boutiller K, VandenBosch KA, Ohki S, Gutierrez-Marcos JF (2014) Central cell-derived peptides regulate early embryo patterning in flowering plants. Science 344(6180):168–172. https://doi.org/10.1126/science.1243005
21. Fiume E, Fletcher JC (2012) Regulation of Arabidopsis embryo and endosperm development by the polypeptide signaling molecule CLE8. Plant Cell 24(3):1000–1012. https://doi.org/10.1105/tpc.111.094839
22. Musielak TJ, Bayer M (2014) YODA signalling in the early Arabidopsis embryo. Biochem Soc Trans 42(2):408–412
23. Liu SL, Adams KL (2010) Dramatic change in function and expression pattern of a gene duplicated by polyploidy created a paternal effect gene in the Brassicaceae. Mol Biol Evol 27(12):2817–2828. https://doi.org/10.1093/molbev/msq169
24. Tang W, Kim TW, Oses-Prieto JA, Sun Y, Deng Z, Zhu S, Wang R, Burlingame AL, Wang ZY (2008) BSKs mediate signal transduction from the receptor kinase BRI1 in Arabidopsis. Science 321(5888):557–560. https://doi.org/10.1126/science.1156973
25. Bayer M, Nawy T, Giglione C, Galli M, Meinnel T, Lukowitz W (2009) Paternal control of embryonic patterning in Arabidopsis thaliana. Science 323(5920):1485–1488. https://doi.org/10.1126/science.1167784

26. Babu Y, Musielak T, Henschen A, Bayer M (2013) Suspensor length determines developmental progression of the embryo in Arabidopsis. Plant Physiol 162(3):1448–1458. https://doi.org/10.1104/pp.113.217166
27. Ueda M, Aichinger E, Gong W, Groot E, Verstraeten I, Vu LD, De Smet I, Higashiyama T, Umeda M, Laux T (2017) Transcriptional integration of paternal and maternal factors in the Arabidopsis zygote. Genes Dev 31(6):617–627. https://doi.org/10.1101/gad.292409.116
28. Haecker A, Gross-Hardt R, Geiges B, Sarkar A, Breuninger H, Herrmann M, Laux T (2004) Expression dynamics of WOX genes mark cell fate decisions during early embryonic patterning in Arabidopsis thaliana. Development 131 (3):657–668. https://doi.org/10.1242/dev.00963
29. Breuninger H, Rikirsch E, Hermann M, Ueda M, Laux T (2008) Differential expression of WOX genes mediates apical-basal axis formation in the Arabidopsis embryo. Dev Cell 14 (6):867–876. https://doi.org/10.1016/j.devcel.2008.03.008
30. Jeong S, Palmer TM, Lukowitz W (2011) The RWP-RK factor GROUNDED promotes embryonic polarity by facilitating YODA MAP kinase signaling. Curr Biol 21 (15):1268–1276. https://doi.org/10.1016/j.cub.2011.06.049
31. Waki T, Hiki T, Watanabe R, Hashimoto T, Nakajima K (2011) The Arabidopsis RWP-RK protein RKD4 triggers gene expression and pattern formation in early embryogenesis. Curr Biol 21(15):1277–1281. https://doi.org/10.1016/j.cub.2011.07.001
32. Rovekamp M, Bowman JL, Grossniklaus U (2016) Marchantia MpRKD regulates the gametophyte-sporophyte transition by keeping egg cells quiescent in the absence of fertilization. Curr Biol 26(13):1782–1789. https://doi.org/10.1016/j.cub.2016.05.028
33. Zhou X, Liu Z, Shen K, Zhao P, Sun MX (2020) Cell lineage-specific transcriptome analysis for interpreting cell fate specification of proembryos. Nat Commun 11(1):1366. https://doi.org/10.1038/s41467-020-15189-w
34. Friml J, Vieten A, Sauer M, Weijers D, Schwarz H, Hamann T, Offringa R, Jurgens G (2003) Efflux-dependent auxin gradients establish the apical-basal axis of Arabidopsis. Nature 426(6963):147–153. https://doi.org/10.1038/nature02085
35. Robert HS, Park C, Gutierrez CL, Wojcikowska B, Pencik A, Novak O, Chen J, Grunewald W, Dresselhaus T, Friml J, Laux T (2018) Maternal auxin supply contributes to early embryo patterning in Arabidopsis. Nat Plants 4(8):548–553. https://doi.org/10.1038/s41477-018-0204-z
36. Yoshida S, Barbier de Reuille P, Lane B, Bassel GW, Prusinkiewicz P, Smith RS, Weijers D (2014) Genetic control of plant development by overriding a geometric division rule. Dev Cell 29(1):75–87. https://doi.org/10.1016/j.devcel.2014.02.002
37. Hamann T, Mayer U, Jurgens G (1999) The auxin-insensitive bodenlos mutation affects primary root formation and apical-basal patterning in the Arabidopsis embryo. Development 126(7):1387–1395
38. Robert HS, Crhak Khaitova L, Mroue S, Benkova E (2015) The importance of localized auxin production for morphogenesis of reproductive organs and embryos in Arabidopsis. J Exp Bot 66(16):5029–5042. https://doi.org/10.1093/jxb/erv256
39. Robert HS, Grones P, Stepanova AN, Robles LM, Lokerse AS, Alonso JM, Weijers D, Friml J (2013) Local auxin sources orient the apical-basal axis in Arabidopsis embryos. Curr Biol 23 (24):2506–2512. https://doi.org/10.1016/j.cub.2013.09.039
40. Wabnik K, Robert HS, Smith RS, Friml J (2013) Modeling framework for the establishment of the apical-basal embryonic axis in plants. Curr Biol 23(24):2513–2518. https://doi.org/10.1016/j.cub.2013.10.038
41. Stepanova AN, Robertson-Hoyt J, Yun J, Benavente LM, Xie DY, Dolezal K, Schlereth A, Jurgens G, Alonso JM (2008) TAA1-mediated auxin biosynthesis is essential for hormone crosstalk and plant development. Cell 133(1):177–191. https://doi.org/10.1016/j.cell.2008.01.047
42. Cheng Y, Dai X, Zhao Y (2007) Auxin synthesized by the YUCCA flavin monooxygenases is essential for embryogenesis and leaf formation in Arabidopsis. Plant Cell 19(8):2430–2439. https://doi.org/10.1105/tpc.107.053009
43. Brumos J, Alonso JM, Stepanova AN (2014) Genetic aspects of auxin biosynthesis and its regulation. Physiol Plant 151(1):3–12. https://doi.org/10.1111/ppl.12098
44. Rademacher EH, Lokerse AS, Schlereth A, Llavata-Peris CI, Bayer M, Kientz M, Freire Rios A, Borst JW, Lukowitz W, Jurgens G, Weijers D (2012) Different auxin response machineries control distinct cell fates in the early plant embryo. Dev Cell 22(1):211–222. https://doi.org/10.1016/j.devcel.2011.10.026

45. Liu Y, Li X, Zhao J, Tang X, Tian S, Chen J, Shi C, Wang W, Zhang L, Feng X, Sun MX (2015) Direct evidence that suspensor cells have embryogenic potential that is suppressed by the embryo proper during normal embryogenesis. Proc Natl Acad Sci U S A 112 (40):12432–12437. https://doi.org/10.1073/pnas.1508651112
46. Radoeva T, Albrecht C, Piepers M, de Vries S, Weijers D (2020) Suspensor-derived somatic embryogenesis in Arabidopsis. Development 147(13). https://doi.org/10.1242/dev.188912
47. Lau S, De Smet I, Kolb M, Meinhardt H, Jurgens G (2011) Auxin triggers a genetic switch. Nat Cell Biol 13(5):611–615. https://doi.org/10.1038/ncb2212
48. Jha P, Ochatt SJ, Kumar V (2020) WUSCHEL: a master regulator in plant growth signaling. Plant Cell Rep 39 (4):431–444. https://doi.org/10.1007/s00299-020-02511-5
49. Wu X, Chory J, Weigel D (2007) Combinations of WOX activities regulate tissue proliferation during Arabidopsis embryonic development. Dev Biol 309(2):306–316. https://doi.org/10.1016/j.ydbio.2007.07.019
50. Nawy T, Bayer M, Mravec J, Friml J, Birnbaum KD, Lukowitz W (2010) The GATA factor HANABA TARANU is required to position the proembryo boundary in the early Arabidopsis embryo. Dev Cell 19(1):103–113. https://doi.org/10.1016/j.devcel.2010.06.004
51. Jurgens G, Mayer U, Busch M, Lukowitz W, Laux T (1995) Pattern formation in the Arabidopsis embryo: a genetic perspective. Philos Trans R Soc Lond Ser B Biol Sci 350 (1331):19–25. https://doi.org/10.1098/rstb.1995.0132
52. Hamann T, Benkova E, Baurle I, Kientz M, Jurgens G (2002) The Arabidopsis BODENLOS gene encodes an auxin response protein inhibiting MONOPTEROS-mediated embryo patterning. Genes Dev 16(13):1610–1615. https://doi.org/10.1101/gad.229402
53. Takada S, Iida H (2014) Specification of epidermal cell fate in plant shoots. Front Plant Sci 5:49. https://doi.org/10.3389/fpls.2014.00049
54. Nodine MD, Yadegari R, Tax FE (2007) RPK1 and TOAD2 are two receptor-like kinases redundantly required for arabidopsis embryonic pattern formation. Dev Cell 12 (6):943–956. https://doi.org/10.1016/j.devcel.2007.04.003
55. Javelle M, Vernoud V, Rogowsky PM, Ingram GC (2011) Epidermis: the formation and functions of a fundamental plant tissue. New Phytol 189(1):17–39. https://doi.org/10.1111/j.1469-8137.2010.03514.x
56. Abe M, Katsumata H, Komeda Y, Takahashi T (2003) Regulation of shoot epidermal cell differentiation by a pair of homeodomain proteins in Arabidopsis. Development 130 (4):635–643. https://doi.org/10.1242/dev.00292
57. Abe M, Takahashi T, Komeda Y (2001) Identification of a cis-regulatory element for L1 layer-specific gene expression, which is targeted by an L1-specific homeodomain protein. Plant J 26(5):487–494. https://doi.org/10.1046/j.1365-313x.2001.01047.x
58. Peterson KM, Shyu C, Burr CA, Horst RJ, Kanaoka MM, Omae M, Sato Y, Torii KU (2013) Arabidopsis homeodomain-leucine zipper IV proteins promote stomatal development and ectopically induce stomata beyond the epidermis. Development 140(9):1924–1935. https://doi.org/10.1242/dev.090209
59. Takada S, Takada N, Yoshida A (2013) ATML1 promotes epidermal cell differentiation in Arabidopsis shoots. Development 140 (9):1919–1923. https://doi.org/10.1242/dev.094417
60. Ogawa E, Yamada Y, Sezaki N, Kosaka S, Kondo H, Kamata N, Abe M, Komeda Y, Takahashi T (2015) ATML1 and PDF2 play a redundant and essential role in arabidopsis embryo development. Plant Cell Physiol 56 (6):1183–1192. https://doi.org/10.1093/pcp/pcv045
61. Takada S, Jurgens G (2007) Transcriptional regulation of epidermal cell fate in the Arabidopsis embryo. Development 134 (6):1141–1150. https://doi.org/10.1242/dev.02803
62. Iida H, Yoshida A, Takada S (2019) ATML1 activity is restricted to the outermost cells of the embryo through post-transcriptional repressions. Development 146(4). https://doi.org/10.1242/dev.169300
63. Nodine MD, Bartel DP (2010) MicroRNAs prevent precocious gene expression and enable pattern formation during plant embryogenesis. Genes Dev 24(23):2678–2692. https://doi.org/10.1101/gad.1986710
64. Palovaara J, de Zeeuw T, Weijers D (2016) Tissue and organ initiation in the plant embryo: a first time for everything. Annu Rev Cell Dev Biol 32:47–75. https://doi.org/10.1146/annurev-cellbio-111315-124929

65. Ruonala R, Ko D, Helariutta Y (2017) Genetic Networks in Plant Vascular Development. Annual Review of Genetics, 51(51):335–359. https://doi.org/10.1146/annurev-genet-120116-024525
66. Hardtke CS, Berleth T (1998) The Arabidopsis gene MONOPTEROS encodes a transcription factor mediating embryo axis formation and vascular development. EMBO J 17 (5):1405–1411. https://doi.org/10.1093/emboj/17.5.1405
67. De Rybel B, Moller B, Yoshida S, Grabowicz I, Barbier de Reuille P, Boeren S, Smith RS, Borst JW, Weijers D (2013) A bHLH complex controls embryonic vascular tissue establishment and indeterminate growth in Arabidopsis. Dev Cell 24(4):426–437. https://doi.org/10.1016/j.devcel.2012.12.013
68. De Rybel B, Mahonen AP, Helariutta Y, Weijers D (2016) Plant vascular development: from early specification to differentiation. Nat Rev Mol Cell Biol 17(1):30–40. https://doi.org/10.1038/nrm.2015.6
69. Schlereth A, Moller B, Liu W, Kientz M, Flipse J, Rademacher EH, Schmid M, Jurgens G, Weijers D (2010) MONOPTEROS controls embryonic root initiation by regulating a mobile transcription factor. Nature 464 (7290):913–916. https://doi.org/10.1038/nature08836
70. Dolan L, Janmaat K, Willemsen V, Linstead P, Poethig S, Roberts K, Scheres B (1993) Cellular organisation of the Arabidopsis thaliana root. Development 119(1):71–84
71. Sarkar AK, Luijten M, Miyashima S, Lenhard M, Hashimoto T, Nakajima K, Scheres B, Heidstra R, Laux T (2007) Conserved factors regulate signalling in Arabidopsis thaliana shoot and root stem cell organizers. Nature 446(7137):811–814. https://doi.org/10.1038/nature05703
72. Forzani C, Aichinger E, Sornay E, Willemsen V, Laux T, Dewitte W, Murray JA (2014) WOX5 suppresses CYCLIN D activity to establish quiescence at the center of the root stem cell niche. Curr Biol 24(16):1939–1944. https://doi.org/10.1016/j.cub.2014.07.019
73. Crawford BC, Sewell J, Golembeski G, Roshan C, Long JA, Yanofsky MF (2015) Plant development. Genetic control of distal stem cell fate within root and embryonic meristems. Science 347(6222):655–659. https://doi.org/10.1126/science.aaa0196
74. Liao CY, Smet W, Brunoud G, Yoshida S, Vernoux T, Weijers D (2015) Reporters for sensitive and quantitative measurement of auxin response. Nat Methods 12(3):207–210. https://doi.org/10.1038/nmeth.3279
75. Aida M, Beis D, Heidstra R, Willemsen V, Blilou I, Galinha C, Nussaume L, Noh YS, Amasino R, Scheres B (2004) The PLETHORA genes mediate patterning of the Arabidopsis root stem cell niche. Cell 119 (1):109–120. https://doi.org/10.1016/j.cell.2004.09.018
76. Galinha C, Hofhuis H, Luijten M, Willemsen V, Blilou I, Heidstra R, Scheres B (2007) PLETHORA proteins as dose-dependent master regulators of Arabidopsis root development. Nature 449 (7165):1053–1057. https://doi.org/10.1038/nature06206
77. Smith ZR, Long JA (2010) Control of Arabidopsis apical-basal embryo polarity by antagonistic transcription factors. Nature 464 (7287):423–426. https://doi.org/10.1038/nature08843
78. Mahonen AP, Ten Tusscher K, Siligato R, Smetana O, Diaz-Trivino S, Salojarvi J, Wachsman G, Prasad K, Heidstra R, Scheres B (2014) PLETHORA gradient formation mechanism separates auxin responses. Nature 515(7525):125–129. https://doi.org/10.1038/nature13663
79. Miller LR, Murashige T (1976) Tissue culture propagation of tropical foliage plants. In Vitro 12(12):797–813. https://doi.org/10.1007/BF02796365
80. Laux T, Mayer KF, Berger J, Jurgens G (1996) The WUSCHEL gene is required for shoot and floral meristem integrity in Arabidopsis. Development 122(1):87–96
81. Mayer KF, Schoof H, Haecker A, Lenhard M, Jurgens G, Laux T (1998) Role of WUSCHEL in regulating stem cell fate in the Arabidopsis shoot meristem. Cell 95(6):805–815. https://doi.org/10.1016/s0092-8674(00)81703-1
82. Yadav RK, Perales M, Gruel J, Girke T, Jonsson H, Reddy GV (2011) WUSCHEL protein movement mediates stem cell homeostasis in the Arabidopsis shoot apex. Genes Dev 25(19):2025–2030. https://doi.org/10.1101/gad.17258511
83. Brand U, Fletcher JC, Hobe M, Meyerowitz EM, Simon R (2000) Dependence of stem cell fate in Arabidopsis on a feedback loop regulated by CLV3 activity. Science 289 (5479):617–619. https://doi.org/10.1126/science.289.5479.617
84. Schoof H, Lenhard M, Haecker A, Mayer KF, Jurgens G, Laux T (2000) The stem cell population of Arabidopsis shoot meristems in maintained by a regulatory loop between the CLAVATA and WUSCHEL genes. Cell 100 (6):635–644. https://doi.org/10.1016/s0092-8674(00)80700-x

85. Clark SE, Williams RW, Meyerowitz EM (1997) The CLAVATA1 gene encodes a putative receptor kinase that controls shoot and floral meristem size in Arabidopsis. Cell 89 (4):575–585. https://doi.org/10.1016/s0092-8674(00)80239-1

86. Perales M, Rodriguez K, Snipes S, Yadav RK, Diaz-Mendoza M, Reddy GV (2016) Threshold-dependent transcriptional discrimination underlies stem cell homeostasis. Proc Natl Acad Sci U S A 113(41):E6298–E6306. https://doi.org/10.1073/pnas.1607669113

87. Chickarmane VS, Gordon SP, Tarr PT, Heisler MG, Meyerowitz EM (2012) Cytokinin signaling as a positional cue for patterning the apical-basal axis of the growing Arabidopsis shoot meristem. Proc Natl Acad Sci U S A 109 (10):4002–4007. https://doi.org/10.1073/pnas.1200636109

88. Gordon SP, Chickarmane VS, Ohno C, Meyerowitz EM (2009) Multiple feedback loops through cytokinin signaling control stem cell number within the Arabidopsis shoot meristem. Proc Natl Acad Sci U S A 106 (38):16529–16534. https://doi.org/10.1073/pnas.0908122106

89. Kitagawa M, Jackson D (2019) Control of meristem size. Annu Rev Plant Biol 70:269–291. https://doi.org/10.1146/annurev-arplant-042817-040549

90. Knauer S, Holt AL, Rubio-Somoza I, Tucker EJ, Hinze A, Pisch M, Javelle M, Timmermans MC, Tucker MR, Laux T (2013) A protodermal miR394 signal defines a region of stem cell competence in the Arabidopsis shoot meristem. Dev Cell 24(2):125–132. https://doi.org/10.1016/j.devcel.2012.12.009

91. Zhang Z, Tucker E, Hermann M, Laux T (2017) A molecular framework for the embryonic initiation of shoot meristem stem cells. Dev Cell 40(3):264–277.e264. https://doi.org/10.1016/j.devcel.2017.01.002

92. McConnell JR, Emery J, Eshed Y, Bao N, Bowman J, Barton MK (2001) Role of PHABULOSA and PHAVOLUTA in determining radial patterning in shoots. Nature 411 (6838):709–713. https://doi.org/10.1038/35079635

93. Emery JF, Floyd SK, Alvarez J, Eshed Y, Hawker NP, Izhaki A, Baum SF, Bowman JL (2003) Radial patterning of Arabidopsis shoots by class III HD-ZIP and KANADI genes. Curr Biol 13(20):1768–1774. https://doi.org/10.1016/j.cub.2003.09.035

94. Dello Ioio R, Galinha C, Fletcher AG, Grigg SP, Molnar A, Willemsen V, Scheres B, Sabatini S, Baulcombe D, Maini PK, Tsiantis M (2012) A PHABULOSA/cytokinin feedback loop controls root growth in Arabidopsis. Curr Biol 22(18):1699–1704. https://doi.org/10.1016/j.cub.2012.07.005

The Plant Cell, Vol. 32: 3311–3323, October 2020, www.plantcell.org © 2020 ASPB.

Constitutive Activation of Leucine-Rich Repeat Receptor Kinase Signaling Pathways by BAK1-INTERACTING RECEPTOR-LIKE KINASE3 Chimera[OPEN]

Ulrich Hohmann,[a,1] Priya Ramakrishna,[a] Kai Wang,[b] Laura Lorenzo-Orts,[a,2] Joel Nicolet,[a] Agnes Henschen,[b] Marie Barberon,[a] Martin Bayer,[b,3] and Michael Hothorn[a,3]

[a] Department of Botany and Plant Biology, University of Geneva, 1211 Geneva, Switzerland
[b] Department of Cell Biology, Max Planck Institute for Developmental Biology, 72076 Tübingen, Germany

ORCID IDs: 0000-0003-2124-1439 (U.H.); 0000-0002-7371-6806 (P.R.); 0000-0002-5370-4170 (K.W.); 0000-0001-9532-630X (L.L.-O.); 0000-0002-2129-8884 (J.N.); 0000-0003-2024-0119 (A.H.); 0000-0002-8169-8580 (M. Barberon); 0000-0001-5806-2253 (M. Bayer); 0000-0002-3597-5698 (M.H.)

Receptor kinases with extracellular leucine-rich repeat domains (LRR-RKs) form the largest group of membrane signaling proteins in plants. LRR-RKs can sense small molecule, peptide, or protein ligands and may be activated by ligand-induced interaction with a shape complementary SOMATIC EMBRYOGENESIS RECEPTOR-LIKE KINASE (SERK) coreceptor kinase. We have previously shown that SERKs can also form constitutive, ligand-independent complexes with the LRR ectodomains of BAK1-INTERACTING RECEPTOR-LIKE KINASE3 (BIR3) receptor pseudokinases, negative regulators of LRR-RK signaling. Here, we report that receptor chimera in which the extracellular LRR domain of BIR3 is fused to the cytoplasmic kinase domains of the SERK-dependent LRR-RKs BRASSINOSTEROID INSENSITIVE1, HAESA and ERECTA form tight complexes with endogenous SERK coreceptors in the absence of ligand stimulus. Expression of these chimeras under the control of the endogenous promoter of the respective LRR-RK leads to strong gain-of-function brassinosteroid, floral abscission, and stomatal patterning phenotypes, respectively. Importantly, a BIR3-GASSHO1 (GSO1)/SCHENGEN3 (SGN3) chimera can partially complement *sgn3* Casparian strip formation phenotypes, suggesting that SERK proteins also mediate GSO1/SGN3 receptor activation. Collectively, our protein engineering approach may be used to elucidate the physiological functions of orphan LRR-RKs and to identify their receptor activation mechanism in single transgenic lines.

INTRODUCTION

Plant-unique membrane receptor kinases characterized by an extracellular domain, a single membrane-spanning helix, and a cytoplasmic dual-specificity kinase domain control many aspects of plant growth and development. They form the first layer of the plant immune system and mediate symbiotic interactions (Hohmann et al., 2017). These leucine-rich repeat receptor kinases (LRR-RKs) constitute the largest class of receptor kinases known in plants (Shiu and Bleecker, 2001). Members of the family have been shown to sense small molecule (Wang et al., 2001), peptide (Gómez-Gómez and Boller, 2000; Matsubayashi, 2014; Santiago et al., 2016), and protein (Huang et al., 2016; Lin et al., 2017; Zhang et al., 2017) ligands.

[1] Current address: Institute of Molecular Biotechnology of the Austrian Academy of Sciences (IMBA) & Research Institute of Molecular Pathology (IMP), Vienna Biocenter (VBC), 1030 Vienna, Austria.
[2] Current address: Research Institute of Molecular Pathology (IMP), Vienna Biocenter (VBC), 1030 Vienna, Austria.
[3] Address correspondence to martin.bayer@tuebingen.mpg.de or michael.hothorn@unige.ch.
The author(s) responsible for distribution of materials integral to the findings presented in this article in accordance with the policy described in the Instructions for Authors (www.plantcell.org) are: Martin Bayer (martin.bayer@tuebingen.mpg.de) and Michael Hothorn (michael.hothorn@unige.ch).
[OPEN] Articles can be viewed without a subscription.
www.plantcell.org/cgi/doi/10.1105/tpc.20.00138

Brassinosteroids, whose biosynthesis involves the steroid 5α reductase DE-ETIOLATED2 (DET2; Chory et al., 1991; Noguchi et al., 1999), are a class of phytohormones that are sensed by the ectodomain of the LRR-RK BRASSINOSTEROID INSENSITIVE1 (BRI1) with nanomolar affinity (Wang et al., 2001; Hothorn et al., 2011; Hohmann et al., 2018b). Brassinosteroid binding to the BRI1 ectodomain triggers BRI1 interaction with the LRR domain of a SOMATIC EMBRYOGENESIS RECEPTOR LIKE KINASE (SERK) coreceptor (Hothorn et al., 2011; She et al., 2011; Santiago et al., 2013; Sun et al., 2013; Hohmann et al., 2018b). The formation of this heterodimeric complex at the cell surface promotes interaction and trans-phosphorylation of the receptor and coreceptor kinase domains inside the cell (Wang et al., 2008; Bojar et al., 2014; Hohmann et al., 2018b; Perraki et al., 2018). BRI1 receptor activation initiates a cytoplasmic signaling cascade, which ultimately results in the dephosphorylation and activation of a family of basic helix-loop-helix transcription factors, including the Arabidopsis (*Arabidopsis thaliana*) proteins BRASSINAZOLE-RESISTANT1 (BZR1) and BRI1-EMS-SUPPRESSOR1 (BES1; Wang et al., 2002; Yin et al., 2002; Vert and Chory, 2006; Nosaki et al., 2018). In *bes1-D* plants, BES1 Pro-233 is replaced by a Leu residue, which leads to constitutive brassinosteroid signaling responses by enhancing protein phosphatase 2A–mediated dephosphorylation (Yin et al., 2002; Tang et al., 2011).

The plant-unique mechanism of SERK coreceptor-dependent activation is conserved among many LRR-RKs (Hohmann et al., 2017), for example, the LRR-RK HAESA (HAE), whose functions

include the control of floral organ abscission in Arabidopsis by interacting with the peptide hormone INFLORESCENCE DEFICIENT IN ABSCISSION (IDA; Jinn et al., 2000; Meng et al., 2016; Santiago et al., 2016; Hohmann et al., 2018b). A SERK-dependent mitogen-activated protein kinase (MAPK) signaling pathway (Meng et al., 2015) involves the LRR-RK ERECTA (ER) and its paralogues ERECTA-LIKE1 (ERL1) and ERL2 (Torii et al., 1996; Shpak, 2013) and plays diverse roles in plant development. ERECTA, ERL1, and ERL2 together control stomata development and their correct spacing on the leaf surface (Shpak et al., 2005). Cys-rich EPIDERMAL PATTERNING FACTOR (EPF) peptides bind to the ectodomains of ERECTA, ERL1, and ERL2, which form constitutive complexes with the ectodomain of the receptor-like protein (RLP) TOO MANY MOUTH (TMM; Yang and Sack, 1995; Nadeau and Sack, 2002; Lee et al., 2012, 2015; Lin et al., 2017). Binding of EPF peptides to these LRR-RK/LRR-RLP complexes triggers their interaction with SERK coreceptor kinases (Meng et al., 2015; Lin et al., 2017) that in turn leads to the initiation of a MAPK signaling pathway that includes the MAPK kinase kinase YODA (Bergmann et al., 2004). Stimulation of the ERECTA pathway negatively regulates stomata formation (Lampard et al., 2009).

The determination of complex structures and quantitative biochemical comparisons of different ligand-activated LRR-RK–SERK complexes have revealed a structurally and functionally conserved activation mechanism, relying on the interaction of the ligand-bound receptor LRR ectodomain with the shape-complementary ectodomain of the SERK coreceptor (Santiago et al., 2013, 2016; Wang et al., 2015; Hohmann et al., 2017, 2018b; Lin et al., 2017). The ligand binding specificity of plant LRR-RKs is encoded in their LRR ectodomains (Hohmann et al., 2017; Okuda et al., 2020). The kinase domain of the receptor, not of the SERK coreceptor, confers cytoplasmic signaling specificity (Hohmann et al., 2018b; Chen et al., 2019; Zheng et al., 2019). Recent genetic, biochemical, and structural evidence suggests that not all plant LRR-RKs rely on SERKs as essential coreceptor kinases (Zhang et al., 2017; Anne et al., 2018; Cui et al., 2018; Hu et al., 2018; Smakowska-Luzan et al., 2018).

Protein engineering approaches have previously been used to dissect LRR-RK receptor activation in planta: a fusion protein combining the extracellular and transmembrane domains of BRI1 (outerBRI1 [oBRI1]) with the cytoplasmic kinase domain of the rice (*Oryza sativa*) immune receptor XA21 (innerXA21 [iXA21]) triggered an immune response in rice cells upon stimulation with brassinosteroids (He et al., 2000). We now know that both BRI1 and XA21 rely on SERK coreceptor kinases for receptor activation (Li et al., 2002; Nam and Li, 2002; Santiago et al., 2013; Chen et al., 2014; Hohmann et al., 2018b). The heteromeric nature of LRR-RK–SERK complexes has been validated in planta using similar protein engineering approaches. Coexpression of a chimeric construct between the immune receptor FLAGELLIN SENSING2 (FLS2) and its coreceptor SERK3 (*oFLS2-iSERK3*) with an *oSERK3-iFLS2* construct led to immune signaling after stimulation with the FLS2 ligand flg22 in a transient expression system (Albert et al., 2013). Stable transgenic lines coexpressing *oBRI1-iSERK3* and *oSERK3-iBRI1* constructs partially rescued the BRI1 weak loss-of-function mutant *bri1-301* (Hohmann et al., 2018b).

The signaling specificity of the cytoplasmic kinase domain of LRR-RKs has been dissected using an oBRI-iHAESA chimera, which rescued the floral abscission phenotypes when expressed under the control of the *HAESA* promoter in the *haesa haesa-like2* (*hsl2*) double mutant (Hohmann et al., 2018b). A similar approach recently demonstrated that the LRR-RKs BRI1 and EXCESS MICROSPOROCYTES1 (EMS1) share a common cytoplasmic signaling cascade (Zheng et al., 2019). However, these approaches all rely on ligand stimulus.

Recently, two studies reported a constitutive, ligand-independent interaction between the LRR ectodomains of SERKs and of BAK1-INTERACTING RECEPTOR-LIKE KINASEs (BIRs; Ma et al., 2017; Hohmann et al., 2018a). While BIR1 appears to have a catalytically active cytoplasmic kinase domain, BIR2 to BIR4 are receptor pseudokinases (Gao et al., 2009; Wang et al., 2011; Blaum et al., 2014). Different BIRs have been characterized as negative regulators of plant immunity, floral abscission, and brassinosteroid signaling (Gao et al., 2009; Leslie et al., 2010; Halter et al., 2014; Imkampe et al., 2017). Structural and biochemical analyses now implicate BIR proteins as general negative regulators of SERK coreceptor-mediated LRR-RK signaling pathways (Moussu and Santiago, 2019). The ectodomains of BIR1 to BIR4 bind to SERK ectodomains with dissociation constants in the low micromolar range and target a surface area in SERKs normally required for the interaction with ligand-bound LRR-RKs (Ma et al., 2017; Hohmann et al., 2018a, 2018b). Thus, BIRs can efficiently compete with LRR-RKs for SERK binding, negatively regulating LRR-RK signaling pathways. In line with this observation, the elongated (*elg*) allele of SERK3, which weakens the interaction with BIRs, but not with BRI1, results in a brassinosteroid-specific gain-of-function signaling phenotype, as BRI1 can more efficiently compete with BIRs for coreceptor binding (Jaillais et al., 2011; Hohmann et al., 2018a). Structure-guided mutations in the BIR-SERK ectodomain complex interface (BIR3 residues Phe-146-Ala/Arg-170-Ala) efficiently disrupt BIR-SERK signaling complexes in vitro and in planta (Hohmann et al., 2018a). Here, we present protein fusions of the BIR3 LRR ectodomain and transmembrane helix (oBIR3) with the cytoplasmic domains of different SERK-dependent LRR-RKs (iBRI1, iHAESA, iER, and iFLS2). Expressing these chimeric constructs under the control of endogenous/context-specific promoters, we obtain strong gain-of-function phenotypes for different developmental signaling pathways triggered by LRR-RKs. In addition, an oBIR3-iGSO1/SGN3 chimera supports a SERK-dependent activation mechanism for the LRR-RK GASSHO1 (GSO1; also called SCHENGEN3 [SGN3]) in Casparian strip formation (Pfister et al., 2014; Okuda et al., 2020). Our strategy allows for the identification of gain-of-function phenotypes of orphan LRR-RKs whose ligands are unknown and enables the elucidation of their receptor activation mechanism.

RESULTS

We compared the structure of a previously reported BRI1-brassinolide-SERK1 complex (Protein Data Bank [PDB] ID: 4LSX; http://rcsb.org) with the recently reported structure of a BIR3-SERK1 complex (PDB-ID: 6FG8; Santiago et al., 2013; Hohmann et al., 2018a). The BRI1 and BIR3 ectodomains bind SERK1 using overlapping, but nonidentical, binding surfaces (Figure 1A). As in

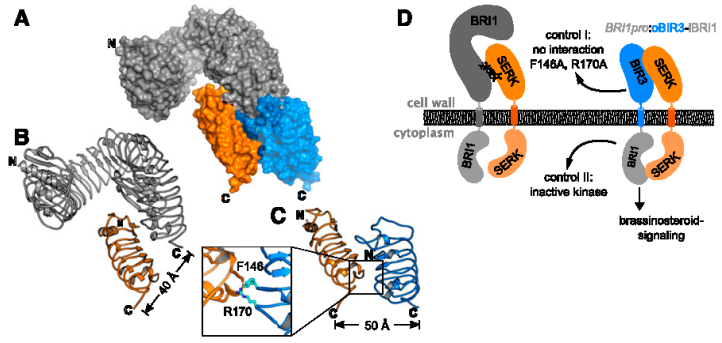

Figure 1. Structural Overview of the BRI1-SERK and BIR3-SERK Complexes.

(A) Surface view of a structural superposition of the BRI1-SERK1 (ectodomains shown in gray and orange, respectively; PDB ID: 4LSX; http://www.rcsb.org/) and SERK1-BIR3 (orange and blue; PDB ID: 6FG8) complexes. The two structures are aligned on SERK1 (root mean square deviation ~0.3 Å comparing 143 corresponding SERK1 C atoms).
(B) and **(C)** Ribbon diagrams of the BRI1-SERK1 **(B)** and BIR3-SERK1 **(C)** complexes, with SERK1 shown in the same orientation. The distances between the respective C termini are indicated (colors as in **[A]**). Inset: close-up view of the BIR3-SERK1 complex interface, with the interface residues Phe-146 and Arg-170 highlighted in bonds representation. Mutation of both residues to Ala disrupts the BIR3-SERK1 complex in vitro and in vivo (Hohmann et al., 2018a).
(D) Schematic overview of an entire BRI1-brassinolide-SERK signaling complex and the envisioned oBIR3-iBRI1-SERK interaction.

the BRI1-SERK1 complex, the C termini of BIR3 and SERK1 are in close proximity in the complex structure (Figures 1B and 1C). Based on their structural similarities, we generated an oBIR3-iBRI1 chimera, in which the BIR3 ectodomain and transmembrane helix are connected to the cytoplasmic domain of BRI1 (see Methods; Figure 1D).

We introduced the oBIR3-iBRI1 chimeric construct, driven by the *BRI1* promoter and with a C-terminal mCitrine fluorescent protein tag, in a previously characterized *bri1* null mutant (Jaillais et al., 2011). We used chimeric constructs encoding oBIR3$^{F146A/R170A}$-iBRI1 and oBIR3-iBRI1^{D1027N} as controls, as they block BIR-SERK complex formation (Hohmann et al., 2018a) and BRI1 kinase activity (Bojar et al., 2014; Hohmann et al., 2018b), respectively. Independent oBIR3-iBRI1 transgenic lines, but none of the control lines, displayed the wavy hypocotyl phenotype characteristic of gain-of-function brassinosteroid mutants (Figure 2A). Importantly, we also observed the wavy hypocotyl phenotype in oBIR3-iBRI1 lines in plants grown in the presence of the brassinosteroid biosynthesis inhibitor brassinazole (BRZ; Figure 2A; Asami et al., 2000). This suggests that oBIR3-iBRI1–triggered brassinosteroid signaling does not depend on endogenous brassinosteroids (Figure 2A). To confirm this hypothesis, we introduced the oBIR3-iBRI1 chimera into the *det2-1* background (Chory et al., 1991), characterized by reduced brassinosteroid levels (Fujioka et al., 1997): all oBIR3-iBRI1 *det2-1* lines, but none of the controls, exhibited a constitutively active phenotype (Figure 2A). Quantification of three independent oBIR3-iBRI1 T3 lines revealed strong gain-of-function phenotypes, which were even more pronounced than the previously reported phenotype of the constitutively active *bes1-1D* mutant (Figure 2A; Supplemental Figure 1B to 1D; Supplemental Data Set; Yin et al., 2002). Introduction of oBIR3-iBRI1 into the *bri1* null or *det2-1* mutants complemented their dwarf phenotype and resulted in extremely elongated petioles, another hallmark of enhanced brassinosteroid signaling (Supplemental Figure 1A). Consistent with a constitutive activation of brassinosteroid signaling, BES1 was dephosphorylated in oBIR3-iBRI1 lines, but not in the control lines (Figure 2B; Supplemental Figure 2). We also detected dephosphorylated BES1 in oBIR3-iBRI1 *det2-1* lines (Figure 2C; Supplemental Figure 2). We next performed coimmunoprecipitation (co-IP) experiments in our stable lines and determined that oBIR3-iBRI1 and oBIR3-iBRI1^{D1027N} efficiently interacted with the endogenous SERK3 coreceptor in vivo, whereas the oBIR3$^{F146A/R170A}$-iBRI1 control, which disrupts the interaction of the isolated BIR3 and SERK1/3 ectodomain in vitro (Hohmann et al., 2018a), could no longer bind SERK3 in planta (Figure 2D; Supplemental Figure 3). Taken together, the BIR3 ectodomain can promote a brassinosteroid-independent interaction with SERK3, and possibly other SERKs in vivo, resulting in a constitutive activation of the brassinosteroid signaling pathway. The control lines further suggest that this signaling complex is formed and stabilized by the ectodomains of BIR3 and SERK3 and requires the catalytic activity of the BRI1 kinase domain for signaling (Figure 2A).

We next tested whether BIR3-based protein chimeras would also activate a functionally distinct LRR-RK signaling pathway. The LRR-RK HAE shares the same overall structure and activation mechanism as BRI1 (Santiago et al., 2013, 2016; Hohmann et al., 2018b), but the two receptors control very different developmental processes (Li and Chory, 1997; Jinn et al., 2000). We introduced an oBIR3-iHAE fusion construct (Figure 3A) with a C-terminal mCitrine tag driven by the *HAE* promoter into the *hae hsl2* mutant, which displays delayed floral organ abscission (Stenvik et al., 2008). We observed that only expression of the oBIR3-iHAE chimera, but not that of the control constructs bearing point mutations in the BIR3 or HAE ectodomains, rescued the floral abscission phenotype of the *hae hsl2* mutant (Figures 3B and 3C). In agreement with these results, oBIR3-iHAE and oBIR3-iHAE^{D1027N} interacted with SERK3 in co-IP assays, but not oBIR3$^{F146A/R170A}$-iHAE (Figure 3D).

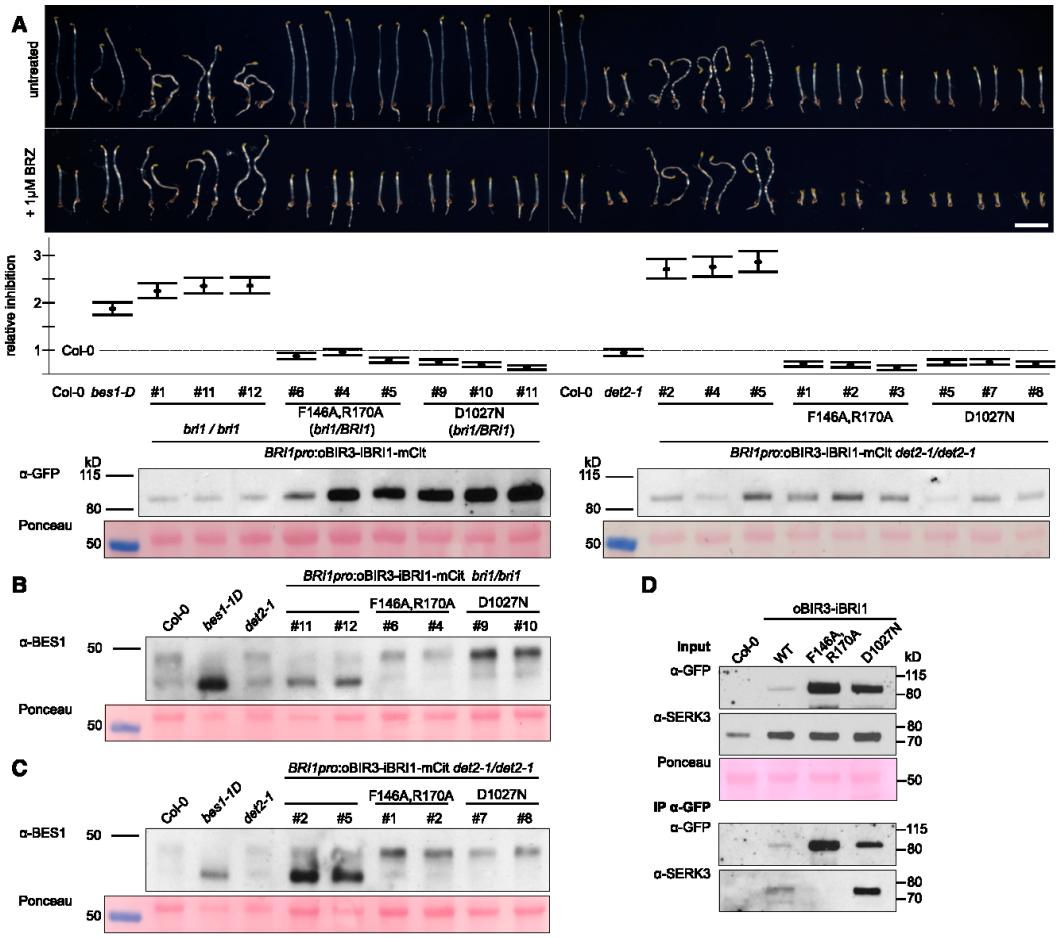

Figure 2. oBIR3-iBRI1 Chimeras Constitutively Activate Brassinosteroid Signaling.

(A) Hypocotyl growth assay of dark-grown seedlings in the presence and absence of the BR biosynthesis inhibitor BRZ. Representative seedlings are shown in the top panel, with the quantification of the data (relative inhibition of hypocotyl growth in the presence of BRZ plotted together with lower and upper confidence intervals) below. For each sample $n = 50$ hypocotyls from five different half-strength MS plates were measured. The # numbers indicate independent lines. Steady state protein levels were quantified by immunoblot with an anti-GFP antibody (detecting the mCitrine tag present in each chimera); the Ponceau-stained membrane is shown as loading control. Homozygous *bri1-null* plants could be obtained only upon expression of oBIR3-iBRI1, but not of the control chimeras. Bar = 0.5 cm.

(B) and **(C)** Anti-BES1 immunoblot on oBIR3-iBRI chimeras in the *bri1*-null **(B)** and *det2* **(C)** backgrounds, with the corresponding Ponceau-stained membranes.

(D) co-IP experiment of oBIR3-iBRI1 chimera and SERK3. Shown alongside are the input immunoblots and the Ponceau-stained membrane. WT, wild type.

SERK proteins were previously shown to allow for receptor activation of the ERECTA family of receptor kinases during protoderm formation and stomatal patterning (Meng et al., 2015). ERECTA forms constitutive complexes with the LRR-RLP TMM to sense EPF peptides in stomatal patterning (Yang and Sack, 1995; Nadeau and Sack, 2002; Lee et al., 2012, 2015; Lin et al., 2017). However, it is not understood at the mechanistic level how SERK coreceptor kinases allow for receptor activation of this LRR-RK/LRR-RLP signaling complex (Lin et al., 2017). To test for the conservation of the receptor activation mechanism between BRI1, HAESA, and ERECTA, we expressed a chimeric oBIR3-iER construct with a C-terminal yellow fluorescent protein for energy transfer (YPet) specifically in the stomata lineage by using the meristemoid-specific *MUTE* promoter (Figure 4A; Pillitteri et al.,

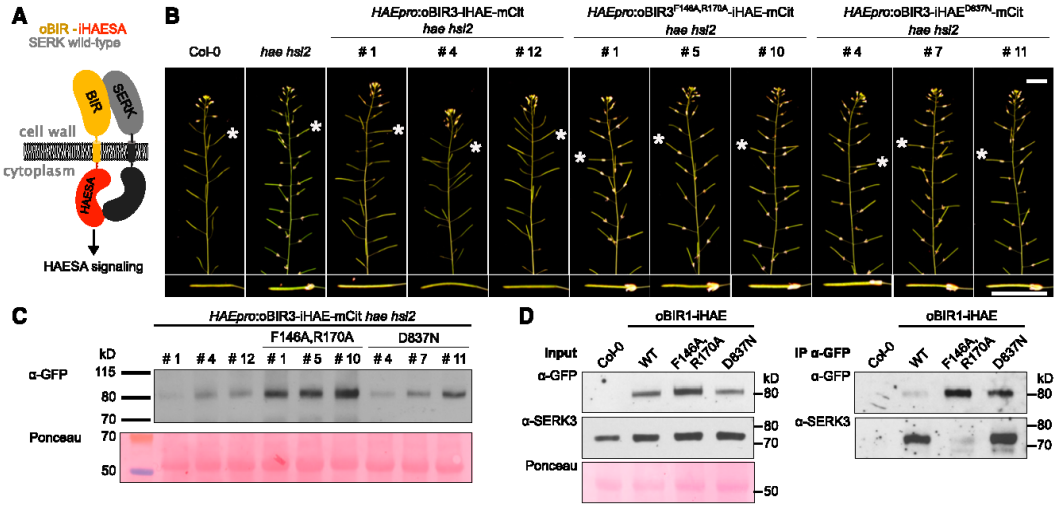

Figure 3. oBIR3-iHAE Chimeras Restore Floral Organ Shedding in *hae hsl2* Mutant Plants.

(A) Cartoon representation of the oBIR3-iHAE chimera.
(B) Representative inflorescences of ~9-week-old Arabidopsis Col-0, *hae hsl2*, and oBIR3-iHAE chimera, with one silique (indicated with a white star) shown magnified below. The # numbers indicate independent lines. Bars = 2 cm.
(C) Steady state protein levels are visualized by immunoblot with an anti-GFP antibody (detecting the mCitrine tag present in each chimera). The Ponceau-stained membrane is shown as loading control.
(D) co-IP experiment of oBIR3-iHAE chimera and SERK3. Shown alongside are the input immunoblots and the Ponceau-stained membrane from input samples (left). WT, wild type.

2007). Previous experiments demonstrated that constitutive activation of the ERECTA pathway in differentiating meristemoids leads to developmental arrest of guard mother cells (GMCs; Lampard et al., 2009). To validate the signaling specificity of our oBIR3-iER chimera, we also expressed a chimeric fusion of the innate immunity receptor FLS2 (Gómez-Gómez and Boller, 2000) driven by the *MUTE* promoter (oBIR3-iFLS2-YPet; Figure 4A; Supplemental Data Set).

Because of the low abundance of our oBIR3-iER and oBIR3-iFLS2 chimeric fusions in meristemoids, we did not perform immunoblot analyses. We did however confirm that all chimeric constructs were expressed and that the fusion proteins localized to the plasma membrane in meristemoids (Supplemental Figure 4). We selected three representative lines according to their YPet fluorescence. The oBIR3-iER lines showed a drastic reduction in mature stomata and an increase in meristemoid-like cells at the leaf surface (Figures 4B and 4C). Consistent with these observations, the oBIR3-iER chimeras downregulated *MUTE* expression (Figure 4D). By contrast, none of the oBIR3-iFLS2 lines displayed any significant deviation from the wild-type stomata phenotype, even though the transgenes were expressed at a similar or higher level than the *BIR3-ER* chimeric constructs (Figure 4G).

To analyze the observed phenotype at a molecular level, we determined the transcript levels of the GMC-specific transcription factor *FAMA* (Ohashi-Ito and Bergmann, 2006) and the guard cell–specific Dof-type transcription factor *STOMATAL CARPENTER1* (*SCAP1*; Negi et al., 2013). The three independent BIR3-ER lines displayed a strong reduction in *FAMA* and *SCAP1* expression (Figures 4E and 4F), suggesting that the abnormal epidermal cells were arrested at the meristemoid stage and did not express GMC-specific or guard cell–specific genes. None of the oBIR3-iFLS2 lines showed a reduction in *FAMA* or *SCAP1* expression. While *SCAP1* transcript levels did not differ significantly from the wild type, *FAMA* expression was significantly upregulated in these lines relative to the wild type (Figures 4E and 4F).

Finally, we tested whether a fusion between the BIR3 ectodomain and the LRR-RK GSO1/SGN3 (Tsuwamoto et al., 2008; Pfister et al., 2014) would restore the apoplastic barrier defects of the *sgn3-3* mutant (Pfister et al., 2014). GSO1/SGN3 directly senses the peptide ligands CASPARIAN STRIP INTEGRITY FACTOR1 (CIF1) and CIF2 to ensure proper formation of the Casparian strip, an endodermal diffusion barrier enabling selective nutrient uptake in the root (Pfister et al., 2014; Doblas et al., 2017; Nakayama et al., 2017; Okuda et al., 2020). A biochemical interaction screen recently identified SERK proteins as putative coreceptor kinases for GSO1/SGN3 (Okuda et al., 2020), but it is presently unclear whether SERKs mediate GSO1/SGN3 receptor activation in vivo (Figure 5A). We introduced chimeric constructs, driven by the *SGN3* promoter and encoding the chimeric proteins oBIR3-iSGN3, oBIR3-iSGN3^{F146A,R170A}, and oBIR3-iSGN3^{D1102N} into the *sgn3-3* mutant background (Figure 5B). As previously described, the *sgn3-3* mutant has a nonfunctional apoplastic barrier that can be visualized and quantified by visualizing the

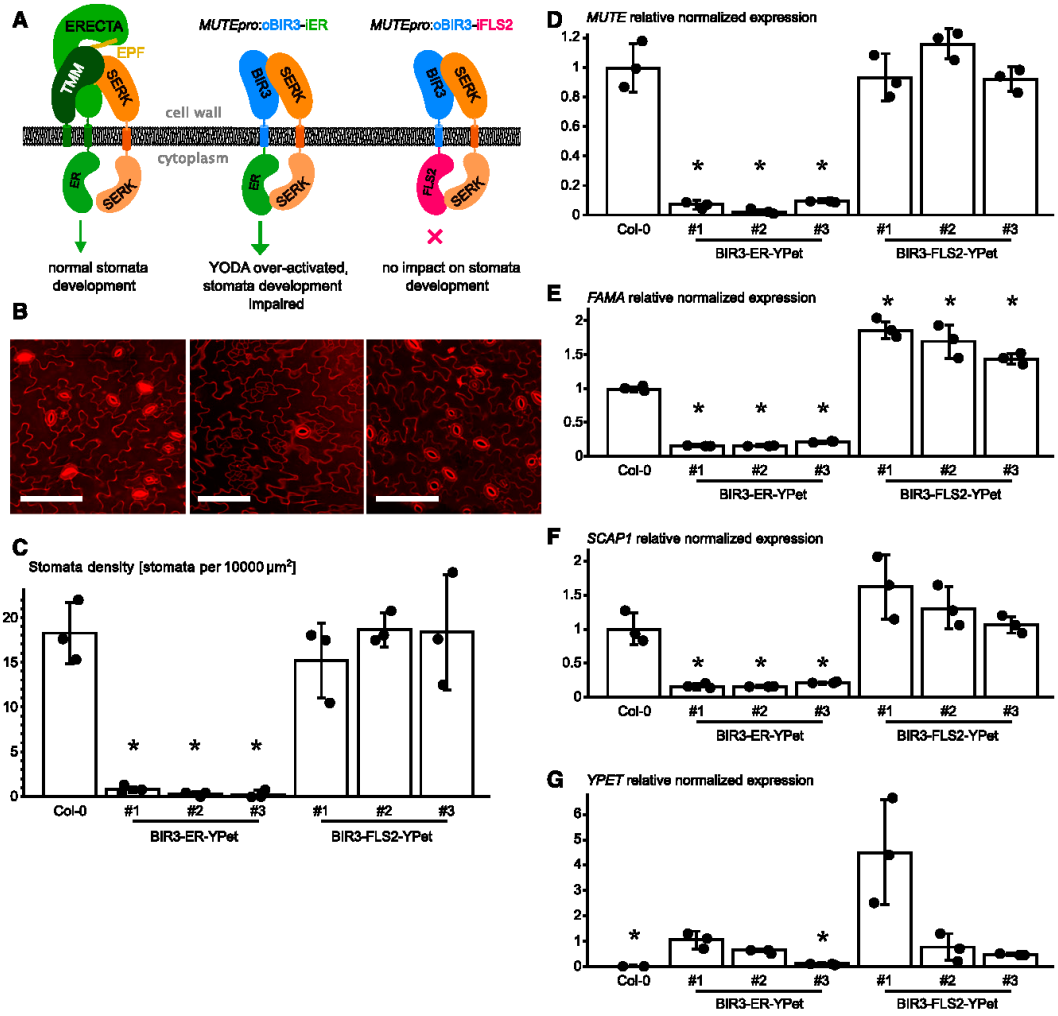

Figure 4. BIR3 chimeras Reveal a Conserved Receptor Activation Mechanism in the LRR-RK ERECTA.

(A) Schematic overview of the ectopically expressed BIR chimera. The receptor kinase ERECTA (ER) interacts with SERK-coreceptor kinases upon ligand (EPF) binding and regulates stomata development (left). Expression of an oBIR3-iER chimera in the epidermis under the MUTE promoter (*MUTEpro*) leads to pathway over-activation and the loss of stomata (middle), while the expression of an oBIR3-iFLS2 chimera has no effect on stomata development.
(B) Confocal microscopy images of PI-stained epidermis of the indicated genotype. Representative images of Col-0 (left), BIR3-ER-YPet (center), and BIR3-FLS2-YPet (right) are shown. Bar = 100 µm.
(C) Abaxial stomata density of cotyledons (# numbers indicate independent lines). The average value of stomata density for three individual plants of each transgenic line is shown. Error bars depict SDs. Individual data points are shown as dots. Significant differences to the wild type are indicated by an asterisk (*t* test; $P < 0.05$).
(D) Expression level of the respective transgenes detected by RT-qPCR of *MUTE*. Data are shown as means ± SD ($n = 3$). Individual data points are shown as dots. Expression in the wild type was arbitrarily set to 1. Significant differences to the wild-type levels are indicated by an asterisk (*t* test; $P < 0.05$).
(E) Relative normalized expression of *FAMA*. Normalized expression values of *FAMA* determined by RT-qPCR are shown as means ± SD ($n = 3$). Individual data points are shown as dots. Expression in the wild type was arbitrarily set to 1. Significant differences to the wild-type levels are indicated by an asterisk (*t* test; $P < 0.05$).

uptake of the apoplastic tracer propidium iodide (PI) along the root and its access to the central vasculature (Figure 5C). We established that the oBIR3-iSGN3 chimera, but none of the point mutants, partially rescued the *sgn3-3* apoplastic defects (Figures 5C and 5D; Supplemental Data Set), indicating a SERK-mediated GSO1/SGN3 receptor activation mechanism in Casparian strip formation. Notably, BIR ectodomains specifically bind the ectodomains of SERKs (Ma et al., 2017; Hohmann et al., 2018a), while not forming complexes with the LRR ectodomain of the sequence-related NSP-INTERACTING KINASE1 (NIK1; Figure 6). This result suggests that SERK coreceptor kinases may have redundant functions in SGN3/GSO1 signaling in the endodermis (Pfister et al. , 2014; Okuda et al., 2020).

DISCUSSION

The identification of a constitutive, ligand-independent interaction between the LRR ectodomains of two plant membrane signaling proteins prompted us to investigate whether protein chimeras between the BIR3 ectodomain and the cytoplasmic domain of various receptor kinases might lead to constitutively active signaling complexes. Despite the significant structural differences between the LRR-RK-SERK and BIR-SERK complexes, our data demonstrate that a wide range of oBIR3-iLRR-RK chimeras are functional in planta.

Expression of the oBIR3-iBRI1 chimera resulted in a strong, constitutive activation of the brassinosteroid signaling pathway. The gain-of-function effect was more pronounced than in the previously described *BRI1*^{sud1} and *SERK3*^{elongated} alleles (Jaillais et al., 2011; Belkhadir et al., 2012; Hohmann et al., 2018a) and was comparable to the constitutive activation of BES1 (Figure 2A; Yin et al., 2002). The constitutive signaling activity of the oBIR3-iBRI1 chimera depends on (1) the ability of the BIR3 ectodomain to bind SERK ectodomains and (2) the kinase activity of the BRI1 cytosolic segment (Figure 2). These results reinforce the notion that formation of the heterodimeric extracellular signaling complex drives LRR-RK receptor activation and that signaling specificity is encoded in the kinase domain of the receptor, not the coreceptor (Bojar et al., 2014; Hohmann et al., 2018b; Zheng et al., 2019). The similar phenotypes seen in oBIR3-iBRI1 lines and *bes1-1D* plants suggest that little signal amplification occurs throughout the brassinosteroid signaling pathway (Figure 2).

We noted that different active signaling chimeras accumulated to low protein levels, whereas their corresponding noninteracting or kinase-dead controls accumulated to higher levels (Figures 2A, 3C, and 5B). We speculate that expression, protein accumulation, and/or protein stability of the constitutively active chimeras may be negatively regulated to dampen their signaling capacity. Such regulation may be achieved in part by known processes regulating LRR-RK internalization and degradation in plants (Russinova et al., 2004; Robatzek et al., 2006; Geldner et al., 2007; Beck et al., 2012; Irani et al., 2012; Doblas et al., 2017; Zhou et al., 2018).

Analysis of the oBIR3-iHAE chimeric receptor revealed a strongly conserved activation mechanism between different SERK-dependent LRR-RK signaling pathways, as previously suggested (Figure 3; Hohmann et al., 2018b). In addition, our experiments imply that BIR ectodomains can interact with SERK proteins in the abscission zone and thus that BIR proteins may act as negative regulators of HAESA- and HSL2-mediated signaling cascades in the wild-type plants (Figure 3). In this respect, it is worth noting that the *bir1* suppressor *SOBIR1/EVERSHED* was previously characterized as a genetic component of the floral abscission signaling pathway (Leslie et al., 2010).

The ERECTA family of kinases require SERK coreceptor kinases to control stomatal patterning and immune responses (Meng et al., 2015; Jordá et al., 2016). Our functional oBIR3-iER chimera now suggests that, despite the requirement for TMM, EPF-bound ER signaling complexes are activated by SERK proteins in very similar ways as those previously reported for other LRR-RKs (Figure 4; Hohmann et al., 2017). Expression of the oBIR3-iER chimera in meristemoid cells led to a similar phenotype as that described for the expression of constitutively active versions of YODA, MAPPK KINASE4 (MKK4), and MKK5 (Lampard et al., 2009). This similarity in phenotypes therefore indicates that the oBIR3-iER chimera displays constitutive, ligand-independent signaling activity. The specificity of signal transduction appears to be largely maintained, as expression of *oBIR3-iFLS2* led to the wild-type–like stomatal development. At the molecular level, we observed a significant increase in *FAMA* expression for all tested oBIR3-iFLS2 lines and a decrease in *MUTE* expression in oBIR3-iER lines. These results are consistent with an antagonistic regulation of these two pathways (Sun et al., 2018). The upregulation of *FAMA* expression, however, did not significantly alter stomata density, likely because the transcriptional activation of the *oBIR3-iFLS2* construct in this experiment was restricted to meristemoid cells by the use of the *MUTE* promoter and might be compensated by post-transcriptional regulation.

Expression of an oBIR3-iSGN3 chimera partially rescued the Casparian strip phenotype of *sgn3-3* plants (Figure 5). BIR ectodomains specifically interacted with SERKs, but not with related LRR-RKs, in vitro (Figure 6). This result suggests that SGN3/GSO1 requires SERKs for receptor activation.

Taken together, our simple, Lego-style assembly of BIR3 chimeras (Figure 7) and the availability of suitable control lines now allow for the genetic characterization of orphan LRR-RKs with unknown/unclear loss-of-function phenotypes and the dissection

Figure 4. (continued).

(F) Relative normalized expression of *SCAP1*. Normalized expression values determined by RT-qPCR are shown as means ± SD ($n = 3$). Individual data points are shown as dots. Expression in the wild type was arbitrarily set to 1. Significant differences to the wild-type levels are indicated by an asterisk (*t* test; $P < 0.05$).

(G) Expression level of the respective transgenes detected by RT-qPCR of YPet. Data are shown as means ± SD ($n = 3$). Individual data points are shown as dots. Expression in the oBIR3-iER-YPET line #1 was arbitrarily set to 1. Significant differences in transgene expression to line #1 is indicated by an asterisk (*t* test; $P < 0.05$).

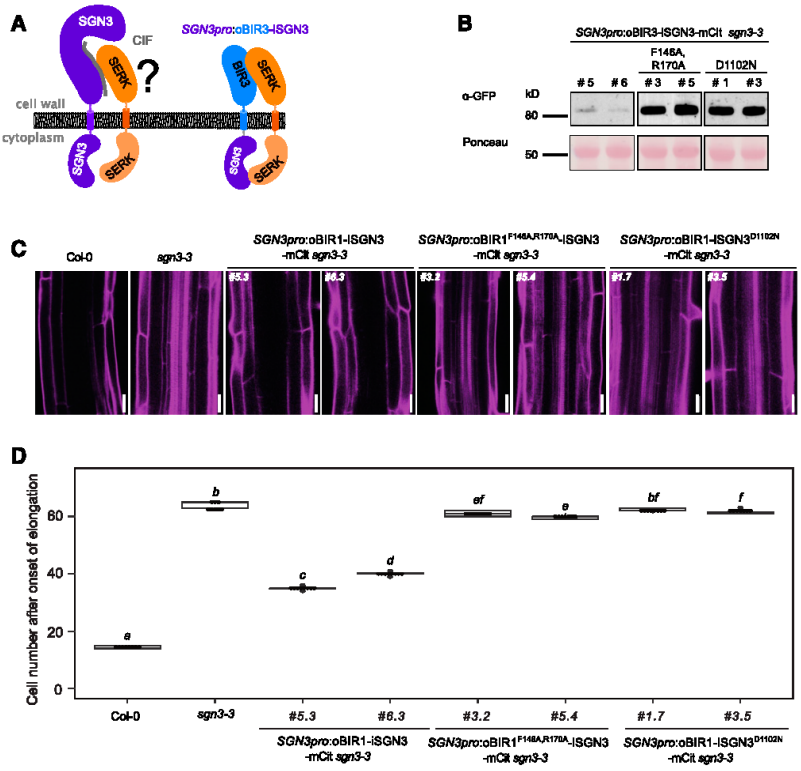

Figure 5. oBIR3-iSGN3 Chimeras Suggest a Role for SERK Proteins in Casparian Strip Formation.

(A) Schematic overview of a biochemically defined SGN3-CIF-SERK signaling complex. The oBIR3-iSGN3 chimera is shown alongside.
(B) Steady state protein levels are visualized by immunoblot with an anti-GFP antibody (detecting the mCitrine tag present in each chimera). The Ponceau-stained membrane is shown as loading control.
(C) Complementation of the *sgn3-3* endodermal barrier defect by the chimeric construct *SGN3pro:oBIR3-iSGN3*. Visualization of endodermal defects with the apoplastic tracer PI, which can reach the stele in barrier-defective plants but is blocked at the endodermis of plants with functional barriers. Pictures were taken around the 50th endodermal cell from the onset of elongation. Bar = 20 μm.
(D) Quantification of the PI block, measured as the number of endodermal cells after the onset of elongation where the PI block is observed. Data are presented as box plots with dot plots overlaid ($n > 7$). For multiple comparisons between genotypes, Kruskal-Wallis test was performed and nonparametric Tukey's test was subsequently used as a multiple comparison procedure. Different letters indicate significant difference ($P < 0.05$).

of their potential activation mechanism. BIR3 protein chimeras may also be of use for biochemical or genetic interaction screens in which a constitutively active form of the receptor is desirable.

METHODS

Plant Materials, Growth Conditions, and Generation of Transgenic Lines

To design chimeric receptor kinases, we predicted the transmembrane helix of all LRR-RKs using TMHMM version 2.0 (https://services.healthtech.dtu.dk/service.php?TMHMM-2.0; Krogh et al., 2001). We fused the native signal peptide, extracellular domain, and the transmembrane helix from Arabidopsis BIR3 (residues 1 to 246) to the juxtamembrane and kinase domains of the respective receptor (BRI1 residues 815 to 1196, HAE residues 649 to 999, and SGN3 residues 899 to 1249). We added no additional linker sequences (Figure 7). We PCR amplified all fragments from Arabidopsis (accession Columbia-0 [Col-0]) genomic or cDNA and cloned the resulting PCR products into pDONR221 (Thermo Fisher Scientific) using Gibson-cloning technology. We introduced mutations through site-directed mutagenesis (Supplemental Table 1). We assembled binary vectors via multi-site Gateway technology into the binary vector pB7m34GW, conferring Basta resistance gene (Thermo Fisher Scientific). We introduced all constructs into Agrobacterium (*Agrobacterium tumefaciens*) strain C58C1 harboring the pGV2260 plasmid and transformed Arabidopsis (*Arabidopsis thaliana*) plants using the floral dip method (Clough and Bent, 1998). For each construct, we selected 12 primary transformants. We confirmed the presence of a single insertion by segregation in T2 lines of which we

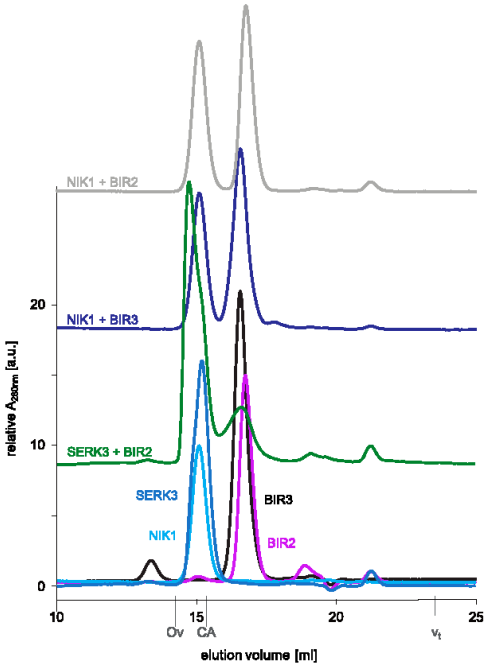

Figure 6. LRR Ectodomains of BIRs and NIK1 Do Not Interact in Vitro.

Analytical size-exclusion chromatography binding experiments using the NIK1, BIR2, and BIR3 ectodomains. BIR2 (gray absorption trace) and BIR3 (in dark blue) do not form a complex with NIK1, as their respective elution volumes correspond to that of the isolated protein (BIR2 in magenta, BIR3 in black, NIK1 in light blue). By contrast, SERK3 and BIR2 form a complex (green absorption trace), resulting in a peak elution volume distinct from isolated SERK3 or BIR2 (SERK3 in medium blue). The NIK1 LRR domain shares 49% protein sequence identity with the SERK1 ectodomain. The total volume (*vt*) is shown together with elution volumes for molecular mass standards (Ov, ovalbumin, 44 kD; CA, carbonic anhydrase, 29 kD). a.u., arbitrary units.

selected three independent lines based on protein accumulation for subsequent analysis. We analyzed all lines in the T3 generation. All transgenic lines generated in the course of this study are listed in Supplemental Table 2.

We used the *bri1* null allele GABI_134E10 (Jaillais et al., 2011), *bes1-1D* (ABRC CS65988; Yin et al., 2002), and *det2-1* (ABRC CS6159; Chory et al., 1991). The mutants *hae hsl2* and *sgn3-3* were previously reported by Stenvik et al. (2008) and Pfister et al. (2014). All plants were grown in soil (Einheitserde Classic, ref. CL Ton Kokos mix containing white peat moss, coco fiber, and clay with 30% [v/v] perlite added) under 50% humidity at 21°C and a 16-h-light/8-h dark cycle (photosynthetic active radiation was ~150 μmol m^{-2} s^{-1} originating from Sylvania–T8 luxline plus, half F58W/T8/840 bulbs [4000 K/5200 lumen] and half F58W/T8/830 [3000 K/5200 lumen] light bulbs).

To generate the chimeric *MUTEpro:oBIR3-iFLS2-YPet* and *MUTEpro:oBIR3-iER-YPet* constructs, we synthesized (Baseclear) a 1946-bp DNA fragment encoding the N-terminal extracellular domain of BIR3 (residues 1 to 245), followed by a short multiple cloning site, the coding sequence of YPet, and a 411-bp terminator sequence from the Arabidopsis *UBQ10* gene. We inserted the synthetic DNA fragment in the T-DNA of a modified pCambia3300 binary vector. We PCR amplified a 2432-bp promoter region from the Arabidopsis *MUTE* gene from Col-0 genomic DNA and inserted the resulting PCR product directly upstream of the synthetic *BIR3* fusion construct by in-fusion cloning (Clontech). We PCR amplified the coding regions for the intracellular domains of ER (residues 581 to 976) and FLS2 (residues 807 to 1173) from cDNAs derived from Arabidopsis seedlings and inserted in frame between the coding region of the BIR3 extracellular domain and the YPet coding region (Figure 7). All constructs were confirmed by Sanger sequencing.

Hypocotyl Growth Assay

Seeds were surface sterilized, stratified at 4°C for 2 d, and plated on half-strength Murashige and Skoog (MS) medium containing 0.8% (w/v) agar and supplemented with 1 μM BRZ from a 10 mM stock solution in 100% DMSO (Tokyo Chemical Industry) or, for the controls, with 0.1% (v/v) DMSO. Following a 1-h light exposure to induce germination, we wrapped the plates in aluminum foil and incubated them in the dark at 22°C for 5 d. We then scanned the plates at 600 dots per inch resolution on a regular flatbed scanner (CanoScan 9000F; Canon), measured hypocotyl lengths using Fiji (Schindelin et al., 2012), and analyzed the results in R version 3.6.1 (R Core Team, 2014) using the packages mratios (Kitsche and Hothorn, 2014) and multcomp (Hothorn et al., 2008). Rather than P-values, we report unadjusted 95% confidence limits for fold-changes. We used a mixed-effects model for the ratio of a given line to the wild-type Col-0, allowing for heterogeneous variances, to analyze log-transformed end point hypocotyl lengths. To evaluate treatment-by-mutant interactions, we calculated the 95% two-sided confidence intervals for the relative inhibition (Col-0: untreated versus BRZ-treated hypocotyl length)/(any genotype: untreated versus BRZ-treated hypocotyl length) for the log-transformed length.

Plant Protein Extraction and Immunoprecipitation

We sowed surface-sterilized seeds on half-strength MS medium with 0.8% (w/v) agar and allowed seedlings to grow for ~14 d after release from stratification. We harvested seedlings, padded them dry carefully on paper towels, snap-froze them in liquid nitrogen, and ground them to a fine powder using a pre-cooled mortar and pestle. We resuspended 1 g of powder per sample in 3 mL of ice-cold extraction buffer (50 mM Bis-Tris, pH 7.0, 150 mM NaCl, 10% [v/v] glycerol, 1% [v/v] Triton X-100, 5 mM DTT, and protease inhibitor cocktail [P9599; Sigma-Aldrich]) and agitated gently at 4°C for 1 h. Subsequently, we centrifuged samples (30 min at 16,000*g* and 4°C), transferred the supernatant to a fresh tube, and estimated protein concentration by Bradford assay against a BSA standard curve.

For each co-IP, we incubated 20 mg of total protein in a volume of 5 mL with 50 μL of antiGFP superparamagnetic MicroBeads (Miltenyi Biotec) for 1 h at 4°C with gentle agitation. Using a magnetic rack and μMACS columns (washed once with extraction buffer; Miltenyi Biotec), we collected the beads and then washed them four times with 1 mL of ice-cold extraction buffer. We then eluted bound proteins twice in 20 μL of extraction buffer pre-heated to 95°C. We separated samples on 10% SDS-PAGE gels and analyzed resolved proteins by standard immunoblot using the following antibodies: anti-GFP antibody coupled to horseradish peroxidase (anti-GFP-HRP, 130-091-833; Miltenyi Biotec) at 1:2000 dilution to detect mCitrine; anti-SERK3 (Bojar et al., 2014) at 1:5000 dilution in conjunction with a secondary anti-rabbit HRP antibody (1:10,000, no. 401353; Calbiochem) to detect SERK3.

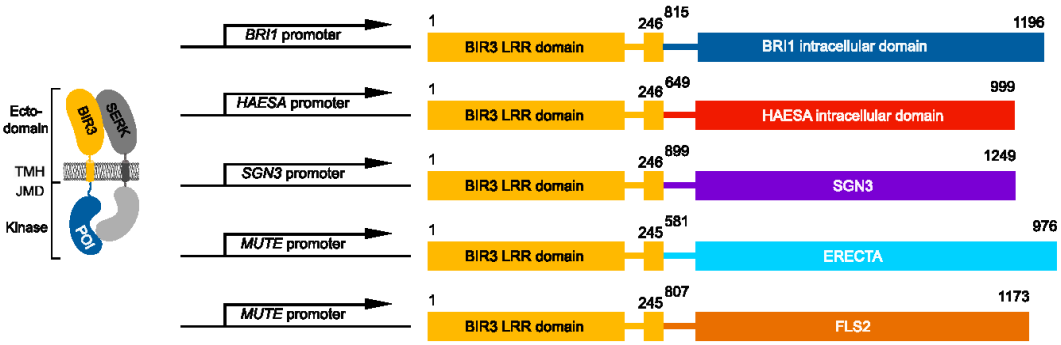

Figure 7. Design Principles of BIR Chimeras.

Schematic overview of selected BIR3 chimeras used in this study. Chimeric constructs are expressed under the endogenous promoter of the respective receptor gene. JMD, juxtamembrane domain; POI, protein of interest; TMH, transmembrane helix.

Immunoblot for BES1

For each sample, we harvested ~100 μg of 7-d-old seedlings grown on half-strength MS medium with 0.8% (w/v) agar, froze the tissue in liquid nitrogen, and ground it to a fine powder using a bead mill (MM400; Retsch). We resuspended samples in ~200 μL of ice-cold extraction buffer (25 mM Tris-HCl, pH 7.5, 150 mM NaCl, 1% (w/v) SDS, 10 mM DTT, and protease inhibitor cocktail [P9599; Sigma-Aldrich]), and incubated them with gentle agitation for 1 h at 4°C before centrifugation for 30 min at 4°C and 16,000*g*. We transferred the supernatant to a fresh tube and assessed their protein concentration by Bradford assay. We separated 80 μg of total protein on a 12% SDS-PAGE gel and analyzed the resolved proteins by immunoblot (primary antibody: anti-BES1, 1:2000 [Yin et al., 2002]; secondary antibody: anti-rabbit HRP [1:10,000, no. 40135; Calbiochem).

Stomata Density Measurements and Microscopy

We used 7-d-old T2 seedlings resistant to Basta to determine stomata density. For confocal imaging, we incubated seedlings in a 10 mg/L PI solution for 30 min and then washed them with water. We imaged the abaxial epidermal regions of cotyledons using a confocal LSM 780 non-linear optical microscope (Zeiss) equipped with a Plan-Apochromat 25×/0.8 Imm Corr differential interference contrast objective. We visualized PI staining with an excitation wavelength of 514 nm and recorded emission between 566 nm and 643 nm. We counted mature stomata over a 0.5 mm by 0.5 mm epidermal area for three seedlings per line. For analysis of fluorescent protein accumulation, we stained 2-d-old seedlings with PI solution and imaged them by confocal microscopy as described above. In addition, we recorded YPet fluorescence by excitation at 514 nm and recorded emission between 517 nm and 544 nm.

Gene Expression Analysis

We used 7-d-old T2 seedlings to analyze transcript levels for the transgene and the endogenous genes. For each independent line, we extracted RNA from 24 pooled T2 seedlings using the RNase Plant Mini Kit (Qiagen). We synthesized first-strand cDNAs with the RevertAid First Strand cDNA Synthesis Kit (Thermo Fisher Scientific). We measured the relative abundance of the endogenous *FAMA* and *SCAP1* transcripts as well as chimeric *YPet*-containing *BIR3* transcripts by RT-qPCR; program: 1. 50°C for 10 min, 2. 95°C for 5 min, 3. 95°C for 10 s, 4. 60°C for 30 s, Plate Read; repeat step 3 – 4 40 times; 5. 95°C for 10 s, 6. ramp 65°C to 95 and increase 0.5°C every 5 s, Plate Read). We used the expression levels of endogenous *ACTIN2* for normalization.

PI Permeability Assay and Confocal Microscopy of the Wild-Type and Complemented *sgn3-3* Plants

We performed PI permeability assays on 5-d-old seedlings. Briefly, we stained the seedlings in the dark for 10 min in 10 μg/mL PI, rinsed them twice in water, and quantified the staining as previously described by Naseer et al. (2012). We counted endodermal cells using an epifluorescence microscope (Leica). We acquired representative confocal images with an SP8 microscope (Leica), with excitation and detection windows set as follows for PI: excitation, 488 nm; emission, 500 to 550 nm. We processed and analyzed confocal images using ImageJ (Schindelin et al., 2012). We performed all statistical analyses in R (R Core Team, 2014). For multiple comparisons between genotypes, we performed the Kruskal-Wallis test and nonparametric Tukey's test as a multiple comparison procedure. Different letters indicate significant differences ($P < 0.05$). Data are presented as box plots overlaid with dot plots.

Protein Expression, Purification, and Size-Exclusion Chromatography

We PCR amplified the coding regions of Arabidopsis NIK1$^{32-248}$ and SERK3$^{1-220}$ from Arabidopsis Col-0 cDNAs, and PCR-amplified Arabidopsis BIR2$^{1-222}$ and BIR3$^{1-213}$ from Arabidopsis Col-0 genomic DNA, before cloning all PCR products into a modified pFastBac vector (Geneva Biotech), providing a tobacco etch virus protease–cleavable C-terminal StrepII-9xHis tag. We fused NIK1 to an N-terminal azurocidin secretion peptide. We expressed proteins by infection of cabbage looper (*Trichoplusia ni*) cells (strain Tnao38; Hashimoto et al., 2010) with 15 mL of *Autographa californica* nucleopolyhedrovirus in 250 mL of cells at a density of ~2 × 10^6 cells mL^{-1} (multiplicity of infection was ~3), followed by incubation for 26 h at 28°C and 110 rpm shaking and then for another 48 h at 22°C and 110 rpm. We purified the secreted proteins from the supernatant by sequential Ni^{2+} (HisTrap excel; GE Healthcare; equilibrated in 25 mM KP_i pH 7.8, 500 mM NaCl) and StrepII (Strep-Tactin XT; IBA; equilibrated in 25 mM Tris-HCl, pH 8.0, 250 mM NaCl, and 1 mM EDTA) affinity chromatography followed by size-exclusion chromatography on a HiLoad 16/600 Superdex 200-pg column (GE Healthcare), equilibrated in 20 mM sodium citrate, pH 5.0, and 250 mM NaCl. The theoretical molecular weight

of the purified ectodomains is 23.6 kD for $NIK1^{32-248}$, 24.6 kD for $SERK3^{26-220}$, 23.4 kD for BIR^{21-222}, and 24.0 kD for $BIR3^{25-213}$.

For analytical size-exclusion chromatography experiments, we pre-equilibrated a Superdex 200 increase 10/300 GL column (GE Healthcare) in 20 mM sodium citrate, pH 5.0, and 250 mM NaCl. For each run, we injected 40 μg of the individual NIK1, SERK3, BIR2, or BIR3 ectodomains in a volume of 100 μL and monitored elution at a rate of 0.75 mL min^{-1} by UV light absorbance at 280 nm. To probe interactions between NIK1, SERK3, BIR2, and BIR3, we mixed 40 μg of the respective proteins in a total volume of 100 μL and incubated the mixture on ice for 30 min before analysis as outlined above.

Accession Numbers

Sequence data from this article can be found in the National Center for Biotechnology Information and The Arabidopsis Information Resource databases under the following accession numbers: *BRI1* (At4g39400); *BIR2* (At3g28450); *BIR3* (At1g27190); *SERK1* (At1g71830); *SERK3* (At4g33430); *BES1* (At1g19350); *HAE* (At4g28490); *HSL2* (At5g65710); *ER* (At2g26330); *FLS2* (At5g46330); *MUTE* (At3g06120); *UBQ10* (At4g05320); *FAMA* (At3g24140); *SCAP* (At5g65590); *ACTIN2* (At3g18780); *GSO1/SGN3* (At4g20140).

Supplemental Data

Supplemental Figure 1. Rosette phenotypes of plants expressing oBIR3-iBRI1 chimeras and raw data for the hypocotyl growth assays (supports Figure 2A).

Supplemental Figure 2. Full immunoblot films and Ponceau-stained membranes (supports Figures 2A to 2C).

Supplemental Figure 3. Full immunoblot films and Ponceau-stained membranes (supports Figures 2D, 3C, and D3D).

Supplemental Figure 4. Accumulation and subcellular localization of oBIR3-iER and oBIR3-iFLS2 chimeras (supports Figure 4).

Supplemental Table 1. Primers used in this study.

Supplemental Table 2. Transgenic lines created in this study.

Supplemental Data Set. Summary of statistical analyses in this study.

ACKNOWLEDGMENTS

We thank Jenny Russinova for providing us with the BES1 antibody. This work was supported by the Swiss National Science Foundation (grant 31003A_176237 to M.H., grant 31CP30_180213 to M.H., and grant 3003A_179159 to M. Barberon), the Howard Hughes Medical Institute (International Research Scholar Award to M.H.), the Max Planck Society, and the Deutsche Forschungsgemeinschaft (grant SFB 1101/B01 to M. Bayer).

AUTHOR CONTRIBUTIONS

U.H., M. Bayer, and M.H. designed the project and the experiments. U.H., P.R., K.W., L.L.-O., J.N., and A.H. performed the experiments. U.H., P.R., K.W., M. Barberon, M. Bayer, and M.H. analyzed the data and prepared the figures. Funding was secured by M. Barberon, M. Bayer, and M.H.

Received February 20, 2020; revised July 22, 2020; accepted August 12, 2020; published August 13, 2020.

REFERENCES

Albert, M., Jehle, A.K., Fürst, U., Chinchilla, D., Boller, T., and Felix, G. (2013). A two-hybrid-receptor assay demonstrates heteromer formation as switch-on for plant immune receptors. Plant Physiol. **163:** 1504–1509.

Anne, P., Amiguet-Vercher, A., Brandt, B., Kalmbach, L., Geldner, N., Hothorn, M., and Hardtke, C.S. (2018). CLERK is a novel receptor kinase required for sensing of root-active CLE peptides in *Arabidopsis*. Development **145:** dev162354.

Asami, T., Min, Y.K., Nagata, N., Yamagishi, K., Takatsuto, S., Fujioka, S., Murofushi, N., Yamaguchi, I., and Yoshida, S. (2000). Characterization of brassinazole, a triazole-type brassinosteroid biosynthesis inhibitor. Plant Physiol. **123:** 93–100.

Beck, M., Zhou, J., Faulkner, C., MacLean, D., and Robatzek, S. (2012). Spatio-temporal cellular dynamics of the Arabidopsis flagellin receptor reveal activation status-dependent endosomal sorting. Plant Cell **24:** 4205–4219.

Belkhadir, Y., Jaillais, Y., Epple, P., Balsemão-Pires, E., Dangl, J.L., and Chory, J. (2012). Brassinosteroids modulate the efficiency of plant immune responses to microbe-associated molecular patterns. Proc. Natl. Acad. Sci. USA **109:** 297–302.

Bergmann, D.C., Lukowitz, W., and Somerville, C.R. (2004). Stomatal development and pattern controlled by a MAPKK kinase. Science **304:** 1494–1497.

Blaum, B.S., Mazzotta, S., Nöldeke, E.R., Halter, T., Madlung, J., Kemmerling, B., and Stehle, T. (2014). Structure of the pseudokinase domain of BIR2, a regulator of BAK1-mediated immune signaling in Arabidopsis. J. Struct. Biol. **186:** 112–121.

Bojar, D., Martinez, J., Santiago, J., Rybin, V., Bayliss, R., and Hothorn, M. (2014). Crystal structures of the phosphorylated BRI1 kinase domain and implications for brassinosteroid signal initiation. Plant J. **78:** 31–43.

Chen, W., Lv, M., Wang, Y., Wang, P.-A., Cui, Y., Li, M., Wang, R., Gou, X., and Li, J. (2019). BES1 is activated by EMS1-TPD1-SERK1/2-mediated signaling to control tapetum development in Arabidopsis thaliana. Nat. Commun. **10:** 4164.

Chen, X., Zuo, S., Schwessinger, B., Chern, M., Canlas, P.E., Ruan, D., Zhou, X., Wang, J., Daudi, A., Petzold, C.J., Heazlewood, J.L., and Ronald, P.C. (2014). An XA21-associated kinase (OsSERK2) regulates immunity mediated by the XA21 and XA3 immune receptors. Mol. Plant **7:** 874–892.

Chory, J., Nagpal, P., and Peto, C.A. (1991). Phenotypic and genetic analysis of det2, a new mutant that affects light-regulated seedling development in Arabidopsis. Plant Cell **3:** 445–459.

Clough, S.J., and Bent, A.F. (1998). Floral dip: A simplified method for Agrobacterium-mediated transformation of Arabidopsis thaliana. Plant J. **16:** 735–743.

Cui, Y., et al. (2018). CIK receptor kinases determine cell fate specification during early anther development in Arabidopsis. Plant Cell **30:** 2383–2401.

Doblas, V.G., Smakowska-Luzan, E., Fujita, S., Alassimone, J., Barberon, M., Madalinski, M., Belkhadir, Y., and Geldner, N. (2017). Root diffusion barrier control by a vasculature-derived peptide binding to the SGN3 receptor. Science **355:** 280–284.

Fujioka, S., Li, J., Choi, Y.H., Seto, H., Takatsuto, S., Noguchi, T., Watanabe, T., Kuriyama, H., Yokota, T., Chory, J., and Sakurai, A. (1997). The Arabidopsis deetiolated2 mutant is blocked early in brassinosteroid biosynthesis. Plant Cell **9:** 1951–1962.

Gao, M., Wang, X., Wang, D., Xu, F., Ding, X., Zhang, Z., Bi, D., Cheng, Y.T., Chen, S., Li, X., and Zhang, Y. (2009). Regulation of cell death and innate immunity by two receptor-like kinases in Arabidopsis. Cell Host Microbe **6:** 34–44.

Geldner, N., Hyman, D.L., Wang, X., Schumacher, K., and Chory, J. (2007). Endosomal signaling of plant steroid receptor kinase BRI1. Genes Dev. **21:** 1598–1602.

Gómez-Gómez, L., and Boller, T. (2000). FLS2: an LRR receptor-like kinase involved in the perception of the bacterial elicitor flagellin in Arabidopsis. Mol. Cell **5:** 1003–1011.

Halter, T., et al. (2014). The leucine-rich repeat receptor kinase BIR2 is a negative regulator of BAK1 in plant immunity. Curr. Biol. **24:** 134–143.

Hashimoto, Y., Zhang, S., and Blissard, G.W. (2010). Ao38, a new cell line from eggs of the black witch moth, *Ascalapha odorata* (Lepidoptera: Noctuidae), is permissive for AcMNPV infection and produces high levels of recombinant proteins. BMC Biotechnol. **10:** 50.

He, Z., Wang, Z.Y., Li, J., Zhu, Q., Lamb, C., Ronald, P., and Chory, J. (2000). Perception of brassinosteroids by the extracellular domain of the receptor kinase BRI1. Science **288:** 2360–2363.

Hohmann, U., Lau, K., and Hothorn, M. (2017). The structural basis of ligand perception and signal activation by receptor kinases. Annu. Rev. Plant Biol. **68:** 109–137.

Hohmann, U., Nicolet, J., Moretti, A., Hothorn, L.A., and Hothorn, M. (2018a). The SERK3 elongated allele defines a role for BIR ectodomains in brassinosteroid signalling. Nat. Plants **4:** 345–351.

Hohmann, U., Santiago, J., Nicolet, J., Olsson, V., Spiga, F.M., Hothorn, L.A., Butenko, M.A., and Hothorn, M. (2018b). Mechanistic basis for the activation of plant membrane receptor kinases by SERK-family coreceptors. Proc. Natl. Acad. Sci. USA **115:** 3488–3493.

Hothorn, M., Belkhadir, Y., Dreux, M., Dabi, T., Noel, J.P., Wilson, I.A., and Chory, J. (2011). Structural basis of steroid hormone perception by the receptor kinase BRI1. Nature **474:** 467–471.

Hothorn, T., Bretz, F., and Westfall, P. (2008). Simultaneous inference in general parametric models. Biom. J. **50:** 346–363.

Hu, C., et al. (2018). A group of receptor kinases are essential for CLAVATA signalling to maintain stem cell homeostasis. Nat. Plants **4:** 205–211.

Huang, J., Zhang, T., Linstroth, L., Tillman, Z., Otegui, M.S., Owen, H.A., and Zhao, D. (2016). Control of anther cell differentiation by the small protein ligand TPD1 and its receptor EMS1 in Arabidopsis. PLoS Genet. **12:** e1006147.

Imkampe, J., et al. (2017). The Arabidopsis leucine-rich repeat receptor kinase BIR3 negatively regulates BAK1 receptor complex formation and stabilizes BAK1. Plant Cell **29:** 2285–2303.

Irani, N.G., et al. (2012). Fluorescent castasterone reveals BRI1 signaling from the plasma membrane. Nat. Chem. Biol. **8:** 583–589.

Jaillais, Y., Belkhadir, Y., Balsemão-Pires, E., Dangl, J.L., and Chory, J. (2011). Extracellular leucine-rich repeats as a platform for receptor/coreceptor complex formation. Proc. Natl. Acad. Sci. USA **108:** 8503–8507.

Jinn, T.L., Stone, J.M., and Walker, J.C. (2000). HAESA, an Arabidopsis leucine-rich repeat receptor kinase, controls floral organ abscission. Genes Dev. **14:** 108–117.

Jordá, L., Sopeña-Torres, S., Escudero, V., Nuñez-Corcuera, B., Delgado-Cerezo, M., Torii, K.U., and Molina, A. (2016). ERECTA and BAK1 receptor like kinases interact to regulate immune responses in Arabidopsis. Front. Plant Sci. **7:** 897.

Kitsche, A., and Hothorn, L.A. (2014). Testing for qualitative interaction using ratios of treatment differences. Stat. Med. **33:** 1477–1489.

Krogh, A., Larsson, B., von Heijne, G., and Sonnhammer, E.L. (2001). Predicting transmembrane protein topology with a hidden Markov model: application to complete genomes. J. Mol. Biol. **305:** 567–580.

Lampard, G.R., Lukowitz, W., Ellis, B.E., and Bergmann, D.C. (2009). Novel and expanded roles for MAPK signaling in Arabidopsis stomatal cell fate revealed by cell type-specific manipulations. Plant Cell **21:** 3506–3517.

Lee, J.S., Hnilova, M., Maes, M., Lin, Y.-C.L., Putarjunan, A., Han, S.-K., Avila, J., and Torii, K.U. (2015). Competitive binding of antagonistic peptides fine-tunes stomatal patterning. Nature **522:** 439–443.

Lee, J.S., Kuroha, T., Hnilova, M., Khatayevich, D., Kanaoka, M.M., McAbee, J.M., Sarikaya, M., Tamerler, C., and Torii, K.U. (2012). Direct interaction of ligand-receptor pairs specifying stomatal patterning. Genes Dev. **26:** 126–136.

Leslie, M.E., Lewis, M.W., Youn, J.-Y., Daniels, M.J., and Liljegren, S.J. (2010). The EVERSHED receptor-like kinase modulates floral organ shedding in Arabidopsis. Development **137:** 467–476.

Li, J., and Chory, J. (1997). A putative leucine-rich repeat receptor kinase involved in brassinosteroid signal transduction. Cell **90:** 929–938.

Li, J., Wen, J., Lease, K.A., Doke, J.T., Tax, F.E., and Walker, J.C. (2002). BAK1, an Arabidopsis LRR receptor-like protein kinase, interacts with BRI1 and modulates brassinosteroid signaling. Cell **110:** 213–222.

Lin, G., Zhang, L., Han, Z., Yang, X., Liu, W., Li, E., Chang, J., Qi, Y., Shpak, E.D., and Chai, J. (2017). A receptor-like protein acts as a specificity switch for the regulation of stomatal development. Genes Dev. **31:** 927–938.

Ma, C., Liu, Y., Bai, B., Han, Z., Tang, J., Zhang, H., Yaghmaiean, H., Zhang, Y., and Chai, J. (2017). Structural basis for BIR1-mediated negative regulation of plant immunity. Cell Res. **27:** 1521–1524.

Matsubayashi, Y. (2014). Posttranslationally modified small-peptide signals in plants. Annu. Rev. Plant Biol. **65:** 385–413.

Meng, X., Chen, X., Mang, H., Liu, C., Yu, X., Gao, X., Torii, K.U., He, P., and Shan, L. (2015). Differential function of arabidopsis SERK family receptor-like kinases in stomatal patterning. Curr. Biol. **25:** 2361–2372.

Meng, X., Zhou, J., Tang, J., Li, B., de Oliveira, M.V.V., Chai, J., He, P., and Shan, L. (2016). Ligand-induced receptor-like kinase complex regulates floral organ abscission in Arabidopsis. Cell Rep. **14:** 1330–1338.

Moussu, S., and Santiago, J. (2019). Structural biology of cell surface receptor-ligand interactions. Curr. Opin. Plant Biol. **52:** 38–45.

Nadeau, J.A., and Sack, F.D. (2002). Control of stomatal distribution on the Arabidopsis leaf surface. Science **296:** 1697–1700.

Nakayama, T., Shinohara, H., Tanaka, M., Baba, K., Ogawa-Ohnishi, M., and Matsubayashi, Y. (2017). A peptide hormone required for Casparian strip diffusion barrier formation in Arabidopsis roots. Science **355:** 284–286.

Nam, K.H., and Li, J. (2002). BRI1/BAK1, a receptor kinase pair mediating brassinosteroid signaling. Cell **110:** 203–212.

Naseer, S., Lee, Y., Lapierre, C., Franke, R., Nawrath, C., and Geldner, N. (2012). Casparian strip diffusion barrier in Arabidopsis is made of a lignin polymer without suberin. Proc. Natl. Acad. Sci. USA **109:** 10101–10106.

Negi, J., Moriwaki, K., Konishi, M., Yokoyama, R., Nakano, T., Kusumi, K., Hashimoto-Sugimoto, M., Schroeder, J.I., Nishitani, K., Yanagisawa, S., and Iba, K. (2013). A Dof transcription factor, SCAP1, is essential for the development of functional stomata in Arabidopsis. Curr. Biol. **23:** 479–484.

Noguchi, T., Fujioka, S., Takatsuto, S., Sakurai, A., Yoshida, S., Li, J., and Chory, J. (1999). Arabidopsis det2 is defective in the conversion of (24R)-24-methylcholest-4-En-3-one to (24R)-24-methyl-

5alpha-cholestan-3-one in brassinosteroid biosynthesis. Plant Physiol. **120:** 833–840.

Nosaki, S., Miyakawa, T., Xu, Y., Nakamura, A., Hirabayashi, K., Asami, T., Nakano, T., and Tanokura, M. (2018). Structural basis for brassinosteroid response by BIL1/BZR1. Nat. Plants **4:** 771–776.

Ohashi-Ito, K., and Bergmann, D.C. (2006). Arabidopsis FAMA controls the final proliferation/differentiation switch during stomatal development. Plant Cell **18:** 2493–2505.

Okuda, S., Fujita, S., Moretti, A., Hohmann, U., Doblas, V.G., Ma, Y., Pfister, A., Brandt, B., Geldner, N., and Hothorn, M. (2020). Molecular mechanism for the recognition of sequence-divergent CIF peptides by the plant receptor kinases GSO1/SGN3 and GSO2. Proc. Natl. Acad. Sci. USA **117:** 2693–2703.

Perraki, A., et al. (2018). Phosphocode-dependent functional dichotomy of a common co-receptor in plant signalling. Nature **561:** 248–252.

Pfister, A., et al. (2014). A receptor-like kinase mutant with absent endodermal diffusion barrier displays selective nutrient homeostasis defects. eLife **3:** e03115.

Pillitteri, L.J., Sloan, D.B., Bogenschutz, N.L., and Torii, K.U. (2007). Termination of asymmetric cell division and differentiation of stomata. Nature **445:** 501–505.

R Core Team (2014). R: A language and environment for statistical computing.. (Vienna: R Foundation for Statistical Computing).

Robatzek, S., Chinchilla, D., and Boller, T. (2006). Ligand-induced endocytosis of the pattern recognition receptor FLS2 in Arabidopsis. Genes Dev. **20:** 537–542.

Russinova, E., Borst, J.-W., Kwaaitaal, M., Caño-Delgado, A., Yin, Y., Chory, J., and de Vries, S.C. (2004). Heterodimerization and endocytosis of Arabidopsis brassinosteroid receptors BRI1 and AtSERK3 (BAK1). Plant Cell **16:** 3216–3229.

Santiago, J., Brandt, B., Wildhagen, M., Hohmann, U., Hothorn, L.A., Butenko, M.A., and Hothorn, M. (2016). Mechanistic insight into a peptide hormone signaling complex mediating floral organ abscission. eLife **5:** e15075.

Santiago, J., Henzler, C., and Hothorn, M. (2013). Molecular mechanism for plant steroid receptor activation by somatic embryogenesis co-receptor kinases. Science **341:** 889–892.

Schindelin, J., et al. (2012). Fiji: An open-source platform for biological-image analysis. Nat. Methods **9:** 676–682.

She, J., Han, Z., Kim, T.-W., Wang, J., Cheng, W., Chang, J., Shi, S., Wang, J., Yang, M., Wang, Z.-Y., and Chai, J. (2011). Structural insight into brassinosteroid perception by BRI1. Nature **474:** 472–476.

Shiu, S.H., and Bleecker, A.B. (2001). Receptor-like kinases from Arabidopsis form a monophyletic gene family related to animal receptor kinases. Proc. Natl. Acad. Sci. USA **98:** 10763–10768.

Shpak, E.D. (2013). Diverse roles of ERECTA family genes in plant development. J. Integr. Plant Biol. **55:** 1238–1250.

Shpak, E.D., McAbee, J.M., Pillitteri, L.J., and Torii, K.U. (2005). Stomatal patterning and differentiation by synergistic interactions of receptor kinases. Science **309:** 290–293.

Smakowska-Luzan, E., et al. (2018). An extracellular network of Arabidopsis leucine-rich repeat receptor kinases. Nature **553:** 342–346.

Stenvik, G.-E., Tandstad, N.M., Guo, Y., Shi, C.-L., Kristiansen, W., Holmgren, A., Clark, S.E., Aalen, R.B., and Butenko, M.A. (2008). The EPIP peptide of INFLORESCENCE DEFICIENT IN ABSCISSION is sufficient to induce abscission in arabidopsis through the receptor-like kinases HAESA and HAESA-LIKE2. Plant Cell **20:** 1805–1817.

Sun, T., Nitta, Y., Zhang, Q., Wu, D., Tian, H., Lee, J.S., and Zhang, Y. (2018). Antagonistic interactions between two MAP kinase cascades in plant development and immune signaling. EMBO Rep. **19:** 19.

Sun, Y., Han, Z., Tang, J., Hu, Z., Chai, C., Zhou, B., and Chai, J. (2013). Structure reveals that BAK1 as a co-receptor recognizes the BRI1-bound brassinolide. Cell Res. **23:** 1326–1329.

Tang, W., et al. (2011). PP2A activates brassinosteroid-responsive gene expression and plant growth by dephosphorylating BZR1. Nat. Cell Biol. **13:** 124–131.

Torii, K.U., Mitsukawa, N., Oosumi, T., Matsuura, Y., Yokoyama, R., Whittier, R.F., and Komeda, Y. (1996). The Arabidopsis ERECTA gene encodes a putative receptor protein kinase with extracellular leucine-rich repeats. Plant Cell **8:** 735–746.

Tsuwamoto, R., Fukuoka, H., and Takahata, Y. (2008). GASSHO1 and GASSHO2 encoding a putative leucine-rich repeat transmembrane-type receptor kinase are essential for the normal development of the epidermal surface in Arabidopsis embryos. Plant J. **54:** 30–42.

Vert, G., and Chory, J. (2006). Downstream nuclear events in brassinosteroid signalling. Nature **441:** 96–100.

Wang, J., Li, H., Han, Z., Zhang, H., Wang, T., Lin, G., Chang, J., Yang, W., and Chai, J. (2015). Allosteric receptor activation by the plant peptide hormone phytosulfokine. Nature **525:** 265–268.

Wang, X., Kota, U., He, K., Blackburn, K., Li, J., Goshe, M.B., Huber, S.C., and Clouse, S.D. (2008). Sequential transphosphorylation of the BRI1/BAK1 receptor kinase complex impacts early events in brassinosteroid signaling. Dev. Cell **15:** 220–235.

Wang, Z., Meng, P., Zhang, X., Ren, D., and Yang, S. (2011). BON1 interacts with the protein kinases BIR1 and BAK1 in modulation of temperature-dependent plant growth and cell death in Arabidopsis. Plant J. **67:** 1081–1093.

Wang, Z.Y., Nakano, T., Gendron, J., He, J., Chen, M., Vafeados, D., Yang, Y., Fujioka, S., Yoshida, S., Asami, T., and Chory, J. (2002). Nuclear-localized BZR1 mediates brassinosteroid-induced growth and feedback suppression of brassinosteroid biosynthesis. Dev. Cell **2:** 505–513.

Wang, Z.Y., Seto, H., Fujioka, S., Yoshida, S., and Chory, J. (2001). BRI1 is a critical component of a plasma-membrane receptor for plant steroids. Nature **410:** 380–383.

Yang, M., and Sack, F.D. (1995). The too many mouths and four lips mutations affect stomatal production in Arabidopsis. Plant Cell **7:** 2227–2239.

Yin, Y., Wang, Z.Y., Mora-Garcia, S., Li, J., Yoshida, S., Asami, T., and Chory, J. (2002). BES1 accumulates in the nucleus in response to brassinosteroids to regulate gene expression and promote stem elongation. Cell **109:** 181–191.

Zhang, X., Liu, W., Nagae, T.T., Takeuchi, H., Zhang, H., Han, Z., Higashiyama, T., and Chai, J. (2017). Structural basis for receptor recognition of pollen tube attraction peptides. Nat. Commun. **8:** 1331.

Zheng, B., Bai, Q., Wu, L., Liu, H., Liu, Y., Xu, W., Li, G., Ren, H., She, X., and Wu, G. (2019). EMS1 and BRI1 control separate biological processes via extracellular domain diversity and intracellular domain conservation. Nat. Commun. **10:** 4165.

Zhou, J., et al. (2018). Regulation of *Arabidopsis* brassinosteroid receptor BRI1 endocytosis and degradation by plant U-box PUB12/PUB13-mediated ubiquitination. Proc. Natl. Acad. Sci. USA **115:** E1906–E1915.

Constitutive Activation of Leucine-Rich Repeat Receptor Kinase Signaling Pathways by BAK1-INTERACTING RECEPTOR-LIKE KINASE3 Chimera

Ulrich Hohmann, Priya Ramakrishna, Kai Wang, Laura Lorenzo-Orts, Joel Nicolet, Agnes Henschen, Marie Barberon, Martin Bayer and Michael Hothorn

Plant Cell 2020;32;3311-3323; originally published online August 13, 2020;
DOI 10.1105/tpc.20.00138

Available online at www.sciencedirect.com

ScienceDirect

Current Opinion in Plant Biology

Square one: zygote polarity and early embryogenesis in flowering plants

Kai Wang, Houming Chen, Yingjing Miao and Martin Bayer

In the last two decades, work on auxin signaling has helped to understand many aspects of the fundamental process underlying the specification of tissue types in the plant embryo. However, the immediate steps after fertilization including the polarization of the zygote and the initial body axis formation remained poorly understood. Valuable insight into these enigmatic processes has been gained by studying fertilization in grasses. Recent technical advances in transcriptomics of developing embryos with high spatial and temporal resolution give an emerging picture of the rapid changes of the zygotic developmental program. Together with the use of live imaging of novel fluorescent marker lines, these data are now the basis of unraveling the very first steps of the embryonic patterning process.

Address
Max Planck Institute for Developmental Biology, Department of Cell Biology, Max-Planck-Ring 5, 72076 Tübingen, Germany

Corresponding author: Bayer, Martin (martin.bayer@tuebingen.mpg.de)

Current Opinion in Plant Biology 2020, **53**:128–133

This review comes from a themed issue on **Growth and development**

Edited by **Marcus Heisler** and **Alexis Maizel**

For a complete overview see the Issue and the Editorial

Available online 11th November 2019

https://doi.org/10.1016/j.pbi.2019.10.002

Introduction

In embryogenesis, a single cell generally develops into a miniature version of the adult organism. In plants, however, the final body architecture is determined post-embryonically, likely as adaption to their sessile life. Plant embryos represent primitive versions of seedlings and only a few basic cell types are established during embryogenesis [1] (Figure 1).

Fertilization of the egg cell marks the beginning of a new sporophytic generation, starting with the zygote. In many angiosperm species, the zygote divides asymmetrically, often after an initial phase of cell elongation [2]. The apical daughter cell will always form at least part of the embryo. The basal daughter cell contains a large central vacuole and its descendants will mainly contribute extra-embryonic tissue [3]. In *Brassicaceae*, embryogenesis follows an invariable series of cell divisions, in which the apical cell forms a spherical proembryo (Figure 1a). The basal daughter cell undergoes a series of transverse mitotic divisions to form the filamentous suspensor. Except the uppermost cell, the suspensor is extra-embryonic, connects the embryo with maternal seed tissue, and does not contribute to the later plant seedling. Therefore, in *Brassicaceae*, the first zygotic division already marks the boundary between embryonic and extra-embryonic development [4]. In other flowering plants, however, the patterning process can be less stereotypic and in some cases there is no clear boundary between embryonic and suspensor tissue (Figure 2). Cells derived from the first apical cell can also differentiate into suspensor cells, as seen in some members of the *Caryophyllaceae*. In a similar manner, descendants of the basal cell might also contribute to large portions of the proembryo as in some *Asteraceae* family members [3]. Therefore, patterning seems to be mainly influenced by position-dependent cues and the concept of cell lineages apparently does not apply in the early plant embryo. Nonetheless, a universal feature of embryogenesis in seed plants is the polarity of the first zygotic division with the apical daughter cell always contributing to the embryo. This division seems to be an essential step in axis formation of the angiosperm embryo and it is therefore a fundamental question how the zygote is polarized.

Early morphological changes

In flowering plants, already the egg cell is a polar structure with the nucleus at the apex and a large central vacuole at the basal pole [5] (Figure 1b). Microtubules are preferentially oriented in a longitudinal direction [6•]. Directly after fertilization, however, this polarity seems to be lost as the large vacuole is broken up into smaller, evenly distributed vacuoles and the nucleus moves to a central position [5,7]. After this transient apolar phase, polarity is reestablished and the zygote starts to elongate in a similar fashion as tip-growing cells such as pollen tubes or root hair cells [6•,7]. In Arabidopsis, the zygote grows threefold in size whereas in many grasses there is barely any noticeable growth at this stage [3]. The first hallmark of polarity reestablishment happens at this stage as the nucleus moves out of the center to an apical position, followed by an asymmetric division. What kind of positional information determines the direction of cell elongation and the position of the cell division plane?

In many animals, the sperm entry site can function as positional cue [8,9]. In a similar fashion, the brown alga *Fucus* relies on the position of sperm entry in the absence

Figure 1

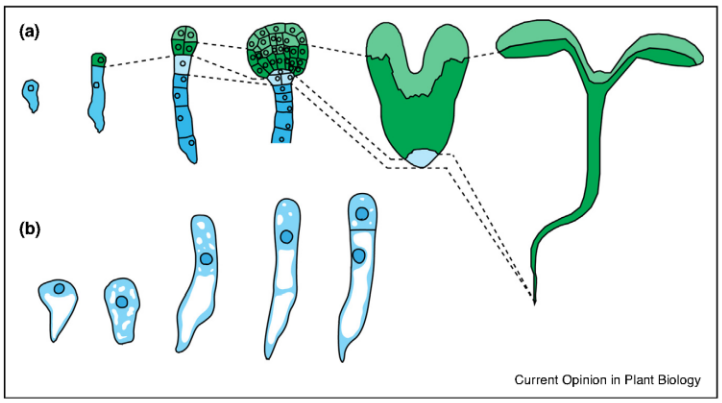

Embryogenesis in Arabidopsis.
(a) After the first zygotic division, the apical cell forms the spherical embryo (green) while the basal cell forms the mostly extra-embryonic suspensor (blue). The final seedling is mainly formed by the upper tier (light green) and lower tier (dark green) of the embryo proper. Only the upper-most suspensor cell (light blue) in direct contact with the embryo proper contributes to the embryonic root. The rest of the suspensor (dark blue) remains extra-embryonic. **(b)** In accordance with morphological criteria, egg cell polarity is lost in the early zygote. The large central vacuole (white) at the basal pole of the egg cell is partitioned into smaller evenly distributed vacuoles. During cell elongation, the zygote repolarized and the nucleus moves to the apex before the first asymmetric division. During zygotic cell elongation, a large central vacuole is reformed at the basal pole.

of other polarizing cues [10]. In flowering plants, however, *in vitro* experiments with rice gametes would argue against positional information provided by the sperm entry site as there was no correlation between its position and polarity of the zygote [11]. Fusion with the sperm, on the other hand, seems to be a necessary trigger for egg activation as it causes Calcium influx and initiates karyogamy and the activation of a zygotic transcriptional program [12] which cannot be achieved by artificial fusion of two egg cells.

In rice, egg activation possibly involves the paternally provided AP2 transcription factor OsASGR-BBML1 [13••]. Overexpression of BBML1 in the egg cell leads to proliferation without fertilization. Dominant negative versions of BBML1 lead to developmental arrest if expressed in the zygote. As ectopic overexpression of BBM induces embryogenesis in somatic cells in Arabidopsis [14], this family of transcription factors could be part of a two-component system of maternal and paternal factors that initiate a zygotic transcriptional program similar to the BELL/KNOX transcriptional regulators in the unicellular alga *Chlamydomonas reinhardtii* [15]

Zygotic gene expression

There have been conflicting reports about the timing of the maternal-to-zygotic transition and the degree of maternal and paternal contribution to early embryogenesis of flowering plants [16–21,22•]. Recent advances in manual isolation of single cells made it possible to generate transcriptional profiles of gametic cells and early embryos with much higher temporal and spatial resolution and lower contamination by surrounding maternal tissue [13••,23••,24••]. With these latest transcriptomic data from grasses and Arabidopsis, a clear picture is emerging.

In animals, the maternal-to-zygotic transition follows two phases. At the beginning, development is regulated purely post-transcriptionally by maternal mRNAs and proteins stored in the oocyte. Later, as the zygotic genome is activated, maternal RNAs are depleted and zygotic mRNAs take over functionally [25]. In flowering plants, there seems to be in principle a similar progressive activation of zygotic bi-parental transcripts [13••,23••,24••]. However, this transition seems to happen rapidly in the zygote. In Arabidopsis, sperm-specific transcripts can be detected in zygotes at 14 hours after pollination (hap) but are dramatically reduced or absent in zygotes at 24 hap. At the same time, egg cell-specific transcripts are rapidly eliminated and several thousand genes are upregulated in the zygote compared to the egg cell [24••]. In Arabidospsis, it has been shown that already the first zygotic cell division relies on *de novo* transcription [24••]. The onset of zygotic transcription is accompanied by rapid turn-over of gametic histones and replacement by zygotic histones [26]. These new data therefore further support the view that zygotic genome activation happens very rapidly in flowering plants as previously proposed by Nodine and Bartel [20]. However,

Figure 2

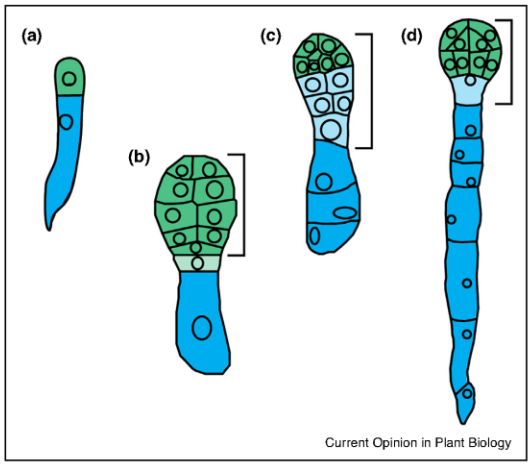

Clonal origin of embryonic structures (after [3], modified).
(a) The first cell division gives rise to an apical (green) and basal (blue) daughter cell. **(b)** Suspensor cells derived from the apical cell in *Sagina procumbens* (*Caryophyllaceae*); shown in light green. **(c)** Cells originating from the basal cell contribute substantially to the embryo proper in *Geum urbanum* (*Asteraceae*); depicted in light blue. **(d)** In *Brassicaceae*, only the upper-most descendent of the basal cell (light blue) contributes to the embryo. Cells contributing to the later seedling are marked by brackets.

these rapid transcriptome changes and the observed intracellular reorganization of the zygote raise the question if polarization of this cell relies on pre-existing parental factors or if polarity establishment is an intrinsic zygotic process.

MAP kinase signaling

Polarity of the zygote and differentiation of the first daughter cells seem to be at least in part controlled by a MAP kinase-dependent signaling pathway. This pathway includes the MAP kinases MPK3 and MPK6, the MAPK kinases MKK4 and MKK5 as well as the MAPKK kinase YODA (YDA) [27–29] (Figure 3). Loss of YDA impairs zygote elongation and results in symmetric cell division. Furthermore, both daughter cells adopt embryo-like division patterns, resulting in embryos lacking a recognizable suspensor. Constitutive activation of the YDA pathway leads to structures entirely consisting of suspensor-like cells [27]. This pathway therefore seems to promote zygote elongation and polarity and suppresses embryonic development in the basal daughter cell [30].

One of the direct phosphorylation targets of this signaling cascade is the transcription factor WRKY2. Together with the HOMEODOMAIN GLABROUS (HDG) transcription factors HDG11/12, WRKY2 activates expression of *WUSCHEL-RELATED HOMEOBOX 8* (*WOX8*) [31,32]. *WOX8* and *WOX9* are necessary for correct suspensor development and expression of several developmentally important genes in the embryo [33]. *WOX* genes generally play important roles as transcriptional repressor in stem cell niches. However, these members of the evolutionarily more ancient *WOX9* clade rather seem to act as transcriptional activators [34].

As the *wrky2* mutant recapitulates certain aspects of the *yda* phenotype but lacks others, there are likely additional targets of the YDA-dependent signaling cascade in the zygote. Potential targets could be transcription factor complexes including the RWP-RK protein GRD/RKD4, although GRD itself does not seem to be a direct target [35,36]. Mutant *grd* embryos in principle resemble *yda* embryos albeit the phenotype is less pronounced. Some members of the *RKD* family play a pivotal role in the egg-to-zygote transition [37,38]. It is therefore tempting to speculate that YDA might be involved in setting up a zygotic genome program via GRD regulation. As the overexpression of RKD4 can induce somatic embryogenesis [36], a role of RKD4 in activating a zygotic transcriptome seems at least plausible.

YDA is activated in the zygote by the BRASSINOSTEROID SIGNALING KINASE family members BSK1 and BSK2 [39••]. These membrane-associated proteins directly interact with the YDA kinase domain, possibly in a phosphorylation-dependent manner. BSK family proteins have been described as integral part of SOMATIC EMBRYOGENESIS RECEPTOR KINASE (SERK)-dependent receptor complexes in various signaling pathways [40–42]. These leucine-rich repeat containing co-receptors are involved in YDA-dependent developmental processes [43]. However, the receptor teaming up with the SERK co-receptors upstream of YDA in the embryo as well as possible ligands are still unknown.

Possible candidates include peptides of the EMBRYO SURROUNDING FACTOR (ESF) family. Downregulation by RNAi causes mild suspensor defects that can be rescued by expression of a constitutively active variant of *YDA* [44]. The spatial and temporal information provided by these possible ligands is, however, presently unclear.

In *Brassicaceae*, an additional way of YDA activation exists in the zygote. The unusual BSK family member SHORT SUSPENSOR (SSP/BSK12) accumulates specifically in the zygote, apparently translated from paternally inherited transcripts [45]. The SSP protein lacks a regulatory intra-molecular interaction typically seen in BSK proteins [39••]. Resembling a constitutively active version of BSK1, SSP can activate YDA directly after fertilization possibly without involving canonical receptor activation (Figure 3). As *ssp* mutants show slower embryonic development and a less defined boundary between embryo and suspensor, much like many species outside the

Figure 3

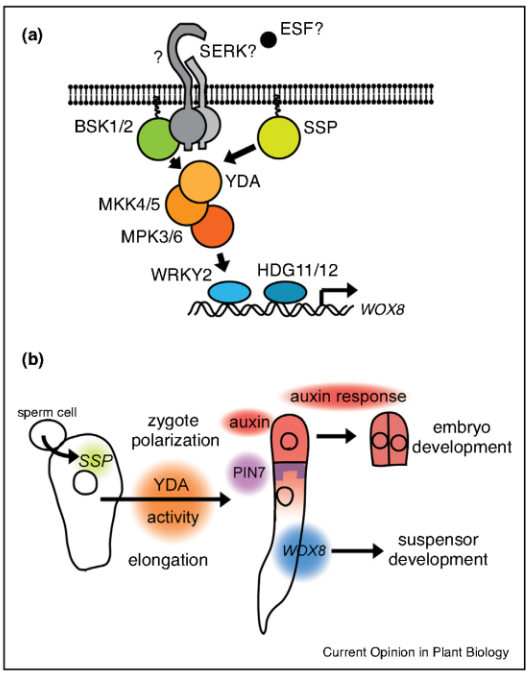

Signaling events in the early embryo.
(a) Schematic depiction of the embryonic YDA signaling pathways. The MAPKKK YDA can be activated by a possible receptor kinase complex including the membrane-associated proteins BSK1/2. In addition, paternally provided SSP directly activates YDA in *Brassicaceae*. **(b)** Consecutive signaling events in the early embryo. YDA activity contributes to zygote elongation, asymmetric cell division, and differential *WOX8* expression. A local, PIN7-mediated auxin maximum in the apical daughter cell initiates 3-dimensional growth of the embryo proper.

Brassicaceae family, this paternal input might provide a beneficial boost of YDA activity contributing to the rapid life cycle of *Brassicaceae* family members [45,46].

Auxin signaling

Many developmental processes in plants start with an asymmetric division and almost universally seem to involve the plant hormone auxin [47–49]. In the zygote, however, direct evidence for a role of auxin in regulating the first asymmetric division is lacking [30]. As the zygote seems to elongate in a tip-growing manner similar to pollen tubes or root hair cells, there is the possibility that this division actually resembles a rather specialized case independent of auxin signaling. The resulting daughter cells, however, show differential expression of genes involved in auxin response and transport. PIN7 in the basal cell is thought to initiate basal-to-apical auxin transport [50]. According to this model, three-dimensional growth of the embryo is then initiated by an auxin response maximum in the apical cell, re-orienting the cell division plane [48]. Auxin responses in the apical cell, therefore, seem to be an essential part of initiating embryonic development. Since the differential auxin response in the two zygotic daughter cells relies on already differentially expressed genes of auxin transport and response [50,51], this raises the question if auxin signaling in this context mainly amplifies and firmly establishes already pre-existing, transient differences.

Auxin transport is intimately linked to auxin synthesis and recent seemingly conflicting reports indicate possibly several sources [52–54,55••]. Consistent with PIN7-mediated transport from the basal cell, auxin might initially be synthesized in maternal cells in the micropylar region that are in direct contact with the basal daughter cell [55••]. However, once suspensor differentiation is initiated in the basal cell, the suspensor itself seems to become an auxin source [54].

Conclusions

Recent advances in live imaging and novel fluorescent markers [6•,7,56] as well as transcriptomic approaches [13••,23••,24••] have yielded new insights into the enigmatic processes that lead to symmetry breaking in the zygote. Polarity information seems to be ubiquitous in plant cells and interpreted at least in part by the recently discovered SOSEKI proteins [57••]. Their role in zygote polarization, however, has to be investigated in detail. It is still an open question if cell polarity in the zygote is inherited from the parental generation or established *de novo*. Does this process rely on external cues or is it directed by an intrinsic mechanism possibly including mechanical forces? How does the MAP kinase-WRKY-WOX pathway integrate with auxin signaling in establishing different cell identities? Recently described MPK-dependent phosphorylation of PIN proteins might suggest that this interaction could be rather direct [58•,59•]. With the recently developed and refined methods, future research will help to answer these fundamental questions at the very first step of plant development.

Conflict of interest statement

Nothing declared.

Acknowledgements

We apologize to our colleagues whose work we have not included in this manuscript due to space restrictions. We would like to thank Daniel Slane and Gerd Jürgens for critical reading of the manuscript and helpful discussions. Research in our group is supported by the German Science Foundation (Deutsche Forschungsgemeinschaft – DFG: SFB1101/B01 to M.B.), the Chinese Scholarship Council (Fellowship No. 201806320131 to Y.M.), and the Max Planck Society. The authors declare no conflict of interest.

References and recommended reading

Papers of particular interest, published within the period of review, have been highlighted as:

- • of special interest
- •• of outstanding interest

1. Lau S, Slane D, Herud O, Kong JX, Jurgens G: **Early embryogenesis in flowering plants: setting up the basic body pattern**. *Annu Rev Plant Biol* 2012, **63**:483-506.

2. Johri BM, Ambegaokar KB, Srivastava PS: *Comparative Embryology of Angiosperms*. Berlin: Springer-Verlag; 1992.

3. Maheshwari P: *An Introduction to the Embryology of the Angiosperms*. New York: McGraw-Hill; 1950.

4. Bayer M, Slane D, Jurgens G: **Early plant embryogenesis-dark ages or dark matter?** *Curr Opin Plant Biol* 2017, **35**:30-36.

5. Faure JE, Rotman N, Fortune P, Dumas C: **Fertilization in *Arabidopsis thaliana* wild type: developmental stages and time course**. *Plant J* 2002, **30**:481-488.

6. • Kimata Y, Higaki T, Kawashima T, Kurihara D, Sato Y, Yamada T, Hasezawa S, Berger F, Higashiyama T, Ueda M: **Cytoskeleton dynamics control the first asymmetric cell division in Arabidopsis zygote**. *Proc Natl Acad Sci U S A* 2016, **113**:14157-14162.

This study uses novel fluorescent marker lines and sophisticated live imaging to describe the dynamics of the cytoskeleton during zygote elongation and the first mitotic division.

7. Kimata Y, Kato T, Higaki T, Kurihara D, Yamada T, Segami S, Morita MT, Maeshima M, Hasezawa S, Higashiyama T *et al.*: **Polar vacuolar distribution is essential for accurate asymmetric division of Arabidopsis zygotes**. *Proc Natl Acad Sci U S A* 2019, **116**:2338-2343.

8. Piotrowska K, Zernicka-Goetz M: **Role for sperm in spatial patterning of the early mouse embryo**. *Nature* 2001, **409**:517-521.

9. Marston DJ, Goldstein B: **Symmetry breaking in *C. elegans*: another gift from the sperm**. *Dev Cell* 2006, **11**:273-274.

10. Hable WE, Kropf DL: **Sperm entry induces polarity in fucoid zygotes**. *Development* 2000, **127**:493-501.

11. Nakajima K, Uchiumi T, Okamoto T: **Positional relationship between the gamete fusion site and the first division plane in the rice zygote**. *J Exp Bot* 2010, **61**:3101-3105.

12. Antoine AF, Faure JE, Cordeiro S, Dumas C, Rougier M, Feijo JA: **A calcium influx is triggered and propagates in the zygote as a wavefront during in vitro fertilization of flowering plants**. *Proc Natl Acad Sci U S A* 2000, **97**:10643-10648.

13. •• Rahman MH, Toda E, Kobayashi M, Kudo T, Koshimizu S, Takahara M, Iwami M, Watanabe Y, Sekimoto H, Yano K, Okamoto T: **Expression of genes from paternal alleles in rice zygotes and involvement of OsASGR-BBML1 in initiation of zygotic development**. *Plant Cell Physiol* 2019, **60**:725-737.

By SNP-based transcriptome analysis of hybrid zygotes, this study identified 23 genes expressed from the paternal allele. Among those genes, OsASGR-BBML1 plays a crucial role in egg cell activation and initiating a zygotic genome program.

14. Horstman A, Li M, Heidmann I, Weemen M, Chen B, Muino JM, Angenent GC, Boutilier K: **The BABY BOOM transcription factor activates the LEC1-ABI3-FUS3-LEC2 network to induce somatic embryogenesis**. *Plant Physiol* 2017, **175**:848-857.

15. Goodenough U, Lin H, Lee JH: **Sex determination in *Chlamydomonas***. *Semin Cell Dev Biol* 2007, **18**:350-361.

16. Meyer S, Scholten S: **Equivalent parental contribution to early plant zygotic development**. *Curr Biol* 2007, **17**:1686-1691.

17. Pillot M, Baroux C, Vazquez MA, Autran D, Leblanc O, Vielle-Calzada JP, Grossniklaus U, Grimanelli D: **Embryo and endosperm inherit distinct chromatin and transcriptional states from the female gametes in Arabidopsis**. *Plant Cell* 2010, **22**:307-320.

18. Autran D, Baroux C, Raissig MT, Lenormand T, Wittig M, Grob S, Steimer A, Barann M, Klostermeier UC, Leblanc O *et al.*: **Maternal epigenetic pathways control parental contributions to Arabidopsis early embryogenesis**. *Cell* 2011, **145**:707-719.

19. Zhao J, Xin H, Qu L, Ning J, Peng X, Yan T, Ma L, Li S, Sun MX: **Dynamic changes of transcript profiles after fertilization are associated with de novo transcription and maternal elimination in tobacco zygote, and mark the onset of the maternal-to-zygotic transition**. *Plant J* 2011, **65**:131-145.

20. Nodine MD, Bartel DP: **Maternal and paternal genomes contribute equally to the transcriptome of early plant embryos**. *Nature* 2012, **482**:94-97.

21. Del Toro-De Leon G, Lepe-Soltero D, Gillmor CS: **Zygotic genome activation in isogenic and hybrid plant embryos**. *Curr Opin Plant Biol* 2016, **29**:148-153.

22. • Schon MA, Nodine MD: **Widespread contamination of Arabidopsis embryo and endosperm transcriptome data sets**. *Plant Cell* 2017, **29**:608-617.

Using an *in silico* approach, the authors assessed the contamination of embryonic transcriptome data by RNA derived from surrounding maternal and endosperm tissue. They conclude that previous data universally included maternal contamination leading to possible misinterpretations.

23. •• Chen J, Strieder N, Krohn NG, Cyprys P, Sprunck S, Engelmann JC, Dresselhaus T: **Zygotic genome activation occurs shortly after fertilization in maize**. *Plant Cell* 2017, **29**:2106-2125.

This work provides transcriptome data of gametes and zygotes as well as apical and basal cells of maize embryos. This study therefore provides a complete set of transcriptome data prefertilization and post-fertilization with high temporal resolution. The data clearly demonstrate that zygotic genome activation happens shortly after fertilization in the zygote.

24. •• Zhao P, Zhou X, Shen K, Liu Z, Cheng T, Liu D, Cheng Y, Peng X, Sun MX: **Two-step maternal-to-zygotic transition with two-phase parental genome contributions**. *Dev Cell* 2019, **49**:882-893 e885.

In this work, the authors present transcriptome data of Arabidopsis egg cells, zygotes, and embryos after the first division. The transcriptome data include SNP-based analysis of parental origin of the transcripts. Zygote were analyzed before (14 hour after pollination) and during elongation (24 hour after pollination). This work therefore provides very high temporal resolution and identifies a two-phased zygotic genome activation.

25. Vastenhouw NL, Cao WX, Lipshitz HD: **The maternal-to-zygotic transition revisited**. *Development* 2019, **146**.

26. Ingouff M, Rademacher S, Holec S, Soljic L, Xin N, Readshaw A, Foo SH, Lahouze B, Sprunck S, Berger F: **Zygotic resetting of the HISTONE 3 variant repertoire participates in epigenetic reprogramming in Arabidopsis**. *Curr Biol* 2010, **20**:2137-2143.

27. Lukowitz W, Roeder A, Parmenter D, Somerville C: **A MAPKK kinase gene regulates extra-embryonic cell fate in Arabidopsis**. *Cell* 2004, **116**:109-119.

28. Wang H, Ngwenyama N, Liu Y, Walker JC, Zhang S: **Stomatal development and patterning are regulated by environmentally responsive mitogen-activated protein kinases in Arabidopsis**. *Plant Cell* 2007, **19**:63-73.

29. Zhang M, Wu H, Su J, Wang H, Zhu Q, Liu Y, Xu J, Lukowitz W, Zhang S: **Maternal control of embryogenesis by MPK6 and its upstream MKK4/MKK5 in Arabidopsis**. *Plant J* 2017, **92**:1005-1019.

30. Musielak TJ, Bayer M: **YODA signalling in the early Arabidopsis embryo**. *Biochem Soc Trans* 2014, **42**:408-412.

31. Ueda M, Zhang Z, Laux T: **Transcriptional activation of Arabidopsis axis patterning genes WOX8/9 links zygote polarity to embryo development**. *Dev Cell* 2011, **20**:264-270.

32. Ueda M, Aichinger E, Gong W, Groot E, Verstraeten I, Vu LD, De Smet I, Higashiyama T, Umeda M, Laux T: **Transcriptional integration of paternal and maternal factors in the Arabidopsis zygote**. *Genes Dev* 2017, **31**:617-627.

33. Breuninger H, Rikirsch E, Hermann M, Ueda M, Laux T: **Differential expression of WOX genes mediates apical-basal axis formation in the Arabidopsis embryo**. *Dev Cell* 2008, **14**:867-876.

Appendix

34. Dolzblasz A, Nardmann J, Clerici E, Causier B, van der Graaff E, Chen J, Davies B, Werr W, Laux T: **Stem cell regulation by Arabidopsis WOX genes**. *Mol Plant* 2016, **9**:1028-1039.

35. Jeong S, Palmer TM, Lukowitz W: **The RWP-RK factor GROUNDED promotes embryonic polarity by facilitating YODA MAP kinase signaling**. *Curr Biol* 2011, **21**:1268-1276.

36. Waki T, Hiki T, Watanabe R, Hashimoto T, Nakajima K: **The Arabidopsis RWP-RK protein RKD4 triggers gene expression and pattern formation in early embryogenesis**. *Curr Biol* 2011, **21**:1277-1281.

37. Koi S, Hisanaga T, Sato K, Shimamura M, Yamato KT, Ishizaki K, Kohchi T, Nakajima K: **An evolutionarily conserved plant RKD Factor controls germ cell differentiation**. *Curr Biol* 2016, **26**:1775-1781.

38. Rovekamp M, Bowman JL, Grossniklaus U: **Marchantia MpRKD regulates the gametophyte-sporophyte transition by keeping egg cells quiescent in the absence of fertilization**. *Curr Biol* 2016, **26**:1782-1789.

39. •• Neu A, Eilbert E, Asseck LY, Slane D, Henschen A, Wang K, Burgel P, Hildebrandt M, Musielak TJ, Kolb M *et al.*: **Constitutive signaling activity of a receptor-associated protein links fertilization with embryonic patterning in Arabidopsis thaliana**. *Proc Natl Acad Sci U S A* 2019, **116**:5795-5804.
The BRASSINOSTEROID SIGNALING KINASES BSK1 and BSK2 act in parallel upstream of YDA in various signaling pathways. As these proteins are universal components of SERK-dependent signaling pathways, this study suggests that the embryonic YDA pathway is activated by a SERK-dependent receptor complex. Furthermore, the authors show that the unusual BSK family member SSP/BSK12 mimics a constitutively active form of BSK1 and can activate YDA possibly without involving canonical receptor activation.

40. Shi H, Yan H, Li J, Tang D: **BSK1, a receptor-like cytoplasmic kinase, involved in both BR signaling and innate immunity in Arabidopsis**. *Plant Signal Behav* 2013, **8**.

41. Majhi BB, Sreeramulu S, Sessa G: **BRASSINOSTEROID-SIGNALING KINASE5 associates with immune receptors and is required for immune responses**. *Plant Physiol* 2019, **180**:1166-1184.

42. Zhao Y, Wu G, Shi H, Tang D: **RECEPTOR-LIKE KINASE 902 associates with and phosphorylates BRASSINOSTEROID-SIGNALING KINASE1 to regulate plant immunity**. *Mol Plant* 2019, **12**:59-70.

43. Meng X, Chen X, Mang H, Liu C, Yu X, Gao X, Torii KU, He P, Shan L: **Differential function of Arabidopsis SERK family receptor-like kinases in stomatal patterning**. *Curr Biol* 2015, **25**:2361-2372.

44. Costa LM, Marshall E, Tesfaye M, Silverstein KA, Mori M, Umetsu Y, Otterbach SL, Papareddy R, Dickinson HG, Boutiller K *et al.*: **Central cell-derived peptides regulate early embryo patterning in flowering plants**. *Science* 2014, **344**:168-172.

45. Bayer M, Nawy T, Giglione C, Galli M, Meinnel T, Lukowitz W: **Paternal control of embryonic patterning in *Arabidopsis thaliana***. *Science* 2009, **323**:1485-1488.

46. Babu Y, Musielak T, Henschen A, Bayer M: **Suspensor length determines developmental progression of the embryo in Arabidopsis**. *Plant Physiol* 2013, **162**:1448-1458.

47. De Smet I, Beeckman T: **Asymmetric cell division in land plants and algae: the driving force for differentiation**. *Nat Rev Mol Cell Biol* 2011, **12**:177-188.

48. Yoshida S, Barbier de Reuille P, Lane B, Bassel GW, Prusinkiewicz P, Smith RS, Weijers D: **Genetic control of plant development by overriding a geometric division rule**. *Dev Cell* 2014, **29**:75-87.

49. Shao W, Dong J: **Polarity in plant asymmetric cell division: division orientation and cell fate differentiation**. *Dev Biol* 2016, **419**:121-131.

50. Friml J, Vieten A, Sauer M, Weijers D, Schwarz H, Hamann T, Offringa R, Jurgens G: **Efflux-dependent auxin gradients establish the apical-basal axis of Arabidopsis**. *Nature* 2003, **426**:147-153.

51. Rademacher EH, Lokerse AS, Schlereth A, Llavata-Peris CI, Bayer M, Kientz M, Freire Rios A, Borst JW, Lukowitz W, Jurgens G, Weijers D: **Different auxin response machineries control distinct cell fates in the early plant embryo**. *Dev Cell* 2012, **22**:211-222.

52. Cheng Y, Dai X, Zhao Y: **Auxin synthesized by the YUCCA flavin monooxygenases is essential for embryogenesis and leaf formation in Arabidopsis**. *Plant Cell* 2007, **19**:2430-2439.

53. Robert HS, Grones P, Stepanova AN, Robles LM, Lokerse AS, Alonso JM, Weijers D, Friml J: **Local auxin sources orient the apical-basal axis in Arabidopsis embryos**. *Curr Biol* 2013, **23**:2506-2512.

54. Robert HS, Crhak Khaitova L, Mroue S, Benkova E: **The importance of localized auxin production for morphogenesis of reproductive organs and embryos in Arabidopsis**. *J Exp Bot* 2015, **66**:5029-5042.

55. •• Robert HS, Park C, Gutierrez CL, Wojcikowska B, Pencik A, Novak O, Chen J, Grunewald W, Dresselhaus T, Friml J, Laux T: **Maternal auxin supply contributes to early embryo patterning in Arabidopsis**. *Nat Plants* 2018, **4**:548-553.
This study identifies the maternal integument tissue at the micropolar end as source of auxin during early phases of embryogenesis.

56. Liao CY, Weijers D: **A toolkit for studying cellular reorganization during early embryogenesis in *Arabidopsis thaliana***. *Plant J* 2018, **93**:963-976.

57. •• Yoshida S, van der Schuren A, van Dop M, van Galen L, Saiga S, Adibi M, Moller B, Ten Hove CA, Marhavy P, Smith R *et al.*: **A SOSEKI-based coordinate system interprets global polarity cues in Arabidopsis**. *Nat Plants* 2019, **5**:160-166.
On the basis of conserved domain structure, the authors identified an apparently evolutionarily conserved family of proteins. The SOSEKI proteins show specific intra-cellular localization according to intrinsic polarity cues and seem to be involved in their interpretation.

58. • Jia W, Li B, Li S, Liang Y, Wu X, Ma M, Wang J, Gao J, Cai Y, Zhang Y *et al.*: **Mitogen-activated protein kinase cascade MKK7-MPK6 plays important roles in plant development and regulates shoot branching by phosphorylating PIN1 in Arabidopsis**. *PLoS Biol* 2016, **14**:e1002550.
Phosphorylation of PIN1 by MPK6 was demonstrated *in vivo* and therefore indicates a direct link between MAP kinase signaling and regulation of auxin transport.

59. • Dory M, Hatzimasoura E, Kallai BM, Nagy SK, Jager K, Darula Z, Nadai TV, Meszaros T, Lopez-Juez E, Barnabas B *et al.*: **Coevolving MAPK and PID phosphosites indicate an ancient environmental control of PIN auxin transporters in land plants**. *FEBS Lett* 2018, **592**:89-102.
This study describes conserved MAP kinase phosphorylation sites in PIN proteins. These data suggest a direct link between receptor kinase signaling and auxin transport.

PNAS PNAS PNAS

Constitutive signaling activity of a receptor-associated protein links fertilization with embryonic patterning in *Arabidopsis thaliana*

Ancilla Neu[a], Emily Eilbert[b], Lisa Y. Asseck[c], Daniel Slane[a], Agnes Henschen[a], Kai Wang[a], Patrick Bürgel[a], Melanie Hildebrandt[a], Thomas J. Musielak[a], Martina Kolb[a], Wolfgang Lukowitz[b], Christopher Grefen[c,d], and Martin Bayer[a,1]

[a]Department of Cell Biology, Max Planck Institute for Developmental Biology, 72076 Tuebingen, Germany; [b]Department of Plant Biology, University of Georgia, Athens, GA 30602; [c]Developmental Genetics, Centre for Plant Molecular Biology, University of Tuebingen, 72076 Tuebingen, Germany; and [d]Department of Molecular & Cellular Botany, Ruhr-University Bochum, 44780 Bochum, Germany

Edited by Dolf Weijers, Wageningen University, Wageningen, The Netherlands, and accepted by Editorial Board Member Caroline Dean January 28, 2019 (received for review September 13, 2018)

In flowering plants, the asymmetrical division of the zygote is the first hallmark of apical-basal polarity of the embryo and is controlled by a MAP kinase pathway that includes the MAPKKK YODA (YDA). In *Arabidopsis*, YDA is activated by the membrane-associated pseudokinase SHORT SUSPENSOR (SSP) through an unusual parent-of-origin effect: *SSP* transcripts accumulate specifically in sperm cells but are translationally silent. Only after fertilization is SSP protein transiently produced in the zygote, presumably from paternally inherited transcripts. *SSP* is a recently diverged, Brassicaceae-specific member of the *BRASSINOSTEROID SIGNALING KINASE* (*BSK*) family. BSK proteins typically play broadly overlapping roles as receptor-associated signaling partners in various receptor kinase pathways involved in growth and innate immunity. This raises two questions: How did a protein with generic function involved in signal relay acquire the property of a signal-like patterning cue, and how is the early patterning process activated in plants outside the Brassicaceae family, where *SSP* orthologs are absent? Here, we show that *Arabidopsis BSK1* and *BSK2*, two dose paralogs of *SSP* that are conserved in flowering plants, are involved in several YDA-dependent signaling events, including embryogenesis. However, the contribution of SSP to YDA activation in the early embryo does not overlap with the contributions of BSK1 and BSK2. The loss of an intramolecular regulatory interaction enables SSP to constitutively activate the YDA signaling pathway, and thus initiates apical-basal patterning as soon as SSP protein is translated after fertilization and without the necessity of invoking canonical receptor activation.

Arabidopsis thaliana | evolution | MAP kinase signaling | embryogenesis | BRASSINOSTEROID SIGNALING KINASE

The organization of complex multicellular bodies is driven by the sequential creation of cells with distinct properties. In higher plants, this process generally starts soon after fertilization, as the division of the zygote is typically asymmetrical, giving rise to daughter cells with different developmental fates (1). Early development of the flowering plant *Arabidopsis thaliana* and other members of the Brassicaceae family proceeds in a strictly stereotypic pattern, making it easy to follow the fate of individual cells (1). The smaller apical daughter of the *Arabidopsis* zygote always forms the embryo proper, while the larger basal cell develops into a filamentous support structure, called the suspensor, that connects the developing embryo with maternal seed tissue and serves as a conduit for nutrients and hormones (2). Only the uppermost cell of the suspensor contributes to the embryo, forming part of the embryonic root pole, while all other suspensor cells remain extraembryonic (3). Thus, the zygotic division already marks embryonic vs. extraembryonic cell fate.

In other plant species, however, plant embryos often do not show a well-defined boundary between embryonic and extraembryonic cell identity based on morphological criteria. In some cases of grasses, the patterning process even seems to take place at later developmental stages involving a larger number of cells (4). The stereotypic, early patterning of Brassicaceae embryos creates all essential cell types by a minimum of cell divisions, and might therefore be an adaption to the rapid life cycle typically seen in many species of this family.

Genetic evidence has established that apical-basal patterning in *Arabidopsis* is controlled by MAP kinase signaling. The MAPKK kinase YODA (YDA) acts in the zygote to promote elongation and embryonic polarity (5). Loss of YDA activity leads to more equal zygote divisions, and derivatives of the basal daughter cell subsequently typically adopt an embryonic division pattern that can result in embryos without a recognizable suspensor (6). Similar effects are observed with loss of the MAPK kinases MKK4 and MKK5 or the MAP kinases MPK3 and MPK6 (7, 8). Engineered constitutive activity of YDA leads to supernumerary suspensor cells and, in many cases, produces filamentous structures without a recognizable embryo (6). It has been concluded that signaling through the YDA MAP kinase

Significance

In flowering plants, membrane-associated kinases of the BRASSINOSTEROID SIGNALING KINASE (BSK) family are ubiquitous, receptor-associated signaling partners in various receptor kinase pathways, where they function in signaling relay. The Brassicaceae-specific BSK family member SHORT SUSPENSOR (SSP), however, acts as a patterning cue in the zygote, initiating the apical-basal patterning process in a signal-like manner. The SSP protein has lost a regulatory, intramolecular interaction and activates the MAPKKK YODA signaling pathway constitutively, in principle, enabling the protein to initiate embryonic patterning without receptor activation. We further show that the BSK family members BSK1 and BSK2, both conserved in flowering plants, activate the same signaling pathway in parallel to SSP and might constitute remnants of an older, canonical signaling pathway still active in *Arabidopsis*.

Author contributions: W.L., C.G., and M.B. designed research; A.N., E.E., L.Y.A., D.S., A.H., K.W., P.B., M.H., T.J.M., M.K., W.L., C.G., and M.B. performed research; A.N., E.E., L.Y.A., D.S., K.W., T.J.M., M.K., W.L., C.G., and M.B. analyzed data; and W.L., C.G., and M.B. wrote the paper.

The authors declare no conflict of interest.

This article is a PNAS Direct Submission. D.W. is a guest editor invited by the Editorial Board.

[1]To whom correspondence should be addressed. Email: martin.bayer@tuebingen.mpg.de.

This article contains supporting information online at www.pnas.org/lookup/suppl/doi:10.1073/pnas.1815866116/-/DCSupplemental.

cascade is setting up apical-basal polarity in the early embryo and promotes extraembryonic differentiation.

Postembryonically, mutant *yda* seedlings are dwarfed and display various morphological alterations in comparison to wild type, reflecting the involvement of the MAP kinase cascade in a number of other signaling events (9, 10). In epidermal patterning, for example, YDA acts as part of a canonical signaling pathway downstream of a receptor complex that includes receptor kinases of the ERECTA family (ERf) and the SOMATIC EMBRYOGENESIS RECEPTOR KINASE (SERK) family to regulate spacing of stomata in the epidermis of leaves (11). However, the available evidence suggests that YDA activation in the zygote may involve different mechanisms.

In the context of the embryo, YDA is, at least in part, activated by the action of a membrane-associated pseudokinase called SHORT SUSPENSOR (SSP) (12). *SSP* transcripts accumulate specifically in the two sperm cells in the pollen, and SSP protein has only been detected transiently after fertilization in the zygote, presumably translated from inherited, previously translationally silent paternal transcripts (12). Overexpression of *SSP* can activate the YDA MAP kinase cascade in other tissues; by analogy, it has been proposed that SSP protein acts in a signal-like manner to trigger YDA activation in the zygote (12).

SSP is a member of the multigene family of *BRASSINOSTEROID SIGNALING KINASE* (*BSK*) genes. BSKs function as cytoplasmic signaling partners in various SERK-dependent receptor kinase pathways involved in plant growth, innate immunity, and abiotic stress response (13–15). BSK proteins are thought to be phosphorylated upon receptor activation and have been proposed to recruit downstream signaling components in a phosphorylation-dependent manner (16, 17). Most of the *BSK* genes seem to have overlapping functions, as obvious phenotypic alterations have only been described for higher order mutants (18). Interestingly, *SSP* is of very recent evolutionary origin, splitting from its sister gene *BSK1* about 23 million years ago in the last whole-genome duplication within the Brassicaceae (19). While *BSK1* evolved under purifying selection, *SSP* has diverged considerably from the common ancestor; in addition, *BSK1* remains ubiquitously expressed throughout plant development, like most *BSK* genes, whereas *SSP* expression has become tightly restricted to the male germ line (12, 19). How can the evolution of *SSP* from an ancestral role similar to other *BSK* genes (general, functionally redundant signaling components in receptor kinase pathways) to a factor providing patterning cues in early embryonic development be rationalized?

Here, we show that *BSK1*, the sister gene of *SSP*, together with *BSK2*, a second close paralog within the same family, act in parallel to *SSP* upstream of *YDA* in the zygote and early embryo, and might therefore constitute remnants of an older prototype of the embryonic YDA pathway. Furthermore, we demonstrate that *BSK1* and *BSK2* also take part in YDA-dependent signaling events outside the embryo, determining plant growth, inflorescence architecture, and stomatal patterning. A detailed comparison between the biochemical properties and structure of BSK1 vs. SSP reveals that *SSP* likely neofunctionalized through loss of negative regulation. By acquiring properties that enable constitutive activation of the YDA pathway, SSP can now directly link the onset of zygotic transcription after the fertilization event to the onset of apical-basal pattering.

Results

BSK1 and _BSK2_ Contribute to Embryonic Patterning, Independent of _SSP_. Embryos mutant for *ssp* display a significantly less severe phenotype than *yda* mutant embryos (12) (Fig. 1), implying that other factors contributing to activation of the YDA MAP kinase cascade in the zygote should exist. *BSK1* may be such a factor since it shares a recent evolutionary origin with *SSP* (19) (*SI Appendix*, Fig. S1). However, *bsk1* single mutants did not show any obvious differences from wild-type embryos (Fig. 1*A*). Transcriptome datasets of early embryos revealed high expression levels of *BSK2*, a close homolog of *BSK1* (20, 21) (*SI Appendix*, Fig. S2*A*). These findings could be confirmed by reporter gene analysis (*SI Appendix*, Fig. S2 *B–E*), and we therefore included *bsk2* mutants in our studies. While *bsk2* embryos were indistinguishable from wild type, the phenotype of *bsk1 bsk2* double mutants was strikingly reminiscent of *ssp* (12) (Fig. 1).

The first observable effect caused by mutations in YDA signaling is drastically reduced elongation of the zygote (6). The *bsk1 bsk2* double mutants similarly exhibit reduced zygotic cell growth, which results in a smaller basal cell in comparison to wild type after the first zygotic division (Fig. 1*C*). Again, similar to other mutations in the pathway, the basal cell of *bsk1 bsk2* embryos produces a suspensor of reduced length (Fig. 1 *A* and *B*), frequently showing aberrant divisions in a vertical plane (*SI Appendix*, Fig. S3). The phenotype of *ssp bsk1 bsk2* triple-mutant embryos is stronger than the phenotype of either *ssp* single or *bsk1 bsk2* double mutants (Fig. 1), suggesting an additive effect, and only slightly weaker than the phenotype of *yda* mutants (Fig. 1 *A* and *B*).

BSK1 and BSK2 Act in Postembryonic Signaling Events. Since *BSK1* and *BSK2* are ubiquitously expressed throughout plant development [determined by AtGenExpress (22)], we next investigated whether they act in YDA-dependent signaling events outside of the embryo. YDA signaling is, among other developmental decisions, necessary for rosette growth and inflorescence architecture, as well as epidermal patterning. In all three instances, *YDA* acts downstream of receptor kinases of the ERf: Mutations in ERf/YDA pathway components result in severely dwarfed plants with smaller rosette leaves and more compressed inflorescences, as well as massive stomata clustering (23–25). Single mutants of *bsk1* or *bsk2* display no obvious alterations in these traits (Fig. 2 and *SI Appendix*, Fig. S4 *A–C*). In contrast, the *bsk1 bsk2* double mutants recapitulate the phenotype of *yda* or *erf* mutants, displaying strikingly smaller rosettes (Fig. 2*B* and *SI Appendix*, Fig. S4*B*), more compact inflorescences (Fig. 2*A* and *SI Appendix*, Fig. S4*A*), and clustered stomata (Fig. 2*C* and *SI Appendix*, Fig. S4*C*). These observations indicate that BSK1 and BSK2 might be general signaling components in YDA-dependent pathways. The additional loss of *SSP* in the *bsk1 bsk2 ssp* triple mutant does not result in any further enhancement of postembryonic defects (Fig. 2 and *SI Appendix*, Fig. S4 *A–C*), confirming that *SSP* function is confined to the embryo.

BSK1 and _BSK2_ Act Genetically Upstream of YDA. BSK family kinases are membrane-associated proteins, and genetic and biochemical evidence showed that *SSP* acts upstream of *YDA* in a linear pathway (12, 26). To test the idea that BSK1 and BSK2 similarly act upstream of the YDA MAP kinase cascade, we created *bsk1 bsk2 ssp* triple mutants that additionally carry a constitutively active version of *YDA* (*YDA-CA*). The *YDA-CA* transgene rescues the *yda* loss-of-function mutant and creates a strong gain-of-function effect, resulting in a leaf epidermis devoid of stomata and consisting almost entirely of pavement cells (9) (Fig. 2*C*). The *YDA-CA* variant was not only able to rescue the genetic defects in stomatal patterning of *bsk1 bsk2 ssp* triple mutants but displayed an epidermal phenotype highly similar to *YDA-CA* seedlings (Fig. 2*C* and *SI Appendix*, Fig. S4*C*). This epistatic behavior of *YDA-CA* strongly argues for a function of *BSK1* and *BSK2* in the ERf/YDA pathway and indicates that *BSK1* and *BSK2* act genetically upstream of *YDA*.

We could furthermore observe a similar epistatic behavior of *YDA-CA* in *bsk1 bsk2 ssp* triple-mutant embryos that were genetically rescued by a *YDA-CA* transgene (*SI Appendix*, Fig. S5). This further supports the notion that *BSK1* and *BSK2* act upstream of *YDA* and might be rather ubiquitous constituents of YDA-dependent signaling pathways.

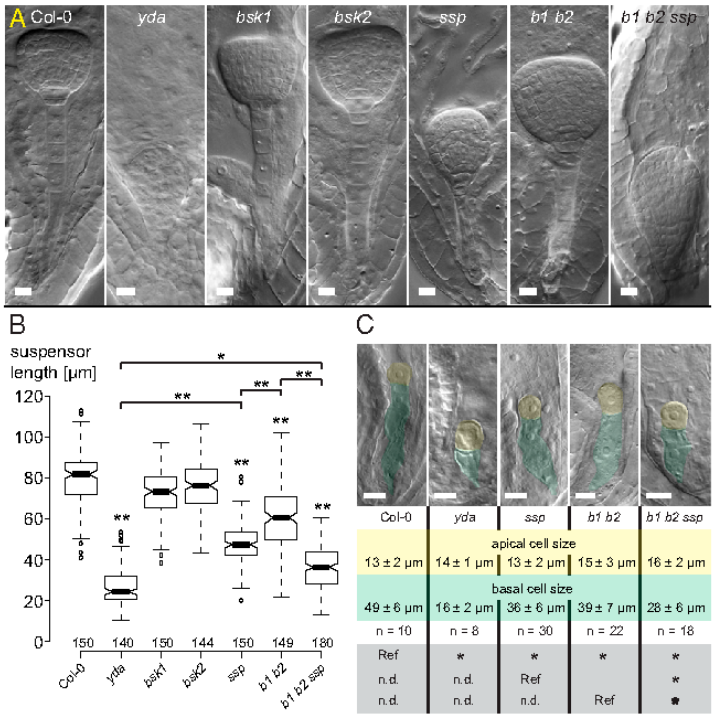

Fig. 1. Functional importance of BSK family kinases in early embryogenesis. (*A*) Nomarsky images of transition-stage embryos in whole-mount cleared seeds of wild-type Col-0, *yda*, *bsk1-2*, *bsk2-2*, and *ssp-2* single mutants, as well as *bsk1 bsk2* double mutants (*b1 b2*) and *bsk1 bsk2 ssp* triple mutants (*b1 b2 ssp*). (Scale bars: 10 µm.) (*B*) Box plot diagram of suspensor length measurements for >100 embryos. The total number of analyzed embryos is depicted above the *x* axis. The box plot diagram shows the median as center lines, and the 25th and 75th percentiles are indicated by box limits. Whiskers show 1.5× interquartile distance. Outliers are represented by dots. Statistically significant differences from wild type were determined by the Mann–Whitney *U* test (***P* < 0.001; **P* < 0.01). Statistically significant differences in other pairwise comparisons are indicated by brackets. (*C*) Nomarsky images of embryos at the one-cell stage in whole-mount cleared seeds. The average sizes of the apical (yellow) and basal (green) daughter cells with the SD and number of analyzed embryos are given below the image. Furthermore, significant differences in pairwise comparisons to the indicated reference (Ref) determined by the Mann–Whitney *U* test (**P* < 0.001) are indicated below the image (gray). Apical cells are false-colored in yellow, and basal cells are shown in green. (Scale bars: 10 µm.)

***BSK1* Cannot Compensate for the Loss of *SSP* in the Zygote and Early Embryo.** Our genetic analysis revealed that *SSP* and *BSK1*/*BSK2* contribute additively to zygote elongation and suspensor development. *SSP* mRNA is supplied paternally by the pollen (12), suggesting the possibility that SSP may mediate early activation of the YDA pathway, before BSK1/BSK2 proteins may be able to accumulate. To test the hypothesis that the specific contribution of *SSP* to early development results from pollen-specific expression, we expressed *SSP* and *BSK1* genomic coding regions under control of the male germ line-specific *MGH3* promoter and the *SSP* promoter, and tested the ability of these constructs to complement the *ssp* mutant phenotype (Figs. 3 and 4). Surprisingly, none of the *pMGH3::BSK1* or *pSSP::BSK1* lines showed genetic rescue of the *ssp* loss-of-function phenotype, while all *pMGH3::SSP* or *pSSP::SSP* transgenic lines used for the analysis rescued the *ssp* embryonic phenotype. This clearly indicates that SSP and BSK1 proteins differ in their potential to activate the embryonic YDA pathway and implies that neofunctionalization of *SSP* did not merely involve a simple change in expression pattern but also changes to the protein properties.

***SSP* Expression Constitutively Activates Downstream Target Genes.** Ectopic overexpression of *SSP* in seedlings evokes a strong gain-of-function effect similar to constitutively active versions of *YDA* (12). Most strikingly, this phenotype manifests itself in an almost complete lack of stomata on the leaf surface (9, 12). In contrast, similar experiments with *BSK1* were previously reported to have little or no effect on plant architecture (27). To corroborate and refine these findings, we examined the effect of overexpressing *BSK1* from the strong, ubiquitously active CaMV 35S promoter on stomata density in detail and found no obvious changes compared with wild type (*SI Appendix*, Fig. S6). The growth defects and the clustered stomata phenotype of the *bsk1 bsk2 ssp* triple mutant were rescued to various degrees by the *p35S::BSK1* transgene in all transgenic lines tested, indicating that the transgene is functional. Furthermore, these plants displayed a wild-type growth phenotype, and no obvious gain-of-function effects were recognizable. This suggests that, in contrast to SSP, the presence of the BSK1 protein alone is not sufficient to hyperactivate the YDA pathway, despite being an integral part of this pathway. To directly test the hypothesis that *SSP*, but not *BSK1*, overexpression leads to strong activation of YDA target genes, we monitored the transcription of *EPF2* in suspension culture-derived protoplasts (Fig. 5*A*). The *EPF2* gene is a target of the ERf/YDA pathway, it encodes one of the ligands of ERf receptors (28), and its expression is negatively regulated by the YDA MAP kinase cascade (29). As predicted from previous reports, the expression of *YDA-CA* led to down-regulation of *EPF2* expression in comparison to samples in which an inactive, kinase-dead (KD) version of *YDA* (*YDA-KD*) was expressed (Fig. 5*A*).

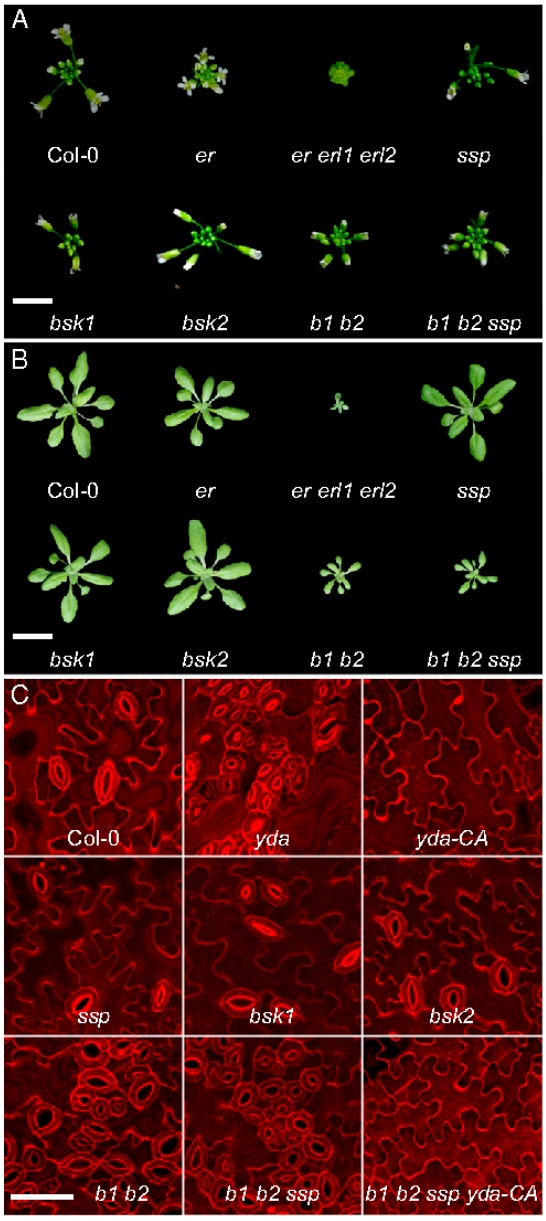

Fig. 2. Phenotypic analysis of YDA-dependent plant development. (*A*) Inflorescence development of wild-type Col-0 in comparison to single-, double-, and triple-mutant combinations of ERf kinases and BSK family kinases. The *bsk1 bsk2* double mutant (*b1 b2*) and *bsk1 bsk2 ssp* triple mutant (*b1 b2 ssp*) show more compact inflorescences very similar to *erecta* (*er*) single mutants and *erecta erecta-like1 erecta-like2* (*er erl1 erl2*) triple mutants. (Scale bar: 5 mm.) (*B*) Rosette leaves at the time of bolting. No obvious difference in rosette diameter can be seen in *bsk1-2*, *bsk2-2*, or *ssp* single mutants in comparison to wild type. The *bsk1 bsk2* double mutant, however, shows a reduced rosette size similar to plants with reduced ERf receptor signaling (*SI Appendix*, Fig. S4). (Scale bar: 2 cm.) (*C*) Epidermal phenotype of 10 d-old seedlings of wild-type Col-0, *bsk1*, *bsk2*, *ssp*, *bsk1 bsk2* double mutants (*b1 b2*), and *bsk1 bsk2 ssp* triple mutants (*b1 b2 ssp*), as well as *bsk1 bsk2 ssp triple* mutants carrying a constitutively active variant of *yda* (*b1 b2 ssp yda-CA*). Loss-of-function *yda* mutants and a constitutively active variant of *YDA* (*yda-CA*) are shown as controls. (Scale bar: 50 μm.)

Expression of *BSK1* had no detectable effect on *EPF2* expression, supporting the notion that the signaling activity of BSK1 is predominantly regulated by receptor-mediated phosphorylation (27) rather than protein abundance. In stark contrast, *SSP* expression leads to strong down-regulation of *EPF2* in a similar way as in samples expressing *YDA-CA* (Fig. 5*A*).

In this overexpression experiment, *SSP* appeared to activate the YDA MAP kinase cascade in a manner that did not involve the canonical ligands of the pathway. To test this idea, we transiently expressed *BSK1* and *SSP* in *Arabidopsis* protoplasts and monitored the activation of MPK3 and MPK6 using a phosphorylation-specific antibody against the activation loop (Fig. 5*B*). As a positive control, we expressed *YDA-CA* and observed a strong increase in signal intensity compared with cells expressing the nonfunctional YDA-KD. The expression of *BSK1* did not noticeably influence the amount of phosphorylated MPK3 or MPK6, while the expression of *SSP* led to a strong increase in activated MPK3 and MPK6 (Fig. 5*B*). The overall MPK6 abundance, as measurable with antibody binding independent of phosphorylation status, did not change in any of these experiments.

Taken together, our data strongly suggest that the SSP protein is capable of triggering YDA-dependent signaling. In this scenario, SSP would be able to initiate downstream YDA-dependent signaling without canonical receptor activation.

Constitutive Signaling Activity Due to Loss of Intramolecular Interaction. SSP has been described as a quite unusual BSK family member with a conspicuously shorter activation loop in comparison to other BSK family proteins (19). SSP has been regarded as a pseudokinase (12); however, kinase activity assays have not been performed. To test if the differences between SSP and BSK1 can be attributed to increased kinase activity of SSP, we purified YDA, SSP kinase, and BSK1 kinase after heterologous expression in *Escherichia coli* and performed kinase activity assays (*SI Appendix*, Fig. S7). We used full-length YDA as a positive control, which showed readily detectable ATP turnover. In contrast to YDA, however, we could not detect kinase activity for SSP or BSK1. While the ATP turnover for SSP did not differ at all from the negative control, there was a very weak but statistically not significant increase in ATP turnover for BSK1 (not visible in *SI Appendix*, Fig. S7). These results are in agreement with previous reports indicating that kinase activity is not necessary for SSP function and suggest that BSK family proteins might function primarily by recruiting downstream signaling components (12, 16, 19). As we cannot detect any kinase activity for SSP, the constitutive activation of downstream signaling components has to be explained by a different mechanism.

BSK proteins are generally regulated by phosphorylation (27); in the case of rice OsBSK3, it has been shown that phosphorylation breaks a direct and negative auto-regulatory interaction between the C-terminal tetratricopeptide repeat (TPR) motif and the central kinase domain (30), liberating the protein to recruit downstream signaling partners. Given the close structural similarity of BSK proteins, this mode of regulation may well be conserved within the family, and we thus wanted to determine whether similar intramolecular interactions could be detected with *Arabidopsis* BSK1 and SSP, respectively. In a yeast two-hybrid interaction assay, the isolated TPR domain of BSK1 indeed showed clear interaction with its kinase domain. Strikingly, this interaction could not be observed for the closely related SSP TPR domain when tested with the SSP kinase domain (Fig. 6*A*), despite expression of the SSP TPR domain (*SI Appendix*, Fig. S8). We independently confirmed these results in plant cells by transiently expressing the TPR and

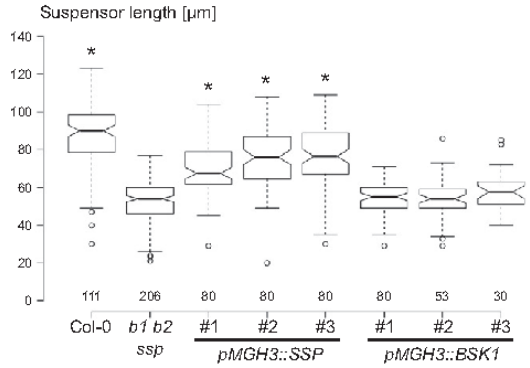

Fig. 3. Genetic rescue of *ssp* mutants by sperm-specific *BSK* gene expression. A box plot diagram of suspensor size measurements 75 h after pollination is shown. Homozygous transgenic lines carrying *pMGH3::SSP* or *pMGH3::BSK1* in a *bsk1 bsk2 ssp* triple-mutant background were used as pollen donors to pollinate wild-type Col-0 plants. Control Col-0 and *bsk1 bsk2 ssp* triple mutants were used as pollen donors in parallel experiments. Without genetic rescue, the paternal effect of the mutant *ssp* allele causes reduced suspensor size in heterozygous embryos. The box plot diagram shows the median as center lines, and the 25th and 75th percentiles are indicated by box limits. Whiskers show 1.5× interquartile distance. Outliers are represented by dots. The total number of embryos for each genotype is given above the *x* axis. Statistically significant differences from the control crosses with homozygous *bsk1 bsk2 ssp* triple mutants as pollen donors are indicated by asterisks (Mann–Whitney *U* test: $*P < 0.01$).

kinase domains of BSK1 and SSP, respectively, as fusion proteins for ratiometric bimolecular fluorescence complementation assays (rBiFCs) (31) in tobacco leaves (Fig. 6*B*). For the most part, the rBiFC assay corroborated our observations in the yeast two-hybrid assay. With the rBiFC assay, we could not detect any interaction of the SSP TPR domain with its kinase domain, while the corresponding TPR domain of BSK1 interacts with the BSK1 kinase domain. In contrast to the yeast experiment, we could also detect an interaction of the BSK1 TPR domain with the SSP kinase domain, possibly indicating that changes within the SSP TPR domain are responsible for neofunctionalization.

The lack of intramolecular, regulatory interaction in SSP might be a simple explanation for its property to evoke a constitutive signaling response. SSP has been described to directly bind the downstream MAPKKK YDA (26), while a direct interaction has been reported for BSK1 with the MAPKKK MKKK5 (32). To rule out the possibility that SSP differs from BSK1 in its ability to directly interact with YDA, we tested the interaction of SSP and BSK1 with different parts of the YDA protein (*SI Appendix*, Fig. S9). In a yeast two-hybrid assay, the TPR motifs of SSP and BSK1 showed binding to the YDA kinase domain, while no interaction with the N-terminal region of YDA could be detected.

These results further support our genetic data and indicate that BSK1 and SSP are both integral parts of YDA-dependent signaling pathways and can both directly interact with YDA. According to the model of regulation by negative intramolecular interaction, the lack of affinity between the SSP TPR and kinase domains may provide a mechanistic basis for the constitutive activation of the YDA pathway evoked by the SSP protein. To explore this possibility and to map SSP-specific protein properties, we expressed chimeric versions of the *SSP* gene, where various parts of the coding regions had been replaced by their BSK1 counterparts under the control of the *SSP* promoter in the *ssp* mutant background, and monitored the genetic rescue of mutant phenotypes (Fig. 4 *A* and *B*). *BSK1* has been shown to be phosphorylated within the activation loop, and this site of phosphorylation is absent in *SSP* (19). It would therefore be conceivable that negatively charged amino acids in the short SSP activation loop mimic constitutive phosphorylation. However, a chimeric BSK1 variant that carries the SSP activation loop did not adopt SSP-like properties, whereas SSP variants with a BSK1 activation loop behaved like the native SSP protein in the genetic rescue experiment, suggesting that the activation loop does not determine the specific property of the SSP protein. An SSP kinase domain paired with a BSK1 TPR motif was also not functional in rescuing the embryonic *ssp* phenotype, whereas a BSK1 kinase domain fused to an SSP TPR motif retained the ability to rescue *ssp-2* mutants. These results demonstrate that, indeed, the structural determinants underlying the different activities of SSP and BSK1 proteins can be largely mapped to the TPR motif. By embedding individual repeat units of BSK1 into an SSP background, we could further show that the third and fourth repeat units of the TRP motif are interchangeable, whereas the presence of the first, cryptic repeat unit or the second repeat unit of BSK1 abolished the function of the chimera. The results clearly demonstrate that the specific signaling property of SSP relies strongly on the SSP TPR motif, which cannot be functionally replaced by the BSK1 TPR domain. Furthermore, neither the activation loop nor the entire SSP kinase domain was sufficient to rescue the *ssp* defects when positioned in the context of the BSK1 protein.

According to our model, the loss of intramolecular interaction would be responsible for the SSP-specific protein properties. The genetic rescue experiments now indicate that this feature can be largely mapped to the TPR domain. One would therefore assume that the ability to evoke a constitutive signaling response in YDA-dependent signaling pathways can also be mapped to the SSP TPR motif. To test this hypothesis, we used chimeric versions of BSK1 and SSP in a protoplast transient expression system and monitored their effect on YDA-dependent target gene expression (Fig. 4*C*). *CYP82C* is transcriptionally up-regulated in protoplasts in response to *YDA-CA* expression. Expression of full-length *SSP* similarly led to a strong increase of *CYP82C* transcripts, as observed with constitutively active *YDA-CA* (Fig. 4*C*). As seen for *EPF2* expression, full-length *BSK1* expression, on the other hand, has no detectable effect on *CYP82C* transcript levels. When testing chimeric constructs, BSK1 protein that carries the SSP TPR motif causes the same up-regulation of target gene expression as full-length SSP and constitutively active YDA-CA. The chimeric SSP protein that harbors a BSK1-derived TPR motif, on the other hand, did not cause activation of *CYP82C* expression. In agreement with our model, only protein variants that cause a constitutive signaling response were also able to rescue the genetic defects of *ssp* mutants (Fig. 4).

Taken together, our data strongly suggest that the SSP protein causes a nonregulated, constitutive activation of YDA-dependent signaling pathways that is most likely the consequence of loss of inhibitory, intramolecular interaction previously demonstrated for BSK family proteins. This lack of regulation, however, can presumably be tolerated by the plant because of the tightly controlled expression pattern of *SSP* that confines the SSP protein to the early embryo (*SI Appendix*, Fig. S2*C*). According to this model, we would predict that prolonged expression of *SSP* in the early embryo should evoke gain-of-function phenotypes. To test this hypothesis, we expressed a functional *SSP-YFP* fusion in the early embryo using a *GAL4-UAS* transactivation system under the control of the ubiquitously active *RPS5a* promoter. Only in F1 embryos that carried the *RPS5a* driver as well as the *pUAS::SSP-YFP* effector constructs could we observe embryos with supernumerary suspensor cells and structures entirely lacking a recognizable proembryo, reminiscent of embryos that carry a constitutively active variant of *YDA* (*SI Appendix*, Fig. S10). Embryos that carried only the driver line or the

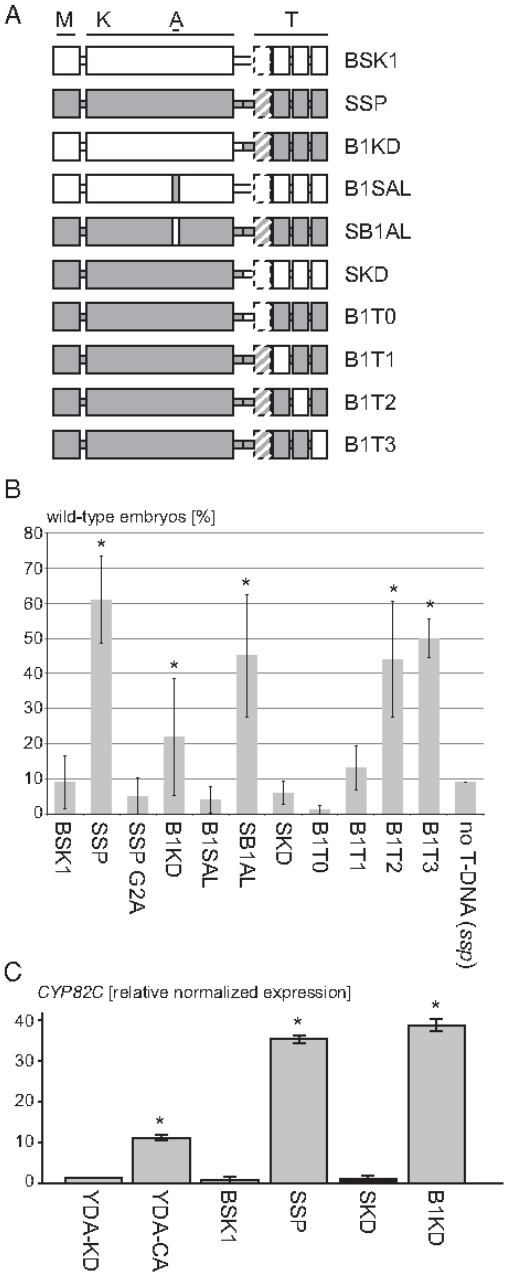

Fig. 4. SSP-specific properties can be mapped to the C-terminal TPR motif. (*A*) To map the structural features underlying the functional difference between the SSP and BSK1 protein, chimeric constructs (described in *Materials and Methods*) were tested for their ability to genetically rescue the *ssp* mutant phenotype. For each construct, 12 independent transgenic lines were analyzed for genetic rescue of the embryonic *ssp* phenotype (>100 embryos each line) in comparison to a full-length *SSP* rescue construct as a positive control and a nonfunctional *SSP* construct [*SSP G2 > A* (12)] as a negative control. Functional protein domains/motifs are depicted as larger rectangular boxes. A, kinase activation loop; K, kinase domain; M, myristoylation motif; T, TPR domain. Each predicted TPR repeat is shown as an individual rectangular box, and the first cryptic repeat is indicated by a dashed line. SSP sequences are depicted in gray, and BSK1 sequences are depicted in white. (*B*) Genetic rescue of *ssp* mutants based on morphological criteria by expression of chimeric *SSP* and *BSK1* variants shown in *A* under control of the *SSP* regulatory sequences. The bar graph shows the number of wild-type embryos as an average percent value with the SD for 12 independent transgenic lines for each construct. Statistically significant differences from the negative control (*ssp*) are indicated (determined by χ^2 test: $^*P < 0.0001$) (details of the analysis and statistical test are provided in Dataset S1, and the heritability of these traits is shown in Dataset S2). (*C*) Transcript levels of *CYP82C* in *Arabidopsis* protoplasts in response to the expression of *SSP* and *BSK1* and chimeric versions determined by qRT-PCR. As controls, a constitutively active variant (*YDA-CA*) and a nonfunctional version of *YDA* (*YDA-KD*) were used. Transcript levels were normalized to *EF2* expression as a reference. Expression levels are given as relative values, with the negative control (*YDA-KD*) arbitrarily set to 1. Significant differences from the negative control (YDA-KD) are indicated (Student's *t* test: $^*P < 0.05$).

effector line did not show any obvious differences from wild-type embryos. Furthermore, transactivation of *BSK1* in the early embryo under control of the same expression system did not lead to any obvious morphological changes in comparison to control plants. Prolonged expression of *SSP* in the embryo therefore evokes a similar gain-of-function phenotype as observed when ectopically expressed in the leaf epidermis, strongly arguing in favor of SSP evoking a constitutive signaling response of YDA-dependent signaling pathways.

Taken together, we could show that SSP exhibits a nonregulated, constitutive signaling activity that is most likely the consequence of loss of inhibitory, intramolecular interaction previously demonstrated for BSK family proteins. Tightly controlled expression of *SSP*, on the other hand, might make posttranslational regulation unnecessary.

Discussion

BSK family proteins have been described to fulfill a role as receptor-associated cytoplasmic kinases in a similar manner as, for example, the interleukin-1 receptor–associated kinases (33). Due to neighboring kinases in the respective receptor complex, these kinases often do not need kinase activity for their function (34, 35). Based on the protein structure of the *Arabidopsis* BSK8 kinase domain, it was proposed that, in general, BSK family kinases are pseudokinases (17). Our kinase assays with BSK1 and SSP kinase domains support this notion. The regulated function of BSK proteins might therefore manifest itself in the passing of signal information by phosphorylation-dependent recruitment of downstream signaling components that, in turn, can be phosphorylated by nearby kinases (16, 30). For BSK1, however, kinase activity in the context of MKKK5 phosphorylation has recently been reported using an antibody against phosphate moieties (32). In agreement with the published data for BSK8 (17) and SSP (12), but in contrast to the previous report regarding BSK1 (32), we could not detect kinase activity for isolated kinase domains of BSK1 and SSP. As we could observe a low but statistically not significant turnover of ATP in the sample containing BSK1, very low kinase activity at our detection limit cannot be ruled out. Furthermore, as our experiments were performed with isolated kinase domains, we cannot exclude the possibility that BSK family proteins possess kinase activity in their native form. In the context of SSP-dependent YDA activation, however, any potential differences in kinase activity between SSP and BSK1 cannot explain the different behavior of these proteins, as swapping kinase domains or the activation loop between SSP and BSK1 in chimeric constructs did not have any effect, while the SSP-specific activation of YDA-dependent target genes depended on the SSP C-terminal TPR motif.

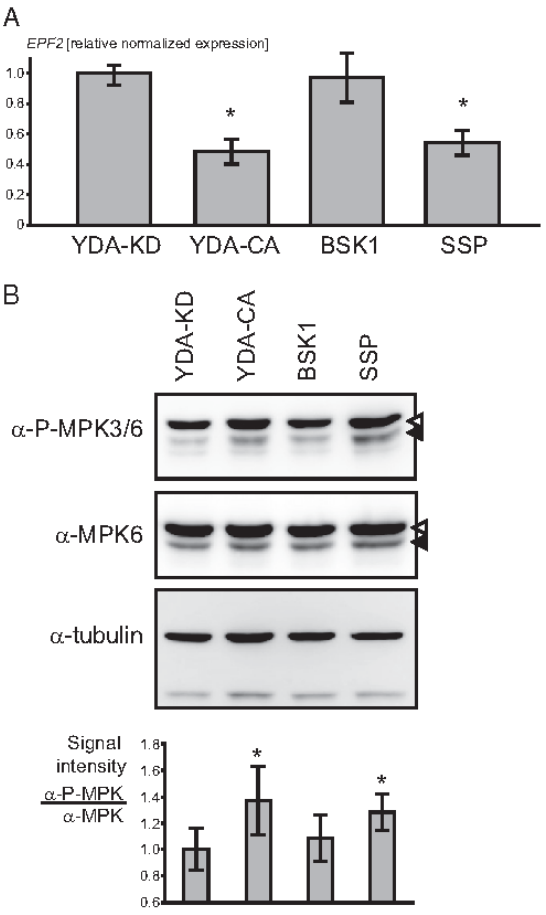

Fig. 5. Activation of the ERf/YDA pathway by ectopic *SSP* expression. (*A*) Transcript levels of *EPF2* in *Arabidopsis* protoplasts in response to expression of *SSP* and *BSK1* determined by qRT-PCR. As controls, a constitutively active variant (*YDA-CA*) and a nonfunctional version of *YDA* (*YDA-KD*) were used. Transcript levels were normalized to *EF2* expression as a reference. Expression levels are given as relative values with the negative control (*YDA-KD*) arbitrarily set to 1. Significant differences from the negative control (*YDA-KD*) are indicated by asterisks (Student's *t* test: $*P < 0.05$). (*B*) Phosphorylation of MPK3 and MPK6 in response to YDA activation detected by Western blotting with a phosphorylation-sensitive antibody against the activation loop of both kinases. As loading controls, phosphorylation-independent antibodies against MPK6 and tubulin were used. Note that the polyclonal antibody against MPK6 also detects MPK3 (black arrowhead). The MPK3 and MPK6 proteins have expected sizes of 42.7 kDa (black arrowhead) and 45.1 kDa (white arrowhead), respectively. The bar graph gives the relative amount of phosphorylated MPK6 in relation to total MPK6 as inferred by the signal intensity of the corresponding Western blots. Average values and SDs of three Western blots are shown. Significant differences from the negative control (YDA-KD) are indicated (Student's *t* test: $*P < 0.05$).

BSK family proteins have been functionally described in the context of brassinosteroid signaling in combination with the receptor kinases BRI1 and BAK1/SERK3 regulating plant growth (16, 27). In this context, several BSKs act in a genetically redundant manner, while BSK3 seems to be more prominently involved (18). BSK1 also interacts with the receptor kinases FLS2 and BAK1/SERK3 in the context of innate immunity responses (14, 36). For BSK5, a role in response to abiotic stress has been postulated (15). Our data now introduce BSK1 and BSK2 as signaling partners of the ERf/YDA signaling pathway, a pathway in which coreceptors of the SERK family also participate (11). Therefore, BSK family kinases could well be rather general downstream signaling partners of SERK-dependent receptor complexes in various (MAP kinase) signaling pathways. Several other receptor pathways with related leucine-rich receptor kinases, such as HAE, HSL2, PXY, and EMS1, have been described as SERK-dependent, and some of them rely on a MAP kinase cascade, including MPK6 (37–39). It will be interesting to see if BSK family kinases also play a role in these pathways.

In the context of brassinosteroid signaling, *BSK* genes supposedly act in a genetically redundant manner (18). It is therefore quite surprising, and in contrast to previous reports, that *bsk1* and *bsk2* double mutants show strong growth defects. This is probably due to the allele choice in previous studies, as the *bsk1-3* (SAIL_140_C04) allele is not a null allele (*SI Appendix*, Fig. S11), while our work was carried out with the *bsk1-2* allele, which does not produce functional BSK1 protein (13) (*SI Appendix*, Fig. S11). Interestingly, the *bsk1-2 bsk2-2* double mutant shows an epidermal phenotype with clusters of stomata almost as dramatic as *yda* loss-of-function mutants (Fig. 2 and *SI Appendix*, Fig. S4). Therefore, the other 10 *BSK* genes might play only a minor role in the context of ERf/YDA signaling and might be more prominently involved in other SERK-dependent signaling pathways. In a similar manner, the *bsk1 bsk2 ssp* triple mutant shows aberrant suspensor development very similar to *yda* loss-of-function mutants. Again, this would argue in favor of functional specificity of different *BSK* genes.

BSK1 and *BSK2* seem to be evolutionarily conserved as they can be found in basal angiosperms such as *Amborella trichopoda* (*SI Appendix*, Fig. S1). *SSP* orthologs, however, only exist in members of the Brassicaceae family and evolved during the last whole-genome duplication of the core Brassicaceae as a duplicate of *BSK1* (19). The involvement of *BSK1* and *BSK2* in the embryonic YDA pathway, as well as the ERf/YDA pathway, therefore most likely reflects an ancestral state, with *SSP* being an embryo-specific innovation of the Brassicaceae. The loss-of-function phenotype of the *bsk1 bsk2* double mutant, on the other hand, demonstrates that BSK1 and BSK2 still contribute to YDA activation in the early embryo. This suggests that a more ancient prototype of YDA activation, possibly via a receptor complex, might still be functional during embryogenesis in *Arabidopsis*. This would also imply that in non-Brassicaceae plants, apical-basal polarity of the zygote could solely rely on BSK1/BSK2-dependent activation of YDA. As many of these plants have embryos with a poorly defined embryo-suspensor boundary quite similar to *ssp* mutant embryos in *Arabidopsis*, it would be fascinating to see what consequences introducing a functional *SSP* gene would have on the early embryonic patterning of these plant species.

SSP contributes to YDA activation in the early *Arabidopsis* embryo in such a way that it cannot be replaced by *BSK1*. It has been shown that BSK1 is phosphorylated by BRI1 at the activation loop at serine 231, a residue that is conserved among *Arabidopsis* BSK proteins, and also in CDG1, a further cytoplasmic kinase targeted by BRI1 (40). In SSP, however, this serine residue is missing and might indicate that SSP relies on a different mode of regulation than the other BSK proteins. Our data suggest that SSP acts like a deregulated, constitutively active variant of BSK1 since the presence of the protein is sufficient to activate the MPK6-dependent MAP kinase cascade and has the same impact on target genes as constitutively active YDA.

Kinases are usually highly regulated proteins and are only activated during signaling events. Constitutively active variants occur only rarely and are often associated with diseases [e.g.,

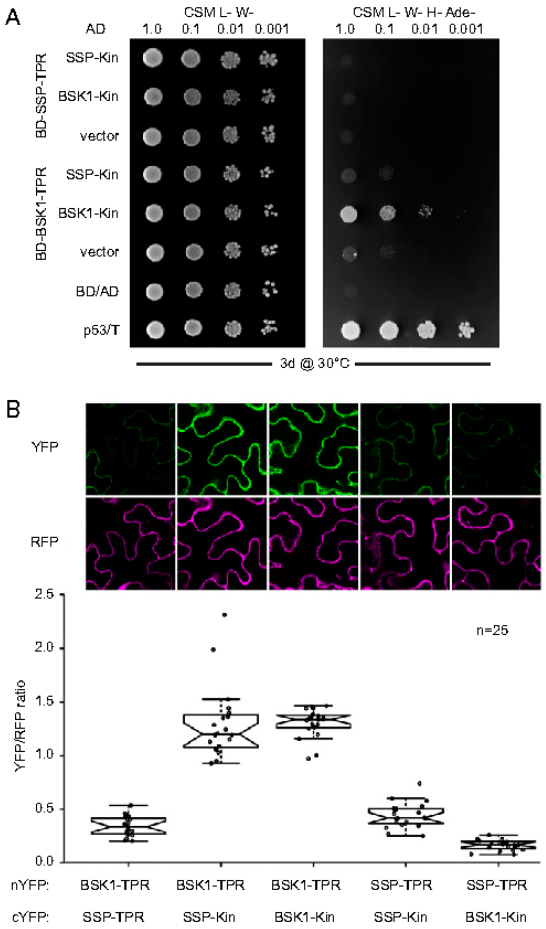

Fig. 6. SSP has lost the competence for intramolecular interaction. (*A*) Yeast two-hybrid assay to test for interaction between the TPR and kinase domains of SSP and BSK1. Serial dilutions of yeast cells containing the GAL4-DNA binding domain (BD) fused to the TPR domain of SSP or BSK1 plus the GAL4 activation domain (AD) fused to the kinase domains of SSP or BSK1, respectively, were dropped on vector-selective [complete supplement medium without leucine and tryptophan (CSM L- W-)] and interaction-selective medium (CSM L- W- H- Ade-). Growth was monitored after 3 d at 30 °C. pGADT7 empty vector was used as a negative control ("vector"). (*B*) Interaction tests using rBiFC. (*Top*) Confocal images of transiently transformed *N. benthamiana* leaf epidermal cells representing the median value of RFP and YFP fluorescence for each experiment are shown. (*Bottom*) Box plot diagram depicts the ratio of the mean fluorescence of YFP against RFP from 25 different, randomly chosen leaf sections. Center lines of boxes represent the median, with outer limits at the 25th and 75th percentiles. Notches indicate 95% confidence intervals. Tukey whiskers extend to 1.5× the interquartile ratio.

human epidermal growth factor receptor mutants are associated with cancer (41)]. In extremely rare cases, acquired constitutive activity might be beneficial and functionally important, as is the case for protein kinase CK2 (42). One possible evolutionary scenario for *SSP* would be that an initial event confined *SSP* expression to sperm cells, rendering the duplicated gene functionally irrelevant. In the absence of purifying selection, *SSP* was then free to accumulate mutations that destroyed regulatory regions of the protein, turning it constitutively active. It was speculated that an in-frame deletion in the activation loop of SSP, which occurred early after the whole-genome duplication and encompasses the BRI1-dependent phosphorylation site of BSK1, might be associated with neofunctionalization (19). Our data, however, demonstrate that the specific properties of SSP reside within the C-terminal TPR domain. Rice OsBSK3 has recently been shown to be negatively regulated through an intramolecular interaction of the kinase domain and the TPR motif. Phosphorylation of the kinase domain activation loop interferes with this interaction and allows the protein to interact with downstream signaling partners (30). Intriguingly, the SSP TPR domain has lost its ability to interact with the kinase domain, providing a possible mechanistic basis for the constitutively active properties of SSP. On the other hand, SSP is capable of direct interaction with YDA, as recently reported (26), and we could show that this is a conserved feature of SSP and BSK1. As described for the interaction of BSK1 and MKKK5 (32), SSP and BSK1 seem to interact with the kinase domain of YDA. Perhaps this simple combination, loss of affinity for the intramolecular interaction with retained affinity for the downstream MAPKK kinase partner, is sufficient for SSP to mediate constitutive activation of the pathway. In this scenario, the phosphorylation sites in the activation loop of the kinase domain would be obsolete and a loss of these sites could well be an evolutionary consequence.

The acquired gain-of-function in the SSP protein facilitates YDA activation as soon as the sperm cell fuses with the egg and SSP protein accumulates in the zygote. We have previously shown that the early YDA activation by *SSP* is correlated with faster development of the embryo and a more precisely defined embryo-suspensor boundary, both of which are characteristic features of the Brassicaceae (12, 43). Evolution of *SSP* might therefore be a key innovation that contributes to the reproductive biology of this successful plant family.

Materials and Methods

Plant Material and Growth Conditions. All *A. thaliana* plants used in this study were grown under long-day conditions as described previously (43). The following mutant alleles have been described previously: *bsk1-1* (R443 > Q), *bsk1-2* (SALK_122120), *bsk1-3* (SAIL_140_C04), *ssp-2* (SALK_051462), *yda-1* (Q443 > STOP), and *YDA-CA* (6, 12, 14, 18, 44). The *bsk2-2* (SALK_001600), *er* (SALK_066455), *erl1* (GK_109G04), and *erl2* (GK_486E03) alleles were genotyped using the following gene-specific primers: bsk1-2 LP: ATGAGGTTGCGAGTAGGAT, bsk1-2 RP: CAAAAGCATGACCAATGAGAAG, bsk2-2-F: 5′-GGAAGCGACTGGTGTTGGGAAG-3′, bsk2-2-R: 5′-TGGTCGATCCTTTGCCTCTGA-3′, er-F: 5′-TTCGAAATCGAAAACGGTATG-3′, er-R: 5′-TGTGTGTGAGAAATGGCTCTG-3′, erl1-F: 5′-TTTCCAATCATGATGTTGCAG-3′, erl1-R: 5′-CAAACAATTGCTCCAGCTTTC-3′, erl2-F: 5′-TATCTCCATGGCAACAAGCTC-3′′, erl2-R: 5′-AATGACACATCGCTGAGAAGG-3′, and transfer DNA (T-DNA) primers LBb1.3: 5′-ATTTTGCCGATTTCGGAAC-3′ and GK-LB: 5′-ATATTGACCATCATACTCATTGC-3′, respectively. Multiple mutant combinations were obtained by crossing and PCR-based genotyping of offspring plants.

Plasmid Construction. For the construction of binary vectors *pGreen nos:bar* (*GIIb*) *pMGH3::SSP* and *GIIb pMGH3::BSK1*, the genomic region covering the entire coding region was synthesized, avoiding commonly used restriction sites in the coding region. In addition, the intron 3 (*SSP*) and intron 6 (*BSK1*) were deleted to allow for PCR-based genotyping of *ssp* and *bsk* mutant alleles in the presence of the transgene. The synthesized fragments were cloned into binary vectors containing the *MGH3* expression cassette by ligation-based molecular cloning. Expression of the transgene was confirmed for all lines used in the analysis by RT-PCR on cDNA from mature pollen using primers SSP-qF2/SSP-qR2 and BSK1-qF2/BSK1-qR2, respectively (*SI Appendix*, Table S1). For the *p35S::YDA-CA*, *p35S::YDA-DN*, *p35S::BSK1*, and *p35S::SSP* expression vectors, coding regions, including restriction sites, were amplified by PCR and transferred into *pJIT60* (45) by restriction digest ligation-based cloning. Similarly, for *p35S*-based expression vectors containing chimeric versions of *SSP* and *BSK1*, the chimeric coding region was PCR-amplified and cloned into *pJIT60*. For *pARF13>>NLS-tdtomato* and *pBSK2>>NLS-tdtomato*, the

corresponding promoter fragments (1.97 kb for *ARF13* and 2.83 kb for *BSK2*) were PCR-amplified and replaced the *NTA* promoter in *pNTA>>NLS-tdtomato* (46).

For chimeric *SSP/BSK1* T-DNA constructs, chimeras were based on two pCambia T-DNAs containing an ∼11-kb fragment spanning the entire *SSP* locus, with a *YFP* moiety added in-frame into low-complexity regions of the SSP protein behind the myristoylation motif (after Gly29) or behind the kinase domain (after Ser314) (12). Restriction sites introduced with the *YFP* moiety were used to exchange segments of the *BSK1* genomic sequence encoding for the kinase domain (Gly43-Pro354; "B1KD") or the TPR domain (after Pro-357, "SKD") with the corresponding segments of *SSP*; the *YFP* moiety was deleted in the process to minimize the number of structural changes. Synthetic fragments (purchased from Integrated DNA Technologies) were used for generating T-DNAs harboring an SSP activation loop embedded in a BSK1 kinase domain ("B1SAL": SSP Glu196-Ser206 inserted between BSK1 Lys221 and Val246), a BSK1 activation loop embedded in an SSP kinase domain ("SB1AL": BSK1 Asn222-Arg245 inserted between SSP Lys195 and Val207), and each of the four units of the BSK1 TPR domain embedded in an SSP TPR domain ("B1T0": linker region and first cryptic repeat, BSK1 Pro357-Met400 inserted between SSP Ser314 and Lys316; "B1T1": first repeat, BSK1 Lys401-Pro417 substituting for SSP Lys316-Pro398; "B1T2": second repeat, BSK1 Pro417-Pro452 substituting for SSP Pro398-Pro412; and "B1T3": BSK1 Pro452-end substituting for SSP Pro412-end).

A normal form of SSP ("SSP") and an inactive form, in which the Gly2 position carrying the myristoylate modification changed to Ala ("G2A"), served as controls. The "BSK1" T-DNA was created by inserting the BSK1 coding sequence derived from a cDNA clone between the SSP start and stop codons of the normal form of SSP T-DNA.

Transient Expression in Protoplasts. Dark-grown suspension cell cultures derived from *A. thaliana* Col-0 were grown and transfected as described previously (47). For qRT-PCR analysis, total RNA was extracted as described below.

RT-PCR and qRT-PCR Analysis. For expression analysis in plants as well as protoplasts, total RNA was extracted by using the RNeasy Plant Mini Kit (Qiagen). RNA samples were treated with DNaseI (Fermentas) to remove any residual genomic DNA. RNA was reverse-transcribed to cDNA with the RevertAid First Strand cDNA Synthesis Kit (Fermentas) using oligo(dT) primers.

To detect transcripts and transcript fragments in insertion lines, gene-specific primer pairs upstream, downstream, and flanking the insertion site were used (*SI Appendix*, Table S1). For measurements of transcript levels, qRT-PCR was carried out on a CFX Connect Thermocycler (Bio-Rad) with SsoAdvanced Universal SYBR Green Supermix (Bio-Rad). The PCR was performed with gene-specific primer pairs (*SI Appendix*, Table S1).

Western Blot. For Western blot analysis, protoplasts were pelleted in 240 mM $CaCl_2 \cdot H_2O$ for 2 min at 3,700 × *g*. After addition of lysis buffer [25 mM Tris phosphate (pH 7.8), 2 mM DTT, 2 mM EDTA, 10% glycerol, 1% Triton X-100], total protein was extracted by repeated manual grinding of frozen samples using liquid nitrogen, and standard Laemmli buffer was added to a final 1× concentration followed by heating at 95 °C for 3 min.

Proteins were separated by size by SDS/PAGE and detected by Western blotting as described previously (48). Phosphorylated MPK6 protein was detected with a Phospho-p44/42 MAPK (Erk1/2) (Thr202/Tyr204) (D13.14.4E) XP monoclonal antibody (1:2,000 dilution, no. 4370; Cell Signaling Technology). Overall amount of MPK6 was detected with a polyclonal anti-AtMPK6 antibody (1:2,000 dilution, no. A7104; Sigma–Aldrich). Tubulin abundance was used as a loading control and was detected with a monoclonal antitubulin antibody (1:2,000 dilution; Sigma–Aldrich).

Yeast Two-Hybrid Assay. Constructs used for the yeast two-hybrid analysis were cloned into the high-copy vectors pGADT7-Dest and pGBKT7-Dest, respectively (Clontech Matchmaker). Both vectors were previously modified to allow for Gateway cloning. For Gateway cloning, coding regions of genes of interests were PCR-amplified with primers containing attB sites (*SI Appendix*, Table S1). Plasmids were cotransformed into the two-hybrid strain PJ69-4A via lithium acetate transformation (49). Diploid yeasts were dropped in 10-fold serial dilutions on vector-selective [complete supplement medium (CSM) L- W-] and interaction-selective (CSM L- W- H- Ade-) media and grown at 30 °C for 3 d.

rBiFC. Constructs were cloned into the binary 2in1 vector pBiFCt-2in1-NN (50) and transformed in *Agrobacterium* strain GV3101. Fluorescence intensities for YFP and RFP were measured from *Nicotiana benthamiana* leaves 2 d after infiltration using a Leica SP8 confocal laser scanning microscope at 514-nm and 561-nm excitation wavelengths, respectively. YFP/RFP ratios were calculated from 25 different leaf regions and plotted using BoxPlotR (51).

Protein Expression and Purification. Codon-optimized coding sequences of BSK1, SSP, and YDA kinases encompassing residues 1–292, 1–331, and 1–883, respectively, were cloned into a modified pET vector containing an N-terminal His6-SUMO solubility tag that is removable by tobacco etch virus (TEV) protease-mediated cleavage. OverExpress C41 cells (Lucigen) were transformed with the respective plasmids and grown in LB medium in the presence of kanamycin. Cells were grown at 37 °C to optical densities (OD_{600}) of 0.6, induced with 0.2 mM isopropyl β-D-1-thiogalactopyranoside, and incubated overnight at a temperature of 22 °C. Twelve hours after induction, cells were harvested and stored at −20 °C. Subsequently, pellets were lysed by sonication in lysis buffer supplemented with 0.1% Triton X-100 and 100 μg/mL lysozyme. Buffer conditions were 50 mM Tris (pH 8.0), 150 mM NaCl, 1 mM DTT, and 10 mM imidazole for BSK1 kinase; 50 mM Tris (pH 8.0), 500 mM NaCl, and 10 mM imidazole for SSP kinase; and 50 mM Hepes (pH 7.5), 250 mM NaCl, 1 mM DTT, 10 mM imidazole, and 20% (wt/vol) glycerol for YDA. Cell lysates were then centrifuged at 50,000 × *g* for 30 min to remove insoluble cell debris. The supernatant, supplemented with 2 mM $MgCl_2$, was applied to nickel-nitrilotriacetic acid (Ni-NTA) resin, and the column was washed using 10 column volumes of the respective lysis buffers. The protein was eluted from the resin using lysis buffers supplemented with 200 mM imidazole. YDA protein was left uncleaved, whereas the SUMO tag was removed from BSK1 and SSP kinase constructs by TEV cleavage during dialysis into 25 mM Tris (pH 8.0), 500 mM NaCl, and 1 mM DTT for SSP kinase and into 25 mM Tris (pH 8.0), 150 mM NaCl, and 1 mM DTT for BSK1 kinase. The cleaved tag was removed from the target protein using a second Ni-NTA step in dialysis buffer. Finally, a size exclusion chromatography purification step in kinase buffer [50 mM Tris (pH 8.0), 200 mM NaCl, 1 mM DTT, and 5 mM $MgCl_2$] using a Superdex 200 column yielded pure protein.

Kinase Activity Assay. Kinase activity was determined using the ADP-Glo Assay (Promega). The experiment was carried out according to the manufacturer's recommendations. In brief, kinase reactions were carried out at 22 °C in kinase buffer [50 mM Tris (pH 8.0), 200 mM NaCl, 1 mM DTT, and 5 mM $MgCl_2$] in the presence of 100 μM ATP and 1 μM lysozyme as substrates. The kinase concentrations used in this assay were 10 μM for BSK1 and SSP kinase domains and 1 μM for YDA. The reactions were terminated by flash-freezing aliquots in liquid nitrogen at 0, 30, and 60 min. Subsequently, ADP generation in the samples was determined according to ADP-Glo instructions using a Tecan Infinite F200 plate reader.

Microscopic Analysis of Embryos, Measurements, and Reporter Gene Analysis. Immature seeds were dissected and cleared in Hoyer's solution as described previously (12). Images were taken with a Zeiss Axio Imager.Z1 microscope equipped with an AxioCam HRc camera. Size measurements were performed using measurement tools of ImageJ (NIH) software (52). Box plot analysis was performed with BoxPlotR (51).

Higher order mutants that are homozygous for *bsk1* and *bsk2* (*bsk1 bsk2*; *bsk1 bsk2 ssp*; and *bsk1 bsk2 ssp yda-CA*) show reduced fertility due to early defects in embryo sac development. In these cases, only fertilized seeds were taken into account for measurements.

Confocal scanning microscopy was performed with Zeiss LSM780NLO and Leica SP8 confocal microscopes as described previously (53). For staining of cell outlines, SCRI Renaissance blue SR2200 was used according to published protocols (54, 55).

Phenotypic Analysis of Seedlings and Plants. Images of inflorescences and rosette leaves were taken with a Pentax K-30 digital camera equipped with a 50-mm SMC-M macro lens mounted on a tripod. The area covered by the rosette leaves was determined in images by marking the perimeter of the plant and calculating the selected area using ImageJ software.

For inflorescence images, black neoprene was used as background. Pedicel length of fully open flowers was determined for five independent plants and two flowers each using a caliper.

Epidermal peels (56) were imaged with a Leica SP8 confocal microscope after staining with SR2200 as described previously (54). For propidium iodide (PI) staining, whole cotyledons were submerged in 10 μg/mL PI solution (Sigma–Aldrich) for 15 min. The samples were rinsed twice with water before mounting in water for confocal microscopy. Confocal images of epidermal surfaces were taken with a Leica TCS SP8 confocal microscope equipped with an HC PL APO 20×/0.75 Imm CORR CS2 objective using a 552-nm diode laser line for excitation. Images were acquired as z-stacks and

displayed as maximum projections using ImageJ (52). Stomata index was calculated as the number of stomata per unit area divided by the total number of epidermis cells per unit area multiplied by 100 as described previously (57).

Statistical Analysis of Quantitative Data. The Student's *t* test and Mann–Whitney *U* test were used for statistical analysis if the data showed a normal distribution or deviated from a normal distribution, respectively.

Phylogenetic Analysis. The evolutionary history was inferred by using the maximum likelihood method based on the Jones, Taylor, Thornton (JTT) matrix-based model (58). Initial tree(s) for the heuristic search were obtained by applying the neighbor-joining method to a matrix of pairwise distances estimated using a JTT model. A discrete gamma distribution was used to model evolutionary rate differences among sites [five categories (+G, parameter = 1.6251)]. The tree was drawn to scale, with branch lengths measured in the number of substitutions per site. All positions with less than 95% site coverage were eliminated; that is, fewer than 5% alignment gaps, missing data, and ambiguous bases were allowed at any position. There were 293 positions in total in the final dataset. Evolutionary analyses were conducted in MEGA6 (59).

ACKNOWLEDGMENTS. We thank the Nottingham Arabidopsis Stock Centre for providing T-DNA insertion lines; Sebastian Vorbrugg, Anja Pohl, and Martin Vogt for technical assistance; Sangho Jeong for sharing material; Caterina Brancato for protoplast transfections; and Gerd Jürgens for helpful discussions and comments on the manuscript. Research in our groups is supported by the German Research Foundation (Deutsche Forschungsgemeinschaft) (DFG SFB1101/B01 to M.B. and Emmy Noether Fellowship GR4251/1-1 to C.G.), the National Science Foundation (Award 1257805 to W.L.), and the Max Planck Society.

1. Lau S, Slane D, Herud O, Kong J, Jürgens G (2012) Early embryogenesis in flowering plants: Setting up the basic body pattern. *Annu Rev Plant Biol* 63:483–506.
2. Kawashima T, Goldberg RB (2010) The suspensor: Not just suspending the embryo. *Trends Plant Sci* 15:23–30.
3. Bayer M, Slane D, Jürgens G (2017) Early plant embryogenesis-dark ages or dark matter? *Curr Opin Plant Biol* 35:30–36.
4. Maheshwari P (1950) *An Introduction to the Embryology of the Angiosperms* (McGraw–Hill, New York).
5. Musielak TJ, Bayer M (2014) YODA signalling in the early Arabidopsis embryo. *Biochem Soc Trans* 42:408–412.
6. Lukowitz W, Roeder A, Parmenter D, Somerville C (2004) A MAPKK kinase gene regulates extra-embryonic cell fate in Arabidopsis. *Cell* 116:109–119.
7. Wang H, Ngwenyama N, Liu Y, Walker JC, Zhang S (2007) Stomatal development and patterning are regulated by environmentally responsive mitogen-activated protein kinases in Arabidopsis. *Plant Cell* 19:63–73.
8. Zhang M, et al. (2017) Maternal control of embryogenesis by MPK6 and its upstream MKK4/MKK5 in Arabidopsis. *Plant J* 92:1005–1019.
9. Bergmann DC, Lukowitz W, Somerville CR (2004) Stomatal development and pattern controlled by a MAPKK kinase. *Science* 304:1494–1497.
10. Meng X, et al. (2012) A MAPK cascade downstream of ERECTA receptor-like protein kinase regulates Arabidopsis inflorescence architecture by promoting localized cell proliferation. *Plant Cell* 24:4948–4960.
11. Meng X, et al. (2015) Differential function of Arabidopsis SERK family receptor-like kinases in stomatal patterning. *Curr Biol* 25:2361–2372.
12. Bayer M, et al. (2009) Paternal control of embryonic patterning in Arabidopsis thaliana. *Science* 323:1485–1488.
13. Shi H, Yan H, Li J, Tang D (2013) BSK1, a receptor-like cytoplasmic kinase, involved in both BR signaling and innate immunity in Arabidopsis. *Plant Signal Behav* 8:e24996.
14. Shi H, et al. (2013) BR-SIGNALING KINASE1 physically associates with FLAGELLIN SENSING2 and regulates plant innate immunity in Arabidopsis. *Plant Cell* 25:1143–1157.
15. Li ZY, et al. (2012) A mutation in Arabidopsis BSK5 encoding a brassinosteroid-signaling kinase protein affects responses to salinity and abscisic acid. *Biochem Biophys Res Commun* 426:522–527.
16. Kim TW, Wang ZY (2010) Brassinosteroid signal transduction from receptor kinases to transcription factors. *Annu Rev Plant Biol* 61:681–704.
17. Grütter C, Sreeramulu S, Sessa G, Rauh D (2013) Structural characterization of the RLCK family member BSK8: A pseudokinase with an unprecedented architecture. *J Mol Biol* 425:4455–4467.
18. Sreeramulu S, et al. (2013) BSKs are partially redundant positive regulators of brassinosteroid signaling in Arabidopsis. *Plant J* 74:905–919.
19. Liu SL, Adams KL (2010) Dramatic change in function and expression pattern of a gene duplicated by polyploidy created a paternal effect gene in the Brassicaceae. *Mol Biol Evol* 27:2817–2828.
20. Slane D, et al. (2014) Cell type-specific transcriptome analysis in the early Arabidopsis thaliana embryo. *Development* 141:4831–4840.
21. Nodine MD, Bartel DP (2012) Maternal and paternal genomes contribute equally to the transcriptome of early plant embryos. *Nature* 482:94–97.
22. Schmid M, et al. (2005) A gene expression map of Arabidopsis thaliana development. *Nat Genet* 37:501–506.
23. Torii KU, et al. (1996) The Arabidopsis ERECTA gene encodes a putative receptor protein kinase with extracellular leucine-rich repeats. *Plant Cell* 8:735–746.
24. Shpak ED, McAbee JM, Pillitteri LJ, Torii KU (2005) Stomatal patterning and differentiation by synergistic interactions of receptor kinases. *Science* 309:290–293.
25. Shpak ED (2013) Diverse roles of ERECTA family genes in plant development. *J Integr Plant Biol* 55:1238–1250.
26. Yuan GL, Li HJ, Yang WC (2017) The integration of Gβ and MAPK signaling cascade in zygote development. *Sci Rep* 7:8732.
27. Tang W, et al. (2008) BSKs mediate signal transduction from the receptor kinase BRI1 in Arabidopsis. *Science* 321:557–560.
28. Hunt L, Gray JE (2009) The signaling peptide EPF2 controls asymmetric cell divisions during stomatal development. *Curr Biol* 19:864–869.
29. Horst RJ, et al. (2015) Molecular framework of a regulatory circuit initiating two-dimensional spatial patterning of stomatal lineage. *PLoS Genet* 11:e1005374.
30. Zhang B, et al. (2016) OsBRI1 activates BR signaling by preventing binding between the TPR and kinase domains of OsBSK3 via phosphorylation. *Plant Physiol* 170:1149–1161.
31. Xing S, Wallmeroth N, Berendzen KW, Grefen C (2016) Techniques for the analysis of protein-protein interactions in vivo. *Plant Physiol* 171:727–758.
32. Yan H, et al. (2018) BRASSINOSTEROID-SIGNALING KINASE1 phosphorylates MAPKKK5 to regulate immunity in Arabidopsis. *Plant Physiol* 176:2991–3002.
33. Flannery S, Bowie AG (2010) The interleukin-1 receptor-associated kinases: Critical regulators of innate immune signalling. *Biochem Pharmacol* 80:1981–1991.
34. Janssens S, Beyaert R (2003) Functional diversity and regulation of different interleukin-1 receptor-associated kinase (IRAK) family members. *Mol Cell* 11:293–302.
35. Mendrola JM, Shi F, Park JH, Lemmon MA (2013) Receptor tyrosine kinases with intracellular pseudokinase domains. *Biochem Soc Trans* 41:1029–1036.
36. Wang J, et al. (2017) OsBSK1-2, an orthologous of AtBSK1, is involved in rice immunity. *Front Plant Sci* 8:908.
37. Meng X, et al. (2016) Ligand-induced receptor-like kinase complex regulates floral organ abscission in Arabidopsis. *Cell Reports* 14:1330–1338.
38. Zhang H, et al. (2016) SERK family receptor-like kinases function as co-receptors with PXY for plant vascular development. *Mol Plant* 9:1406–1414.
39. Li Z, et al. (2017) Two SERK receptor-like kinases interact with EMS1 to control anther cell fate determination. *Plant Physiol* 173:326–337.
40. Kim TW, Guan S, Burlingame AL, Wang ZY (2011) The CDG1 kinase mediates brassinosteroid signal transduction from BRI1 receptor kinase to BSU1 phosphatase and GSK3-like kinase BIN2. *Mol Cell* 43:561–571.
41. Valley CC, et al. (2015) Enhanced dimerization drives ligand-independent activity of mutant epidermal growth factor receptor in lung cancer. *Mol Biol Cell* 26:4087–4099.
42. Pinna LA (2003) The raison d'être of constitutively active protein kinases: The lesson of CK2. *Acc Chem Res* 36:378–384.
43. Babu Y, Musielak T, Henschen A, Bayer M (2013) Suspensor length determines developmental progression of the embryo in Arabidopsis. *Plant Physiol* 162:1448–1458.
44. Alonso JM, et al. (2003) Genome-wide insertional mutagenesis of Arabidopsis thaliana. *Science* 301:653–657.
45. Schwechheimer C, Smith C, Bevan MW (1998) The activities of acidic and glutamine-rich transcriptional activation domains in plant cells: Design of modular transcription factors for high-level expression. *Plant Mol Biol* 36:195–204.
46. Kong J, Lau S, Jürgens G (2015) Twin plants from supernumerary egg cells in Arabidopsis. *Curr Biol* 25:225–230.
47. Schütze K, Harter K, Chaban C (2009) Bimolecular fluorescence complementation (BiFC) to study protein-protein interactions in living plant cells. *Methods Mol Biol* 479:189–202.
48. Reichardt I, et al. (2011) Mechanisms of functional specificity among plasma-membrane syntaxins in Arabidopsis. *Traffic* 12:1269–1280.
49. Asseck LY, Wallmeroth N, Grefen C (2018) ER membrane protein interactions using the split-ubiquitin system (SUS). *Methods Mol Biol* 1691:191–203.
50. Grefen C, Blatt MR (2012) A 2in1 cloning system enables ratiometric bimolecular fluorescence complementation (rBiFC). *Biotechniques* 53:311–314.
51. Spitzer M, Wildenhain J, Rappsilber J, Tyers M (2014) BoxPlotR: A web tool for generation of box plots. *Nat Methods* 11:121–122.
52. Schneider CA, Rasband WS, Eliceiri KW (2012) NIH image to ImageJ: 25 years of image analysis. *Nat Methods* 9:671–675.
53. Musielak TJ, Slane D, Liebig C, Bayer M (2016) A versatile optical clearing protocol for deep tissue imaging of fluorescent proteins in Arabidopsis thaliana. *PLoS One* 11:e0161107.
54. Musielak TJ, Schenkel L, Kolb M, Henschen A, Bayer M (2015) A simple and versatile cell wall staining protocol to study plant reproduction. *Plant Reprod* 28:161–169.
55. Musielak TJ, Bürgel P, Kolb M, Bayer M (2016) Use of SCRI renaissance 2200 (SR2200) as a versatile dye for imaging of developing embryos, whole ovules, pollen tubes and roots. *Bio Protoc* 6:e1935.
56. Eisele JF, Fäßler F, Bürgel PF, Chaban C (2016) A rapid and simple method for microscopy-based stomata analyses. *PLoS One* 11:e0164576.
57. Salisbury EJ (1928) On the causes and ecological significance of stomatal frequency, with special reference to the woodland flora. *Philos Trans R Soc B* 216:1–65.
58. Jones DT, Taylor WR, Thornton JM (1992) The rapid generation of mutation data matrices from protein sequences. *Comput Appl Biosci* 8:275–282.
59. Tamura K, Stecher G, Peterson D, Filipski A, Kumar S (2013) MEGA6: Molecular Evolutionary Genetics Analysis version 6.0. *Mol Biol Evol* 30:2725–2729.

A filament-like embryo system to study the suspensor-embryo transition

Authors

Kai Wang, Yingjing Miao, Marina Ortega-Perez, Houming Chen, Martin Bayer*

Affiliation

Max Planck Institute for Developmental Biology, Department of Cell Biology, Max-Planck-Ring 5, 72076 Tübingen, Germany

* Correspondence: martin.bayer@tuebingen.mpg.de

Abstract

During embryogenesis of flowering plants, the embryo proper is connected with the mother tissue through the suspensor. Although the suspensor is eventually degraded during seed maturation, it is indispensable for delivery of nutrition and phytohormones during early embryogenesis. The differentiation to produce the two functionally different structures takes place very early. The suspensor contains most of the cells derived from the basal daughter cell after an asymmetric zygote division, while descendants of the apical daughter cell mainly contribute to the embryo proper. However, what mechanism regulates the distinct differentiations and whether the differentiation directions are alterable are largely unknown. The Brassicaceae embryogenesis follows a very stereotypical development process. A filamentous suspensor is generated by horizontal divisions of the basal daughter cell, and a clear boundary between the suspensor and the embryo proper is formed, thus providing an advantageous model to study the mechanism of cell differentiations. Several researches have indicated that the suspensor has a potential to transit into an embryo in Arabidopsis and *Brassica napus*. The function of Auxin is emphasized in regulating the suspensor-to-embryo (suspensor-embryo) transition. Here, through activating YDA pathway in early embryogenesis, we generated filament-like embryos in Arabidopsis to study the suspensor-embryo transition. The development of twin proembryos derived from these filaments was easy to follow, and twin healthy seedlings were finally generated. Through using transgenic fluorescent marker lines, we indicated that the filamentous embryo was in an undifferentiated status. Strong auxin response was not observed in early filamentous embryos. Later, we observed the maximum auxin response in the suspensor cells. Taken together, we developed an elegant system that can be used to study the mechanism of embryonic transition. Our preliminary results implies that it is important to have an early inhibition of auxin response in the whole embryo and a late activation of auxin response in the suspensor for the suspensor-embryo transition.

Keywords

YDA signaling, SSP, MPK6, cell lineage, filament-like embryo, twin embryos, embryonic transition, cell identity, auxin response

Introduction

Embryogenesis is the initiating step of the development of multicellular organisms. Different from animal embryogenesis, embryos of flowering plants have a file of cells connected with the mother tissue, called suspensor, most part of which is degraded during embryo maturation (Maheshwari, 1950). Considered to hold and provide nutrition and phytohormone for the embryo proper above, suspensor structures are quite diverse among the plant kingdom (Kawashima and Goldberg, 2010). As both the suspensor and the embryo proper are formed from the zygote, an important issue is to dissect how the differentiation directions are determined. In many plant species, the embryogenesis is flexible and the boundary between embryonic and suspensor tissue is difficult to distinguish (Wang et al., 2020). By contrast, *Brassicaceae* embryogenesis follows a very stereotypical development process. After an asymmetric division of the zygote, cell fates of two daughter cells are determined. The small apical cell develops into a spherical embryo proper while the large basal cell divides horizontally to form a filament-like suspensor. Except the uppermost suspensor cell that contributes to the hypophysis, the suspensor is degraded in the end (Wang et al., 2020). Thus, Brassicaceae provide a practical tool to study the mechanism of cell differentiations during embryogenesis.

In Arabidopsis, zygotic polarity is regulated by a Mitogen-activated protein kinase (MAPK) cascade: YODA(YDA, MKKK4)-MKK4/5-MPK3/6 (Bayer et al., 2017). The *yda*, *mkk4 mkk5* and *mpk3 mpk6* mutants show symmetric zygote divisions, and their basal daughter cells adopt embryo-like development, leading to embryos without suspensor (Lukowitz et al., 2004; Wang et al., 2007; Zhang et al., 2017). In transgenic lines expressing a constitutively active version of YDA (yda-CA), the first zygote division becomes more asymmetric and filament-like embryos without embryo proper are formed, which results in embryonic lethality (Lukowitz et al., 2004). Thus, the YDA cascade promotes suspensor differentiation and inhibits proembryo differentiation. The BR-signaling kinase 1 (BSK1), BSK2 and SHORT SUSPENSOR (SSP/BSK12) function upstream of the YDA cascade. Different from BSK1/2, SSP is a constitutive input for YDA signaling with an unusual paternal-of-origin effect (Bayer et al., 2009; Neu et al., 2019). The YDA cascade regulates zygote polarity by phosphorylating the transcription factor WRKY2, which in turn activates *WOX8* expression. During embryogenesis, *WOX8* is expressed from the zygote stage onward and marks suspensor identity (Breuninger et al., 2008; Ueda et al., 2011).

Recent transcriptome data of developing zygotes and isolated cell lineages of 1-cell embryos and 32-cell embryos showed that the basal cell and early suspensor cells have quite close transcriptional states in Arabidopsis. However, their transcriptional states are much different from that of the zygote, suggesting that the basal cell lineage has differentiated from the zygote (Zhou et al., 2020). However, suspensor cells are still capable of becoming embryos. *Liu et al.* showed that when a young proembryo was removed by laser ablation, a new embryo proper was developed from the remnant top suspensor cell. This potential was possessed only by early basal cell lineage as suspensor cells no longer own the ability after the globular stage (Liu et al., 2015). Thus, the embryonic potential of the early basal cell lineage might be suppressed by the normal embryo proper (Marsden and Meinke, 1985). Consistent with this theory, secondary embryos were formed from suspensor cells when the original embryo proper was abnormal in *sus* mutants (Schwartz et al., 1994). However, secondary embryos are still developed from suspensor cells in some mutants like *twn1* and *twn2* although their embryo propers appear normal (Vernon and Meinke, 1994; Zhang and Somerville, 1997).

Development of the apical daughter cell is regulated by auxin which is initially transported from the basal cell by PIN7 (Friml et al., 2003). Compared to the basal cell, the apical cell shows stronger DR5 response (Friml et al., 2003). When the apical auxin response was suppressed by direct inhibition or decreased auxin influx, the apical cell divided horizontally and gave rise to an abnormal embryo proper (Hamann et al., 1999; Friml et al., 2003). Recent data suggests that auxin transported from surrounding maternal tissue is responsible for auxin response in the apical cell (Robert et al., 2018). Later on, strong auxin response is mainly taking place in the hypophysis, which is vital for the root initiation (Hamann et al., 1999; Friml et al., 2003; Lau et al., 2012). Collective observations imply that local auxin response may be also involved in the suspensor-embryo transition. In the laser ablation system, strong DR5:GFP signal was observed in the remnant top suspensor cell after removal of the early embryo proper (Liu et al., 2015). Similarly, in some knock-out lines where embryo-like proliferation in the suspensor was observed, maximum DR5:GFP response was found in suspensor cells before the initiation of secondary embryos (Xiang et al., 2011; Zhang et al., 2020). Thus, it is tempting to presume that increased auxin response in suspensor cells promotes the transition. However, other studies showed that inhibiting auxin response in suspensor cells promotes this transition. BODENLOS/INDOLE-3-ACETIC ACID INDUCIBLE 12 (BDL, IAA12) is an AUX/IAA protein that inhibits auxin response. When the stabilized *bdl*, a dominant-active version of *BDL* (Hamann et al., 1999; Dharmasiri et al., 2005), was trans-activated in the whole embryo (*RPS5A>>bdl*) or only in the early suspensor (*M0171>>bdl*), embryo-like proliferations were observed in the suspensor, suggesting that the suspensor-embryo transition is inhibited by local auxin response (Rademacher et al., 2012; Radoeva et al., 2019). However, compared to *M0171>>bdl*, twin seedlings were more frequently generated in *RPS5A>>bdl* (Rademacher et al., 2012; Radoeva et al., 2019). As formation of the embryo proper on top was also abnormal in *RPS5A>>bdl* (Rademacher et al., 2012; Yoshida et al., 2014), the suspensor-embryo transition might be further facilitated by the abnormal embryo proper in this system.

Removing the embryo proper through the laser ablation system is an elegant tool to study the transition of suspensor cells without above embryo proper. However, the thick covering ovule tissue reduced precision during ablation (Liu et al., 2015). The microspore-derived embryo in *Brassica napus* provides another strategy to address the transition. When cultured with a special media, the microspore of *Brassica napus* can divide horizontally into a suspensor-like filament and then generates proembryos on top, in the middle or at several positions of the long filament (Supena et al., 2008). This suspensor-like filament system will provide tempting information regarding the suspensor-embryo transition. In Arabidopsis filament-like embryo can also be induced by activating the YDA pathway (Lukowitz et al., 2004).

To check what mechanism triggers/inhibits the embryonic transition of the early basal cell lineage, we generated filament-like embryos in Arabidopsis through activating the embryonic YDA pathway in different degrees. By following the embryonic development of these transgenic lines, we detected their ability to produce multiple embryos and multiple seedlings, and chose pS4:SSP-YFP lines for further analysis. By using different fluorescent marker lines, we found that early filamentous embryos resemble the basal cell lineage. Auxin response was not observed in filament-like embryos. Then obvious auxin response was observed in putative hypophysis and tips of cotyledon primordia, suggesting the normal embryonic development of apical embryos. In contrast, the maximum auxin response was detected in suspensors cells. The maximum auxin response in the vertically divided suspensor cell implied initiation of the suspensor-embryo transition. Taken together, we developed an easy method to study the suspensor-embryo transition. Our results suggest that an early inhibition of auxin response in the whole

embryo and a late activation of auxin response in the basal cells are both important for the suspensor-embryo transition.

Results

Continuously activating the embryonic YDA signaling leads to filament-like embryos

First, we checked embryogenesis of *yda-CA* transgenic lines. Although long filament-like embryos were formed (Lukowitz et al., 2004), the *yda-CA* lines showed severe stomata defects, arrested inflorescence development, abnormal silique shapes and reduced ovule formation (not shown), consistent with previous observations (Bergmann et al., 2004; Meng et al., 2012). These defects together contribute to a severe loss of fertility. To avoid the fertility defect, we tried to activate the YDA pathway specifically in the embryo sack. Replacing Tyr 144 by Cys in MPK6 (MPK6-CA) caused a strong activation of MPK6 which functions downstream of YDA (Wang et al., 2007; Berriri et al., 2012; Zhang et al., 2017). Therefore, we tried to trans-activate MPK6-CA by the *RPS5A* promoter (*RPS5A*$_{pro}$*>>MPK6-CA*) in the embryo using the GAL4-UAS two-component expression system (Haseloff, 1999; Weijers et al., 2006).

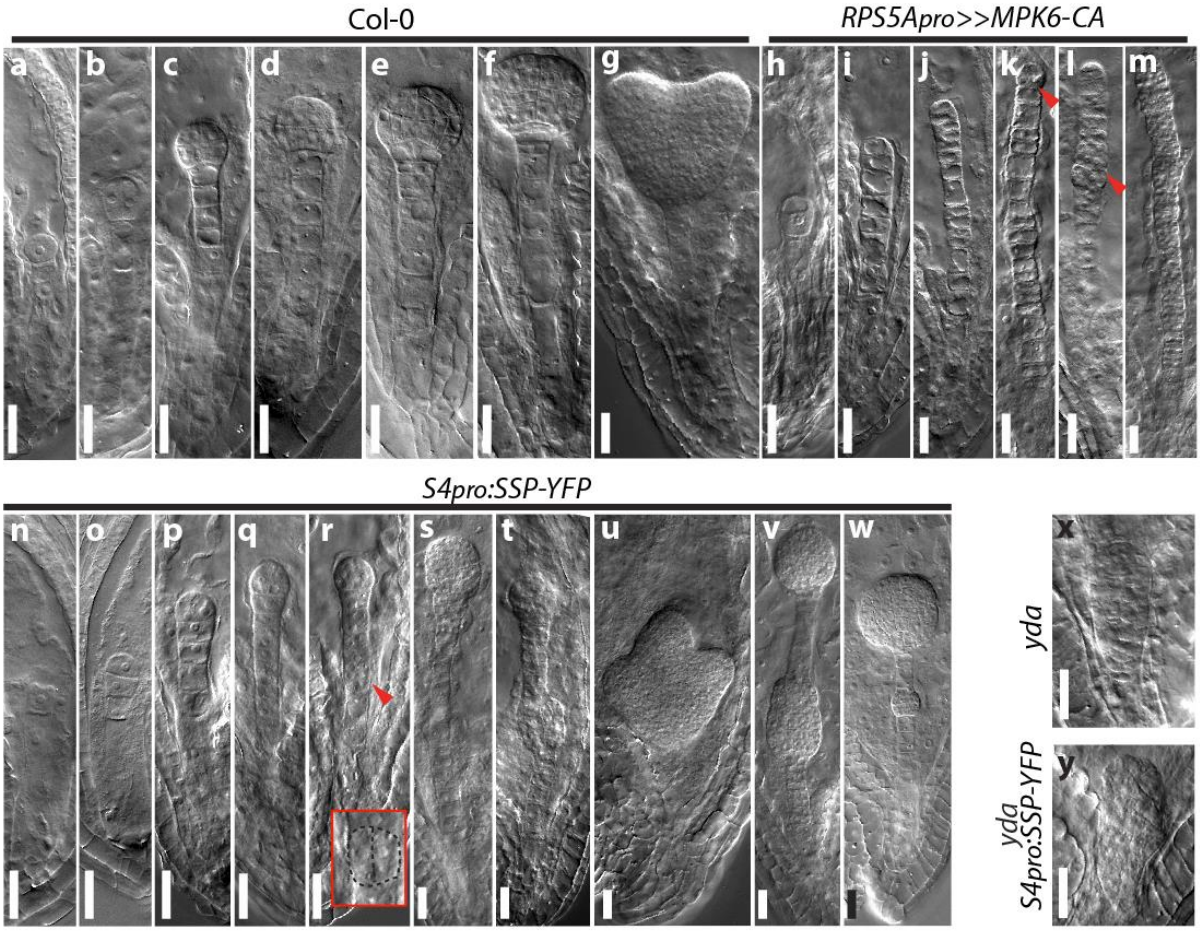

Figure 1. Embryonic development of Col-0, *RPS5A*$_{pro}$*>>MPK6-CA* and *S4*$_{pro}$*:SSP-YFP* in early embryonic stages.
a-**g**, The embryonic development of Col-0 in 1 DAP at the 1-cell stage (**a**) or the 2-cell stage (**b**), 2 DAP at the 8-cell stage (**c**), 2.5 DAP at the 32-cell stage (**d**) or the early globular stage (**e**), 3 DAP at the later globular stage (**f**), and 4 DAP at the heart stage (**g**). **h**-**m**, The embryonic development of *RPS5A*$_{pro}$*>>MPK6-CA* in 1 DAP (**h**), 2 DAP (**i**), 2.5 DAP (**j**), 3 DAP (**k** and **l**) and 4 DAP (**m**). **k** and

l, Filament-like embryos with the first vertical division either in the uppermost apical cell (**k**, arrowhead) or in middle cells (**l**, arrowhead). **n**-**w**, The embryonic development of *S4$_{pro}$:SSP-YFP* in 1 DAP (**n** and **o**), 1.5 DAP (**p**), 2 DAP (**q** and **r**), 3 DAP (**s** and **t**) and 4 DAP (**u**-**w**). **r**, the 2-DAP embryo with an additional vertical division within basal cells (arrowhead and the enlarged image with dished lines). **s**, the 3-DAP embryo containing an embryo-like cell cluster on top and a very long basal part. **t**, the 3-DAP embryo containing twin embryo-like cell clusters . **u**-**w**, 4-DAP embryos containing triple cotyledon primordia (**u**) or twin embryo-like cell clusters (**v** and **w**). **x**, the *yda* early embryo. **y**, the *yda S4$_{pro}$:SSP-YFP* early embryo. DAP: day after pollination. Scale bar represents 20 μm in all panels.

After hand pollination, long filament-like embryos were formed in *RPS5a>>MPK6-CA* at early stages, indicating strong activation of the YDA pathway (Figure 1a-l). During the growth of filaments, the first vertical division is mainly observed on the top (Figure 1k). However, the embryo-like development was also sometime observed in the middle of filaments (Figure 1l). This observation resembles the microspore system that the embryonic fate is not always first delivered to the apical (Supena et al., 2008). These long filaments first developed into thick sticks (Figure 1m). Then, several embryo-like structures were generated (Figure 2b and 2h), implying that the MPK6 inhibition of embryonic differentiation was partly overcome in the end. However, these structures cannot develop into intact seedlings after germination (Figure 2n), indicating that normal embryogenesis was severely retarded by continuous activation of the YDA pathway.

Lines and crosses	Vertical division of basal cells at 2 DAP	twin embryos at 3DAP	twin embryos at 4DAP	multiple embryos at 5 DAP	Single seedling with >2 cotyledons primordia	multiple seedlings
S4$_{pro}$:SSP-YFP #3	0% (0/82)	14% (14/100)	21.01% (25/119)	27.97% (40/143)	19.18% (14/73)	9.59% (7/73)
S4$_{pro}$:SSP-YFP #10	0% (0/56)	6.54% (7/107)	7.89% (6/76)	23.96% (46/192)	10.64% (20/188)	8.51% (16/188)
S4$_{pro}$:SSP-YFP #14	1.47% (3/204)	5.08% (6/118)	5.02% (11/219)	19.67% (71/361)	25.74% (35/136)	7.35% (10/136)
S4$_{pro}$:SSP-YFP #14 x Col-0	-	-	-	22.60% (33/146)	-	-
Col-0 x *S4$_{pro}$:SSP-YFP #14*	-	-	-	3.16% (3/95)	-	-

Table 1. The ratio of multiple embryos and seedlings in different lines and crosses

The numbers are listed below the ratio. The crosses are given as female x male. DAP: day after pollination. ">2" means more than two. "-"indicates the ratio was not calculated.

Specifically enhancing YDA signaling at early stages promotes twin embryos formation

Since continuous activation of the embryonic YDA pathway caused a strong embryonic defect, enhancing the YDA signaling only at early stages might be a better approach to facilitate embryonic transition from filament-like embryos. SSP is a strong input to the embryonic YDA pathway (Bayer et al., 2009; Neu et al., 2019). The *At3g10100* promoter is mainly active during early embryogenesis (Slane et al., 2014). Thus we use this promoter (here after called the *S4* promoter) to express *SSP* fused with a YFP (*S4$_{pro}$:SSP-YFP*) in the *ssp-2* mutant background. In this way, we expected to stimulate YDA signal at early stages and shut it down at late stages. Three lines with strong phenotypes were chosen for analysis. 2 days after pollination (DAP), *S4$_{pro}$:SSP-YFP* embryos developed into filaments (Figure 1n-r). Occasionally, a vertical division was observed in basal cells of line *#14* (Figure 1r and Table 1). 3 DAP, a long filamentous basal part with a proembryo-like cluster was generated (Figure 1s). In addition, twin embryo-like clusters were occasionally observed in ovules (Figure 1t and Table 1). 4 DAP, twin clusters were constantly expanding (Figure 1v,w)

and embryos containing three cotyledon primordia were observed (Figure 1u). Twin/triple embryos were more frequently observed at 5 DAP, indicating that filament-derived secondary embryos were generated continuously (Table 1). These tri-cotyledon embryos and multiple embryos underwent normal embryogenesis although their developments were strongly delayed compared to wild type (Figure 2). Interestingly, twin embryos can also develop in opposite orientations (Figure 2e, k). After seed germination, we often observed tri-cotyledon seedlings, twin-root seedlings and twin/triple seedlings (Figure 2 and Table 1).

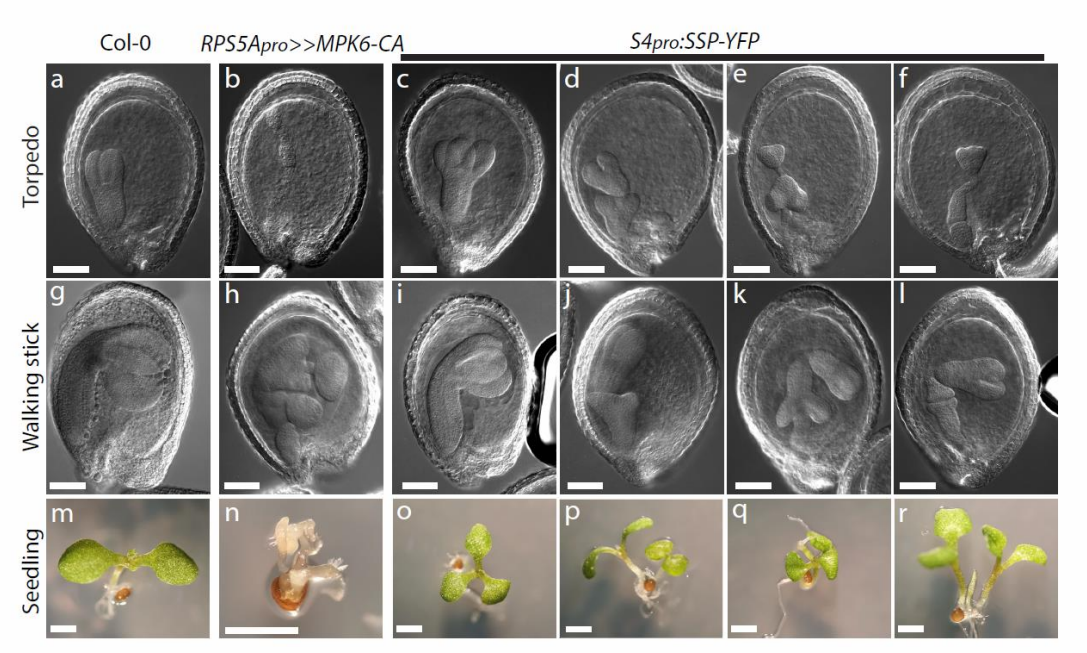

Figure 2. Late embryonic phenotypes and seedling phenotypes of Col-0, *RPS5A$_{pro}$>>MPK6-CA* and *S4$_{pro}$:SSP-YFP.*
a-**l**, ovules of late embryonic stages in Col-0, *RPS5A$_{pro}$>>MPK6-CA* and *S4$_{pro}$:SSP-YFP* stained with Hoyer's solution. **a** and **g**, Col-0 embryos at the torpedo stage (**a**) and the walking-stick stage (**g**). **b** and **h**, *RPS5A$_{pro}$>>MPK6-CA* embryos at the torpedo stage (**b**) and the walking-stick stage (**h**). **c**-**f** and **i**-**l**, *S4pro:SSP-YFP* embryos of the torpedo (**c**-**f**) stage and walking-stick stage (**i**-**l**) with triple cotyledons (**c** and **i**), twin embryos growing in either the normal orientation (**d** and **j**) or reverse orientations (**e** and **k**), and triple embryos (**f** and **l**). **m**-**r**, 5 DAP seedlings of Col-0 (**m**), *RPS5A$_{pro}$>>MPK6-CA* (**n**), and *S4$_{pro}$:SSP-YFP* (**o**-**r**) containing tri-cotyledons (**o**), twin seedlings (**p**), twin roots (**q**) or triple seedlings (**r**). DAP: days after germination. The scale bars represent 100 µm in **a**-**l** and 1 mm in **m**-**r**.

Endogenous SSP is only shortly active in the zygote (Bayer et al., 2009). We then wonder whether the filament-like embryos were indeed caused by activation of the YDA pathway. In *yda/+* mutants, a quarter embryos show severe development defects (Lukowitz et al., 2004). In *S4$_{pro}$:SSP-YFP yda-11/+* , 26.73% (54/202) embryos showed severe elongation defects, indicating that the embryonic phenotypes of *S4$_{pro}$:SSP-YFP* were primarily induced by activating the YDA pathway. In contrast to *pRPS5A$_{pro}$>>MPK6-CA* seedlings, *S4$_{pro}$:SSP-YFP* seedlings grew and flowered normally in soil (not shown). Thus, the influence of *S4$_{pro}$:SSP-YFP* transgene was only restricted to the embryo. These transgenic lines provide good models to study the suspensor-embryonic transition.

SSP-YFP transgene changed activity of the S4 promoter

As the S4 promoter is mainly active in early embryos and *SSP-YFP* inhibition of embryonic differentiation was removed during cell proliferation, we wonder how long and where *SSP-YFP* was expressed. In *S4$_{pro}$:nGFP*, nuclear-localized GFP was observed in the zygote and early embryos. The signal became weaker from the globular stage onward and disappeared after the heart stage (Figure 3a-e). Similar to *S4$_{pro}$:nGFP*, membrane-localized YFP signal was also detected in the whole *S4$_{pro}$*:SSP-YFP embryo during early stages (Figure 3f-i). However, the signal was still obvious in the center of expanding cell clusters while it was attenuated in other cells (Figure 3j-k). YFP signal was barely detected in heart embryos and torpedo embryos (Figure 3i-m). As the S4 promoter is more active in early embryos, these cells with higher SSP-YFP signal (Figure 3j-k) may be still in the early stage while surrounding cells had differentiated further. Taken together, the activity of S4 promoter is also influenced by the expression of SSP-YFP, implying that cell identities might have been altered in these embryo-like clusters.

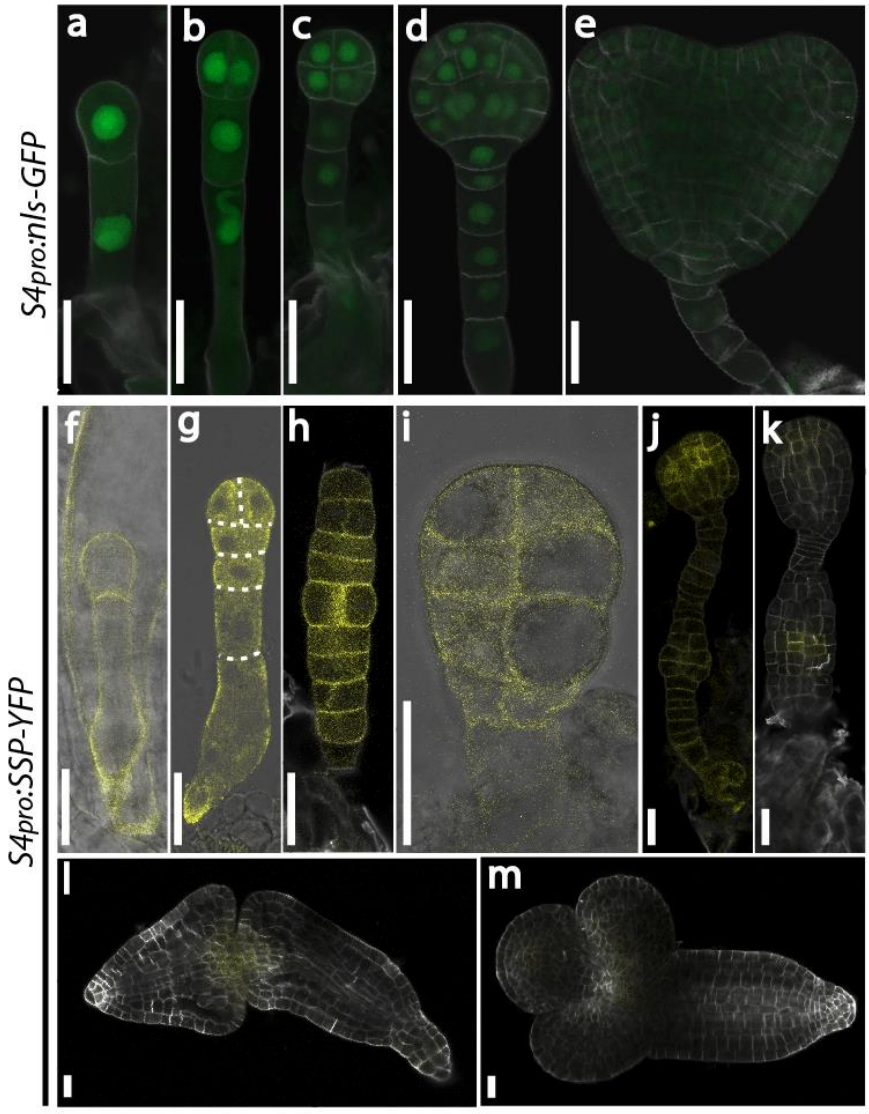

Figure 3. Expression of *SSP-YFP* in *S4$_{pro}$:SSP-YFP* embryos.
a-**e**, GFP signals in *S4$_{pro}$:nls-GFP* 1-cell embryo (**a**), 2-cell embryo (**b**), 8-cell embryo (**c**), globular embryo (**d**) and heart embryo (**e**). **f**-**m**, membrane-localized YFP signals in *S4$_{pro}$:SSP-YFP* 1-cell embryo (**f**), early embryo showing first vertical division (**g**), filament-like embryo (**h**), apical cells of an early embryo (**i**), embryos containing twin proembryo-like early clusters (**j**) or further-

proliferated clusters (**k**), twin embryos at the heart stage (**l**), and the torpedo embryo containing three cotyledon primordia (**m**). The very apical cells of the embryo in **h** were lost during sampling. Large vacuoles were observed in apical cells (**i**). Dashed lines in **g** indicate cell walls. Scale bar represents 20 µm in all panels.

The filamentous embryo has the identity of early basal cells

To check cells identities of *S4$_{pro}$:SSP-YFP* early embryos, different promoter marker lines were crossed with *S4$_{pro}$:SSP-YFP*. From the reciprocal crosses experiment between *S4$_{pro}$:SSP-YFP* and Col-0, we found that higher frequency of twin embryos were observed when using *S4$_{pro}$:SSP-YFP* as mother, which was equivalent to self-crossed *S4$_{pro}$:SSP-YFP* (Table 1), suggesting a strong maternal contribution to YDA activation in our transgenic system. Therefore, *S4$_{pro}$:SSP-YFP* was always used in the maternal side to cross with fluorescent markers lines. F1 embryos were checked directly from crosses.

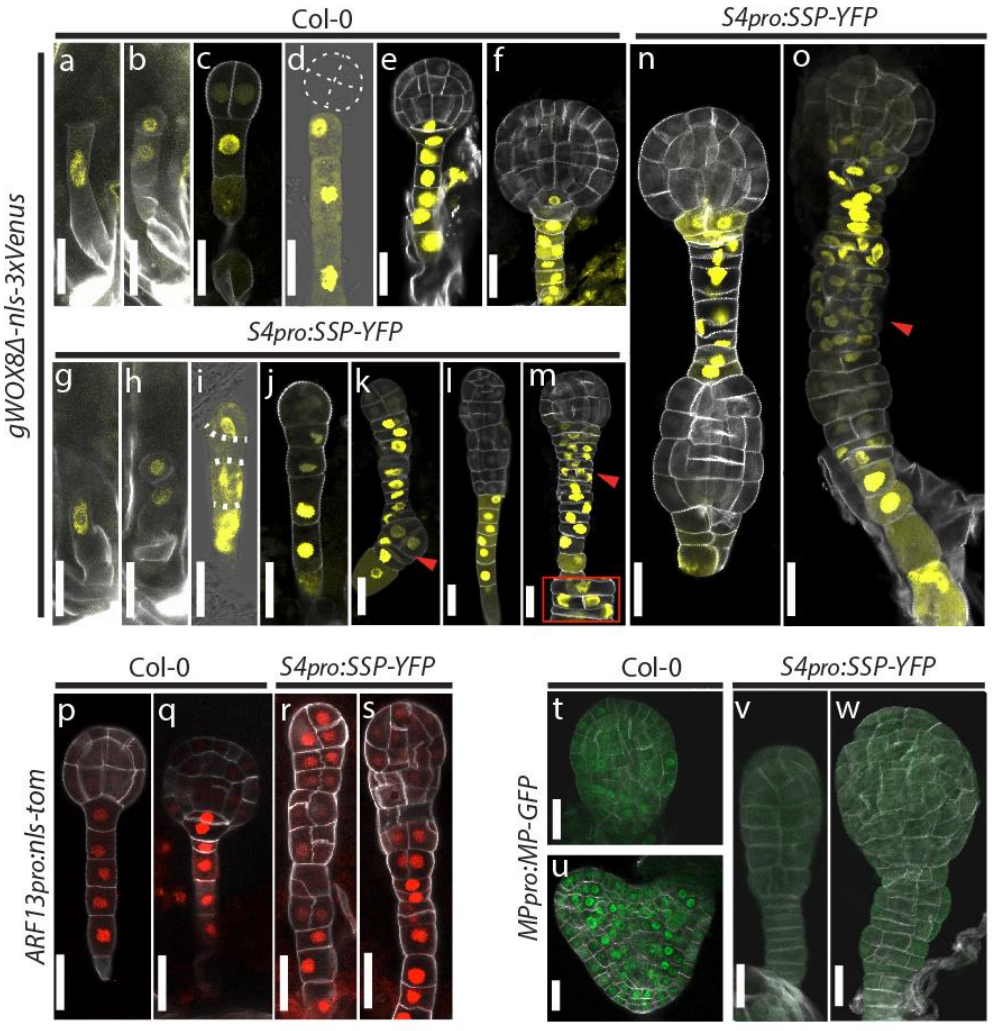

Figure 4. The expression patterns of fluorescent markers in Col-0 and *S4$_{pro}$:SSP-YFP* lines.

a-**f**, the *gWOX8Δ-nls-3xVenus* signal in Col-0 zygote (**a**), 1-cell embryo (**b**), 2-cell embryo (**c**), 8-cell embryo (**d**), early globular embryo (**e**) and late globular embryo (**f**). **g**-**o**, the *gWOX8Δ-nls-3xVenus* signal in *S4$_{pro}$:SSP-YFP* zygote (**g**), 1-cell embryo (**h**) and embryos of different stages and shapes (**i**-**o**). **i**, the early embryo with a horizontal division of the apical daughter cell of the zygote. **j**, the filament-like embryo with the first vertical division of the top apical cell. **k**, the filamentous embryo showing the first vertical division of basal cells (arrowhead). **l**, the embryo containing an apical stick-like cell cluster. **m**, the early embryo containing a proembryo-like cluster on top and the first vertical division of basal cells (arrowhead and the enlarged box). **n** and **o**, embryos containing twin proembryo-like cell clusters. **p**-**s**, the *ARF13$_{pro}$:nls-Tom* signal in Col-0 32-cell embryo (**p**) and globular embryo (**q**),

and in the *S4$_{pro}$:SSP-YFP* filament-like embryo (**r**) and the embryo with a proliferated apical cluster(**s**). **t**-**w**, the *MP$_{pro}$:MP-GFP* signal in Col-0 globular embryo (**t**) and heart embryo (**u**), and in *S4$_{pro}$:SSP-YFP* embryos in early stage (**v**) or a bit late stage (**w**) . Dashed lines in **d** and **i** indicate the cell wall. Scale bar represents 20 µm in all panels.

gWOX8Δ-NLS-3xVenus was used to mark suspensor identity (Breuninger et al., 2008). In wild-type background, Venus signal was detected in the elongating zygote and both daughter cells (Figure 4a,b). At the 2-cell stage, weak Venus signal was still detected in the apical cells (Figure 4c). From the 8-cell stage onward, Venus signal was only observed in suspensor cells (Figure 4d-f). In contrast, obvious YFP signal was observed in apical cells of filamentous embryos in *S4$_{pro}$:SSP-YFP* (Figure 4i-k), suggesting that the embryonic identity had not been acquired yet. *ARF13* is also specifically expressed in the suspensor (Breuninger et al., 2008; Schlereth et al., 2010). In *ARF13$_{pro}$:nls-Tom*, ARF13 promoter was fused with a nuclear localization signal sequence and Tomato RFP sequence. Specific Tomato signal was observed in the wild-type suspensor (Figure 4p,q), whereas strong Tomato signal was detected in the whole early filamentous embryo in *S4$_{pro}$:SSP-YFP* although some apical cells divided vertically (Figure 4r). Combined together, these results suggest the filamentous embryo in *S4$_{pro}$:SSP-YFP* is a file of cells with most likely basal cell identity.

The expanding cell clusters did not fully obtain proembryo identity

In *S4$_{pro}$:SSP-YFP*, proembryo-like clusters were generated from the filamentous embryos (Figure 1). While strong *gWOX8Δ-NLS-3xVenus* and *ARF13$_{pro}$:nls-Tom* signals were observed in the basal part of these embryos, the apical clusters did not show strong fluorescent signals despite the abnormal shapes (Figure 4i-n). These observations imply that these clusters might have obtained embryonic identity. Sometimes, when basal cells divided vertically, the *gWOX8Δ-NLS-3xVenus* signal in daughter cells became weaker (Figure 4k). These cells may undergo proliferation to generate another embryo-like cluster (Figure 4n). In addition, we also sometime observed strong Venus signal in these daughter cells (Figure 4m). It seems plausible that these daughter cells may proliferate into cell clusters partly with the suspensor identity (Figure 4o). Some cells in this basal cluster may eventually obtain the embryonic fate as *gWOX8Δ-NLS-3xVenus* signal in these cells was weaker than the others (Figure 4o).

Although these proembryo-like clusters showed weak suspensor identity, whether these clusters really gained the embryonic identity was not clear. *MONOPTEROS/Auxin Response Factor 5 (MP/ARF5)* is specifically expressed in the embryo proper (Schlereth et al., 2010). We make the *MP$_{pro}$:MP-nGFP* line where the MP promoter was fused with the MP genomic sequence and a nuclear-localized GFP sequence. In wild type, despite a weak gain-of function phenotype during embryogenesis, the MP-GFP signal was specifically detected in the embryo proper (Figure 4t,u). However, the MP-GFP signal was not observed in *S4$_{pro}$:SSP-YFP* embryo-like clusters in the early stage or a bit late stage (Figure 4v,w). Taken together, although the proembryo-like clusters in *S4$_{pro}$:SSP-YFP* have weak suspensor identity, they have not fully acquired the embryonic identity yet. The embryonic identity in these clusters could be directly suppressed by YDA activation since SSP-YFP signal was detected in cell clusters (Figure 3j,k). Importantly, although the SSP-YFP signal was strong in early basal cells, these cells can divide vertically and then generate clusters, suggesting that these basal cells have overcome SSP inhibition. How can these cells override SSP inhibition to divide vertically?

Altered Auxin response in *S4$_{pro}$:SSP-YFP*

Auxin response is crucial for embryonic development of the apical daughter cell after zygote division. When auxin response is blocked, the apical daughter cell divides horizontally like the basal daughter cell and the embryonic development is deregulated. Several studies have linked auxin response with suspensor-embryo transition. To check whether auxin response is deregulated in *S4$_{pro}$:SSP-YFP*, we checked the DR5:GFP signals in Col-0 and *S4$_{pro}$:SSP-YFP*. 4 DAP, maximum DR5 response was observed in wild-type hypophysis (Figure 5a), whereas GFP signal was not observed in filament-like embryos in *S4$_{pro}$:SSP-YFP* (Figure 5b), suggesting that the YDA signal has a primary inhibition on auxin response. Intriguingly, in proembryo-like clusters of *S4$_{pro}$:SSP-YFP* embryos, weak DR5:GFP signal was still detected in the putative hypophysis region (Figure 5c,d), suggesting that the apical-basal axis was partly established. Strong DR5:GFP signal was observed in the hypophysis of wild type and *S4$_{pro}$:SSP-YFP* embryos at 5 DAP (Figure 5e-g). Obvious DR5:GFP signal was also detected in cotyledon primordia of these embryos though the signal in *S4$_{pro}$:SSP-YFP* was weaker than in wild type. These results demonstrate that embryogenesis of the proembryo-like clusters was delayed, yet not fully blocked. This is consistent with the observation that healthy tri-cotyledon seedlings and twin seedlings were generated eventually. As the SSP-YFP signal was very weak during the heart stage (Figure 3l), the direct inhibition of the SSP-YFP on cell differentiation might has been erased from this stage onward. Strikingly, the maximum auxin response in *S4$_{pro}$:SSP-YFP* embryos had shifted to basal cells at 3 DAP (Figure 5c). At this stage, we also directly observed the maximum DR5:GFP signal in the dividing basal cells (Figure 5d), reminiscent of the auxin response in wild-type apical daughter cell after zygote division. It seems plausible that the increased auxin response in basal cells serves as an momentum for the embryonic transition.

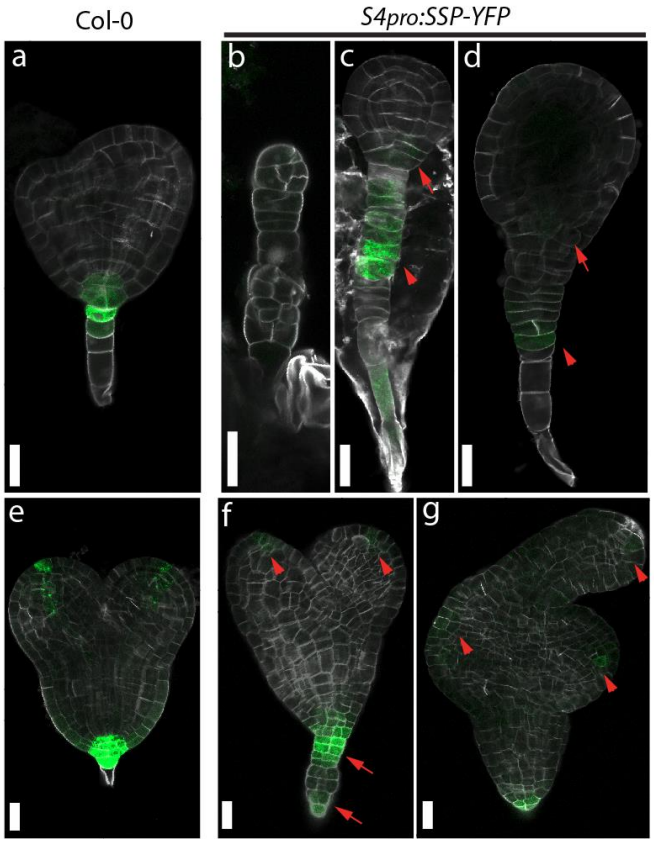

Figure 5. DR5 response in Col-0 and *S4$_{pro}$:SSP-YFP* embryos.

a-**g**, *DR5:GFP* signal in Col-0 embryos (**a** and **e**) and *S4$_{pro}$:SSP-YFP* embryos (**b**-**d**, **f**, **g**) at 4 DAP (**a**-**d**) and 5 DAP (**e**-**g**). **b**-**d**, *S4$_{pro}$:SSP-YFP* 4-DAP embryos with a filamentous structure (**b**), a long basal part (**c**)or the first vertical division in basal cells (**d**). Arrows in **c** and **d** indicate the DR5:GFP signal in putative hypophysis. Arrowheads in **c** and **d** indicate the maximum auxin response in basal cells. **f** and **g**, heart stage *S4$_{pro}$:SSP-YFP* embryos containing two (**f**) or three (**g**) cotyledon primordia. Arrowheads in **f** and **g** show the DR5:GFP signal in tips of cotyledon primordia. Strong DR5 signal was also observed in the basal part of twin clusters (**f**, arrow). Scale bar represents 20 µm in all panels.

Discussion

Enhancing the YDA signal in early embryos promotes the generation of twin seedlings

In this study, we tried three different strategies to activate the embryonic YDA pathway, aiming to produce filament-like embryos. In *yda-CA*, although filamentous embryos were produced (Lukowitz et al., 2004; Musielak and Bayer, 2014), the development is hard to follow because of strong fertility defects. Thus, we tried to specifically enhance the YDA signal in the embryo by the GAL4-UAS system. Similar to *yda-CA*, long filament-like embryos were formed in *RPS5A$_{pro}$>>MPK6-CA* (Figure 1). However, the embryonic development was severely delayed or blocked because of continuously activation of the YDA signaling (Figure 1 and Figure 2). Although multiple embryo-like clusters were formed, mature embryos were barely observed, making it hard to depict the developmental process(Figure 2). Finally, by enhancing YDA signaling at early embryonic stages, we developed an approach to convert filament-like embryos into twin embryos and finally into healthy twin seedlings(Figure 1 and Figure 2). Reciprocal crosses between wild type and *S4$_{pro}$:SSP-YFP* indicates that the maternal expressed *SSP-YFP* played a major role in the YDA activation in our system. The endogenous SSP regulates embryogenesis with a paternal effect (Bayer et al., 2009). Our result implies that *SSP* promoter sequence is vital for the paternal manner of SSP.

Basal cells in filamentous embryos have embryonic potential

In *RPS5A$_{pro}$>>MPK6-CA*, first embryo-like proliferation can be initiated in the middle of filamentous embryos (Figure 1), suggesting that the first embryonic transition is not solely possessed by top apical cells. Different from *RPS5A$_{pro}$>>MPK6-CA*, filament-like embryos was shorter in *S4$_{pro}$:SSP-YFP*. Besides, first embryo-like proliferation was only initiated from the apical part and were formed earlier in *S4$_{pro}$:SSP-YFP*, suggesting that the level of activation on the YDA signaling was weaker in *S4$_{pro}$:SSP-YFP*. By crossing *S4$_{pro}$:SSP-YFP* with early suspensor marker lines *gWOX8Δ-NLS-3xVenus* and *ARF13$_{pro}$:nls-Tom*, we found that the filamentous have the identity of early basal cells (Figure 4). Second proembryo-like clusters were initiated from these cells (Figure 1), suggesting that these cells have embryonic potential. Even 5 DAP, new embryo-like clusters were still initiated from the basal part (Table 1), indicating that this potential can endure for quite long time. That explains why only 7%~10% twin seedlings were formed eventually while 20%~30% twin embryos were generated (Table 1). According to *Liu et al.,* when proembryo was removed after the globular stage, suspensor cells did not have the embryonic potential (Liu et al., 2015). Thus we prefer to call these basal cells along *S4$_{pro}$:SSP-YFP* filamentous embryo “basal lineage ground cells (BLGCs)” that can either develop into a suspensor or convert into an embryo.

Embryonic transition and feedback in our system

Although the *S4* promoter is mainly active at early stage, we observed longer SSP-YFP signals when using *S4* promoter (Figure 3). In wild type, *SSP* transcripts were only detected in the pollen and zygote (Bayer et al., 2009; Zhao et al., 2019). Although 225bp *SSP* 5' UTR was fused with the S4 promoter in our construct, this is unlikely the reason of prolonged expression. As activated YDA signaling prevented differentiation in the beginning, the BLGCs will strongly activate the *S4* promoter activity. Then increased SSP-YFP expression activated the YDA signaling, which in turn promoted the generation of more BLGCs. In proembryo-like clusters, SSP-YFP is mainly localized in the center (Figure 3). Since the *S4* promoter is more active at early stages, it seems plausible that these cells containing stronger SSP-YFP signal were still in very early embryonic stages, which also contribute to prolonged SSP-YFP expression. Accordingly, surrounding cells containing lower SSP-YFP signal may have differentiated further. However, although *gWOX8Δ-NLS-3xVenus* and $ARF13_{pro}$*:nls-Tom* patterns partly mimic that of wild type in these clusters, MP_{pro}*:MP-GFP* was not observed (Figure 4), suggesting that the proembryo identity was only partly acquired in these clusters. That might explain why triple cotyledon primordia were frequently formed (Figure 1). As $S4_{pro}$*:SSP-YFP* seems to establish a positive feedback loop, activating YDA pathway at early stages without a possible feedback onto the promoter would be an even better method to study the BLGCs-embryo transition. Expressing SSP-YFP with a strong promoter that is solely active in the egg cell and/or zygote would be fascinating.

The initiation of embryonic transition from basal lineage ground cells

We showed that enhanced YDA signaling inhibits embryonic development primarily. During filament elongation, some BLGCs finally adopted vertical division and tried to proliferate into an embryo. Thus, these cells have at least partly overcome the inhibition of YDA signaling. Interestingly, this violation is not negatively correlated with SSP-YFP signal strength since vertically divided BLGCs still showed strong SSP-YFP signal like other BLGCs (Figure 3). This suggests that some BLGCs may gained signals for the vertical division, although the following transition processes were still strongly suppressed by YDA signaling in early stages. Auxin response in apical daughter cells is vital for its vertical division. Thus, we wonder whether auxin response in BLGCs is different from that of wild-type suspensor cells. As most vertical division of BLGCs were observed from 3 DAP to 4 DAP, we checked the DR5:GFP activity in $S4_{pro}$*:SSP-YFP* mainly at that stages. Twin embryos were observed when auxin response was suppressed by expressing stabilized *bdl* (Rademacher et al., 2012; Radoeva et al., 2019). Similarly, auxin response was presumably suppressed in the very early stage in our system. Before the initiation of second embryo, DR5 activity was very weak in the putative hypophysis of the top cell cluster, also reflecting a retarded auxin response (Figure 5). Strikingly, we observed strong DR5 activity in BLGCs before and right after their vertical division (Figure 5). This observation is consistent with other researches (Liu et al., 2015; Zhang et al., 2020), strongly suggesting the role of auxin response in BLGC-embryo transition.

It was proposed that the embryonic potential of suspensor cells might be suppressed by the normal embryo proper (Marsden and Meinke, 1985). As the embryonic identity of the apical cluster was acquired quite late, its inhibition on BLGCs, if exists, might not occur in the early stage so that BLGC-embryo transition can happen. This might be related to auxin contribution. In our system when the above embryo proper is abnormal, auxin transported from the bottom and/or embryo proper may converged in some BLGCs, resulting in a strong auxin response to diminish YDA signaling inhibition. Similar regulation could

happen in wild type as YDA signaling regulates suspensor development and vertical division was also observed in *yda* basal cells (Lukowitz et al., 2004).

Materials and Methods

Plant Materials and Growth Conditions

The *yda-11* (SALKseq_078777) and *ssp-2* (SALK_051462) mutants were described previously (Bayer et al., 2009) (See Methods in Chapter II). Seeds used in this study were sterilized with 70% ethanol, and then transferred to half-strength Murashige and Skoog (½ MS) medium containing 1% (w/v) sucrose and 1% (w/v) agar (pH = 5.7)(Murashige and Skoog, 1962) at 4°C in dark for 2 days. Then seeds and seedlings were geminated and grown under long-day conditions as described previously (Babu et al., 2013).

Plasmid constructions and transgenic lines

To make $S4_{pro}$*:SSP-YFP*, 1750 bp sequence upstream of *At3g10100* start codon was fused with *SSP* genomic sequence and 153bp SSP 3' UTR. A Citrine YFP was introduced in between SSP kinase domain and SSP TPR domain as described before (Bayer et al., 2009). The whole expression cassette was synthesized on the pUC57 vector and then introduced to the pBay-bar vector (Wang et al., 2021). To make UAS_{pro}*:MPK6-CA*, 3 times UAS sequence was fused in pGreenII vector with MPK6 CDS containing a Y144>C mutation. In $ARF13_{pro}$*:nls-Tom*, 2 kb sequence upstream of *ARF13* start codon was fused with *Tomato RFP* and a nuclear localization sequence in pGreenII vector. *gWOX8Δ-NLS-3xVenus* was kindly provided by Thomas Laux (Ueda et al., 2011). Transgenic lines were generated by floral dip using *Agrobacterium tumefaciens* GV3101 (Van Larebeke et al., 1974). $S4_{pro}$*:SSP-YFP* was transformed into *ssp-2*. UAS_{pro}*:MPK6-CA* and $ARF13_{pro}$*:nls-Tom* were transformed into Col-0. Transgenic seeds were screen on ½ MS containing 50 mg/L phosphinothricin. $S4_{pro}$*:SSP-YFP #14* was crossed with *yda11/+* to get $S4_{pro}$*:SSP-YFP yda/+*. $RPS5A_{pro}$*:GAL4-VP16* (Weijers et al., 2006), *DR5:GFP:ER* (Weijers et al., 2006), MP_{pro}*:MP-GFP* and $S4_{pro}$*:nls-GFP* (Slane et al., 2014) were described before.

DIC microscopy

For differential interference contrast (DIC) imaging, ovules were hand-pollinated and incubated in Hoyer´s solution (Lukowitz et al., 2004) at room temperature (incubating 1 day for ovules collected 1 DAP (day after pollination), 2 days for ovules collected 2 DAP, and so on). For embryos of $RPS5A_{pro}$*>>MPK6-CA*, UAS_{pro}*:MPK6-CA* was crosses with $RPS5A_{pro}$*:GAL4-VP16* and F1 embryos were collected. To count the ratio of horizontal division of the apical daughter cell, 1.5-DAP ovules were collected for imaging. DIC images were taken with a Zeiss Axio Imager and AxioVision 4 software.

Confocal microscopy

A Zeiss LSM 780 NLO microscope with ZEN 2.0 software and a Leica TCS SP8 microscope with LAS X software were used for confocal microscopy. Embryos were dissected from ovules using a Zeiss Stemi 2000 binocular and shape needles. For cell wall imaging, dissected embryos were incubated in SCRI Renaissance 2200 (SR2200) staining solution for 5-10 min, and confocal images were obtained with 405 nm excitation wavelength and 415-475 nm detection wavelength (Musielak et al., 2015). GFP images were obtained with 488 nm excitation wavelength and 496-533 nm detection wavelength. For YFP imaging, 514 nm laser wavelength was used for excitation, wavelength between 526 nm and 553 nm was recorded. For RFP imaging, 561 nm excitation wavelength and 580-633 nm detection wavelength were used.

Seedling phenotyping

Seedlings were grown on ½ MS medium for 7 days before counting different phenotypes. Seedling images were taken with a Zeiss Stemi 2000 binocular equipped with a camera.

References

Babu, Y., Musielak, T., Henschen, A., and Bayer, M. (2013). Suspensor length determines developmental progression of the embryo in Arabidopsis. Plant Physiol **162,** 1448-1458.

Bayer, M., Slane, D., and Jurgens, G. (2017). Early plant embryogenesis-dark ages or dark matter? Curr Opin Plant Biol **35,** 30-36.

Bayer, M., Nawy, T., Giglione, C., Galli, M., Meinnel, T., and Lukowitz, W. (2009). Paternal control of embryonic patterning in Arabidopsis thaliana. Science **323,** 1485-1488.

Bergmann, D.C., Lukowitz, W., and Somerville, C.R. (2004). Stomatal development and pattern controlled by a MAPKK kinase. Science **304,** 1494-1497.

Berriri, S., Garcia, A.V., Frey, N.F.D., Rozhon, W., Pateyron, S., Leonhardt, N., Montillet, J.L., Leung, J., Hirt, H., and Colcombet, J. (2012). Constitutively Active Mitogen-Activated Protein Kinase Versions Reveal Functions of Arabidopsis MPK4 in Pathogen Defense Signaling. Plant Cell **24,** 4281-4293.

Breuninger, H., Rikirsch, E., Hermann, M., Ueda, M., and Laux, T. (2008). Differential expression of WOX genes mediates apical-basal axis formation in the Arabidopsis embryo. Dev Cell **14,** 867-876.

Dharmasiri, N., Dharmasiri, S., Weijers, D., Lechner, E., Yamada, M., Hobbie, L., Ehrismann, J.S., Jurgens, G., and Estelle, M. (2005). Plant development is regulated by a family of auxin receptor F box proteins. Developmental Cell **9,** 109-119.

Friml, J., Vieten, A., Sauer, M., Weijers, D., Schwarz, H., Hamann, T., Offringa, R., and Jurgens, G. (2003). Efflux-dependent auxin gradients establish the apical-basal axis of Arabidopsis. Nature **426,** 147-153.

Hamann, T., Mayer, U., and Jurgens, G. (1999). The auxin-insensitive bodenlos mutation affects primary root formation and apical-basal patterning in the Arabidopsis embryo. Development **126,** 1387-1395.

Haseloff, J. (1999). GFP variants for multispectral imaging of living cells. Method Cell Biol **58,** 139-+.

Kawashima, T., and Goldberg, R.B. (2010). The suspensor: not just suspending the embryo. Trends Plant Sci **15,** 23-30.

Lau, S., Slane, D., Herud, O., Kong, J., and Jurgens, G. (2012). Early embryogenesis in flowering plants: setting up the basic body pattern. Annu Rev Plant Biol **63,** 483-506.

Liu, Y., Li, X.B., Zhao, J., Tang, X.C., Tian, S.J., Chen, J.Y., Shi, C., Wang, W., Zhang, L.Y., Feng, X.Z., and Sun, M.X. (2015). Direct evidence that suspensor cells have embryogenic potential that is suppressed by the embryo proper during normal embryogenesis. P Natl Acad Sci USA **112,** 12432-12437.

Lukowitz, W., Roeder, A., Parmenter, D., and Somerville, C. (2004). A MAPKK kinase gene regulates extra-embryonic cell fate in Arabidopsis. Cell **116,** 109-119.

Maheshwari, P. (1950). An introduction to the embryology of angiosperms. (New York,: McGraw-Hill).

Marsden, M.P.F., and Meinke, D.W. (1985). Abnormal-Development of the Suspensor in an Embryo-Lethal Mutant of Arabidopsis-Thaliana. Am J Bot **72,** 1801-1812.

Meng, X.Z., Wang, H.C., He, Y.X., Liu, Y.D., Walker, J.C., Torii, K.U., and Zhang, S.Q. (2012). A MAPK Cascade Downstream of ERECTA Receptor-Like Protein Kinase Regulates Arabidopsis Inflorescence Architecture by Promoting Localized Cell Proliferation. Plant Cell **24,** 4948-4960.

Murashige, T., and Skoog, F. (1962). A Revised Medium for Rapid Growth and Bio Assays with Tobacco Tissue Cultures. Physiol Plantarum **15,** 473-497.

Musielak, T.J., and Bayer, M. (2014). YODA signalling in the early Arabidopsis embryo. Biochem Soc Trans **42,** 408-412.

Musielak, T.J., Schenkel, L., Kolb, M., Henschen, A., and Bayer, M. (2015). A simple and versatile cell wall staining protocol to study plant reproduction. Plant Reproduction **28,** 161-169.

Neu, A., Eilbert, E., Asseck, L.Y., Slane, D., Henschen, A., Wang, K., Burgel, P., Hildebrandt, M., Musielak, T.J., Kolb, M., Lukowitz, W., Grefen, C., and Bayer, M. (2019). Constitutive signaling activity of a receptor-associated protein links fertilization with embryonic patterning in Arabidopsis thaliana. Proc Natl Acad Sci U S A **116,** 5795-5804.

Rademacher, E.H., Lokerse, A.S., Schlereth, A., Llavata-Peris, C.I., Bayer, M., Kientz, M., Freire Rios, A., Borst, J.W., Lukowitz, W., Jurgens, G., and Weijers, D. (2012). Different auxin response machineries control distinct cell fates in the early plant embryo. Dev Cell **22,** 211-222.

Radoeva, T., Lokerse, A.S., Llavata-Peris, C.I., Wendrich, J.R., Xiang, D., Liao, C.Y., Vlaar, L., Boekschoten, M., Hooiveld, G., Datla, R., and Weijers, D. (2019). A Robust Auxin Response Network Controls Embryo and Suspensor Development through a Basic Helix Loop Helix Transcriptional Module. Plant Cell **31,** 52-67.

Robert, H.S., Park, C., Gutierrez, C.L., Wojcikowska, B., Pencik, A., Novak, O., Chen, J., Grunewald, W., Dresselhaus, T., Friml, J., and Laux, T. (2018). Maternal auxin supply contributes to early embryo patterning in Arabidopsis. Nat Plants **4,** 548-553.

Schlereth, A., Moller, B., Liu, W., Kientz, M., Flipse, J., Rademacher, E.H., Schmid, M., Jurgens, G., and Weijers, D. (2010). MONOPTEROS controls embryonic root initiation by regulating a mobile transcription factor. Nature **464,** 913-916.

Schwartz, B.W., Yeung, E.C., and Meinke, D.W. (1994). Disruption of Morphogenesis and Transformation of the Suspensor in Abnormal Suspensor Mutants of Arabidopsis. Development **120,** 3235-3245.

Slane, D., Kong, J., Berendzen, K.W., Kilian, J., Henschen, A., Kolb, M., Schmid, M., Harter, K., Mayer, U., De Smet, I., Bayer, M., and Jurgens, G. (2014). Cell type-specific transcriptome analysis in the early Arabidopsis thaliana embryo. Development **141,** 4831-4840.

Supena, E.D., Winarto, B., Riksen, T., Dubas, E., van Lammeren, A., Offringa, R., Boutilier, K., and Custers, J. (2008). Regeneration of zygotic-like microspore-derived embryos suggests an important role for the suspensor in early embryo patterning. J Exp Bot **59,** 803-814.

Ueda, M., Zhang, Z., and Laux, T. (2011). Transcriptional activation of Arabidopsis axis patterning genes WOX8/9 links zygote polarity to embryo development. Dev Cell **20,** 264-270.

Van Larebeke, N., Engler, G., Holsters, M., Van den Elsacker, S., Zaenen, I., Schilperoort, R.A., and Schell, J. (1974). Large plasmid in Agrobacterium tumefaciens essential for crown gall-inducing ability. Nature **252,** 169-170.

Vernon, D.M., and Meinke, D.W. (1994). Embryogenic transformation of the suspensor in twin, a polyembryonic mutant of Arabidopsis. Dev Biol **165,** 566-573.

Wang, H., Ngwenyama, N., Liu, Y., Walker, J.C., and Zhang, S. (2007). Stomatal development and patterning are regulated by environmentally responsive mitogen-activated protein kinases in Arabidopsis. Plant Cell **19,** 63-73.

Wang, K., Chen, H., Miao, Y., and Bayer, M. (2020). Square one: zygote polarity and early embryogenesis in flowering plants. Curr Opin Plant Biol **53,** 128-133.

Wang, K., Chen, H., Ortega-Perez, M., Miao, Y., Ma, Y., Henschen, A., Lohmann, J.U., Laubinger, S., and Bayer, M. (2021). Independent parental contributions initiate zygote polarization in Arabidopsis thaliana. Curr Biol.

Weijers, D., Schlereth, A., Ehrismann, J.S., Schwank, G., Kientz, M., and Jurgens, G. (2006). Auxin triggers transient local signaling for cell specification in Arabidopsis embryogenesis. Developmental Cell **10,** 265-270.

Xiang, D., Yang, H., Venglat, P., Cao, Y., Wen, R., Ren, M., Stone, S., Wang, E., Wang, H., Xiao, W., Weijers, D., Berleth, T., Laux, T., Selvaraj, G., and Datla, R. (2011). POPCORN functions in the auxin pathway to regulate embryonic body plan and meristem organization in Arabidopsis. Plant Cell **23,** 4348-4367.

Yoshida, S., Barbier de Reuille, P., Lane, B., Bassel, G.W., Prusinkiewicz, P., Smith, R.S., and Weijers, D. (2014). Genetic control of plant development by overriding a geometric division rule. Dev Cell **29,** 75-87.

Zhang, J.Z., and Somerville, C.R. (1997). Suspensor-derived polyembryony caused by altered expression of valyl-tRNA synthetase in the twn2 mutant of Arabidopsis. Proc Natl Acad Sci U S A **94,** 7349-7355.

Zhang, M., Xu, X., Zheng, Y., Zhang, Y., Deng, X., Luo, S., Wu, Q., Xu, J., and Zhang, S. (2020). Expression of a plastid-localized sugar transporter in the suspensor is critical to embryogenesis. Plant Physiol.

Zhang, M.M., Wu, H.J., Su, J.B., Wang, H.C., Zhu, Q.K., Liu, Y.D., Xu, J., Lukowitz, W., and Zhang, S.Q. (2017). Maternal control of embryogenesis by MPK6 and its upstream MKK4/MKK5 in Arabidopsis. Plant J **92,** 1005-1019.

Zhao, P., Zhou, X., Shen, K., Liu, Z., Cheng, T., Liu, D., Cheng, Y., Peng, X., and Sun, M.X. (2019). Two-Step Maternal-to-Zygotic Transition with Two-Phase Parental Genome Contributions. Dev Cell.

Zhou, X., Liu, Z., Shen, K., Zhao, P., and Sun, M.X. (2020). Cell lineage-specific transcriptome analysis for interpreting cell fate specification of proembryos. Nat Commun **11,** 1366.